AN INVESTIGATION INTO THE FUNCTION OF TWO S100 PROTEINS, S100A12 AND MRP-14

Matthew James Robinson

October 2000

This thesis is presented in part fulfilment of the
requirements for the degree of Doctor of Philosophy
at the University of London

Supervisors

Dr. Nancy Hogg
Leukocyte Adhesion Laboratory
Imperial Cancer Research Fund
London

Prof. Bastien Gomperts
Department of Physiology
University College London
London

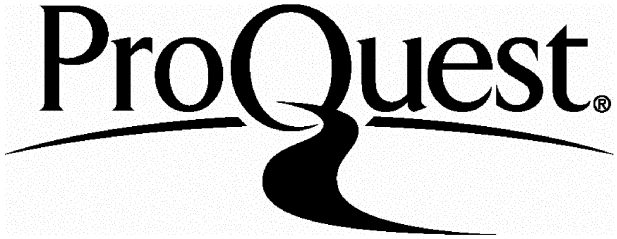

DEDICATION

To my parents
who deserve so much, but got this!

ABSTRACT

MRP-8 and MRP-14 (S100A8 and S100A9) are homologous members of the S100 family of small acidic calcium binding proteins. These proteins are highly expressed as a complex by neutrophils, comprising 45% of the total cytosolic protein. Monocytes and certain squamous epithelia also express MRP-8 and MRP-14. Another closely related S100 protein, S100A12, is expressed by neutrophils. S100A12 was cloned, and the recombinant protein expressed and purified. Immunohistochemistry showed S100A12 expression by squamous epithelia was similar to but more restricted than MRP-14 expression. S100A12 and MRP-14 failed to co-immunoprecipitate from neutrophil lysate, indicating that S100A12 does not exist in the complex with the MRP proteins.

Previous work in our laboratory showed that recombinant MRP-14 (rMRP-14) activated the leukocyte integrin Mac-1 (CD11b/CD18) on neutrophils (Newton and Hogg, 1998). Further work demonstrated that rMRP-14 induced Mac-1 expression on T lymphoblasts and stimulated binding to the Mac-1 ligand fibrinogen (Newton, 1997). However, detailed analysis of the rMRP-14 induced adhesion of T lymphocytes and neutrophils to fibrinogen proved it was not mediated by Mac-1. The cell adhesion was dependent on rMRP-14 binding to fibrinogen and other Mac-1 ligands, such as denatured BSA. The rMRP-14 induced expression of Mac-1 on T lymphoblasts has also proved to be an artefact

rMRP-14 bound heparin with high affinity. This interaction with heparin was different in nature to the binding to fibrinogen, and was probably maintained by ionic bonds formed with the sulphate substitutions. The binding site for heparin was discrete and distinct from the proteinaceous ligand-binding site. Further, rMRP-14 bound to the cell surface of T lymphoblasts and the microvascular endothelial cell line, HMEC-1. Initial studies indicate that the rMRP-14 bound to cell surface proteoglycans.

It is proposed that the adhesion of neutrophils and T lymphoblasts is mediated by rMRP-14 binding both the immobilised ligand and the cell surfaces, thus acting as a "molecular glue".

ACKNOWLEDGEMENTS

First and foremost I would like to thank Nancy for her almost relentless optimism, help, guidance and assistance over what must have seemed four long years. The creative environment she fosters in the Lab will be hard to find elsewhere. I am also grateful to the members of the MacLab, past and present, as they made my time at the ICRF all the more enjoyable and fruitful. Specific thanks must go to: Jo "open for surgery" Porter, Richard May for his testosterone and understanding of football, Bec "not quite as tall as my stories" Newton, Birgit Leitinger for being the other voice in lab meeting, Paula Stanley for getting my project started so quickly, Josie Hobbs for trying to organise me in between her other engagements, Madelon Bracke who's never short of outfits or conversation, Robbie Henderson for looking like my student and Kiki Tanousis who never lets the lunchtime conversation run dry. I am especially grateful to Kathy O'Connor, who cleaned up before and after me, never complained and was always cheery.

On a more technical note, I thank George Elia for performing the immunohistochemistry presented in this thesis. I am also grateful to Phillip Tessier and Richard May, who contributed massively to the air pouch experiments.

Finally, I'm most grateful to Ali for support and encouragement above and beyond the call of duty.

TABLE OF CONTENTS

CHAPTER 2: MATERIALS AND METHODS

CHAPTER 3: INITIAL CHARACTERISATION OF S100A12

CHAPTER 4: THE PROADHESIVE EFFECT OF rMRP-14

CHAPTER 5: rS100 PROTEINS BINDING TO PROTEINACEOUS LIGANDS

CHAPTER 6: rMRP-14 AND rS100A12 BINDING TO CELL SURFACES AND GLYCOSAMINOGLYCANS

CHAPTER 7: DISCUSSION AND FUTURE DIRECTIONS

FIGURES AND TABLES

CHAPTER 1: INTRODUCTION

CHAPTER 3: INITIAL CHARACTERISATION OF S100A12

CHAPTER 4: THE PROADHESIVE EFFECT OF rMRP-14

CHAPTER 5: rS100 PROTEINS BINDING TO PROTEINACEOUS LIGANDS

CHAPTER 6: rMRP-14 AND rS100A12 BINDING TO CELL SURFACES AND GLYCOSAMINOGLYCANS

CHAPTER 7: DISCUSSION AND FUTURE DIRECTIONS

ABBREVIATIONS

Apo-	Calcium free-
BSA	Bovine serum albumin
BCECF-AM	2',7'-bis-(carboxyethyl)-5(6')-carboxyfluorescein acetoxymethyl ester
BrdU	5-Bromo-2'-deoxyuridine
Ca^{2+}	Ionised calcium
Ca^{2+}-	Calcium bound-
$[Ca^{2+}]_i$	Intracellular calcium
CaM	Calmodulin
cDNA	Complementary DNA
CHAPS	3-[(-Cholamidopropyl)dimethylammonio]-1-propane-sulphonate
CR1	Complement receptor 1
DMSO	Dimethyl sulphoxide
dpc	Days post coitum
DTT	DL-Dithiothreitol
E. coli	*Escherichia coli*
EDTA	Ethylenediaminetetraacetic acid
ELISA	Enzyme linked immunosorbent assay
E-selectin	Endothelial-selectin
FA^- BSA	Fatty acid free bovine serum albumin
F-actin	Filamentous actin
FCS	Foetal calf serum
FGF	Fibroblast growth factor
FGFR	Fibroblast growth factor receptor
FITC	Fluorescein isothiocyanate
fMLP	formyl-methionyl-leucyl-phenylalanine

FSG	Fish skin gelatin
GAG	Glycosaminoglcan
Gal	Galactose
GalNAc	D-Galactosamine
gC1qR	Globular C1q receptor
GFAP	Glial fibrillary acidic protein
Glc A	Glucuronic acid
GlcNAc	N-Acetyl-D-glucosamine
GlcNSulpho	N-Sulpho-D-glucosamine
GM-CSF	Granulocyte/macrophage-colony stimulating factor
GROα	Growth regulated oncogene α
GlyCAM-1	Glycosylation-dependent cell adhesion molecule-1
HBSS	Hank's balanced saline solution
H-HBSS	HEPES buffered Hank's balanced salts solution
HMWK	High molecular weight kininogen
ICAM	Intercellular adhesion molecule
Ido A	Iduronic acid
IgSF	Immunoglobulin superfamily
IL-	Interleukin
$InsP_3$	Inositol (1,4,5)-triphosphate
IPTG	Isopropyl-β-D-thiogalactopyranoside
LFA-1	Leukocyte function-associated antigen-1
LPS	Lipopolysaccharide
L-selectin	Leukocyte selectin
mAb	Monoclonal antibody
mRNA	Messenger RNA
MRP	Migration inhibitory factor-related protein
NF-κB	Nuclear factor-κB
NP40	Nonidet P40 or ethylyphenyl-polyethylene glycol

PAF	Platelet activating factor
PBMC	Peripheral blood mononuclear cell
PBSA	Phosphate buffered saline A
PCR	Polymerase chain reaction
PdBu	Phorbol-12,13-dibutyrate
PF-4	Platelet factor-4
pI	Isoelectric point
PKC	Protein kinase C
PLC	Phospholipase C
PMCA	Plasma membrane calcium ATPase pump
PMSF	Phenylmethylsulphonyl fluorine
P-selectin	Platelet-selectin
r	Recombinant
RAGE	Receptor for advanced glycation endproducts
RT	Room temperature
SD	Standard deviation
SDS	Sodium dodecyl sulphate
SDS PAGE	Sodium dodecyl sulphate polyacrylamide gel electrophoresis
SERCA	Sacroplasmic and endoplasmic reticulum calcium ATPase pump
Sgp200	Sulphated glycoprotein 200kDa
sLe^x	Sialyl $lewis^x$
Tblast	T lymphoblast
TBS	Tris buffered saline
TGF-β1	Transforming growth factor-β1
TNF	Tumour necrosis factor
VCAM	Vascular cell adhesion molecule
VLA-4	Very late antigen-4

Chapter 1

INTRODUCTION

1.1 Calcium: A Second Messenger

1.1.a Calcium Signalling

The concentration of ionised calcium (Ca^{2+}) within resting cells is about 100nM, which is approximately four orders of magnitude lower than the extracellular level. Cell signalling can result in transient elevations in intracellular calcium ($[Ca^{2+}]_i$), which in turn initiate many signal transduction pathways. The mechanisms by which the level of $[Ca^{2+}]_i$ is controlled are summarised below, but more comprehensive reviews are (Barritt, 1999; Clapham, 1995).

Ca^{2+} is excluded from the cytosol of a cell by ATPase pumps. Specifically, cytosolic Ca^{2+} is transported into the sarcoplasmic and endoplasmic reticulum by SERCA (sarcoplasmic and endoplasmic reticulum Ca^{2+} ATPase) pumps, and out into the extracellular milieu by PMCA (Plasma Membrane Ca^{2+} ATPase) pumps. Stimulation of the cell then causes the opening of calcium channels in both the plasma membrane and the endoplasmic reticulum, thus allowing the entry of Ca^{2+} back into the cytosol. This influx of Ca^{2+} is typically mediated by one of two pathways depending on the cell type. Excitable cells, such as neurons and muscle cells, express specialised voltage sensitive calcium channels, which mediate a massive increase in cytosolic Ca^{2+} levels. However, most cells are termed "non-excitable", and stimuli cause smaller bursts of elevated $[Ca^{2+}]_i$.

In "non-excitable cells", the calcium flux is predominantly induced by another second messenger, inositol (1,4,5)-triphosphate ($InsP_3$). The ligation of G protein-coupled receptors activates phospholipase Cβ (PLCβ), which cleaves phosphatidylinositol (4,5)-bisphosphate into $InsP_3$ and diacylglycerol. Alternatively, ligand induced autophosphorylation of many tyrosine kinase receptors causes the

translocation of phospholipase Cγ (PLCγ) to the plasma membrane. This similarly results in the production of $InsP_3$ and diacylglycerol. The $InsP_3$ receptor in the membrane of endoplasmic reticulum is a calcium channel, which opens on ligation of the second messenger allowing Ca^{2+} to enter the cytosol. Depletion of calcium ions from this intracellular store stimulates the entry of Ca^{2+} through channels in the plasma membrane. The mechanisms by which this "capacitative entry" is triggered are poorly defined, but it is potentiated by hyperpolarisation caused by opening potassium channels. Capacitative entry produces a more sustained elevation of $[Ca^{2+}]_i$. These elevated levels of $[Ca^{2+}]_i$ are only transient, because the Ca^{2+} is quickly pumped out of the cytosol. This combined with the slow diffusion rate of Ca^{2+} within non-excitable cells means the cellular signal can be very quick and localised.

1.1.b Calcium Binding Proteins

The signal of elevated $[Ca^{2+}]_i$ is transduced by calcium binding proteins (reviewed by (Heizmann and Hunziker, 1991; Ikura, 1996)). Ca^{2+}-binding proteins typically ligate the divalent cation through 6 co-ordinating oxygen atoms of glutamatic or aspartic acid side chains. The most common Ca^{2+}-binding motif is the EF-hand, which characteristically consists of two perpendicular α-helices separated by a 12-residue loop. The sequence of the loop determines the affinity for Ca^{2+}, because it contains the chelating residues. EF-hand motifs usually exist in pairs, with the Ca^{2+}-binding loop regions forming a short anti-parallel β-sheet.

Intracellular calcium-binding proteins can typically be placed into three functional groups: Ca^{2+}-buffering proteins; Ca^{2+}-regulated proteins; and Ca^{2+}-sensor proteins. Ca^{2+}-buffering proteins (e.g. parvalbumin and calbindin D_{28K}) buffer and/or transport Ca^{2+}, and, as such, usually do not undergo a conformational change upon binding Ca^{2+}. In the endoplasmic reticulum these proteins, like calsequestrin, buffer the high concentrations of calcium ions. In the cytosol Ca^{2+}-buffering proteins

control the distribution of Ca^{2+} signals, for example when immobilised these proteins greatly reduce the diffusion of Ca^{2+}, thereby localising the signal.

Ca^{2+}-regulated proteins are effector proteins (e.g. enzymes) directly modulated by binding calcium. These proteins differ in structure from the buffering molecules. Typically, these proteins have an affinity for Ca^{2+} such that the divalent cation is not bound at the low concentration in resting cells, but on elevation it binds to the protein. The proteins usually undergo a Ca^{2+}-induced change in conformation, thereby regulating the function of the protein. For example, the thiol protease m-calpain has an absolute requirement for Ca^{2+} for proteolysis, because ligation of Ca^{2+} by the EF-hands of the regulatory domain causes a conformational change. This is transduced through the molecule re-orientating the catalytic domain, such that the catalytic residues (the catalytic triad) are brought together in the active site (Hosfield et al., 1999).

Ca^{2+}-sensor proteins differ from Ca^{2+}-regulated proteins, because they are not effector molecules. Rather, they modulate the function of one or more effector proteins. Like Ca^{2+}-regulated proteins, these proteins typically bind Ca^{2+} only when Ca^{2+} levels are elevated and undergo a conformational change. The prototype Ca^{2+}-sensor protein is the ubiquitously expressed calmodulin (CaM), which modulates a diverse range of proteins (reviewed by (Chin and Means, 2000)). CaM has two globular domains each containing two EF-hands joined by a short linker. At low concentrations of Ca^{2+}, CaM is Ca^{2+} free (apo), and adopts the closed conformation. Upon elevation of Ca^{2+} levels the EF-hands ligate the divalent cation, which induces a dramatic change to the open conformation. This change in conformation reveals a predominantly hydrophobic and acidic crevice, which is the binding site for Ca^{2+}-dependent targets.

1.2 The S100 Family of Ca^{2+} Binding Proteins

S100 proteins are a family of low molecular weight acidic calcium binding proteins. The nomenclature S100 comes from the solubility of the proteins in saturated ammonium sulphate, which was originally a defining characteristic. Now the family is defined by protein structure (see Section 1.2.a), and comprises 16 known members. During the elucidation of the family and its members, several different nomenclatures have been used. Here I have used the currently favoured nomenclature defined by Schäfer et al. (Schafer et al., 1995), with the exception of MRP-8 (S100A8) and MRP-14 (S100A9). Additional family members are named as in (Donato, 1999).

1.2.a S100 Protein Structure

S100 proteins are characteristically small proteins of 9-14 kDa, with a highly conserved protein structure containing two EF-hand motifs (see Fig 1.1A and reviewed by (Kligman and Hilt, 1988; Zimmer et al., 1995)). The C-terminal EF-hand has a classical structure, as it comprises two α-helices separated by a twelve amino acid Ca^{2+}-binding loop. Six residues in the loop chelate the calcium ion, predominantly through side chain oxygen atoms. However, the N-terminal hand has an unusually long Ca^{2+}-binding loop, which is unique to S100 proteins. The loop is comprised of 14 residues of which only five interact with Ca^{2+}. The S100 proteins share significant sequence homology, with the C-terminal extension (the sequence C-terminal to the classical EF-hand) and "hinge region" (the sequence separating the EF-hands) being most divergent.

Profilaggrin, trychohyalin and repetin comprise a distinct group of S100-like proteins (reviewed by (Schafer and Heizmann, 1996) and (Zimmer et al., 1995)). Each has a N-terminal domain, which has considerable homology with the S100 proteins. These proteins also have additional domains, and may be formed as a result of gene fusion.

A) S100 Protein Structure

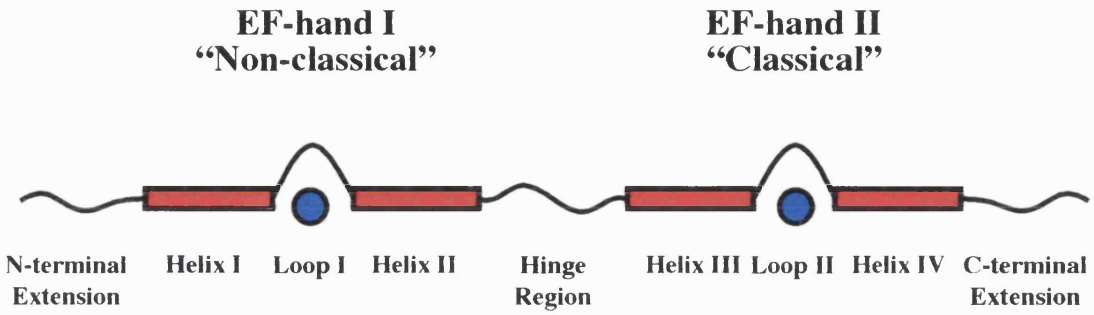

B) S100 Gene Structure

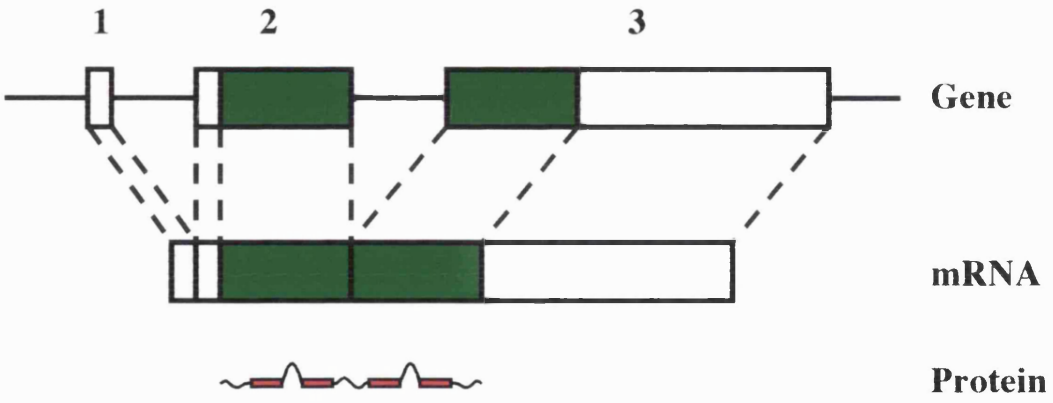

Figure 1.1: The Structure of a Typical S100 Protein and S100 Gene

A) A diagrammatic representation of a typical S100 protein. The α-helices of the EF-hands are denoted with a red box. The areas of little or no secondary structure are represented by a single line. The helix-loop-helix structure of the EF-hands can be seen, with loops I and II interchelating a calcium ion (blue circle).

B) A schematic representation of a typical S100 gene. The white boxes denote untranslated sequences, and the green boxes translated sequences. The characteristic 3 exon structure is shown, where exon 2 encodes for the N-terminal EF-hand and exon 3 the C-terminal EF-hand.

Unusually for EF-hand containing proteins, the S100 proteins typically exist either as a non-covalently linked homodimer, or less frequently as a heterodimer (reviewed by (Donato, 1999)). For example, S100B exists primarily as a homodimer, but can also form heterodimers with S100A1 (Isobe et al., 1981) and S100A6 (Yang et al., 1999). The major exception is calbindin D_{9k}, which does not oligomerise. However, calbindin D_{9k} shares only 25% homology with other S100 proteins, and has unusually short terminal extensions and "hinge region".

All the S100 proteins have been shown to bind Ca^{2+}, with the exception of S100A10. A detailed account is given in (Heizmann and Cox, 1998; Schafer and Heizmann, 1996; Zimmer et al., 1995). Typically, the classical C-terminal EF-hand binds Ca^{2+} with a higher affinity than the non-classical motif. For example, in vitro the classical EF-hand of S100B binds Ca^{2+} with a Kd = 10-50μM, and the non-classical motif with a Kd = 200-500μM (Baudier and Cole, 1989). Additionally, several S100 protein (S100A2, S100A3, S100A5, S100A6, S100A7, S100A12, S100B and MRP-14) have been shown to bind ionic zinc (reviewed by (Heizmann and Cox, 1998; Schafer and Heizmann, 1996)). In the case of both S100A1 and S100B the binding of Zn^{2+} has been shown to increase the affinity of the protein for Ca^{2+} (Baudier et al., 1986).

Within the last 5 years the Ca^{2+}-free (apo) structures of S100A6 (Potts et al., 1995), bovine S100B (see Fig 1.2; (Kilby et al., 1996)) and rat S100B (Drohat et al., 1996), have been solved. All three structures were of homodimers, with each monomer containing the two predicted helix-loop-helix EF-hand motifs. The loop regions of the two EF-hands from the same monomer form a short β-sheet, as observed in several EF-hand structures. Overall the arrangement of the helices was very similar. The only major difference was that the "hinge region" of bovine S100B and S100A6 contained a short α-helix (designated helix IIa), which was almost continuous with helix II. The angle of helix III also differed slightly between the structures. The interface between the monomers is formed largely by helices I and IV, with helix IV running almost antiparallel to the same helix of the complexing

monomer. The interactions between the monomers appear to be maintained predominantly by hydrophobic bonds.

More recently, the structure of several Ca^{2+}-bound (Ca^{2+}-) S100 proteins have been solved, specifically: rat (Drohat et al., 1998), bovine (see Fig 1.2; (Matsumura et al., 1998)) and human S100B (Smith and Shaw, 1998a); S100A6 (Sastry et al., 1998); S100A7 (Brodersen et al., 1999); MRP-8 (Ishikawa et al., 2000); and S100A11 (Rety et al., 2000). When the structures of the Ca^{2+}-S100B molecules were compared to those of apo-S100B (see Fig 1.2 and (Drohat et al., 1998; Matsumura et al., 1998; Smith and Shaw, 1998a; Smith and Shaw, 1998b)), there were many similarities. The secondary structure and the interface between the monomers were virtually unaltered. In fact, helices I, II and IV were nearly superimposable. However, helix III had undergone a major reorientation compared to the other helices. Upon binding calcium, helix III pivots to lie almost perpendicular to helix IV, as opposed to being nearly parallel to helix IV in the apo-structures. Consequently, the loop of the classical Ca^{2+}-binding site tilts inwards, and the N-terminus of helix III and the "hinge region" swing out, away from the compact interior. This effectively exposes many hydrophobic residues of the "hinge region" and C-terminus, with several acidic residues also becoming more solvent accessible (see Fig 1.2B and (Matsumura et al., 1998; Smith and Shaw, 1998a; Smith and Shaw, 1998b)). This has been termed the "open" conformation.

The situation changes dramatically with calbindin D_{9k}, an unusual monomeric S100 protein with shortened "hinge region" and terminal extensions. Ca^{2+}-binding by this unusual S100 protein does not induce major structural changes. Comparing the structures of apo- and Ca^{2+}-Calbindin D_{9k} demonstrated no large reorientation of helix III and no significant change in surface hydrophobicity. Both structures most closely resembled the apo-S100B proteins (Matsumura et al., 1998; Skelton et al., 1994; Smith and Shaw, 1998b). The structure of Ca^{2+}-S100A6 also did not differ greatly from that of the apo-S100A6, suggesting that this protein does not undergo a gross conformational change on binding Ca^{2+} (Potts et al., 1995; Sastry et al., 1998).

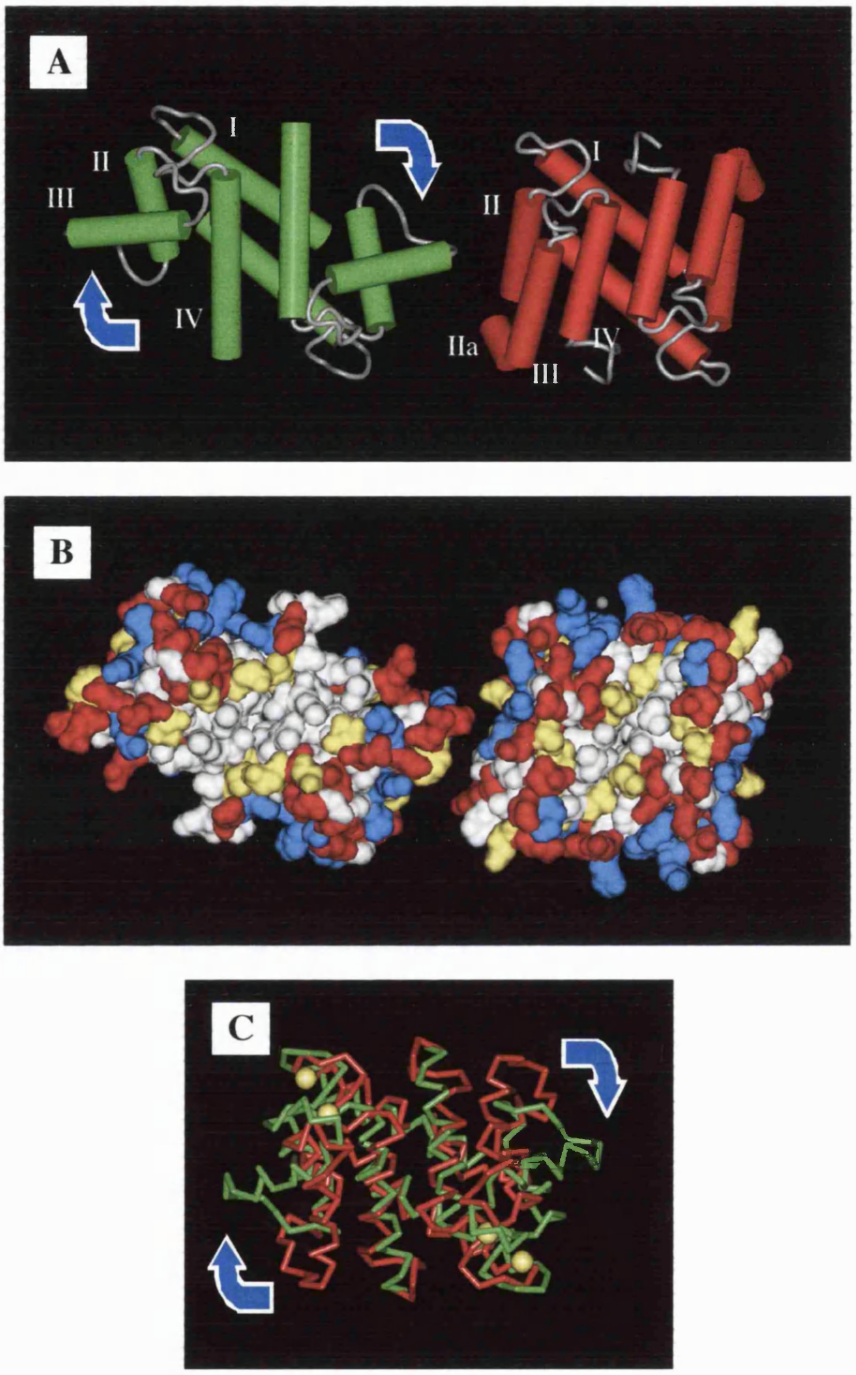

Figure 1.2: The Ca^{2+}-Induced Conformational Change in Bovine S100B
A) Three dimensional representation of bovine S100B in the Ca^{2+}-bound (green) and Ca^{2+}-free (red) conformations. The helix numbers for one monomer are shown in white. **B**) A space fill model of **A** showing hydrophobic residues in white, negatively charged residues in red, positively charged residues in blue and polar residues in yellow. **C**) An overlay of Cα traces of the two conformations of bovine S100B, coloured as in **A** with Ca^{2+} ions in yellow. The blue arrows denote the Ca^{2+}-induced movement of helix III. All structures were drawn by P. Bates (ICRF) using the following co-ordinates: Ca^{2+}-S100B (Matsumura et al., 1998), PDB accession code 1MHO; and Ca^{2+}-free S100B (Kilby et al., 1996), PDB accession code 1CFP.

The structure of MRP-8 has only been solved in the Ca^{2+}-bound form. It is a non-covalently linked homodimer, with a structure similar to Ca^{2+}-S100B (Ishikawa et al., 2000). MRP-8 also has a large hydrophobic pocket. Similarly, the backbone of Ca^{2+}-bound S100A11 was most closely related to Ca^{2+}-S100B (Rety et al., 2000). The EF-hands of S100A10 have either deletions or substitutions, which prevent the binding of Ca^{2+}. As expected, the S100A10 structure lacked Ca^{2+} (Rety et al., 1999), but adopted a "open" conformation most closely related to the Ca^{2+}-bound structures of S100B and S100A11.

The Ca^{2+}-bound structure of S100A7 has been solved in the presence and absence of Zn^{2+} (Brodersen et al., 1999). The Zn^{2+}-free structure differs from the other S100 proteins because the loop of the N-terminal EF-hand is shortened and lacks a crucial Ca^{2+}-binding residue. Thus each S100A7 monomer bound only one Ca^{2+} ion in the C-terminal EF-hand. The homodimer also bound two zinc ions, with each Zn^{2+} being ligated by residues His86 and His90 of one monomer, as well as His17 and Asp24 of the other S100A7 molecule. Residues 86 and 90 are just C-terminal to helix IV, and the other two amino acids are within the loop of the variant EF-hand. Interestingly, the Zn^{2+}-chelating residues lie next to the hydrophobic pocket. The ligation of Zn^{2+} contracted the local area, including the hydrophobic pocket, and opened the structure on the opposing face. It is believed the binding of Zn^{2+} would stabilise the dimer.

The Zn^{2+}-binding residues of S100A7 are only conserved in S100A12 and MRP-14 and partially in S100B, yet S100A2 (Franz et al., 1998), S100A3 (Fritz et al., 1998), S100A5 (Schafer et al., 2000) and S100A6 (Filipek et al., 1990) also bind zinc ions. Additionally, a study indicates S100A3 ligates Zn^{2+} via the thiol groups of cysteines in the C-terminal extension (Fritz et al., 1998). The Zn^{2+} binding residues are also not consistent with the three cysteine residues of S100A2 proposed to ligate zinc ions (Stradal et al., 2000). Therefore, it seems unlikely that the zinc ion binding by S100A7 is universally applicable.

1.2.b Gene Structure and Genome localisation

The gene structure of S100 proteins, like the protein structure, is highly conserved (see Fig 1.1B and (Zimmer et al., 1995)). The intron and exon organisation is identical for all S100 proteins, except S100A5. Characteristically each gene is composed of three exons and two introns. The first exon is not translated in any of the genes. Exon 2 encodes the N-terminal EF-hand, whilst exon 3 codes for the C-terminal EF-hand and 3' untranslated region. The S100A5 gene has 4 exons. Exon 1 remains untranslated. Exon 2 encodes the remaining 5' untranslated sequence, and 13 of the 18 residues of the unusually long N-terminal extension that is particular to S100A5. Exons 3 and 4 are equivalent to exons 2 and 3 of other S100 genes (Engelkamp et al., 1993). The region of the genes encoding the S100-like fragment of profilaggrin and trychohyalin are organised similarly to the S100 genes (see (Zimmer et al., 1996)).

The cDNA sequences are highly conserved, especially between species. Typically, mammalian S100 genes have greater than 75% identity between species, with *Xenopus* genes showing more than 50% identity with the mammalian equivalent. The introns vary greatly in sequence, but, interestingly, the length of the first intron is often conserved between species. The cDNA encoding the different human S100 proteins have an average identity of 47%, with a range of 61-37% (Zimmer et al., 1996).

Where sufficient genomic sequence is available, the S100 genes have a conserved sequence within 300bp of the TATA box. This S100 protein element also exists in S100A1, which does not have a TATA box. However, the current evidence suggests this motif is not just restricted to S100 genes (Engelkamp et al., 1993).

S100A1-A7, MRP-8 (S100A8), MRP-14 (S100A9), S100A12 and S100A13 genes are clustered within about 300kb on human chromosome 1q21 (Engelkamp et al., 1993; Schafer et al., 1995; Wicki et al., 1996). Supergroups exist within this cluster, as a 15kb section encodes the genes for S100A3, S100A4, S100A5 and S100A6 (Engelkamp et al., 1993). MRP-8, S100A12 and MRP-14 are also very

closely linked (Wicki et al., 1996). About 1.5Mb 3' to this cluster, and separated by the epidermal gene cluster, are the genes encoding for S100A10 and S100A11 (Schafer et al., 1995; Wicki et al., 1996). Additionally, the genes for profilaggrin and trychohyalin are located within the epidermal gene cluster (Schafer et al., 1995). Consequently, chromosome 1q21 contains many densely packed genes, including at least 15 encoding for S100 or S100-like proteins. The genes for the other S100 proteins that have been localised are not on chromosome 1.

The murine genes encoding S100A1, MRP-8, MRP-14, S100A13, S100A6, S100A3, S100A4 and S100A5 are clustered on chromosome 3. The genes for murine S100A6, S100A3, S100A4 and S100A5 are located within 35kb and the genes for MRP-8 and MRP-14 also form a supergroup (Ridinger et al., 1998). Therefore it would appear the clustering is largely conserved in the mouse. The functional significance of this clustering is currently unknown, as the genes do not seem to be co-regulated. It is possible that the members of the supergroups may be co-regulated at least in some situations. This is most evident with MRP-8, MRP-14 and S100A12 (see section 1.3.c and Chapter 3).

1.2.c Expression of S100 proteins

All S100 proteins are expressed in a tissue-specific and cell type-specific pattern (reviewed by (Schafer and Heizmann, 1996) and (McNutt, 1998)), and none are found ubiquitously expressed like calmodulin. Some S100 proteins are expressed by several cell types, for example S100A1 has been detected in neurons, skeletal and heart muscles and the kidney. However, some are very specifically localised, e.g. S100P is found only in the placenta. Additionally, the level of S100 proteins in a particular cell type is often regulated in differentiation. S100 proteins also have been shown to be inducibly expressed, for example intestinal expression of calbindin D_{9k} is stimulated by vitamin D. The levels of S100A4 and S100A6 are regulated in cell

cycle progression (reviewed by (Kligman and Hilt, 1988)). S100A6 is maximally expressed at entry into G_1, and S100A4 in S phase.

S100A2, S100A7, S100A12, S100B, MRP-8 and MRP-14 have been ascribed extracellular functions (see (Donato, 1999) and Sections 1.3.d and 1.4.b), but S100 proteins do not have a hydrophobic leader sequence and have not been localised within vesicles. Despite this, S100A2, S100A4, S100A7, S100B, MRP-8 and MRP-14 have all been shown to be secreted by cultured cells, and the latter three have been found in extracellular fluid (reviewed by (Donato, 1999)). Currently, the mechanism of release is not understood. The secretion of MRP-8 and MRP-14 is reportedly sensitive to microtubule-depolymerising agents, but not inhibitors of vesicular traffic through the endoplasmic reticulum ((Rammes et al., 1997) and see Section 1.3.c.iv).

The cell type specific expression of S100 proteins has allowed for their association with many disease states. S100A2, S100A4, S100A6 and S100B have all been linked with neoplastic disease. Interestingly, S100A4 and A6 are upregulated in ovarian, breast, colon and thyroid cancer, but S100A2 is downregulated in skin, lung, kidney and prostrate cancer (Ilg et al., 1996a). S100B has also been associated with Down's syndrome and Alzheimer's disease (Griffin et al., 1989). The gene encoding S100B is located on chromosome 21 (Duncan et al., 1989), which explains the link with Down's syndrome. MRP-8 and MRP-14 are elevated in inflammation (see Section 1.4.b). S100A7 was first isolated, because it is over-expressed by keratinocytes of psoriatic skin (Madsen et al., 1991).

1.2.d The General Functions of S100 Proteins

Generally, the functions of S100 proteins are poorly defined. No S100 protein has been assigned an enzymatic activity, and, for the main part, these proteins have been proposed to function as transducers and modulators of a Ca^{2+} signal.

Further, the tissue specific expression of the S100 proteins implies that they mediate cell type specific responses to the ubiquitous second messenger Ca^{2+}.

1.2.d.i S100 proteins Can Act as Ca^{2+}-Sensors

Ca^{2+}-sensory proteins alter the activity of effector molecules in a calcium dependent manner (see Section 1.1.b). This is frequently achieved by Ca^{2+}-dependent binding to the effector molecule, which then leads to the change in activity. The majority of interactions between S100 proteins and target molecules are Ca^{2+}-dependent, with characteristically two molecules of the target protein binding to a S100 homodimer. This is typified by the Ca^{2+} induced binding of S100B to the regulatory domain of p53 (Baudier et al., 1992). S100B undergoes a Ca^{2+} induced conformational change, which reveals a hydrophobic and acidic crevice made by the "hinge region" and the helices of the classical EF-hand of each monomer (see Section 1.2.a and Fig 1.2). Biophysical data indicates that a similar increase in hydrophobicity occurs when many other S100 proteins bind calcium (reviewed by (Donato, 1999)). This S100 crevice is similar to the Ca^{2+}-dependent binding site of calmodulin, the prototype Ca^{2+}-sensory protein (Chin and Means, 2000). The structure of S100B complexed with a peptide of p53 (residues 367-388) has been solved (Rustandi et al., 2000). The peptide, as predicted, bound to the hydrophobic pocket, with most of the interacting residues being hidden in the Ca^{2+}-free conformation of S100B.

To act as a Ca^{2+}-sensor this Ca^{2+}-dependent binding must modulate the activity of the effector molecule, thereby transducing the Ca^{2+} signal. The Ca^{2+}-induced S100 protein binding to a target protein has been shown to modulate the function of the target by a number of different mechanisms. Below I have outlined the most common mechanisms by which this occurs. Firstly, S100 proteins can directly interact with and activate an enzyme, for example Ca^{2+}-S100B binds to and activates Ndr protein kinase (Millward et al., 1998). Secondly, S100 proteins can

inhibit cytoskeleton assembly by binding to cytoskeletal components and blocking their association. This is typified by S100B and S100A1 sequestering of the intermediate filament subunits, glial fibrillary acidic protein (GFAP) and desmin (Garbuglia et al., 1999). Thirdly, S100 proteins have been shown to bind to modulator proteins, thereby affecting the function of a third protein. An example of this is S100A6 interacting with caldesmon, removing its inhibition of actomyosin ATPase (Mani et al., 1992). Fourthly, S100 proteins frequently bind to a potential phosphorylation site on a target protein, thus preventing the phosphorylation of a specific protein without inhibiting the kinase responsible. Possibly the best-studied example of this mechanism is S100B binding to the regulatory subunit of p53, which prevents the phosphorylation by protein kinase C (PKC) (Baudier et al., 1992). Finally, S100A1 and S100B are also able to block the interaction of specific basic helix-loop-helix (bHLH) transcription factors with DNA (Baudier et al., 1995; Onions et al., 1997).

Interestingly, the targets of S100 proteins appear to be very diverse. One exception is the annexin family of phospholipid and membrane binding proteins, as five S100 proteins have been shown to bind to one or more members of this family (reviewed by (Donato, 1999)). The structure of two S100 proteins bound to analogous annexin peptides have been solved. The binding of S100A10 to annexin II is independent of calcium, because S100A10 does not bind Ca^{2+}. Rather, S100A10 is permanently in the "open" conformation. The crystal structure of S100A10 complexed with a peptide from annexin II shows that the binding site is similar to that of the p53 peptide site on S100B, but that the interacting residues are different (Rety et al., 1999). S100A11 binds to annexin I by a Ca^{2+}-dependent mechanism (Mailliard et al., 1996). The structure of S100A11 with an annexin I peptide shows that the binding site is very similar to that on S100A10, and that the interaction involves some of the same residues (Rety et al., 2000).

1.2.d.ii S100 Proteins Can Act as Ca^{2+}-Buffering Proteins

The monomeric S100 protein calbindin D_{9k} does not appear to act as a Ca^{2+}-sensor. Calbindin D_{9k} does not undergo a gross conformational change on Ca^{2+}-binding (Skelton et al., 1994), and has not been shown to interact with target proteins. Thus, it is proposed that calbindin D_{9k} acts as a calcium buffering protein (see Section 1.1.b). Therefore, S100 proteins are able to modulate a Ca^{2+} signal, as well as to transduce it.

1.2.d.iii Some Specific Functions of S100 Proteins

The S100 proteins are proposed to be specific transducers and modulators of a Ca^{2+} signal. However, some have been shown to have additional Ca^{2+}-independent roles, and extracellular functions. The most clearly elucidated Ca^{2+}-dependent and -independent functions of S100 proteins are summarised below, with the exception of MRP-8 and MRP-14 (see Sections 1.3.d and 1.4.b) and S100A12 (see Section 3.1).

1.2.d.iii.1 S100B

S100B is primarily expressed in the brain, and has been shown to bind 24 proteins in a Ca^{2+}-dependent fashion (reviewed by (Zimmer et al., 1995) and (Donato, 1999)). In many situations S100B is proposed to block phosphorylation sites. This S100 protein inhibits assembly of type III intermediate filaments and microtubules, and stimulates the actomyosin ATPase by interacting with the inhibitory proteins, caldesmon and calponin. Therefore, S100B may be a major regulator of the cytoskeleton. S100B also regulates energy metabolism by activating and inhibiting enzymes. S100B modulates cell signalling by interacting with kinases as well as adenylate and guanylate cyclases.

Extracellular homodimeric S100B promotes neurite extension, via induction of an increase in $[Ca^{2+}]_i$ (Barger et al., 1992). This neurotropic effect only occurs at low concentrations, as higher concentrations of the homodimer can induce apoptosis (Fulle et al., 1997). S100B can also stimulate the expression of β-amyloid precursor protein in neuronal cultures (Li et al., 1998). Therefore, the elevated level of S100B in Down's syndrome and Alzheimer's disease may contribute to the neuropathology of these diseases. Currently, no receptor for S100B has been identified.

1.2.d.iii.2 S100A1

The target proteins of S100B and S100A1 are very similar, which is reflected in their high homology of 60% (see (Donato, 1999)). The only known S100A1 specific role is the direct regulation of Ca^{2+} homeostasis by increasing the affinity of the Ca^{2+} release channel, ryanodine receptor, for its ligand (Treves et al., 1997). S100A1 has not been ascribed an extracellular function or been associated with any pathologies.

1.2.d.iii.3 S100A4

S100A4 is highly expressed in the cells of kidneys, salivary glands, stomach and intestine, that are involved in ion transport. S100A4 has also been detected in neurons, smooth muscle cells and some leukocytes. The expression and putative functions have recently been reviewed in (Barraclough, 1998). S100A4 was first identified because it is associated with increased proliferation, morphological changes and metastatic potential in cultured cells. This S100 protein has also been linked to metastasis/malignancy in human tumour biopsies. Transfection of benign cell lines with S100A4 induced metastatic activity in vivo (Davies et al., 1993), and similar results were obtained with a transgenic model (Davies et al., 1996). Therefore, S100A4 appears to have a role in metastasis.

Unfortunately the mechanism by which S100A4 induces a metastatic phenotype is unknown, but an increase in motility and altered morphology has been proposed. S100A4 has been shown to interact with F-actin, tropomyosin and myosin. The interaction with myosin prevents phosphorylation by PKC, and also inhibits its ATPase activity (see (Barraclough, 1998)).

1.2.d.iii.4 S100A6

S100A6 is primarily expressed in fibroblasts and epithelial cells (Kuznicki et al., 1992), and is upregulated by growth factors (Calabretta et al., 1986). S100A6 is also over-expressed in many tumours (Ilg et al., 1996a). Again the function of S100A6 has not been defined, but some characteristics have been elucidated. Ca^{2+} induces S100A6 to bind cytoskeletal associated proteins, such as tropomyosin (Golitsina et al., 1996) and caldesmon (Mani and Kay, 1995), annexins XI-A (Sudo and Hidaka, 1999), II and VI (Zeng et al., 1993), as well as glyceraldehyde-3-phosphate dehydrogenase (Zeng et al., 1993). Interestingly, S100A6 also associates with plasma and nuclear membranes in a Ca^{2+}-dependent manner, but is localised to the cytoplasm during cell division (Stradal and Gimona, 1999).

1.2.d.iii.5 S100A10

S100A10, the only S100 protein that does not bind Ca^{2+}, interacts with and inhibits cytosolic phospholipase A_2 (PLA_2) (Wu et al., 1997). However, S100A10 is most well characterised as a regulator of annexin II, with which it forms a heterotetrameric complex (annexin II_2-$S100A10_2$). Annexin II_2-$S100A10_2$ binds to glial fibrillary acidic protein (GFAP), and stimulates assembly of the type III intermediate filaments. Interestingly, this appears to oppose the effect of S100B, which binds to GFAP at a different site (Bianchi et al., 1995; Garbuglia et al., 1995). The heterotetramer also shows Ca^{2+}-dependent binding to and bundling of F-actin (Ikebuchi and Waisman, 1990). The heterotetramer is also strongly implicated in

Ca^{2+}-triggered exocytosis by adrenal chromaffin cells (reviewed by (Burgoyne et al., 1991)). Specifically, annexin II_2-$S100A10_2$ contributes to Ca^{2+}-induced membrane localisation of vesicles as well as Ca^{2+}-triggered granule fusion and aggregation. There is also evidence that the heterotetramer can link F-actin to the membrane (reviewed in (Gerke and Moss, 1997)). Thus, it has been hypothesised that this annexin/S100 complex is involved in linking the cytoskeleton with cell membranes, vesicles and other cellular components.

1.2.d.iii.6 S100A11

S100A11 binds to F-actin (Sakaguchi et al., 2000), and inhibits actin-activated myosin Mg^{2+}-ATPase (Zhao et al., 2000) in a Ca^{2+}-dependent manner. Interestingly, in fibroblasts S100A11 is predominantly associated with actin filaments of leading edge pseudopodia, and overexpression of the protein leads to increased pseudopodia formation (Sakaguchi et al., 2000). S100A11 associates with annexin I, and the heterotetramer (annexin I_2-$S100A11_2$) may contribute to the formation of the cornified envelope in epidermal keratinocytes (reviewed by (Donato, 1999)). Upon confluency, cytoplasmic S100A11 in fibroblasts is phosphorylated, which results in translocation to the nucleus. This has been associated with contact inhibition, and does not occur in immortalised cells (Sakaguchi et al., 2000).

1.3 The MRP Proteins

Migration inhibitory factor-related protein (MRP) –8 and –14 are two highly homologous S100 proteins designated S100A8 and S100A9, respectively (Schafer et al., 1995). MRP-8 is a 10.8kDa protein, and has also been named p8, L1 light chain, calgranulin A and cystic fibrosis antigen (CFA). MRP-14 is the largest known S100 protein with a molecular weight of 13.6kDa. Previous nomenclature for MRP-14

includes p14, L1 heavy chain and calgranulin B. The MRP proteins are known to form a heterodimer (Edgeworth et al., 1991), which has been named calprotectin. The 8 and 14 refers to the molecular weights of the molecules as determined by SDS PAGE.

1.3.a Protein Structure

Both MRP-8 and -14 have a protein structure characteristic of S100 proteins, with a N-terminal "non-classical" EF-hand and C-terminal "classical" EF-hand. MRP-14 is unusually large for an S100 protein, because it has an elongated C-terminal extension (reviewed by (Kerkhoff et al., 1998) and see Fig 1.3). The proteins have largely been studied in mouse and human systems. Both the MRP proteins share about 59% identity between the mouse and human, which is more divergent than interspecies comparisons of other S100 proteins (Lagasse and Weissman, 1992). This may explain some of the discrepancies observed between the two species that are discussed below.

1.3.a.i MRP-8

The crystal structure of Ca^{2+} bound MRP-8 shows a homodimer, with a fold typical of S100 proteins. This Ca^{2+}-MRP-8 had a large exposed hydrophobic cleft similar to the target protein-binding site of Ca^{2+}-S100B. It was thought the C-terminal EF-hand of MRP-8 may not bind Ca^{2+}, because a highly conserved glutamic acid residue in the unusual Ca^{2+} binding loop is substituted for an aspartic acid. Interestingly, a water molecule bridges this aspartic acid residue with the Ca^{2+}, whereas in other S100 proteins (except S100A7 and S100A10) the Ca^{2+} ion is directly chelated by the glutamic acid (Ishikawa et al., 2000).

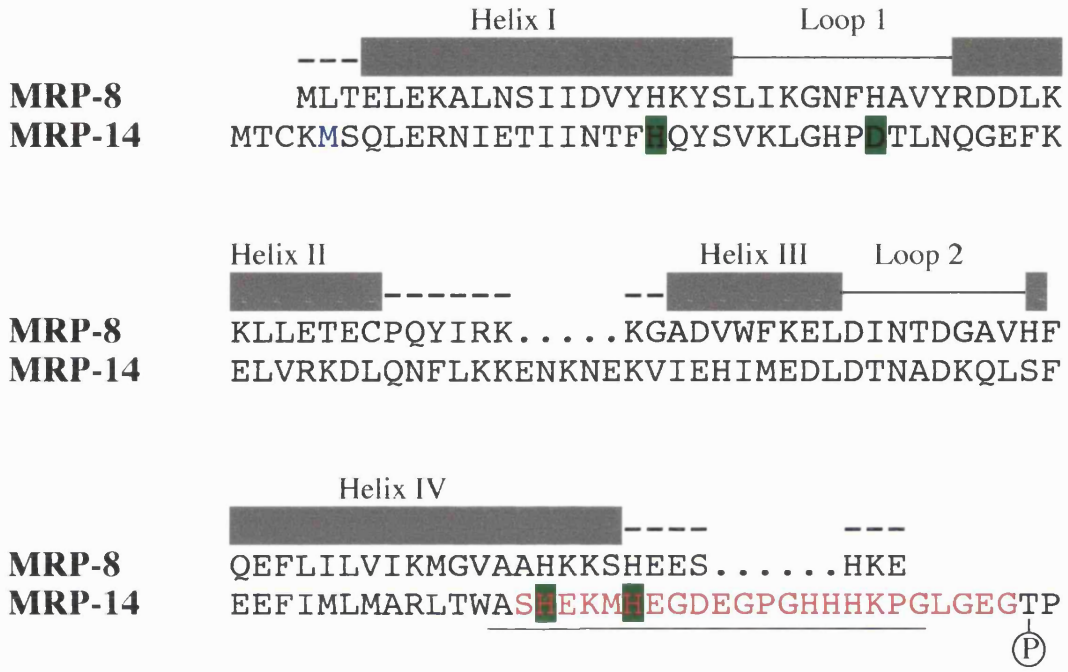

Figure 1.3: The Sequence of MRP-8 and -14
The amino acid sequence of human MRP-8 and -14 aligned by BLOSUM 30. The secondary structure of MRP-8 is shown above, as determined from the crystal structure of the homodimer (Ishikawa et al., 2000). The alternative start site of MRP-14, Met 5, is shown in blue. The zinc binding residues of S100A7 that are conserved in MRP-14 are highlighted in green. The MRP-14 residues that are identical to the first 20 amino acids of NIF-1 are underlined. The sequences homologous to those in domain 5 of high molecular weight kininogen are in red. The phosphorylation site on MRP-14, Thr 113, is also indicated.

1.3.a.ii MRP-14

Human MRP-14 is the only S100 protein known to exist as two isoforms. Both isoforms are synthesised simultaneously from a single mRNA species, as it has two alternative start sites. One isoform lacks the first four residues, which include the only cysteine residue in human MRP-14 (van den Bos et al., 1996). No differences in expression, localisation or function of the isoforms have been reported.

Both human and mouse MRP-14 have been shown to bind Zn^{2+} independently of Ca^{2+} (Raftery et al., 1996). MRP-14 of both species have the four residues of S100A7 shown to chelate Zn^{2+} (Brodersen et al., 1999). This includes the His.X.X.X.His motif, located in the C-terminal extension, that is often found in Zn^{2+}-binding proteins. Human MRP-14 has only one such motif at a similar location to S100A7, near to helix IV. Mouse MRP-14 has an additional His.X.X.X.His motif towards the end of the C-terminal extension, and deletion of this appears to greatly diminish Zn^{2+}-binding (Raftery et al., 1999). So the precise Zn^{2+}-binding site still awaits clarification.

Twenty amino acids (89-108) of the elongated C-terminal extension of human MRP-14 show complete identity with the first twenty residues of neutrophil immobilising factor (NIF) –1 (Freemont et al., 1989). NIF-1 inhibits the random migration and chemotaxis of neutrophils by an unknown mechanism (Watt et al., 1983). This extension of MRP-14, specifically residues 90-112, also has significant homology to the HG and HGK regions of the plasma glycoprotein high molecular weight kininogen (HMWK) (Hessian et al., 1995). These regions of HMWK are in domain 5, which forms part of the light chain on cleavage. Domain 5 of HMWK has been implicated in the binding of surfaces that initiate the contact activation of the intrinsic coagulation/kinin-forming cascade (see (Kaplan et al., 1997)). Domain 5 also, at least in part, mediates binding to endothelial cells via interactions with cytokeratin-1 (Hasan et al., 1998), gC1qR (Joseph et al., 1996) and heparan sulphate proteoglycans (Renne et al., 2000).

A small proportion of human MRP-14 in resting neutrophils and monocytes is phosphorylated on the penultimate residue, threonine 113 (Edgeworth et al., 1989). The proportion of MRP-14 phosphorylated increases significantly upon treating the cells with a calcium ionophore or calcium dependent activators, such as fMLP (Edgeworth et al., 1989; Guignard et al., 1996). The kinase responsible for this is unknown, but believed not to be protein kinase C (PKC) as phorbol esters do not induce phosphorylation of MRP-14 (Edgeworth et al., 1989). Interestingly, this amino acid is not conserved in murine MRP-14.

1.3.a.iii Complexes of the MRP Proteins

MRP-8 and –14 primarily exist as a heterodimer, which forms independently of calcium (Edgeworth et al., 1991). The binding of Ca^{2+} and Zn^{2+} by the heterodimer induce a conformational change. In particular, Ca^{2+} causes the exposure of several hydrophobic residues (Kerkhoff et al., 1999a), which is reminiscent of the creation of a hydrophobic crevice on S100B. The binding of Zn^{2+} by the Ca^{2+}-bound complex limits the solvent accessibility of these exposed hydrophobic residues (Kerkhoff et al., 1999a), which is consistent with the Zn^{2+} induced contraction of the hydrophobic pocket observed in S100A7 (Brodersen et al., 1999). Ca^{2+} also results in the formation of higher complexes, namely MRP-8_2-MRP-14 and MRP-8_2-MRP-14_2 (Teigelkamp et al., 1991). Interestingly, both MRP-8 and MRP-14 can form homodimers, but these do not pack as tightly as the heterodimer (Hunter and Chazin, 1998). This is thought to explain why the MRP proteins preferentially form the heterodimer in vitro and in vivo.

1.3.b Gene structure and Genome localisation

The human genes for MRP-8 and MRP-14 have a three exon structure typical of S100 proteins (see Section 1.2.b), and are spliced to produce a single mRNA species (Lagasse and Clerc, 1988). There is a single copy of each gene in the mouse

and human genomes, which have been localised to the S100 clusters on human chromosome 1q21 (Schafer et al., 1995) and mouse chromosome 3 (Ridinger et al., 1998). In both these species, MRP-8 and –14 are very closely linked and form a supergroup, but interestingly in humans the genes are separated by a third member of the supergroup, S100A12 (Wicki et al., 1996).

1.3.c Expression

MRP-8 and -14 are expressed in a cell type specific manner, and, in the virtually all situations, are co-expressed. Both the MRP proteins are believed to be restricted largely to leukocytes of the myeloid lineage and certain epithelial cells. Additionally, the expression of the MRP proteins in both lineages is regulated in differentiation (reviewed by (Hessian et al., 1993)). The exception is murine MRP-8 (also known at CP-10), and to a lesser extent murine MRP-14, which also can be detected in endothelial cells activated by proinflammatory stimuli both in vitro and in vivo (Yen et al., 1997).

1.3.c.i Myeloid Expression

Together MRP-8 and –14 comprise approximately 45% of the cytosolic protein in circulating neutrophils. Neutrophils may therefore contain millimolar levels of the MRPs. Monocytes also have a high level of the MRP proteins, but this is about 40 fold lower than in neutrophils (Edgeworth et al., 1991). Circulating lymphocytes, eosinophils and platelets do not express either MRP-8 or –14 (Hogg et al., 1989).

The expression of MRP-8 and –14 is regulated in differentiation. In the bone marrow of adult mice, virtually all the MRP positive cells were determined to be late myeloid cells by expression of Mac-1 and Gr-1, as well as nuclear morphology (Lagasse and Weissman, 1992). Consistent with this, the immature human myeloid

cell lines HL-60 and U-937 express very little or no MRPs (Hogg et al., 1989). Interestingly, HL-60 cells differentiated into monocytes by 1α,25-dihydroxy-vitamin D_3 and into granulocytes by DMSO express both the MRPs (Koike et al., 1992).

Resident tissue macrophages do not express MRP-8 and –14, which suggests further regulation of these proteins in differentiation (Hogg et al., 1989; Odink et al., 1987). In thioglycollate-induced peritonitis, a murine model of macrophage differentiation, infiltrating monocytes harvested after 4 hours were MRP-8 and –14 positive, whereas the macrophages harvested after four days were negative for both MRP proteins (Lagasse and Weissman, 1992). This indicates that tissue macrophages are derived from MRP positive monocytes, and that the expression is downregulated during differentiation. This is further supported by the MRP proteins being detected in early infiltrating cells (Hogg et al., 1989). In chronic inflammatory situations, such as rheumatoid arthritis, macrophages are MRP-8 and –14 positive (Hogg et al., 1985; Odink et al., 1987; Zwadlo et al., 1988). Alternatively, in some examples of acute inflammation, for example gingivitis and psoriasis, macrophages express MRP-14, but not MRP-8 (Delabie et al., 1990; Odink et al., 1987; Zwadlo et al., 1988). Therefore, the expression of MRP-8 and –14 by cells of the monocyte/macrophage lineage is tightly controlled in differentiation and inflammation.

1.3.c.ii Epithelial Expression

Normal and secretory epithelia do not express MRP-8 and –14, but the proteins are expressed by mucosal squamous epithelial of the mouth, tongue, oesophagus and cervix. The expression is turned on early in differentiation, as the proteins are detected in most supra-basal cells (Brandtzaeg et al., 1987; Wilkinson et al., 1988). MRP-8 and –14, which are not normally found in skin, have been detected in lesional keratinocytes of several inflammatory dermatoses, such as psoriasis, eczema and lupus erythematosus. In these pathologies, the proteins were

mostly restricted to the more mature middle and upper epidermal layers (strata spinous and granular). However, basal layer cells that are positive for the MRP proteins have been detected in lupus erythematosus and some psoriatic biopsies (Gabrielsen et al., 1986; Kunz et al., 1992; Wilkinson et al., 1988). Some squamous cell carcinomas of the lung and skin also express MRP-8 and –14 (Wilkinson et al., 1988).

Some epithelial cell lines express the MRP proteins, and this correlates with the ability of the cell lines to differentiate. Cultured normal human keratinocytes also express high levels of MRP-8 and –14 (Saintigny et al., 1992). This expression by cultured normal keratinocytes, but not normal epidermis, may indicate a link between these proteins and high rates of proliferation. This is supported by mucosal squamous epithelia having a high proliferative rate, as compared to other epithelia. The correlation between the MRPs and hyperproliferation is also consistent with the expression by squamous cell carcinomas. Additionally, some of the inflammatory dermatoses are associated with an increase in proliferation, for example, psoriasis. However, the proliferating basal keratinocytes in most examples are negative for MRP-8 and -14. Therefore, it has been proposed that these proteins are associated with the differentiation of hyperproliferating epithelia.

1.3.c.iii Subcellular Localisation

In resting neutrophils and monocytes, MRP-8 and –14 are localised almost entirely in the cytosol (Edgeworth et al., 1991). Activation of both of these myeloid cell types induces the translocation of MRP-8 and -14 to the membrane and cytoskeleton. This subcellular relocalisation is dependent on the influx of Ca^{2+}, and can also be induced with Ca^{2+} ionophores (Burwinkel et al., 1994; Lemarchand et al., 1992). Specifically, MRP-8 and –14 interact with the vimentin type III intermediate filaments of cultured monocytes and macrophages isolated from inflammatory sites (Burwinkel et al., 1994; Roth et al., 1993). Both unphosphorylated and

phosphorylated MRP-14 translocate from the cytosol to the membrane and cytoskeleton, but it is more pronounced for the phosphorylated molecules (Guignard et al., 1996; van den Bos et al., 1996).

Ca^{2+} ionophore treatment of a human squamous carcinoma cell line also induced the MRP proteins to translocate to membrane and cytoskeletal fractions. In this cell line, the MRPs associated with keratin intermediate filaments (Goebeler et al., 1995). When MRP-8 or MRP-14 were transfected singly into an embryonic lung cell line, both translocated to the membrane and cytoskeletal fractions in a similar fashion to the co-transfected proteins (Roth et al., 1993). Thus MRP-8, MRP-14 and the heterodimer translocate to the membrane and intermediate filaments of a cell following Ca^{2+} influx.

About twenty percent of circulating monocytes express heterodimeric MRP-8 and –14 on the cell surface (Zwadlo et al., 1986). The level of MRP expression is increasedby culture and treatment with various stimuli, including Ca^{2+} ionophores. Interestingly, MRP expressing monocytes secrete 4-100 fold more TNF-α and IL-1β, than non-expressing monocytes (Bhardwaj et al., 1992). Neutrophils do not express surface MRP proteins (Hogg et al., 1989).

1.3.c.iv Extracellular Expression

MRP-8 and –14 are not synthesised with a leader sequence, and are not localised to granular structures within cells (Edgeworth et al., 1991). However, there is a lot of evidence that these proteins exist extracellularly in vivo. A diffuse staining of the MRPs has been observed associated with infiltrating myeloid cells in tissues (Hogg et al., 1985). The vascular endothelium of venules proximal to chronic inflammatory sites, such as in Crohn's disease and rheumatoid arthritis, stain positive for MRP-8 and –14 ((Hogg et al., 1989) also see Fig 1.5). The mRNA encoding the MRP proteins cannot be detected in the endothelium, and therefore it is assumed the proteins are released by migrating myeloid cells (P. Tessier and N. Hogg,

unpublished data). MRP-8 and –14 can also be detected in the plasma of normal healthy humans, and the level is significantly increased in: infectious diseases, especially bacterial; chronic inflammatory conditions, such as rheumatic diseases and Crohn's disease; cystic fibrosis; and leukaemias. The elevation in plasma MRPs in cystic fibrosis is probably due to the associated chronic inflammation. The MRP proteins have also been detected in cerebrospinal fluids, oral fluid, urine, faeces and synovial fluid (reviewed by (Johne et al., 1997)).

In vitro cultured human monocytes and in vitro derived macrophages spontaneously release the MRP proteins into the culture medium. The level of release by cultured monocytes is increased by stimulation with Pokeweed mitogen (Lugering et al., 1997), GM-CSF, IL-1β, phorbol ester and LPS (Rammes et al., 1997). The phorbol ester activated release was reduced by inhibitors of energy metabolism, protein kinase C and microtubules, but not inhibitors of protein synthesis, the classical ER/golgi pathway or the actin cytoskeleton (Rammes et al., 1997). This not only distinguishes the secretion from that of the ER/golgi pathway, but the dependency on microtubules also differentiates it from the IL-1-like alternative route. Interestingly, in some situations, e.g. phorbol ester stimulated monocytes, more MRP-14 than MRP-8 is released (Rammes et al., 1997). This mirrors the relative plasma levels of MRP-8 and –14 observed in cystic fibrosis (Bruggen et al., 1988). Therefore, there is a lot of evidence in vivo and in vitro for the release of the MRP proteins, but the mechanism still awaits elucidation.

1.3.d Functions

The primary role of the MRP proteins is thought to be in the inflammatory process, and this is discussed in Section 1.4.b. However, in vitro assays and the MRP-8 "knock out" mouse have suggested several alternative functions for MRP-8 and –14.

1.3.d.i Fatty Acid Binding

The complex of recombinant MRP-8 and –14 from human or mouse binds arachidonic acid with high affinity (Kd=0.13μM for human). Intriguingly, neither of the MRP proteins alone interact with the fatty acid. The binding was Ca^{2+} dependent and inhibited by other unsaturated fatty acids but not saturated fatty acids (Klempt et al., 1997; Siegenthaler et al., 1997). This has also been shown for the native complex isolated from differentiating keratinocytes, psoriatic scales (Siegenthaler et al., 1997) and neutrophils (Kerkhoff et al., 1999b). In fact, the MRP protein complex is the primary fatty acid carrier in neutrophils (Roulin et al., 1999). Ca^{2+} ionophore and phorbol ester stimulated release of arachidonic acid appears to parallel that of the MRP proteins in a lymphoma cell line (HL-60) differentiated towards the granulocyte lineage (Kerkhoff et al., 1999b). Zn^{2+} inhibits the binding of fatty acid molecules, probably by constricting the hydrophobic pocket (Kerkhoff et al., 1999a).

Although the MRP-8/–14 heterodimer is clearly a major fatty acid binding protein of both keratinocytes and neutrophils, the role of this activity in vivo is unknown. The proteins are unlikely to act as an intracellular reservoir for fatty acid molecules, as binding does not occur in the absence of Ca^{2+}. It is more likely the MRPs act as Ca^{2+} dependent fatty acid transporters, maybe orchestrating movement to and/or release from the plasma membrane. Zn^{2+} may limit the role of MRP-8 and –14 as fatty acid binding molecules extracellularly, or alternatively may act as a release mechanism following secretion.

1.3.d.ii Antimicrobial

The MRP protein complex was named calprotectin because it is able to inhibit the growth of several strains of *Candida*, with minimum inhibitory concentrations of 4-128μg/ml. The MRPs also are antibacterial at higher concentrations (Steinbakk et al., 1990). This antimicrobial activity is independent of

Ca^{2+}, but can be completely reversed by low concentrations of Zn^{2+} (Sohnle et al., 1991). It is proposed that because microbes require low concentrations of Zn^{2+}, the MRP complex was chelating essential Zn^{2+}. This was supported by Zn^{2+}-supplemented *Candida* being resistant to MRP induced growth arrest. This was not due to Zn^{2+} inactivation of the MRPs, as the *Candida* did not release Zn^{2+} and the MRP proteins retained their fungicidal activity (Santhanagopalan et al., 1995). Additionally, polyhistidine demonstrates similar antimicrobial activity, which is reversed by Zn^{2+} and histidine modification, like the MRP proteins (Loomans et al., 1998). Therefore, the MRP protein complex-induced microbial growth arrest is likely to be due to Zn^{2+} chelation, and thus reversed directly by Zn^{2+} rather than the Zn^{2+} induced conformational change.

1.3.d.iii Inducer of Cytostasis and Apoptosis

A cell growth inhibitory factor isolated from rat peritoneal exudate cells has been shown to be MRP-8 and –14. The purified MRP protein complex inhibited the growth of mitogen stimulated lymphocytes, bone marrow cells and macrophages, as well as a rat, three murine and a human tumour cell lines (Yui et al., 1995a; Yui et al., 1993). The cytotoxic effect induced apoptosis in a murine lymphoma cell line (EL-4), some apoptosis in normal fibroblasts and no apoptosis in a human leukaemia cell line (MOLT-4). In these cases the effects have been shown to be reversed by Zn^{2+} (Yui et al., 1997; Yui et al., 1995b). Thus, this putative role for the MRP proteins may be mediated by chelation of Zn^{2+}, but a Zn^{2+} inhibited function cannot be excluded. Consequently, the in vivo cytostatic effects are hard to evaluate.

1.3.d.iv Embryo Development

Deletion of the MRP-8 gene in mice is embryonic lethal. The null embryos appear normal until they are reabsorbed by the mother at 9.5-13.5 days post coitum (dpc). This may be related to the expression of MRP-8, but not MRP-14, by some

embryonic trophoblasts, a phagocytic cell originating from the ectoplacental cone, at 6.5-8.5 dpc. Based on the chemotactic activity of murine MRP-8 (see Section 1.4.b.ii), the authors propose that the trophoblast may secrete the S100 protein, and that this contributes to the formation of the foetal-maternal interface (Passey et al., 1999). Interestingly, it has recently been reported that the mRNA for MRP-8 can be detected in many foetal cells, including cytotrophoblasts, of the human placenta during the first two trimesters. However, at term only myeloid cells express the mRNA (Sato et al., 1999). Thus the MRPs could have a role in the development of the foetal-maternal interface.

1.3.d.v Other Putative Functions

The C-terminal extension of MRP-14 is homologous to domain 5 of high molecular weight kininogen (HMWK), which interacts with negatively charged surfaces, such as kaolin. MRP-14, alone or complexed to MRP-8, binds to kaolin, and HMWK or a peptide of the C-terminal extension of MRP-14 can competitively inhibit this. MRP-14 also delayed the onset of intrinsic plasma coagulation in an in vitro assay (Hessian et al., 1995). Therefore MRP-14, alone or as part of a complex, may block HMWK induced intrinsic coagulation.

The MRP protein complex has also been shown to inhibit casein kinases I and II ($K_i \leq 1\mu M$), but not four other kinases. Unlike other examples of S100 mediated inhibition of kinases, this does not appear to be substrate specific, as the MRP protein inhibited phosphorylation of casein and kinase activation of RNA polymerase. The inhibition was also independent of Ca^{2+} (Murao et al., 1989). Casein kinases can regulate gene expression, therefore this may play a role in the differentiation and/or growth arrests of MRP expressing cells.

1.4 Inflammation and the S100 Proteins

Many S100 proteins have been implicated in inflammation. In particular, the MRP proteins have been both directly and indirectly associated with the inflammatory process.

1.4.a The Inflammatory Process

Inflammation is the process by which our bodies resolve tissue injury caused by infection and physical damage. Tissue insult leads to the recruitment of specific sub-populations of leukocytes depending on both the stimuli and the tissue type. The leukocytes then destroy the infectious agent and resolve the injury. The MRP proteins have largely been associated with this recruitment of leukocytes. Therefore, below I have summarised the sequence of events that lead to the extravasation of leukocytes.

1.4.a.i Initiation of Inflammation

Inflammation can be initiated by infectious agents and/or tissue damage. Microbial products, such as lipopolysacchardies (LPS) from gram-negative bacteria and lipoteichoic acid from gram-positive bacteria, induce the release of proinflammatory mediators, including cytokines, from the surrounding tissue and, in particular, from tissue macrophages (Henderson and Wilson, 1996; Hersh et al., 1998). The production of these mediators by macrophages is enhanced by opsonisation of the pathogen with complement molecules and/or antibodies. Additionally, the draining of the inflammatory site by afferent lymphatics and migration of dendritic cells leads to the presentation of the microbial antigens in secondary lymphoid tissues, thus initiating the adaptive immune response. Tissue damage and cell necrosis release intracellular molecules, which also can initiate inflammation (Janeway et al., 1999).

Proinflammatory mediators, such as histamine and TNFα, stimulate local blood vessels to dilate and become more permeable. The resulting increase in blood flow and leakage of fluids causes the heat, redness and swelling that characterise inflammation. Crucially, the endothelial cells of these vessels release leukocyte activating cytokines and become more adhesive (Mantovani et al., 1992; Mantovani et al., 1994). It is the combination of these events that leads to leukocyte recruitment.

1.4.a.ii The Recruitment of Leukocytes

The sub-populations of leukocytes recruited to an inflammatory site depends upon the tissue type and stimuli. Despite this, the mechanism of leukocyte emigration is similar in all cases, and, more surprisingly, is virtually identical to the process of lymphocyte extravasation in homing. In dilated post capillary venules proximal to the inflammatory site, where the shear stress is relatively low, the circulating leukocytes first bind to and then transmigrate through activated endothelium. Four sequential steps mediate this process of leukocyte emigration, known as the adhesion cascade. These steps are leukocyte rolling, activation, firm adhesion and transmigration (See Fig 1.4). This has been reviewed by (Springer, 1994) and (Carlos and Harlan, 1994), and these reviews also cover the following sections (1.4.a.ii.1-4) in detail.

1.4.a.ii.1 Rolling

The first stage of the adhesion cascade is the tethering and slowing of leukocytes. The leukocytes form several temporary interactions with the activated endothelial cells, thus under flow the leukocytes appear to roll along the vasculature. This process is mediated by the interactions of selectins with their carbohydrate ligands (reviewed by (Varki, 1994; Varki, 1997)). Selectins are a family of three membrane bound glycoproteins with C-type lectin domains at the extracellular

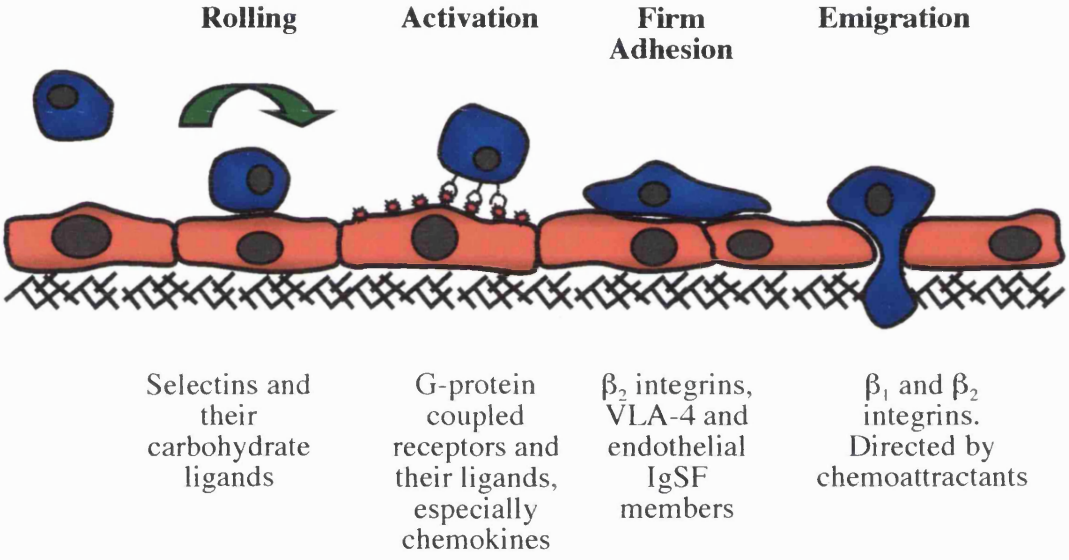

Figure 1.4: Schematic Diagram of the Multistep Model of Leukocyte Emigration

Leukocytes roll along stimulated endothelium via selectins (L-selectin on leukocytes and E- and P-selectins on the endothelium) and their interactions with glycoconjugate ligands. This exposes the leukocyte to activating stimuli, such as chemokines, which results in the integrin-mediated firm adhesion. Then the leukocyte transmigrates through the endothelium into the inflamed tissue.

terminus. This lectin domain binds to specific carbohydrate moieties on proteins and lipids. These glycoconjugates largely consist of glycans that contain specific small sialylated fucosylated oligosaccharides similar to sialyl-lewis^x (sLe^x). The selectin-carbohydrate interactions have rapid association and dissociation constants, which leads to the quick tethering and rolling motions observed in vivo.

P-selectin is normally contained within cytoplasmic granules of platelets and endothelial cells. Activation of these cells leads to degranulation, and the subsequent transient cell surface expression. P-selectin binds to leukocyte sialomucins decorated with O-linked glycans containing sLe^x moieties. The best characterised ligand is the homodimer of P-selectin glycoprotein ligand-1 (PSGL-1). PSGL-1 is expressed by neutrophils, and it alone can mediate neutrophil rolling on P-selectin in vitro (also see (Rosen and Bertozzi, 1996; Varki, 1997)).

E-selectin is expressed transiently by activated endothelium, but is synthesised de novo following stimulation. Consequently, E-selectin expression tends to follow that of P-selectin, but is more prolonged. E-selectin ligands are expressed on neutrophils and subsets of lymphocytes. E-selectin ligand-1 (ESL-1) is expressed on the microvilli of neutrophils, and requires N-linked glycosylations for binding.

L-selectin is expressed by most resting leukocytes, and binds to ligands on the high endothelial venules and endothelium at sites of chronic inflammation. L-selectin binding to four sialomucins expressed specifically on high endothelial venules, CD34, podocalyxin, Sgp200 and GlyCAM-1, is critical to naïve lymphocyte homing to lymphoid organs (also see (Rosen, 1999)). However, the ligands for L-selectin on the inflammatory endothelium are less well characterised. One potential candidate is heparan sulphate bearing proteoglycans (Norgard-Sumnicht, 1993).

Overall, the rapid and weak interactions between selectins and their ligands tether and slow leukocytes in the blood. Crucially this process is independent of leukocyte activation. However, it is this bringing together of the leukocyte and the activated endothelium, that leads to leukocyte activation.

1.4.a.ii.2 Leukocyte Activation

Cytokine activation of endothelial cells leads to the production of several leukocyte chemoattractants. These chemoattractants range from lipid mediators, such as platelet activating factor (PAF), to cytokines. To prevent dilution of these mediators in the blood flow, they bind to low affinity receptors on the endothelium. This effectively presents the chemoattractants to leukocytes rolling down the same endothelium. Therefore, leukocytes, which express the high affinity receptors for the specific chemoattractants, are exposed to and ligate these mediators. These high affinity receptors are of the seven membrane spanning G protein-coupled class, and ligation results in activation of the leukocyte. In summary, activated endothelium expresses mediators, which activate specific slowly rolling leukocytes.

This activation step is thought to be the major stage for selective recruitment of different leukocyte sub-populations. This selectivity by the activating chemoattractants is determined by the receptor expression on the leukocyte sub-populations. For the main part, this specificity is thought to be mediated by one family of chemoattractant cytokines, the chemokines, although other molecules do contribute, e.g. PAF.

The chemokine superfamily (reviewed by (Baggiolini et al., 1997; Schluger and Rom, 1997; Zlotnik and Yoshie, 2000)) can be subdivided into four groups according to the positioning of the first two cysteine residues. These are namely CXC, CC, CX_3C and C, and most chemokines fall within the first two groups. Chemokines are presented on the endothelium by binding to the glycosaminoglycan (GAG) chains of proteoglycans with low affinity (Tanaka et al., 1993). The high affinity G protein-coupled receptors are expressed by specific sub-populations of leukocytes, and ligate one or more members of a group. Therefore, the chemokines expressed at the endothelial surface determine which of the rolling leukocytes are activated. Currently, eighteen receptors and over thirty chemokines have been

identified. This gives the system great flexibility and selectivity. IL-8 has often been defined as the prototype inflammatory chemokine. IL-8 is synthesised and expressed by activated endothelium, and predominantly activates neutrophils (Baggiolini et al., 1994).

1.4.a.ii.3 Firm Adhesion

The activation of rolling leukocytes by ligation of G protein-coupled receptors triggers the firm adhesion of leukocytes on the endothelium (reviewed by (Carlos and Harlan, 1994; Gahmberg et al., 1997a)). This is mediated by the activation of the leukocyte integrins. The integrins on the surface of leukocytes, unlike most other cells, are constitutively maintained in a non-adherent state. Activation of the rolling leukocytes triggers the integrins to bind their endothelial ligands. Leukocyte stimulation can also lead to the increased expression of integrins. This is most dramatic with surface expression of Mac-1 on neutrophils, which can increase by about 10 fold.

Integrins are heterodimeric adhesion molecules composed of non-covalently associated α and β subunits. Three leukocyte integrins primarily mediate this step of the adhesion cascade (reviewed by (Harris et al., 2000)). LFA-1 and Mac-1 share a common β subunit (β_2/CD18), which is specific to haemopoietic cells. LFA-1 has an α_L subunit (CD11a), whereas Mac-1 has an α_m subunit (CD11b). VLA-4 is composed of α_4 (CD49d) and β_1 (CD29) subunits. These integrins can be activated by two mechanisms, which increase either the affinity or avidity of the heterodimer for its ligands (reviewed by (Stewart and Hogg, 1996a)). Stimuli that act via intracellular signals cause the integrin to cluster, but do not increase the affinity for its ligands. This results in an increase in avidity, which is sufficient to mediate firm adhesion. However, integrins can also be activated by cations in vitro. This leads to a conformational change, which results in an increase in affinity. The contribution of this latter form of activation in vivo remains elusive.

The leukocyte integrin ligands expressed on endothelium are members of the immunoglobulin superfamily (reviewed by (Gahmberg et al., 1997a)). Both the β_2 integrins bind to intercellular adhesion molecules (ICAMs)-1 and -2. ICAM-2 is constitutively expressed by endothelium, and therefore may be more involved in lymphocyte homing. ICAM-1, however, is expressed de novo upon activation of endothelial cells. VLA-4 binds to vascular cell adhesion molecule-1 (VCAM-1). VCAM-1, like ICAM-1, is induced on activated endothelium, but the expression is thought to be more restricted.

Therefore, the first three steps of the adhesion cascade result in the firm adhesion of a selected sub-population of leukocytes to the activated endothelium of post capillary venules proximal to the inflammatory site. Following this, the leukocytes transmigrate through the endothelium and into the inflamed tissue.

1.4.a.ii.4 Transmigration

Once firmly adhered to the endothelium, leukocytes migrate along a chemotactic gradient through the endothelium and into the tissue (reviewed by (Bianchi et al., 1997)). The chemoattractants that form the gradient include tissue produced chemokines and other proinflammatory cytokines. Therefore, the same or similar mediators that induce the leukocyte activation step direct this migration, at least in part. Several other molecules also form chemotactic gradients, for example the bacteria products LPS and formyl-peptides.

The initial barrier to overcome is extravasation of the leukocytes through the endothelium (reviewed by (Johnson-Leger et al., 2000)). Whether this requires disruption of the endothelial cell junctions is still unclear. However, it is currently believed, that most leukocytes extravasate through gaps between endothelial cell rather than via transcytosis. Consistent with this, proteases released by activated leukocytes disrupt the VE-cadherin-catenin complex, which maintains the adherens junctions (Moll et al., 1998).

Within interstitial tissues leukocytes continue to follow the chemotactic gradients of soluble factors. Again these are immobilised by low affinity interactions with the extracellular matrix and cell surfaces. In vitro models suggest leukocytes can navigate through serial gradients formed by different chemoattractants due to receptor desensitisation (Foxman et al., 1999; Kitayama et al., 1997), thus leading the cell specifically to the site of inflammation.

1.4.b The MRP Proteins in Inflammation

The MRP proteins have long been associated with inflammation. Initially the link was made with expression: neutrophils, which are recruited in large numbers early in inflammation, contain an extraordinary amount of MRP-8 and –14; macrophage expression of the MRPs are differentially regulated in resting, acutely inflamed and chronically inflamed tissues; and the plasma concentration is elevated in patients with chronic inflammatory diseases (see Section 1.3.c). Possibly the most direct link with expression was the localisation of the MRP proteins to venules proximal to chronic inflammatory sites (see Fig 1.5; (Hogg et al., 1989)). This has led to the hypothesis that the MRPs play a role in the adhesion cascade.

There is also evidence that the MRPs are involved in the activation of monocytes (see Section 1.3.c). Activation of monocytes with various stimuli, including Ca^{2+} ionophores, causes the MRPs to relocate to the intermediate filaments, plasma membrane and cell surface (Burwinkel et al., 1994; Lemarchand et al., 1992). Monocytes expressing surface MRPs secrete more TNF-α and IL-1β, than non-expressing monocytes (Bhardwaj et al., 1992). In vitro cultured human monocytes and in vitro derived macrophages spontaneously release the MRP proteins, and pokeweed mitogen, GM-CSF, IL-1β, phorbol ester and LPS all enhance this (Lugering et al., 1997; Rammes et al., 1997).

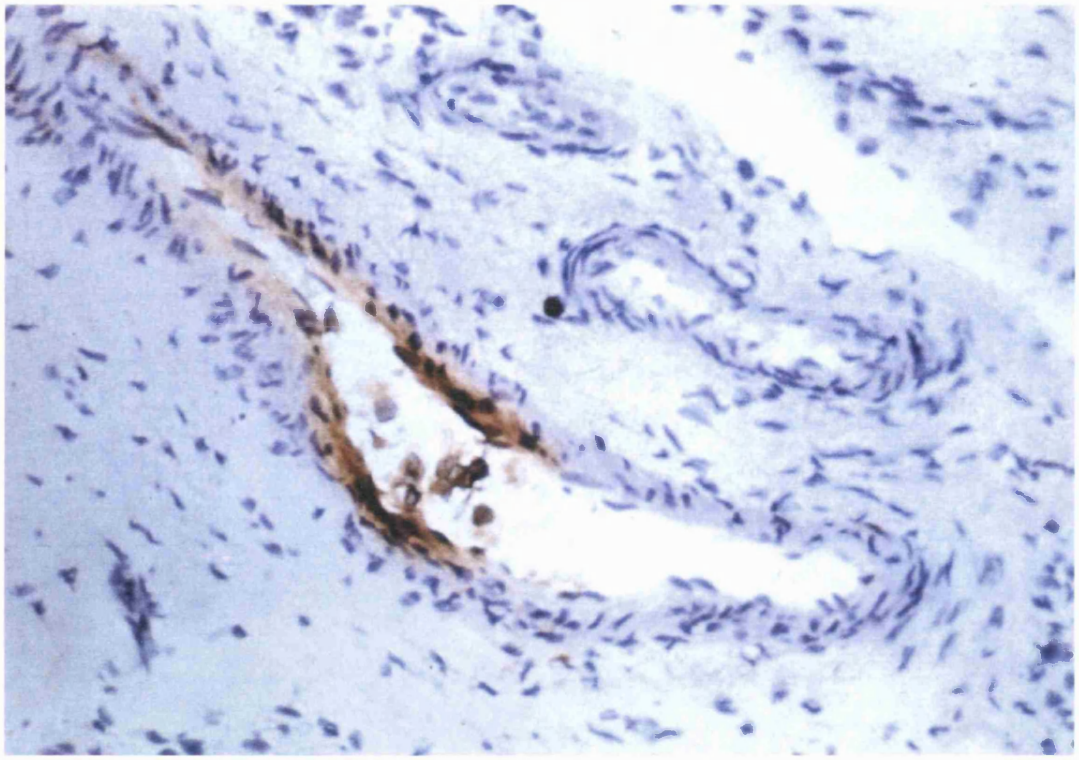

Figure 1.5: MRP-8 and -14 in Rheumatoid Synovium.
Immunohistochemical staining for MRP-8 and -14 in a section from rheumatoid synovium. The MRP complex was found deposited on the surface of the endothelium associated with the positively staining myeloid cells. This was adapted from (Hessian et al., 1993).

The specific roles that have been assigned to the MRP proteins in inflammation are described below.

1.4.b.i MRP-14 Activates Mac-1

In this laboratory R. Newton has shown that recombinant human MRP-14 (rMRP-14) is a novel activator of neutrophil Mac-1 (Newton and Hogg, 1998). This activation appeared to be mediated by a G protein-coupled receptor. However, the activation differed from chemoattractant stimulation, because rMRP-14 did not induce neutrophil shape change, actin polymerisation, Ca^{2+} flux, L-selectin shedding, Mac-1 upregulation or respiratory burst. Additionally, rMRP-14 induced the high affinity conformation of Mac-1. A continuation of this work has shown that rMRP-14 also stimulates Mac-1 mediated adhesion by a pro-monocytic cell line (THP-1) and T lymphoblasts. In the later case, rMRP-14 also caused the induction of cell surface Mac-1 (Newton, 1997).

These observations were particularly interesting given the localisation of the MRPs on inflammatory endothelium, where MRP-14 could act as a potent activator of Mac-1 mediated firm adhesion. The ability of rMRP-14 to induce firm adhesion without activating other potentially damaging neutrophil functions, suggested that MRP-14 could be a unique non-harmful inducer of firm adhesion. rMRP-14 stimulation is similar to the "pure" chemoattractants, like transforming growth factor-β1 (TGF-β1) and substance P. "Pure" chemoattractants induce neutrophil chemotaxis via G protein-coupled receptors, but do not cause Ca^{2+} flux or general neutrophil activation (Haines et al., 1993). Interestingly, rMRP-8 inhibited this rMRP-14 activity (Newton and Hogg, 1998), suggesting it may have a regulatory role.

1.4.b.ii Murine MRP-8 is Chemotactic

Murine MRP-8, also known as CP-10, is potently chemotactic for human and mouse neutrophils and murine macrophages in vitro (Lackmann et al., 1993). Injecting the recombinant and native proteins in vivo causes infiltration of neutrophils followed by mononuclear leukocytes (Devery et al., 1994; Lackmann et al., 1993). Murine MRP-8 chemotaxis is similar to the "pure" chemoattractants and rMRP-14 stimulation, because it is pertussis toxin sensitive and does not induce neutrophils to undergo Ca^{2+} flux, increase Mac-1, shed L-selectin, degranulate or produce a superoxide burst (Cornish et al., 1996; Devery et al., 1994). The chemotaxis in vitro and in vivo can be reproduced by a synthetic peptide identical to the hinge region, suggesting this is the active domain (Lackmann et al., 1993).

However, this may not relate to human MRP-8. The two homologues only share 58% identity, which is very low for cross species homologous S100 proteins. Additionally, the most divergent section is the hinge region. Recombinant human MRP-8 is not chemotactic for human neutrophils (Newton, 1997). In more complete experiments (i.e. with murine MRP-8 as a control), the hinge region of human MRP-8 is not chemotactic for murine leukocytes, and the same region from both species are described as weakly and variably chemotactic for human neutrophils (Lackmann et al., 1993). The species expression of MRP-8 also appears to differ, with activated mouse endothelium expressing MRP-8 in vitro and in vivo (Yen et al., 1997). This is not the case for human endothelium (P. Tessier and N. Hogg, ICRF, personal communication).

1.4.b.iii Other Roles of MRP-8 and MRP-14 in Inflammation

In the avridine-induced mouse model of arthritis, the human MRP-8 and –14 complex reduced the numbers of infiltrating cells, but this was not significant. The injection of an antibody raised to MRP-8 and –14 did cause a significant increase in

the number of infiltrating cells (Brun et al., 1995). This suggests the MRP proteins may have a protective role in chronic inflammation.

The homology of the MRP-14 C-terminal extension and high molecular weight kininogen (HMWK) has led to the proposal that MRP-14 blocks HMWK binding and activation at inflammatory sites (see Section 1.3.d.iv). Therefore, the MRP proteins may aid leukocyte extravasation by reducing fibrin accumulation. The fatty acid and arachidonic acid binding by the MRP proteins (see Section 1.3.d.i) has also been proposed to have a role in inflammation (Kerkhoff et al., 1999c). Unfortunately, whether the MRPs transport, localise, inhibit or mediate the functions of these molecules is unknown.

1.4.c Other S100 Proteins in Inflammation

Three other S100 proteins have been shown to be chemotactic. S100A7, or psoriasin, is an epidermal protein, which is highly upregulated in psoriasis (Madsen et al., 1991). S100A7 is a chemoattractant for CD4 T lymphocytes and neutrophils, but not monocytes or CD8 T cells (Jinquan et al., 1996). The bovine lung protein S100A2 (S100L) is potently chemotactic for guinea pig eosinophils, but not monocytes or neutrophils. Interestingly, the chemotactic activity of S100A2 was inhibited by pertussis toxin, suggesting a G protein-coupled receptor (Komada et al., 1996). Last year murine S100A12 was shown to be chemotactic for monocytes (see Section 3.1).

1.5 Aims

Just prior to the start of this project a third MRP-like S100 protein, S100A12, was isolated ((Dell'Angelica et al., 1994; Ilg et al., 1996b) also see Section 3.1). The major aim of this thesis was to investigate the expression and potential functions of this novel protein. In particular, the work by R. Newton showing that MRP-14 stimulates Mac-1 mediated adhesion of leukocytes (Newton, 1997) was used as a model for the analysis of S100A12.

An additional aim was to investigate the molecular mechanism of MRP-14-induced cell adhesion. The uniqueness of the rMRP-14-mediated upregulation and activation of Mac-1 on T lymphoblasts made this an attractive model system for this study.

Chapter 2

MATERIALS AND METHODS

2.1 Materials

2.1.a Stimuli and Other Reagents

Reagent	Stock Solution	Supplier
BCECF-AM [2',7'-bis-(Carboxyethyl)-5(6')-carboxyfluorescein acetoxymethyl ester]	1mM in DMSO Stored at -20°C	Calbiochem
fMLP (formyl-methionyl-leucyl-phenylalanine)	10mM in ethanol Stored at -20°C	Sigma
Ionomycin	1mM in DMSO Stored at -20°C	Calbiochem
Murine rMRP-14	≈1mg/ml in H-HBSS Stored at -70°C	Provided by R. May (ICRF)
PdBu (Phorbol-12,13-dibutyrate)	2mM in DMSO Stored at -20°C	Calbiochem
Glycated BSA	Made up fresh each time	Sigma

2.1.b Antibodies

2.1.b.i S100 Specific Antisera

The S100 antisera were raised against the rS100 proteins by Murex Biotech. Briefly, the rabbits were immunised, initially with 200 μg rS100 protein, followed by 6 boosts with 100 μg protein over the course of 3 months. The antisera were tested for specificity to the individual recombinant proteins by ELISA titration. Prebleed serum from the rabbit immunised with the S100A12 protein was used as the control antisera.

2.1.b.ii Monoclonal Antibodies

mAb	Epitope	Supplier
10.1	FcγRI (CD64)	Research monoclonal antibody service (RmAbS), ICRF
1F5	MRP-14	RmAbS, ICRF
1H9	MRP-14	RmAbS, ICRF
24	Activation reporter for β_2 integrins	RmAbS, ICRF
2H3*	Mac-1 α subunit (CD11b)	Dr A Bernard, Paris, France
2LPM19c	Mac-1 α subunit (CD11b)	Dr K Pulford, Oxford.
3.9	p150,95 α subunit (CD11c)	RmAbS, ICRF
4U	Unknown intracellular	RmAbS, ICRF
52U	Unknown intracellular	RmAbS, ICRF
6.5E	β_2 subunit (CD18)	Dr M. Robinson, Celltech, Slough
6E1	MRP-14	RmAbS, ICRF
6G4	MRP-14	RmAbS, ICRF
E11	CR1 (CD35)	RmAbS, ICRF
FL18.26	FcγRII (CD32)	Pharmingen
IB4	β_2 subunit (CD18)	Dr A. Law, Oxford
ICRF44	Mac-1 α subunit (CD11b)	RmAbS, ICRF
Lam 1.3	L-selectin (CD62L)	Dr T Tedder, Duke University, NC, USA
MEM170	Mac-1 α subunit (CD11b)	Dr V. Horesji, Prague, Czech Republic
SP-2*	None (null ascites)	RmAbS, ICRF
TS1/18	β_2 subunit (CD18)	RmAbS, ICRF
UCHM1	CD14	RmAbS, ICRF

All mAbs were supplied and used as a purified solution, except the ascites denoted by *.

2.1.b.iii Fab' Preparation

The Fab' preparation of ICRF44 was made by the Immunopure Fab preparation kit (Pierce) as per the manufacturer's instructions. The Fab' preparation of mAb 24 was kindly donated by A. McDowall (ICRF).

2.1.c Glycosaminoglycans

All glycosaminoglycan preparations were supplied by sigma, with the exception of [3H] heparin (NEN). The glycosaminoglycan preparations were made up at 2mg/ml in H-HBSS just prior to use is the assay, except hyaluronan which was solubilised at 50°C in 0.3M Na_2HPO_4 pH 5.4 to give the same final concentration.

2.1.c.i Different Glycosaminoglycans

Glycosaminoglycan	Source
Heparin	Porcine intestinal mucosa
Heparan sulphate	Bovine kidney
Chondroitin-4-sulphate	Bovine trachea
Chondroitin-6-sulphate	Shark cartilage
Dermatan sulphate	Porcine intestinal mucosa
Hyaluronan	Human umbilical Cord
Keratan sulphate	Bovine cornea

2.1.c.ii Chemically Modified Heparin

All chemically modified preparations of heparin were made by a protocol described by Nagasawa and Inoue (Nagasawa and Inoue, 1980) from porcine intestinal mucosa heparin and supplied by Sigma.

2.1.d Buffers and Media

H-HBSS: 10mM HEPES pH7.4 (Sigma) buffered Hank's Balanced Salt Solution (x10 without Mg^{2+} and Ca^{2+}; Gibco BRL)

H-HBSS/cations: H-HBSS + 1mM $CaCl_2$ + 1mM $MgSO_4$ + 10μM $ZnSO_4$

FACS wash: H-HBSS + 0.2% BSA

FACS wash/cations: H-HBSS + 0.2% BSA + 1mM $CaCl_2$ + 1mM $MgSO_4$ + 10μM $ZnSO_4$

FACS Fix: PBSA + 2% formaldehyde

TBS: 50mM Tris, pH 8.0, + 150mM NaCl

0.1M carbonate buffer: 0.013M Na_2CO_3 + 0.087M $NaHCO_3$

PBSA, RPMI-1640, LB agar and LB media were supplied by ICRF Research Cell Service.

2.1.e Cell lines

The cell lines Jurkat E6, Molt-4, Daudi, K562, U937 and THP-1 were maintained in RPMI-1640 with FCS (THP-1 media was also supplemented with 20μM 2-mercaptoethanol) by the ICRF Research Cell Service.

The T lymphoblast cell lines SKW3 and $SK\beta_2.7$ (Weber et al., 1997) were a kind gift from Dr A. Law (Oxford) and cultured in RPMI-1640 with 10% FCS.

The human microvascular endothelial cell line HMEC-1 (Ades et al., 1992) was generously donated by R. Bicknell (ICRF) and was cultured on gelatin coated flasks in DMEM (Sigma) supplemented with 10% FCS (Bioclear), 10ng/ml epidermal growth factor (Sigma) and 1mg/ml hydrocortisone (Sigma). The cells were then cultured on tissue culture plastic for the final passage, and removed with 0.5mM EDTA in PBSA (with 0.25% trypsin when specified) for use in assays.

2.1.f Primers

All primers were synthesised by the ICRF Oligonucleotide Synthesis Service.

P6-1+	TGGGCATATGACAAAACTTGAAGAGCAT
P6-73	GACACCCTCTCTAAGGGTGAG
P6-271R+	AGAGCATATGCTACTCTTTGTGGGTGTG
T7 promoter	GATATCACTCAAGCATAA

2.2 Methods

2.2.a Cloning of S100A12 cDNA

S100A12 cDNA was amplified from a human bone marrow cDNA library (Quick-Clone cDNA; Clontech) by PCR with primers P6-1+ and P6-271R+. The primers were designed from the protein sequence (Yamamura et al., 1996) with flanking Nde 1 sites. Vent DNA polymerase (New England Biolabs) was used for high fidelity. The PCR reaction was performed in 100µl of polymerase buffer (New England Biolabs) containing 1ng cDNA, 2U DNA polymerase, 125mM of each dNTP (Promega) and 0.5ng of both primers. Following a 5min delay at 95°C, the reaction was subjected to 25 cycles of 60sec at 94°C, 60sec at 55°C and 90sec at 72°C. After an extension of 10min at 72°C, the reaction was stopped by cooling to 4°C.

20µl of the PCR product was run on a 1.5% agarose gel, and the band of the correct size excised. After removing the agarose using the Prep-A-Gene kit (performed as per manufacturer's instructions; Bio Rad), the cDNA was digested with 20U of Ndel (New England Biolabs) in 20µl of buffer 4 (New England Biolabs) for 30min at 37°C. This was supplemented with another 20U of Ndel in 20µl of buffer 4, and the incubation repeated. The cDNA was then purified by phenol/chloroform and chloroform extractions, ethanol precipitated and resuspended in water. The pET3a vector (Novagen, Inc.) was digested with Ndel by the same

protocol as above and run on an agarose gel. The linearised plasmid was excised and the agarose removed using a Gene Clean II kit (performed as per manufacturer's instructions; Bio 101). The product was treated with 2 x 1U alkaline phosphatase (Roche) by the same protocol as the NdeI digestion of the cDNA, except the phosphatase buffer (Roche) was used. The vector was then phenol/chloroform and chloroform extracted, ethanol precipitated and resuspended in water. A fraction of both the digested cDNA and vector were then run on an agarose gel and the amount of DNA estimated by eye.

Approximately 5ng of cDNA was ligated to 50ng of pET3a vector by 1U of T4 DNA ligase (Roche) in 23µl of ligase buffer (Roche) at 16°C overnight. 10µl of this ligation were used to transfect supercompetent XL1-Blue MRF *E. coli* (Stratagene) by heat shock at 42°C following the manufacturer's protocol. The transformation mix was then plated out on LB agar plates containing 50µg/ml ampicillin (Sigma). Several colonies were picked and grown overnight at 37°C with shaking in 5ml of LB media containing 50µg/ml ampicillin. The plasmid from the bacteria of 1.5ml of the overnight culture was purified by "Miniprep". Briefly, the bacteria were pelleted by microfuge and resuspended in 100µl of Solution I (50mM glucose, 25mM Tris pH 8.0, 10mM EGTA). After 5min incubation at RT, 200µl of solution II was added (0.2M NaOH, 1%SDS), and the tube mixed before placing on ice for 5min. 150µl of solution III (3MKOAc, 11.5% glacial acetic acid) was added and the tube incubated on ice for another 5min. Following centrifuging in a microfuge at 4°C, the supernatant was phenol/chloroform and chloroform extracted, ethanol precipitated and then resuspended in 50µl of water.

The vector constructed was verified by PCR. The same protocol as for the original amplification was used with the following modifications:1ul of Miniprep DNA was used as a template; the annealing temperature was lowered to 47°C; and the following primer pairs were used.

Insertion Verification:	Primers P6-1 and P6-271R+
S100A12 Specificity:	Primers P6-73 and P6-271R+
Orientation Verification:	Primers T7 promoter and P6-271R+

Two clones, named A and B, were selected and used to seed overnight cultures of 400ml of LB media with ampicillin. The bacteria were pelleted by centrifugation at 3,600 x g for 20min, and the plasmid isolated by Maxiprep kit (performed as per manufacturer's instructions; Qiagen). The sequence of a clone was verified by an automated sequencer with a fluorescence dye terminator cycle reaction kit (performed as per manufacturer's instructions; Perkin-Elmer) using primers P6-1 and P6-271R+.

2.2.b Expression of rS100A12

The Maxiprep DNA was diluted 1 in 100 with water and 10µl used to transfect supercompetent BL21 (DE3) pLysS *E. coli* (Stratagene) as before. The bacteria were plated out on LB agar with ampicillin, and two clones chosen from each transfection (i.e. two clones from clone A and two from clone B).

All four clones and a clone of MRP-14 transformed BL21(DE3) pLysS were used to seed an overnight culture of LB media containing 50µg/ml ampicillin and 35µg/ml chloramphenicol (Sigma). 0.5ml of the culture was then used to seed another 5ml culture of LB media with antibiotics. This was grown for 1hr at 37°C when IPTG (isopropyl-β-D-thiogalactopyranoside; Amersham Pharmacia Biotech) was added to a final concentration of 0.4mM, and the culture grown for a further 2hr. The bacteria from 100µl of culture was pelleted, and the bacteria taken up in sample buffer and analysed by SDS PAGE.

One clone was then chosen for protein expression. An overnight culture of this clone was used to seed several 50ml cultures of LB media with antibiotics. These were grown for 1hr before induction with IPTG as before. The flasks were

then cultured for different times up to 5hr, after which the soluble and insoluble proteins were separated. The bacteria was pelleted and resuspended in 5ml of 50mM Tris pH 8.0, containing 2mM EDTA and 0.1% Triton X-100. The suspension was incubated at 30°C for 15min before sonication (Soniprep 150; Sanyo) twice for 10sec on high power. The insoluble proteins were then pelleted by centrifugation at 12,000 x g for 15min. The pellet was solubilised in sample buffer (see below), and 0.3% of each fraction analysed by SDS PAGE. This clone was stored by adding 2ml of 60% glycerol to 1ml of overnight culture, and freezing at -70°C.

The induction was then scaled up for protein purification. The glycerol stock was streaked out on LB Agar containing 50μg/ml ampicillin, and grown overnight. A single colony was then selected to seed a 20ml overnight culture of LB media containing 50μg/ml ampicillin and 35μg/ml chloramphenicol. 8ml of this culture was then used to seed 500ml of LB media with antibiotics. This culture was grown to an OD_{600nm} of 0.6-1.0, when IPTG was added to 0.4mM. The culture was grown for a further 3hr, after which the bacteria were pelleted at 3,800 x g and then frozen overnight at -20°C. The thawed pellet was taken up in 20ml of resuspension buffer. Initially, 20ml of 25mM Tris pH 7.1 containing 0.1% Triton X-100, 2mM EDTA, 1mM DTT and 20μg/ml PMSF (Phenylmethylsulphonyl fluorine; Sigma) was used as a resuspension buffer for Mono P loading at pH 7.1. However in subsequent experiments and large scale preparations, the Mono P was loaded at pH 8.3, and so the pellet was resuspended in 25mM triethanolamine pH8.3 containing 2mM EDTA, 1mM DTT and 20μg/ml PMSF. The suspension was then sonicated (Soniprep 150; Sanyo) for three times 30sec on high power, and centrifuged at 100,000 x g for 1hr. The supernatant was then analysed by SDS PAGE and used of as the starting material for protein purification.

2.2.c Purification of rS100A12

2.2.c.i Mono P purification

The conditions for Mono P purification were worked out with a 4ml prepacked column (Mono P HR 5/20; Amersham Pharmacia Biotech), and the rS100A12 followed by SDS PAGE analysis. When loaded on to the column in a Tris pH7.1 based buffer, the loading buffer used in rMRP-14 purification (see Section2.2.d), rS100A12 did not bind to the column. However, when loaded on in triethanolamine pH8.3 based buffers, the rS100A12 bound, and was eluted virtually pure. Thus this procedure was used as the basis for the large scale preparation described below.

For large scale preparations a SR10/50 column (Amersham Pharmacia Biotech) packed with 36ml of Mono P Polybuffer Exchange Media 94 (Amersham Pharmacia Biotech) was used. The rS100A12 solution was diluted to 50ml with resuspension buffer, and loaded onto the column that had been pre-equilibrated in loading buffer (25mM triethanolamine, adjusted to pH 8.3 with iminodiacetic acid). The column was washed extensively with loading buffer, and the bound proteins eluted with 100% elution buffer (3% Polybuffer 96 and 7% Polybuffer 74 pH 5.0; both from Amersham Pharmacia Biotech). The fractions were analysed by SDS PAGE, and those containing rS100A12 pooled. This solution of rS100A12 was dialysed overnight at 4°C against hydroxyapatite loading buffer (5mM Na_2HPO_4 pH 8.0, with 0.1M NaCl).

2.2.c.ii Hydroxyapatite Purification

The semi-pure solution of rS100A12 was then split into two and each half loaded on to a 10ml hydroxyapatite column (Bio Rad) pre-equilibrated in loading buffer. Following extensive washing of the column, the rS100A12 was eluted by a gradient of 0-100% elution buffer (500mM Na_2HPO_4 pH 8.0, with 0.1M NaCl) over 100ml. Again the fractions were analysed by SDS PAGE, and the ones containing

high concentrations of rS100A12 pooled. These fractions were dialysed against H-HBSS overnight at 4°C, and then centrifuged at 100,000 x g for 1hr to remove aggregates. The recombinant protein was sterilised by passing through a 0.2μm filter, aliquoted and stored at -70°C. Upon thawing rS100A12 was kept sterile and stored at 4°C for up to 2-4 weeks.

2.2.d Purification of rMRP-8 and rMRP-14

rMRP-8 and –14 were purified by protocols developed by P. Hessian and A. Coffer at the ICRF. These are described in (Newton and Hogg, 1998), and are briefly outlined below.

The BL21 (DE3) pLysS *E. coli* transformed with MRP-14.pET3a and MRP-8.pET3a were grown up, induced, harvested and lysed as for S100A12, except that the MRP-8 bacteria were induced for 5hr. The bacterial pellets from 1l of each culture were resuspended in 40ml 50mM Tris pH8.0 containing 2mM EDTA, 1mM DTT, 20μg/ml PMSF and 20mM $MgCl_2$. The DNA was sheared by adding DNase I (Roche) to a concentration of 100μg/ml, and incubating at RT for 2hr. The inclusion bodies were the pelleted by centrifugation at 12,000 x g, and washed twice with PBSA. The protein was then solubilised in 40ml of 25mM Tris pH8.0 with 6M urea. rMRP-14 was solubilised for 1hr on ice, and then dialysed overnight against 25mM Tris pH 7.1. rMRP-8 was agitated overnight at RT. The purification protocols of these preparations are summarised below.

2.2.d.i rMRP-14

The rMRP-14 was purified by a two step protocol similar to that for rS100A12. The preparation of resolubilised rMRP-14 was loaded onto the 36ml Mono P Polybuffer Exchange column pre-equilibrated in 25mM Tris, pH 7.1, and eluted by 10% Polybuffer 76, pH 4.0. The rMRP-14 containing fractions were then dialysed into hydroxyapatite loading buffer, and purified on a hydroxyapatite column

by the same protocol as rS100A12. The rMRP-14 was dialysed in H-HBSS, centrifuged, filter sterilised, aliquoted and stored as described for rS100A12.

2.2.d.ii rMRP-8

The urea solubilised rMRP-8 was applied to preparative isoelectric focussing (Rotofor; Bio Rad) over a range of pH 3-10 according to the manufacturer's instructions. The fractions were analysed by SDS PAGE and those containing rMRP-8 pooled and dialysed into hydroxyapatite loading buffer. The rMRP-8 was then purified by hydroxyapatite column chromatography, treated and stored, as described for rS100A12, except rMRP-8 was used on the day of thawing.

2.2.e Protein Analysis

2.2.e.i Protein Estimation

The concentration of the rS100 proteins was determined using Bio Rad protein assay dye reagent (as per the manufacturer's instructions; Bio Rad) using γ-globulin standards (0-500μg/ml). The concentration of other proteins and cell lysates were determined by the BCA protein assay reagent kit (as per the manufacturer's instructions; Pierce) using BSA standards (0-500μg/ml; Sigma). Both assays were read by a multiskan plate reader (Titertek), and the concentration of test proteins calculated from the standard curve of protein concentration of standards versus absorbance readings.

2.2.e.ii SDS PAGE

SDS PAGE analysis of S100 proteins was performed essentially following the method of Laemmli et al (Laemmli, 1970). The polyacrylamide gel was composed of a stacking gel layered over a separating gel. The separating gel was

made from 375mM Tris, pH 8.0, containing 17.5% acrylamide and 0.47% bis-acrylamide (from an acrylamide/bis-acrylamide stock solution; Amersham Pharmacia Biotech) as well as 0.1% SDS, 0.04% ammonium persulphate and 1/500 TEMED (Sigma). The stacking gel was made of 125mM Tris, pH 6.8, with 3% acrylamide, 0.08% bis-acrylamide, 0.1% SDS, 0.04% ammonium persulphate and 1/500 TEMED. Proteins for analysis were boiled in sample buffer (125mM Tris, pH 6.8, 25% glycerol, 2% SDS, 1% 2-mercaptoethanol, 0.02% bromophenol blue) for 5min just prior to loading onto the gel. Electrophoresis was performed in an Atto Dual Mini Slab Chamber (Genetic Research Instrumentation Ltd.) with electrophoresis buffer (25mM Tris, 192mM glycine, 0.1% SDS) at 100V through the staking gel and 180V through the separating gel. Rainbow coloured proteins low molecular weight markers (2 to 46kDa; Amersham Pharmacia Biotech) were run under identical conditions on the same gel. Samples not analysed by Western blot were visualised by staining with Coomassie Blue (0.5% w/v Coomassie Blue, 40% ethanol, 10% glacial acetic acid) and destaining with 20% ethanol/10% glacial acetic acid.

When better resolution was required to separate S100A12 and the MRP proteins a tricine based electrophoresis buffer system was used. The cathode buffer was composed of 0.1M Tris pH 8.25, 0.1M Tricine and 0.1% SDS, and the anode buffer was 0.2M Tris pH 8.9.

The integrity of monoclonal antibodies was verified by SDS PAGE performed virtually as above. The samples were run on gels made as above, except that the separating gel contained 10% acrylamide and 0.27% bis-acrylamide. In addition, the antibodies were prepared in the absence of 2-mercaptoethanol and run on gels with 15% acrylamide and 0.4% bis-acrylamide. The antibodies were compared to high molecular weight rainbow markers (14.3-220kDa; Amersham Pharmacia Biotech).

2.2.e.iii Western Blotting

2.5μg recombinant protein, the lysate from 5 x 10^5 cells or the immunoprecipitations from 25 μg of total protein were subjected to SDS PAGE as described above. The samples were then transferred onto a nitrocellulose membrane (Hybond ECL; Amersham Pharmacia Biotech) at 60V for 75min in a Transblot Cell (Bio Rad) containing transfer buffer (25mM Tris, 192mM glycine, 20% methanol). Following confirmation of transfer by 0.1% Ponceau S solution staining (Sigma), the membrane was blocked with PBS/Tween (PBSA + 0.1% Tween 20) containing 5% milk powder for 1hr at RT or overnight at 4°C. The membrane was then incubated with the primary antibody diluted in PBS/Tween for 1hr at RT. After washing three times in PBS/Tween, the membrane was incubated with horseradish peroxidase-conjugated goat anti-rabbit immunoglobulin (Dako) diluted 1 in 5,000 in PBS/Tween for 1hr at RT. The blot was washed again prior to reacting with a chemiluminescent substrate (ECL detection reagents; Amersham Pharmacia Biotech) for 1min. The image was then visualised by exposing the blot to film (Hybond ECL film; Amersham Pharmacia Biotech).

2.2.f Endotoxin Removal

Endotoxin was removed from aliquots of the recombinant S100 proteins prior to in vivo and neutrophil experiments, by a phase separation method originally described by Aida and Pabst (Aida and Pabst, 1990). The protein solutions were briefly vortexed in the presence of 1% Triton X-114 (Sigma), and then placed on ice for 5min. After vortexing again, the samples were placed at 37°C for 5min, and then centrifuged for 10sec in a microfuge. The upper aqueous phase was then removed, and used in assays.

2.2.g Cell Preparations and Lysis

2.2.g.i Neutrophils and Peripheral Blood Mononuclear Cells (PBMCs)

Human neutrophils and PBMCs were isolated from EDTA-anticoagulated whole blood, as described by Dooley et al (Dooley et al., 1982). Basically, the erythrocytes were sedimented by the addition of Dextran T500 (Amersham Pharmacia Biotech) to a final concentration of 0.6%. After 45min at RT, the leukocyte-rich plasma was layered onto a discontinuous gradient of 70% and 80% isotonic Percoll (Amersham Pharmacia Biotech). Following centrifugation at 1137 x g for 15min, the neutrophils were harvested from the interface between the 70% and 80% Percoll, and the PBMCs from the plasma-Percoll interface. The fractionated cells were then washed three times with H-HBSS.

2.2.g.ii T Lymphoblasts

Blood from a buffy coat (National Blood Service) was layered over Lymphoprep (Nycomed) and centrifuged at 1380 x g for 30min. The PBMC fraction was harvested from the Lymphoprep to plasma interface, and washed three times with RPMI-1640. The PBMCs were resuspended in RPMI-1640 + 10% FCS containing 1µg/ml phytohaemagglutinin (PHA; Murex Biotech Ltd.), and cultured for four days at 37°C. The cells were then washed twice with RPMI-1640, and maintained in culture at approximately 10^6 cells/ml in RPMI-1640 + 10% FCS containing 20ng/ml rIL-2 (Chiron UK Ltd). The expanded T lymphoblasts were used after 7-12 days culture in rIL-2.

2.2.g.iii Cell Lysis

Cells were resuspended at 5 x 10^7 cells/ml in chilled lysis buffer (20mM HEPES, 140mM NaCl, 20µg/ml PMSF and 1% NP40), and lysed for 30min on ice with occasional shearing by passing through a 21 Gauge needle. The lysate was then

centrifuged for 10min in a microfuge to remove insoluble material, and the supernatant used for assays. Lysates for immunoprecipitation were used immediately, whilst those analysed by Western blotting were used immediately or aliquoted and stored at -20°C.

2.2.h Cytospins and Immunohistochemistry

2.2.h.i Cytospins Preparation and Staining

1 x 10^4 fractionated PBMCs were centrifuged onto glass slides at 28 x g for 5min (Shandon Cytospin). The slides were then air dried overnight, fixed in acetone for 5min, and stored at -70°C.

The slides were thawed, and the endogenous peroxidase blocked by 0.2% H_2O_2 in methanol for 10min. The slide was then rehydrated, before blocking with normal swine serum diluted 1 in 25 with PBSA for 15min. The slide was then treated with the anti-S100 antisera or control antisera diluted 1 in 500 with PBSA for 35min. Following two washes with PBSA, the cytospin was incubated with biotinylated swine anti-rabbit immunoglobulin (Dako) at 1 in 500 for 35min. The slide was washed again, and incubated with streptavidin-peroxidase conjugate (Dako) diluted 1 in 500 for 30min. After washing, the cytospin was stained with 3,3'-diaminobenzidine (0.5mg/ml in PBSA with 0.07% H_2O_2; Sigma) for 2min. The reaction was stopped by washing with water. The slides were then counterstained with haematoxylin for 30sec, dehydrated and mounted.

2.2.h.ii Immunohistochemistry

Sections of 6μm were cut from paraffin imbedded tissues, dewaxed and the endogenous peroxidase blocked. After rehydration, the sections were treated with 1mg/ml trypsin (BDH, Merck Eurolab) for 15min at 37°C. The sections were then

stained by the same protocol as used for cytospins with the following exception. The antisera were used at an optimal dilution of 1:1000 for S100A12, 1:1000 for MRP-14 and 1:1000 for the control.

2.2.i Coimmunoprecipitations

Purified neutrophils were activated with 100nM fMLP or 1μM ionomycin in H-HBSS/cations at 1 x 10^7 cells/ml for 5 min at 37°C. Untreated and activated neutrophils were then lysed, as described above except at 5 x 10^6 cells/ml. Aliquots of lysate, containing 100μg of total protein, were precleared with 50μl protein A-Sepharose (a 50% slurry in lysis buffer; Amersham Pharmacia Biotech) for 1hr at 4°C. The beads were removed by centrifugation, and 10μl of control or S100 specific antisera was added for 1hr at 4°C. The antibody was then precipitated by adding 50μl protein A-Sepharose for another 1hr and then centrifuging. The beads were washed twice with a high salt buffer (25mM Tris pH 8.0, 0.5M NaCl, 0.5% NP-40, 0.5% sodium deoxycholate, 0.05% SDS), twice with a low salt buffer (as high salt except contains only 0.15M NaCl) and once with a no salt buffer (25mM Tris pH 8.0, 0.05% SDS). The beads were then taken up in 80μl of sample buffer. 20μl of each immunoprecipitate were analysed for S100A12, MRP-8 or MRP-14 by Western blotting.

2.2.j Cell Adhesion Assays

2.2.j.i Ligands and Coating Plates

Fibrinogen (Sigma) was solubilised in 0.1M carbonate buffer, pH 9.5, to 0.5mg/ml, and filtered through a 0.2μm syringe filter. Native bovine serum albumin (BSA; Sigma) was made up to 0.5mg/ml in TBS. Urea treatment was used to make denatured BSA. The BSA was first solubilised in 50mM Tris pH 8.0 containing 8M urea for 2hr at RT to give a final concentration of 4mg/ml. Iodoacetamide (Sigma)

was added to 60mM, and the solution incubated for a further 2hr in the dark. The denatured BSA was then extensively dialysed against TBS over 4-5 days, and centrifuged at 100,000 x g for 1hr to remove aggregates. The solution was then diluted to 0.5mg/ml with TBS.

96 well Maxisorb flat bottom microtitre plates (Nunc-Immunoplates; Gibco BRL) were coated with 50µl/well of ligand overnight at 4°C, except fish skin gelatin (FSG; Sigma) which was left untreated overnight. The plate was then blocked with 150µl/well of 1% FSG in PBSA for 1-2hr at 37°C. The wells were washed three times with 200µl of H-HBSS just prior to use.

2.2.j.ii Neutrophil Adhesion Assay

Neutrophils were labelled by incubation at 5 x 10^6 cells/ml in H-HBSS containing 1µM BCECF-AM (Calbiochem) for 30min at RT. The neutrophils were then washed three times in H-HBSS, and resuspended to 2 x 10^6 cells/ml in the same buffer. 50µl of H-HBSS/2x cations containing 2 x stimulants and blocking agents were added to each well. After 10min, the same volume of labelled neutrophils was then added, and the plate incubated in the dark at RT for 30min. After washing 2-4 times with 150µl/well of H-HBSS, the bound cells were quantified by a Cytofluor Multi-well Plate Reader (Series 4000; Perseptive Biosystems). The percentage of cells bound was determined by comparing fluorescence values to 50µl of labelled cells.

2.2.j.iii T Lymphoblast and Cell Line Adhesion Assays

T lymphoblast and cell lines adhesion assays were performed essentially as for neutrophils with the following exceptions and additions. The cells were labelled with H-HBSS containing 2.5µM BCECF-AM for 30min at 37°C. The labelled cells were added to the plate to give a final concentration of 2 x 10^6 cells/ml, after which

the plate was spun at 262 x g for 1min. The assay was performed at 37°C, rather than RT, and the unbound cells were washed off with warmed H-HBSS/cations.

In some experiments the T lymphoblasts were preincubated with mAbs. In these cases the stimuli and mAb were added to the plate as above, but, following this addition, the plate was incubated on ice for 10min. The cells were then added, and the plate incubated on ice for a further 15min. The cells were then spun onto the ligand, and the plate incubated and washed as in the standard assay.

When the assay was conducted at 4°C, all the buffers (including those to wash the cells) were chilled, and the plate incubated on ice.

Other experiments measured the T lymphoblast adhesion to rMRP-14 pretreated ligands. In these experiments, 50µl of H-HBSS/x2 cations with and without 2µM rMRP-14 was added to each well followed by 50µl of H-HBSS. After 40min incubation at RT, the plate was washed three times with 150µl/well of H-HBSS/cations. 50µl of H-HBSS/x2 cations with or without blocking agents was then added to the plate followed by 50µl of labelled cells. The cells were spun onto the ligand, and the plate incubated and washed as in the standard assay.

2.2.k FACScan Analysis of the Expression of Cell Surface Molecules

The cells were washed three times in FACS wash, and resuspended to 4 x 10^6 cells/ml in the same buffer. 50µl of cells was then added to 50µl of FACS wash/2xcations with 2 x stimuli and 2 x primary antibody in a U-bottomed PVC plate (Dynex Technologies, Inc.). After incubating at 37°C for 30min, the cells were washed three times with 150µl of chilled FACS wash, and resuspended in 100µl of FACS wash containing FITC-conjugated goat anti-mouse IgG (Sigma) at a dilution of 1 in 400. The plate was incubated on ice for 30min before washing again. The cells were then resuspended in 200µl of chilled FACS wash for immediate analysis or 200µl of FACS fix for analysis within 24hr. The fluorescence intensity of at least 5,000 cells was measured by a FACScan flow cytometer (Becton Dickenson).

2.2.l The Air Pouch Model of Chemotaxis

The protocol for this assay was based on that described by Tessier et al (Tessier et al., 1997). Briefly, 8 to 10 week old male C57/BL6 mice were anaesthetised with halothane and injected subcutaneously on the back with 2.5ml of sterile air (day 1). This was repeated on day 4 to generate the air pouch. On day 7, the mice were again anaesthetised, and 1ml of PBSA containing 1mM $CaCl_2$, 1mM $MgSO_4$, 10μM $ZnSO_4$ and the stimuli were injected into the air pouch. The mice were allowed to recover, and were sacrificed by CO_2 asphyxiation after 6hr. The infiltrating cells were harvested from the air pouch by washing with 1ml of PBSA containing 5mM EDTA, followed by another two 2ml washes. The cells were then counted in duplicate with a haemocytometer.

2.2.m rS100 Protein Binding to Proteinaceous Ligands

2.2.m.i The Standard Assay

Ligands were prepared and plates coated, blocked and washed as for the cell adhesion assays (see Section 2.2.j.i). 100μl of the appropriate concentration of rS100 protein in H-HBSS/cations with or without blocking agents was added to the wells in triplicate, and incubated at RT for 40min. The wells were washed three times with 150μl of H-HBSS/cations, and 100μl of S100 specific antisera diluted 1 in 1000 in H-HBSS/cations added for 30min at RT. The plate was washed again, and 100μl of horseradish peroxidase-conjugated goat anti-rabbit immunoglobulin (Dako) diluted 1 in 1000 in H-HBSS/cations added to each well for 30min at RT. After washing, the bound antibody was detected by 75μl/well O-phenylenediamine (made up in 0.067M $NaHPO_4$, 0.033M citric acid and 0.03% H_20_2 as per manufacturer's instructions; Sigma). The reaction was stopped by addition of 50μl

of 3M H_2SO_4 per well, and the absorbance at 492nm read by a Multiskan plate reader (Titertek).

2.2.m.ii Detergent and Salt Washes

In some experiments the sensitivity of the rMRP-14-ligand interaction to NaCl and detergent washes was evaluated. In these cases, the plates were incubated with rMRP-14 as in the standard assay. Following this, the wells were washed three times with 150µl of H-HBSS/cations containing the disruptive agent, and then a further three times with 150µl of H-HBSS/cations. The amount of rS100 protein bound was then determined as for the standard assay.

2.2.m.iii Divalent Cation Dependency

In the experiments to determine the divalent cation dependency of the interaction between rS100 protein and ligands the standard assay was modified as follows. The rS100 protein was incubated with the ligand as before, but the buffer contained either: no divalent cations; 1mM $CaCl_2$ and 1mM $MgSO_4$; 1mM $MgSO_4$ and 10µM $ZnSO_4$; 1mM $CaCl_2$ and 10µM $ZnSO_4$; or all three divalent cations. The wells were then washed three times with 150µl of H-HBSS containing the same cations, and three times with 150µl of H-HBSS containing all the divalent cations. The amount of rS100 protein bound was then measured as for the standard assay.

2.2.n Cell Surface Binding by rS100 Proteins

2.2.n.i Cell Surface Binding Assay

The cells were washed three times in chilled FACS wash, and resuspended to 4 x 10^6 cells/ml in the same buffer. 50µl of cells was then added to 50µl of FACS wash/2xcations containing 2 x rS100 protein with and without 2 x blocking agent in a U-bottomed PVC plate (Dynex Technologies, Inc.). The cells were incubated on

ice for 40min, and then washed three times with 150µl of chilled FACS wash/cations. The cells were resuspended in 100µl of S100 specific antisera diluted 1 in 1000 with FACS wash/cations, and incubated on ice for 30min. After washing, the cells were resuspended in 100µl of FITC-conjugated goat anti-rabbit IgG (each batch was diluted optimally at 1 in 160 to 400; Sigma) in FACS wash/cations. The plate was incubated on ice for 30min, and washed as before. The cells were then prepared for FACScan analysis as described in Section 2.2.k.

2.2.n.ii Divalent Cation Dependency

To determine the divalent cation dependency of rS100 protein binding to cell surfaces, the standard assay was modified as follows. 50µl of cells was then added to 50µl of FACS wash containing 2 x rS100 protein and either: no divalent cations; 1mM $CaCl_2$ and 1mM $MgSO_4$; 1mM $MgSO_4$ and 10µM $ZnSO_4$; 1mM $CaCl_2$ and 10µM $ZnSO_4$; or all three divalent cations. After the cells were incubated on ice for 40min, they were washed three times with 150µl of chilled FACS wash containing the same divalent cations, and then another three times with 150µl of FACS wash/cations. The rMRP-14 bound determined as for the standard assay.

2.2.o Heparin Binding Assay

2.2.o.i The Standard Assay

96 well Immulon 1 flat bottom microtitre plates (Dynex Technologies, Inc.) were coated with 50µl/well of 1H9, 6G4 or purified anti-S100A12 at 100µg/ml in PBSA overnight at 4°C. The plate was then blocked with 150µl/well of 2% FA^- BSA (Fatty acid free; ICN Pharmaceuticals, Inc.) for 1-2 hr at RT. The plate was washed three times with 150µl/well of H-HBSS just prior to use.

50µl of H-HBSS/x2 cations containing 4% FA^- BSA was added to each well followed by 50µl of H-HBSS with or without 0.2µM rS100 protein. After

incubating at RT for 1 hr, the plate was washed three times with 150µl/well of H-HBSS/cations containing 0.1% Tween-20. Next, 50µl of H-HBSS/x2 cations containing 4% FA$^-$ BSA and blocking agents was added to the wells followed by 50µl of H-HBSS containing the x2 [3H] heparin (NEN). The plate was incubated for 1hr (unless otherwise stated) at 37°C, and then washed as before but with warmed buffer. The bound [3H] heparin was solubilised by 0.5M NaOH containing 1% SDS for 30min at 37°C. After which, the contents of each well were added to 5ml of liquid scintillation cocktail (Ecolite +; ICN Pharmaceuticals, Inc.) and counted by a Beckman multi-purpose scintillant counter LS6500 (Beckman Instruments, Inc.). The specific binding was determined by subtraction of binding in the presence of 100µg/ml cold heparin (Sigma).

In assays with blocking agents, a parallel experiment was performed to test whether the blocking agent was able to compete the rMRP-14 from the anchoring mAb. The plates were coated, blocked and washed as above. The incubation with rMRP-14 was the same as above, except the final concentration of rMRP-14 was 0.01µM. After washing, the amount of rMRP-14 bound was determined as for the rS100 protein binding to proteinaceous ligand assay (see Section 2.2.m.i) except the antibodies were incubated in H-HBSS/cations containing 2% FA$^-$ BSA, and the washes contained 0.1% Tween 20.

2.2.o.ii Salt Washes

The salt sensitivity was analysed by the standard assay with an additional wash step following the incubation with [3H] heparin. The extra wash was 3 x 150µl/well of H-HBSS/cations with and without 0.5M NaCl. Like the blocking assays, a parallel experiment determined whether or not rMRP-14 was released from the anchoring mAb.

Chapter 3

INITIAL CHARACTERISATION OF S100A12

3.1 Introduction

In 1995, a MRP-8 polyclonal antibody was reported to cross react with a neutrophil cytosolic protein of approximately 6kDa (Guignard et al., 1995). This protein, later designated S100A12, has been identified and sequenced from pig (Dell'Angelica et al., 1994), human (Ilg et al., 1996b) and rabbit (Yang et al., 1996) neutrophils. S100A12 has also been cloned or isolated from: the surface of the human skin parasite, *Onchocerca volvulus* (Marti et al., 1996); bovine and human cornea (Gottsch and Liu, 1997; Gottsch and Liu, 1998); and bovine amniotic fluid (Hitomi et al., 1996). The numerous independent isolations has lead to several different names for the protein p6, calgranulin C, calgranulin-related protein (CaRP), cornea-associated antigen (CO-Ag) and calcium binding protein in amniotic fluid (CAAF1). Here I have used the S100 nomenclature of S100A12 (Wicki et al., 1996).

S100A12 is most closely homologous to MRP-14, and has a protein and gene structure typical of S100 proteins (Yamamura et al., 1996). Further, the human gene resides between the genes encoding MRP-8 and MRP-14 in the S100 gene cluster (Wicki et al., 1996). Human neutrophils are known to express high levels of S100A12, constituting about 5% of the cytosolic protein (Guignard et al., 1995). The expression by peripheral blood mononuclear cells (PBMCs) has been more controversial. S100A12 was reported to be present in preparations of porcine lymphocytes (Dell'Angelica et al., 1994) and human monocytes, but not in Epstein-Barr virus-transformed B cell lines (Guignard et al., 1995). The expression by lymphocytes is further complicated by reports that the human leukaemic T lymphoblast cell line Jurkat is both positive (Hofmann et al., 1999) and negative (Guignard et al., 1995) for S100A12. However, a recent study has shown that lymphocytes were negative for S100A12, and monocyte preparations were weakly

positive for S100A12, but that the source of the protein was contaminating neutrophils (Vogl et al., 1999).

MRP-8 and –14 are also expressed by a subset of normal stratified squamous epithelia, such as tongue and oesophagus, and by a number of hyperproliferative, neoplastic and malignant epithelia (see Section 1.3.c.ii). However, the expression of S100A12 by non-lymphoid tissue has been less well studied. Northern blot analysis detected S100A12 mRNA in oesophagus, but not prostrate, testis, ovary, small intestine, colon or skin (Yamamura et al., 1996). S100A12 protein was detected in the supra-basal layers of many squamous epithelia in the bovine foetus, including the epidermis, oesophagus and amnion, whereas several other bovine foetal tissues were negative. Additionally, expression was detected in bovine newborn oesophagus and epidermis (Hitomi et al., 1996).

In resting neutrophils S100A12 is cytosolic, but the protein translocates to the membrane upon activation by opsonised zymosan, fMLP, calcium ionophore and arachidonic acid (Guignard et al., 1995). A similar translocation has been observed on addition of calcium to neutrophils lysates (Vogl et al., 1999). This mirrors the subcellular localisation of the MRP proteins in monocytes and neutrophils (see Section 1.3.c.iii). The similar translocation of S100A12 and the MRP proteins, the similar expression patterns and the fact the proteins often co-purify has lead to the proposal that S100A12 may be associated with the MRP protein complex. Contrary to this, S100A12 does not associate with recombinant MRP-8 or -14 or when co-purified with the MRP protein complex and cross linked (Vogl et al., 1999).

Recently, three potential functions of S100A12 have been reported. Firstly, S100A12 positive primary cultured epithelial cells reportedly do not proliferate as determined by BrdU incorporation. Further, the expression of recombinant S100A12 by a cell line, derived from a squamous cell carcinoma of human oesophagus, reduced the number of proliferating cells, thus directly linking S100A12 with growth arrest (Hitomi et al., 1998). Secondly, S100A12 has also been described to have filariacidal and filariastatic activity, because the recombinant protein greatly reduced

the motility of the parasitic nematode, *Brugia malayi* (Gottsch et al., 1999). This is supported by the isolation of S100A12 from another filarial parasite, *Onchocerca volvulus* (Marti et al., 1996). Finally S100A12 was isolated as a ligand for the Receptor for Advanced Glycation End products (RAGE). The following comprehensive study showed that rS100A12 activated NF-κB in human umbilical vein endothelial cells (HuVEC) resulting in upregulation of VCAM-1 and ICAM-1. The recombinant protein was also shown to be chemotactic for human monocytes in vitro, chemotactic for murine leukocytes in vivo, and an inducer of TNFα and IL-1β secretion by macrophages. Additionally, blocking RAGE reduced both acute and chronic inflammatory lesions, thus implying a proinflammatory function for S100A12 (Hofmann et al., 1999).

The aim of this project was to clone human S100A12 and produce the recombinant protein. Antibodies could therefore be raised to further elucidate the expression of S100A12. Whether S100A12 has a similar function to the close homologue rMRP-14 also was investigated.

3.2 Results

3.2.a Cloning of S100A12 cDNA

The cDNA encoding S100A12 was amplified from human bone marrow cDNA using primers designed from the protein sequence (Marti et al., 1996). The 5' primer (P6-1+) contained 18bp based on the protein sequence preceded by a Nde 1 site, which included the start site, and a 4bp tail. The 3' primer (P6-271R+) was designed to comprise the antisense strand to the final 15bp of the S100A12 gene (again based on the protein sequence), preceded by the antisense stop codon, a NdeI site and a 4bp tail. Thus the primers were designed to engineer two NdeI sites, flanking the S100A12 cDNA. The product of the 25-cycle PCR reaction with 1ng of bone marrow cDNA was analysed by agarose electrophoresis. The gel showed a

single product of approximately the predicted size (288bp, Fig 3.1A). This product was cut out of the gel, the agarose removed and the DNA digested with Nde1. The digested cDNA was then ligated with the vector, pET3a, which had previously been treated with Nde1 and alkaline phosphatase.

The ligation product was used to transform competent XL-1 Blue MRF *E. coli*, and the bacteria cloned on ampicillin selection plates. The clones were screened by PCR for the presence of insert, the presence of the S100A12 cDNA, and the orientation of the insert (Fig 3.1B). The presence of an insert was detected with the original primers, P6-1+ and P6271R+. The presence of S100A12 cDNA was checked because the terminal sequences of MRP-8 and S100A12 are quite homologous. This utilised a primer, P6-73, designed from a unique sequence of S100A12 (residues 26-32), and the same 3' primer. The orientation of the insert was verified by PCR amplification using the 5' primer based on the T7 promoter of the vector and P6-271R+. Two clones, named A and B, were determined to have the correct construct and were chosen for sequencing. Both clones had identical nucleotide sequences, which was predicted to translate in to the published amino acid sequence of S100A12 (Fig 3.2, (Marti et al., 1996)). The constructs were purified from both these clones, and used in expression studies.

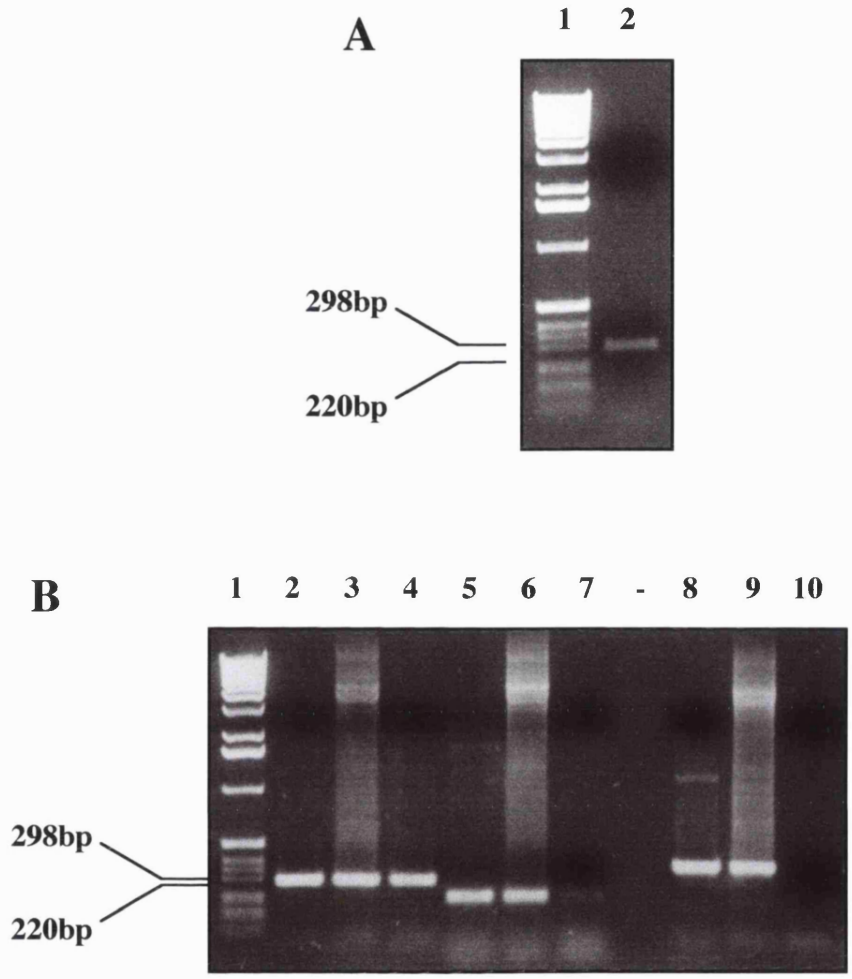

Figure 3.1: PCR Amplification of S100A12 cDNA and PCR Verification of the S100A12/Vector Constructs

A) Agarose gel electrophoresis analysis of the product from the PCR amplification from 1ng bone marrow cDNA, using primers P6-1+ and P6-271R+ (Lane 2).

B) Agarose gel electrophoresis analysis of the PCR screening of XL-1 Blue MRF *E. coli* clones transformed with the S100A12/pET3a ligation product. Three clones, A (Lanes 2, 5 and 8), B (Lanes 3, 6 and 9) and C (Lanes 4, 7 and 10), were subjected to PCR to verify insertion (Lanes 2-4), S100A12 specificity (Lanes 5-7) and orientation (Lanes 8-10). The insertion was verified by primers P6-1+ and P6-271R+; the S100A12 specificity by P6-73 and P6-271R+; and the orientation by the T7 promoter primer and P6-271R+. The size of the products in **A** and **B** was compared with a 1kb DNA ladder (Lanes 1).

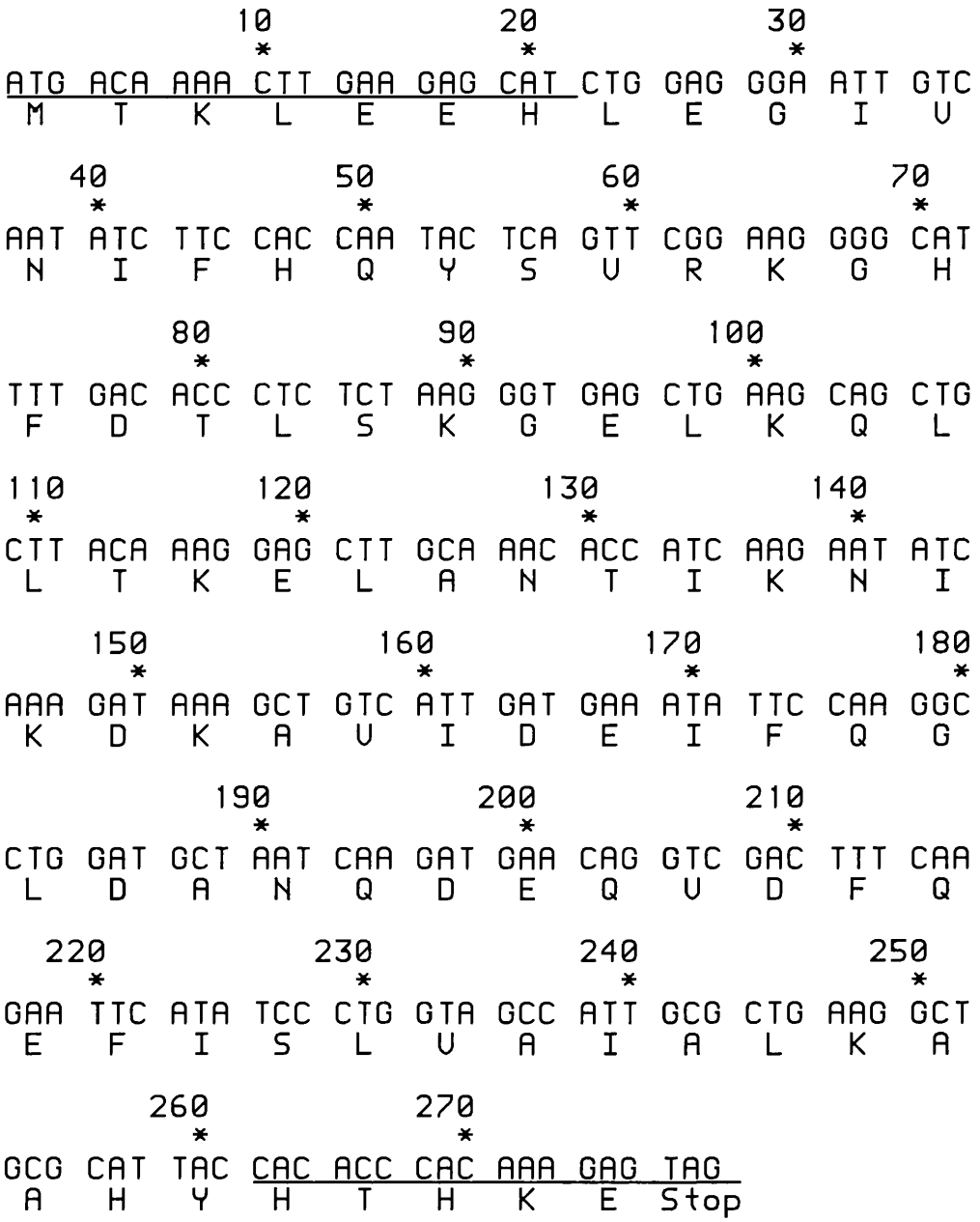

Figure 3.2: cDNA Sequence of Clones A and B

The cDNA (sense strand) and translated protein sequence (single letter code) of Clones A and B of S100A12 cDNA. The underlined sequences denote those encoded by the primers.

3.2.b Expression and Purification of rS100A12

For protein expression the constructs from clones A and B were transfected into competent BL21(DE3) pLysS *E. coli*, and cloned again. The IPTG induced expression of recombinant proteins by MRP-14 transformed BL21(DE3) pLysS was compared to two clones of clone A and two clones of clone B transformed bacteria. SDS PAGE analysis of the total protein showed that all four S100A12 transformants were induced to express high amounts of a protein, which migrated at 6kDa (Fig 3.3A, Lanes 2-5). The expression appeared to be greater than that of rMRP-14 (Fig 3.3A, Lane 1). Clone B/1 BL21(DE3) pLysS *E. coli* (Fig 3.3A, Lane 4) was selected for further studies and will subsequently be known as S100A12-BL21(DE3) pLysS.

An induction time course was performed on S100A12-BL21(DE3) pLysS. At each time point the bacteria were lysed by sonication in 0.1% Triton X-100, and the insoluble material removed by centrifugation. The protein content of both the soluble and insoluble material was analysed by SDS PAGE. There was little leakage from the uninduced pET3a vector (Lanes 1 of Fig 3Bi and ii). The recombinant protein was the major constituent of the soluble material of induced bacteria, with expression peaking at 3-5 hours (Fig 3.3Bi, Lanes 2-7). Little or no rS100A12 could be seen in the insoluble fraction (Fig 3.3Bii).

Finally, the process was scaled up to a 0.5l culture of S100A12-BL21(DE3) pLysS induced with 0.4mM IPTG for 3 hours during the exponential growth phase. The bacteria were lysed by freeze/thaw followed by sonication in 0.1% Triton X-100, and centrifuged to remove insoluble and aggregated material. SDS PAGE analysis of the resultant solution showed rS100A12 to be the primary constituent (Fig 3.3C). This methodology was used in subsequent experiments to prepare the start material for the protein purification.

Because S100A12 is homologous to MRP-14, the initial attempts to purify rS100A12 were based on the protocol for rMRP-14 purification (Newton and Hogg, 1998). rMRP-14 is first purified from a crude preparation by Mono P

chromatofocussing. At neutral pHs only acidic proteins bind the ion exchange resin, and, therefore, rMRP-14 binds the resin whilst most impurities flow through the column. The recombinant protein is further purified by elution with a descending pH gradient formed in situ by the Polybuffer exchanger. When dialysed into the rMRP-14 loading buffer (Tris, pH 7.1), rS100A12 did not bind the Mono P resin (data not shown). This is probably because rS100A12 has a higher pI than rMRP-14. Consequently, the crude rS100A12 then was prepared in a triethanolamine-based buffer, pH 8.3. The crude product was loaded onto the Mono P column, the rS100A12 bound and was eluted off the column, by the Polybuffer system, in virtually pure state (Fig 3.4A and B).

Following Mono P purification, rMRP-14 is further purified by hydroxyapatite column chromatography. Hydroxyapatite resin binds, amongst other macromolecules, calcium binding proteins, and is used to remove remaining bacterial impurities as well as misfolded non-calcium binding recombinant protein. Therefore, it was considered an ideal second step in rS100A12 purification. rS100A12 bound well to the hydroxyapatite resin, and was eluted, with high concentrations of phosphate, largely as a single peak (Fig 3.5A and B).

This two step protocol yielded 70-90mg of rS100A12 per litre of bacterial culture. The product was then dialysed into HEPES buffered HBSS (H-HBSS), and frozen at –70°C in aliquots. The recombinant protein was highly pure and migrated at 6kDa in SDS PAGE, like native S100A12 (Guignard et al., 1995). Coomassie Blue staining of an overloaded SDS PAGE revealed no impurities. Matrix assisted laser desorption (MALDI) mass spectrometric analysis of the product, diluted 1in 10,000 with water, detected a single molecule of 10563Da (D. Pappin, personal communication). This is similar to the predicted mass of rS100A12 (10574Da), with the high salt concentration of buffer probably being responsible for the slight discrepancy. This protocol, therefore, purifies rS100A12 to homogeneity and is similar to the methodology used to purify rMRP-14. The rMRP-14 was functional, as determined by induction of neutrophil adhesion, and also was used to generate specific antibodies.

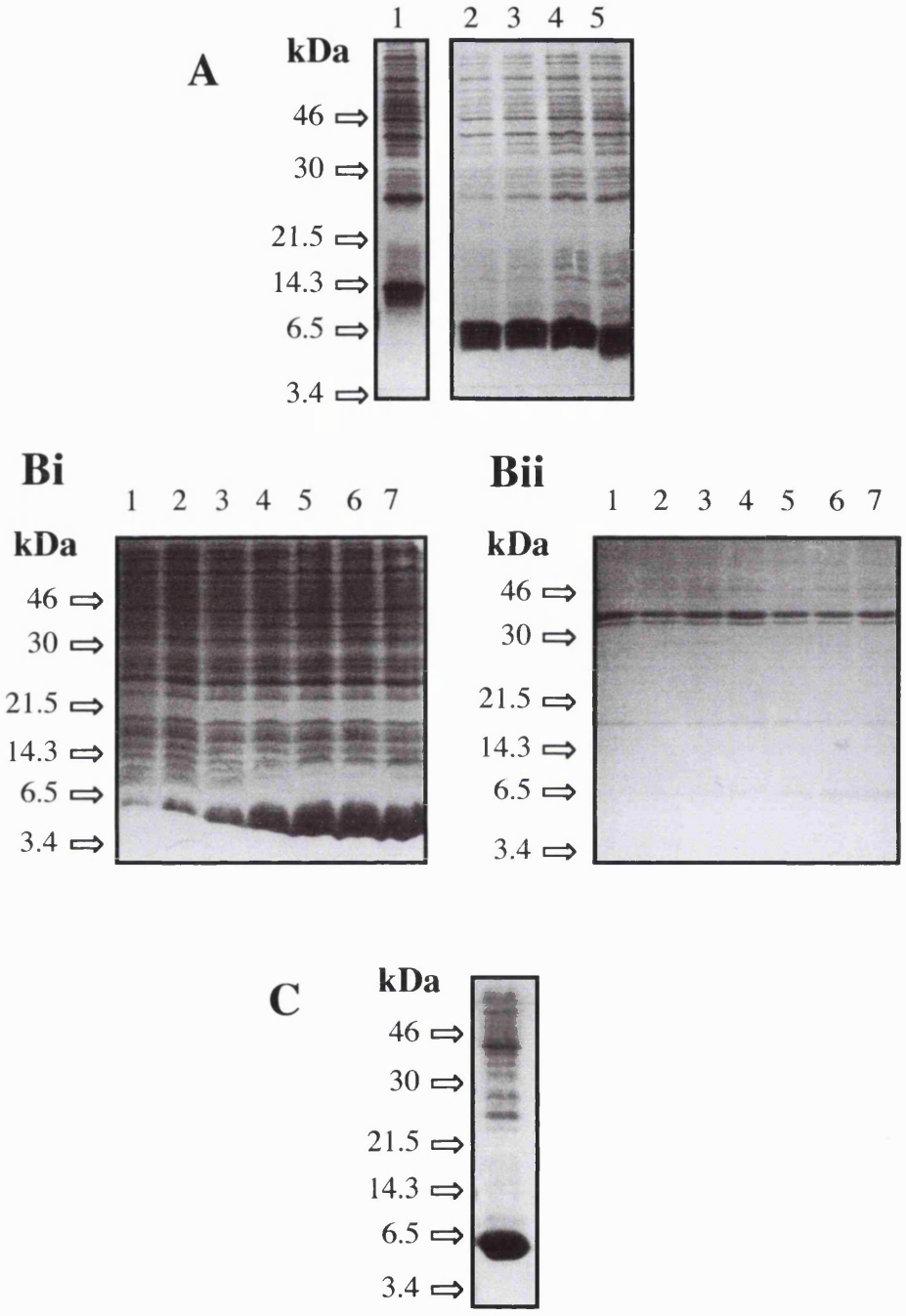

Figure 3.3: Analysis of rS100A12 Expression by *E. coli* by SDS PAGE
A) SDS PAGE analysis of clones of BL21 (DE3) pLysS transformed with MRP-14 (Lane 1), S100A12 clone A (Lanes 2 and 3) and S100A12 clone B (Lanes 4 and 5). Each lane represents the total bacterial protein from 100µl of an exponentially growing culture induced for 2 hours with 0.4mM IPTG. **B**) SDS PAGE analysis of S100A12-BL21 (DE3) pLysS *E. coli*, uninduced (Lane 1) and induced with 0.4mM IPTG for 30 min (Lane 2), 1hr (Lane 3), 2hr (Lane 4), 3hr (Lane 5), 4hr (Lane 6) and 5hr (Lane 7). Each lane represents the total protein solubilised by sonication in 0.1% Triton X-100 (**Bi**) or the recovered insoluble material (**Bii**) from 150µl of culture. **C**) SDS PAGE analysis of a large scale culture, 0.5l, of S100A12-BL21 (DE3) pLysS *E. coli* induced with 0.4mM IPTG for 3 hours.

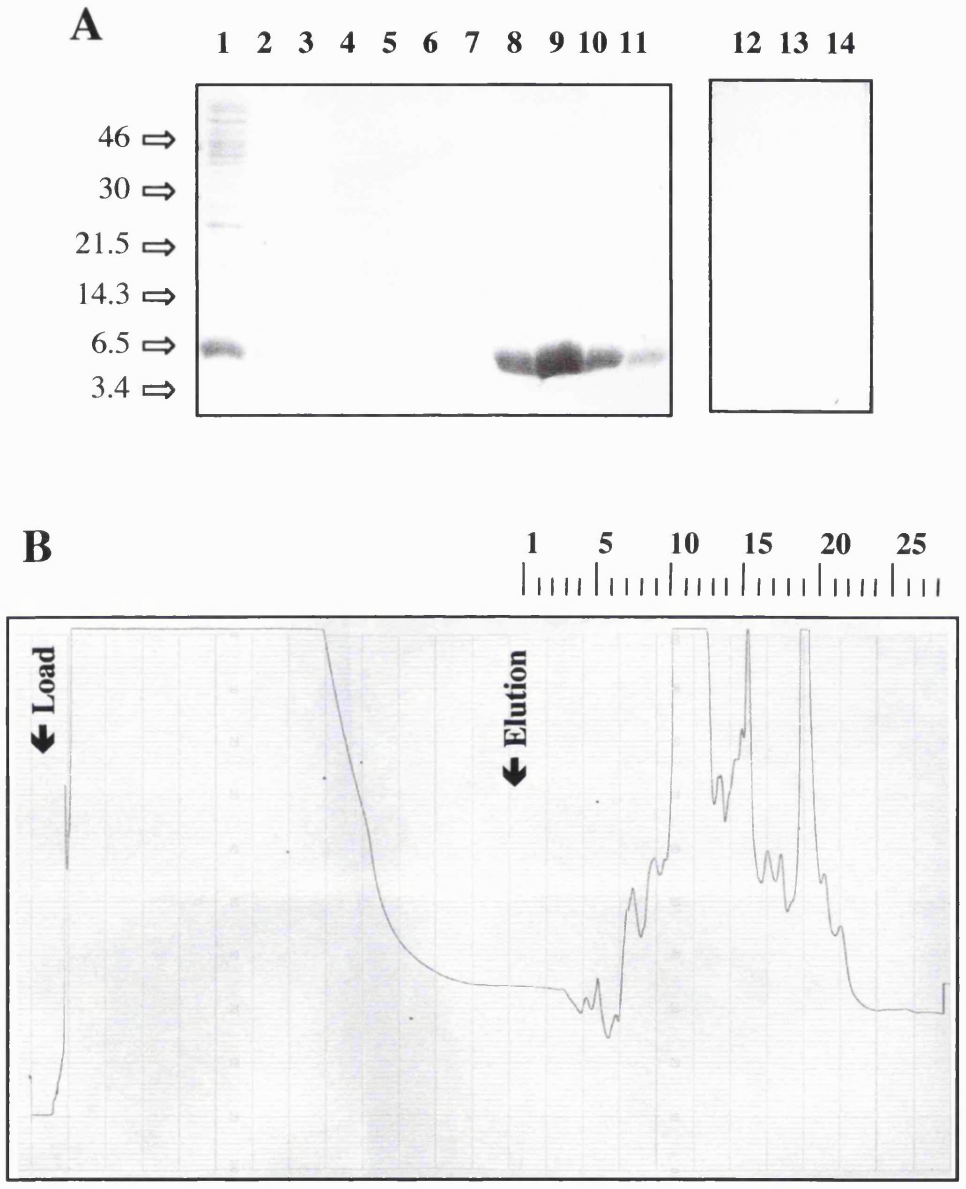

Fig 3.4: Mono P Purification of rS100A12 from Bacterial Lysate
A) SDS PAGE analysis of the purification of rS100A12 from the crude bacterial lysate by Mono P chromatofocussing. Lane 1, crude load; Lane 2, unbound proteins; and Lanes 3-14, fractions 5-16. 10µl of each sample was loaded per lane. Fractions 10-13 were pooled. **B**) The absorbance at 280nm of the flow through of the Mono P chromatofocussing column. The fraction numbers are shown above. Full scale deflection = 1.0.

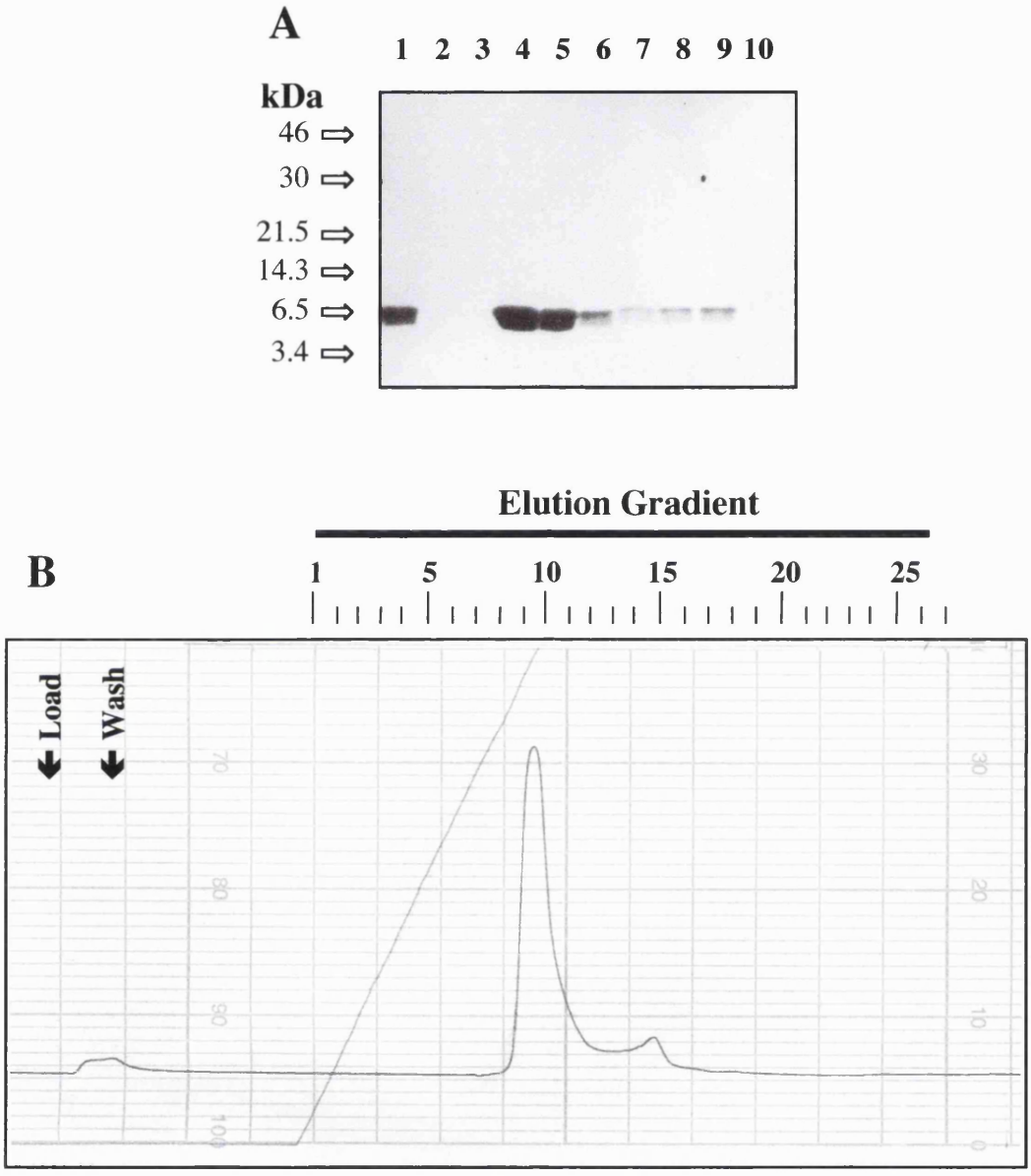

Fig 3.5: Hydroxyapatite Purification of rS100A12 from a Semi-Pure Preparation

A) SDS PAGE analysis of the hydroxyapetite column chromatography purification of rS100A12 already partially purified by Mono P chromatofocussing. Lane 1, load; Lane 2, unbound proteins; and Lanes 3-10, fractions 8-15. 10μl of each sample was loaded per lane. Fractions 9 and 10 were pooled. **B**) The absorbance at 280nm of the flow through of the hydroxyapetite column. The fraction number and the gradient from 0% to 100% Elution Buffer (see Materials and Methods) are shown above. Full scale deflection = 1.0.

3.2.c S100A12 Expression by Circulating Leukocytes

Neutrophils are reported to express S100A12, but the expression by other leukocyte populations, such as monocytes and lymphocytes, has been controversial (Dell'Angelica et al., 1994; Guignard et al., 1995; Hofmann et al., 1999; Vogl et al., 1999). One difficulty in being certain about S100A12 expression has been caused by the use of antisera that cross react with the MRP proteins. A rabbit polyclonal antisera raised against purified rS100A12 did not cross react with recombinant MRP-8 or –14 (Fig 3.6A). Similarly, the antisera raised to rMRP-8 and -14 were quite specific, with only the anti-MRP-14 antibody showing very slight cross reactivity with rMRP-8 (Fig 3.6A). The specificity of the antisera for the native proteins was then determined by Western blot analysis of neutrophil lysate. The polyclonal antibodies raised against rS100A12 and MRP-8 specifically detected a single protein of the correct molecular weight (Fig 3.6B and C). The anti-rMRP-14 antisera detected two proteins, of 14 and 28kDa (Fig 3.6D), with the former probably being MRP-14 and the latter either a complex of MRP-8/MRP-14 or MRP-14/MRP-14. The MRP complexes are often only partially destroyed by boiling in sample buffer (Longbottom et al., 1992). Therefore, all three antisera are specific as determined by Western blot analysis.

To compare S100A12 expression with that of MRP-8 and –14, neutrophils, PBMCs, T lymphoblasts as well as lymphoid, myeloid and endothelial cell lines were analysed by Western blotting. Neutrophils and PBMCs were strongly positive for all three proteins (Fig 3.7A, Lanes 1 and 2). T lymphoblasts, the leukaemic T cell lines Jurkat and Molt-4, the B lymphoblast cell line Daudi, the bone marrow leukaemic cell line K-562, the promonocytic cell line THP-1, the histiocytic lymphoma cell line U-937, the acute promyelocytic leukaemic cell line HL-60 and the microvascular endothelial cell line HMEC-1, were all negative for S100A12, even when the blot was over exposed (Fig 3.7A, Lanes 3-11). Similarly, T lymphoblasts and the tested cell lines did not express MRP-8 and –14 (Fig 3.7A,

Lanes 3-9, 11), except for THP-1 cells which were weakly positive for both MRP proteins (Fig 3.7A, Lanes 10). The anti-actin Western blot showed that the loading of the various cell lines was equivalent to or greater than that of the PBMCs. These results are consistent with MRP-8 and –14 being expressed by mature neutrophils and monocytes (Hessian et al., 1993). S100A12 is also expressed by neutrophils, however the S100A12 positive cell type in PBMCs remained unclear.

To identify which cell types in PBMCs express S100A12, and to exclude contaminating neutrophils as the source of the protein, S100A12 expression was analysed at the single cell level by immunohistochemistry of cytospin preparations. As expected, monocytes and the contaminating neutrophils were positive for MRP-14 (Fig 3.7B). The S100A12 antibody stained the neutrophils confirming the result of the Western blot experiment, and also weakly stained monocytes (Fig. 3-7C). This staining was specific as the control antisera failed to stain any PBMCs under identical conditions (Fig. 3-7D). Lymphocytes were negative for S100A12 and MRP-14. Therefore, it can be concluded that circulating neutrophils and monocytes, but not lymphocytes, express S100A12.

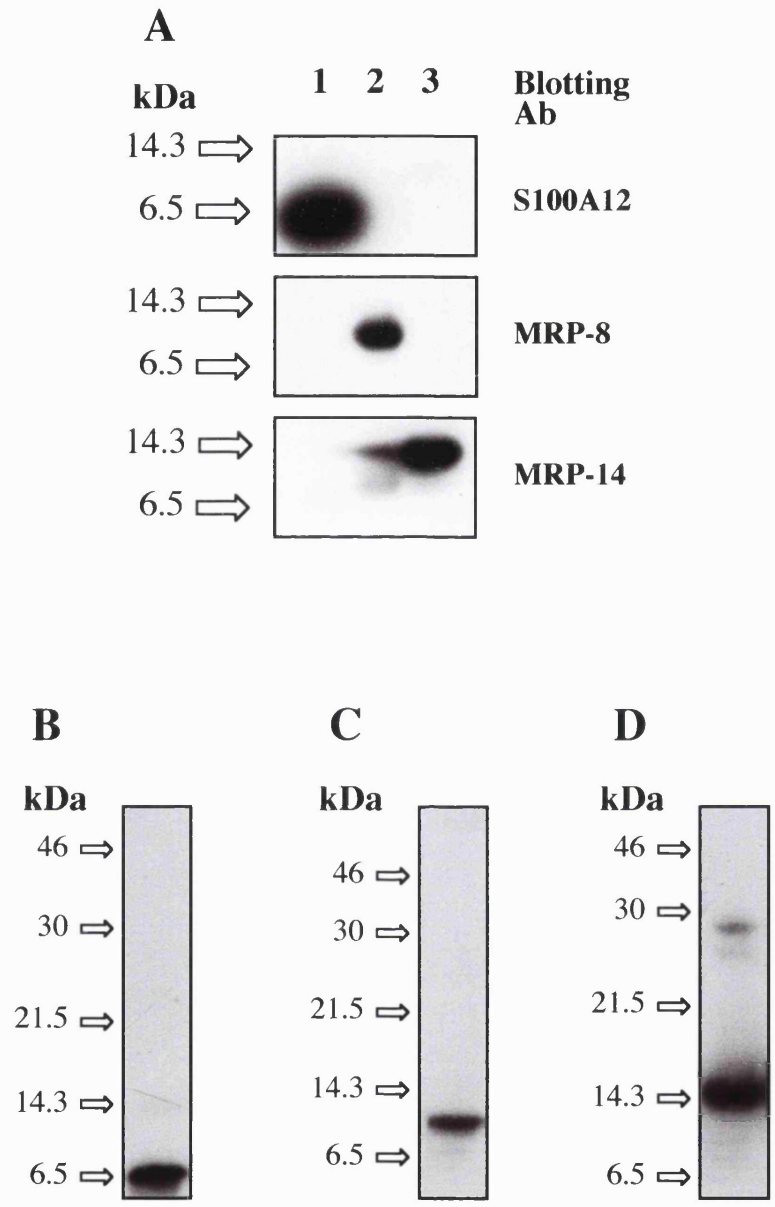

Figure 3.6: Specificity of the S100A12, MRP-8 and MRP-14 Antisera
A) Western blot analysis of 2.5µg of purified rS100A12 (Lane 1), rMRP-8 (Lane 2) and rMRP-14 (Lane 3) using antisera raised against the same recombinant proteins. **B-D**) Neutrophil lysate made with NP40 ($5x10^5$ cells/Lane) analysed by Western blot with S100A12 antisera (**B**), MRP-8 antisera (**C**) and MRP-14 antisera (**D**). The antisera were used at the following dilutions anti-S100A12 at 1 in 10,000, anti-MRP-8 at 1 in 5,000 and anti-MRP-14 at 1 in 50,000.

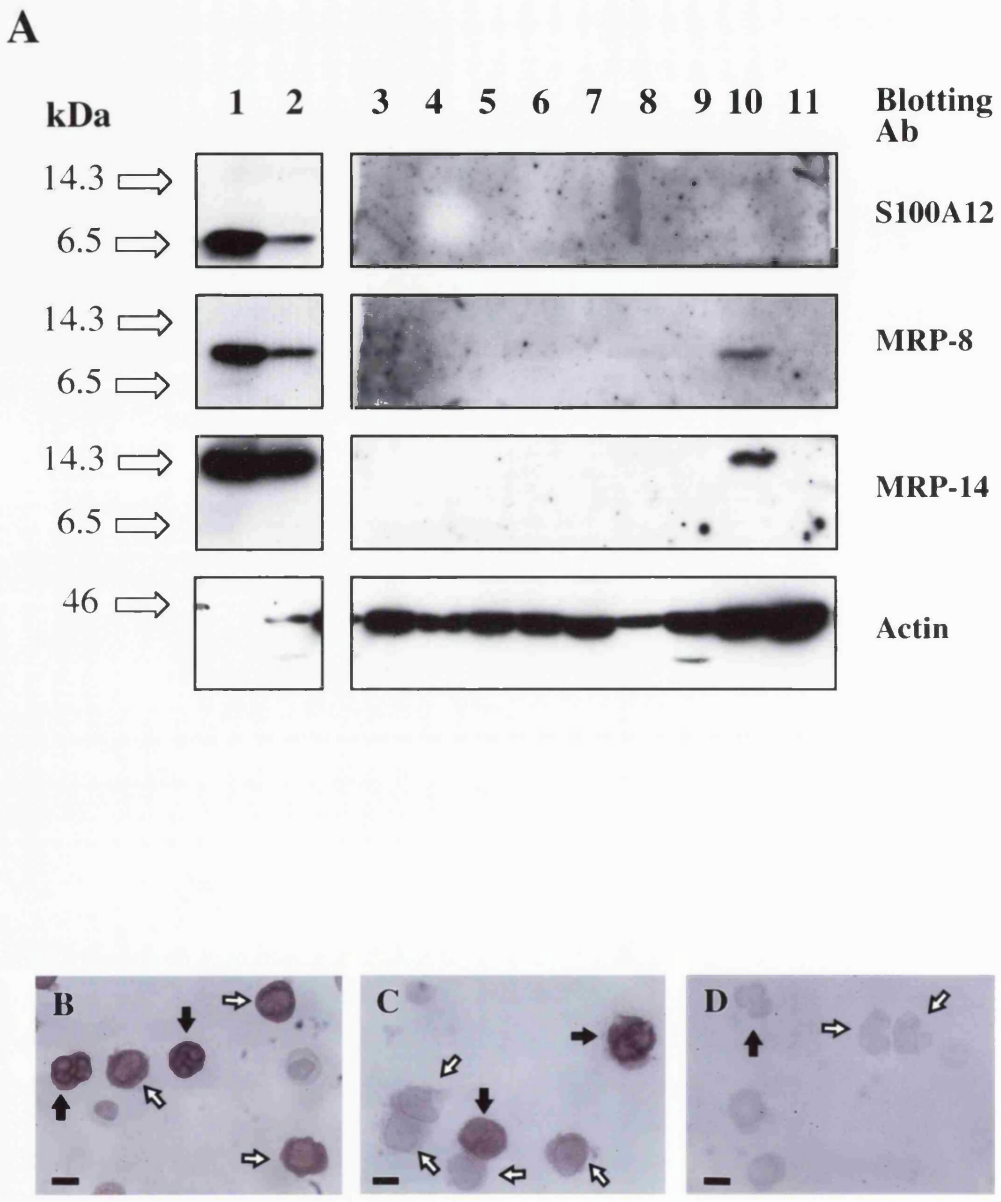

Figure 3.7: S100A12 Expression by Leukocyte Sub-Populations

A) Western blot analysis of purified neutrophils (Lane 1), PBMCs (Lane 2), T lymphoblasts (Lane 3) and cell lines Jurkat E6-1 (Lane 4), Molt-4 (Lane 5), Daudi (Lane 6), K-562 (Lane 7), HL-60 (Lane 8), U-937 (Lane 9), THP-1 (Lane 10) and HMEC-1 (Lane 11) all lysed in 1% NP40 and loaded at $5x10^5$ cells/lane. The monospecific rabbit antisera for S100A12, MRP-8 and MRP-14 were used at 1 in 10,000, 1 in 5,000 and 1 in 50,000, respectively. Lanes 3-11 were overexposed. As a control for protein loading, the cell lysates were blotted for actin (anti-actin used at 1 in 5,000) in parallel (not over exposed). **B-D**) Immunohistochemistry of cytospins of PBMC preparations with MRP-14 (**B**), S100A12 (**C**) and control (**D**) antisera. All antisera were used at 1 in 500. Open arrows denote monocytes and filled arrows denote contaminating neutrophils. Scale bar: 10μm. This immunohistochemistry was performed by G. Elia (Histopathology Unit, ICRF).

3.2.d S100A12 and the Staining of Tissue Leukocytes

A study of S100A12 expression by leukocytes within tissues has never been reported. To initially characterise the expression of rS100A12 by non-circulating leukocytes, spleen and lymph node sections were stained for both S100A12 and MRP-14. The spleen contains many cells that stain strongly for MRP-14. These cells were primarily localised to the perifollicular zone with some dispersed in the red pulp (Fig 3.8A). The S100A12 antisera stained fewer cells and more weakly, but the cells did show a similar distribution (Fig 3.8B). Lymph node also contained S100A12 positive cells, but predominately dispersed throughout the red pulp (See Table 3.1). In both cases the staining was specific as the control sera did not stain any cells (Fig 3.8C and data not shown). The S100 positive cells of the spleen and lymph node that could be identified had a morphology and nucleus typical of neutrophils.

MRP-8 and -14 are generally not expressed by tissue macrophages except in chronic inflammatory conditions (see Section 1.3.c.i). Tissue macrophages and other resident or infiltrating leukocytes were not stained with the S100A12 antisera in any of the normal non-lymphoid tissues studies (Table 3.1). Crohn's disease biopsies typically contain many MRP-8 and –14 positive macrophages and neutrophils (Schmid et al., 1995). When a Crohn's disease biopsy was analysed by immunohistochemistry, the S100A12 antisera stained fewer cells and more weakly than the MRP-14 antibody (Fig 3.9A, data not shown). In particular a leukocyte rich structure stained highly for S100A12. Although all the positive cells could not be identified, at higher magnifications S100A12 staining neutrophils could be seen but not cells with a typical macrophage morphology (data not shown). Again the specificity was determined by the control sera failing to stain any cells (Fig 3.9B).

Overall S100A12 expression in non-circulating leukocytes was similar, but more restricted than that of MRP-14.

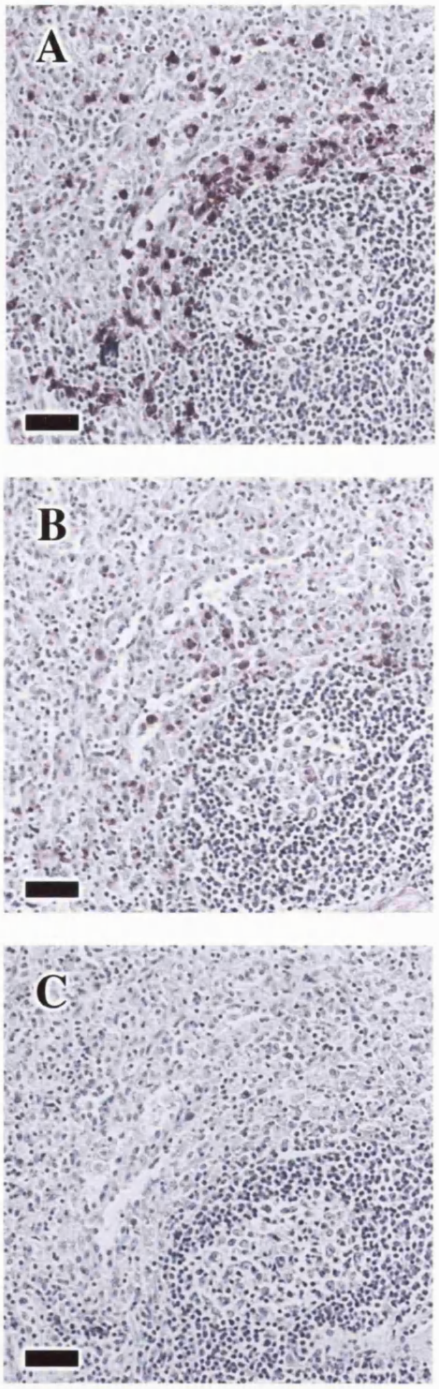

Figure 3.8: S100A12 Expression in the Spleen
Immunohistochemical study of the spleen staining with (**A**) MRP-14 antisera, (**B**) S100A12 antisera and (**C**) control sera at 1 in 1,000. Scale bar: 50μm. This immunohistochemistry was performed by G. Elia (Histopathology Unit, ICRF).

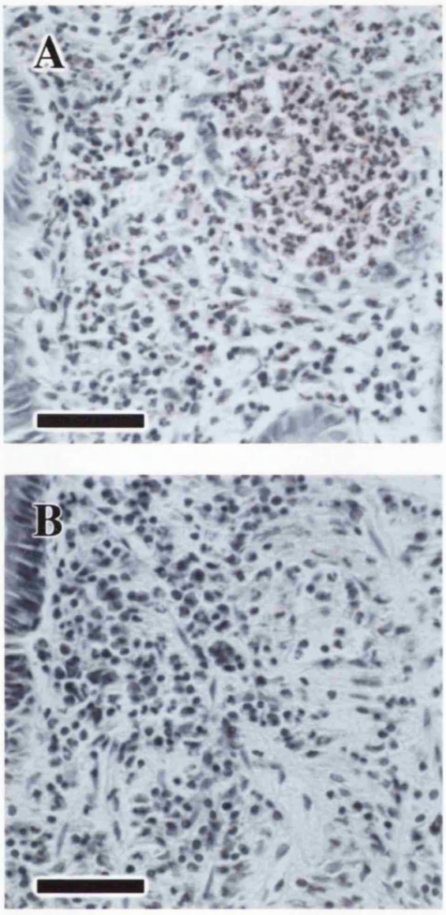

Figure 3.9: S100A12 Expression in Crohn's Disease
Immunohistochemical study of a Crohn's disease biopsy staining with (**A**) S100A12 antisera and (**B**) control sera at 1 in 1,000. Scale bar: 50μm. This immunohistochemistry was performed by G. Elia (Histopathology Unit, ICRF).

3.2.e S100A12 and Epithelial Tissues

MRP-8 and MRP-14 are expressed in various squamous epithelial tissues (see Section 1.3.c.ii), but there has been no comparative study with S100A12. Antisera specific for MRP-14 and S100A12 were used to directly compare the expression patterns of the proteins in consecutive or near consecutive sections of a variety of squamous epithelia. Both S100A12 and MRP-14 are constitutively expressed by the supra-basal cells of the oesophagus (Fig. 3-10B and C). However, the staining intensities did not directly correspond, S100A12 appeared to be most highly expressed by the less mature and smaller spinal cells, whereas MRP-14 was elevated in the later spinal and granular layers.

The expression of the MRP proteins by normal skin is less clear. Although skin is usually negative for both MRP-8 and MRP-14 (Brandtzaeg et al., 1987; Kunz et al., 1992), occasionally patchy MRP expression can be seen. Three different skin biopsies were negative for S100A12, even when MRP-14 staining was observed (Fig. 3-10E and F). The epithelial sheaths of hair follicles express high levels of MRP-14, regardless of the surrounding squamous epithelium, but were also negative for S100A12 (data not shown). The uppermost layer of human foetal scalp skin stained strongly for MRP-14, but this tissue was also negative for S100A12 (Fig. 3-10H and I). As reported, psoriatic skin stained for MRP-14 in all layers, including the proliferating basal layer (Brandtzaeg et al., 1987; Kunz et al., 1992). Two psoriatic biopsies were positive for S100A12, but the staining pattern was different from that of MRP-14 (Fig. 3-10K and L). Rather than the fairly even staining of MRP-14, the expression of S100A12 by basal and adjacent spinal layers was patchy and weak, with the more mature granular and horny layers staining strongly and more evenly. In each of these epithelial tissues the staining was specific as the control sera did not stain any epithelial cells (Fig 3.10A, D, G and J)

The observations above, combined with lack of S100A12 staining of the MRP-14 positive thymus endothelium (Table 3.1), clearly show that S100A12

expression in squamous epithelium is similar, but more restricted than that of MRP-14. Further, no staining of S100A12 was observed in tonsil, thymus, lung, salivary gland, stomach, colon, appendix, kidney and foetal trachea (see Table 3.1).

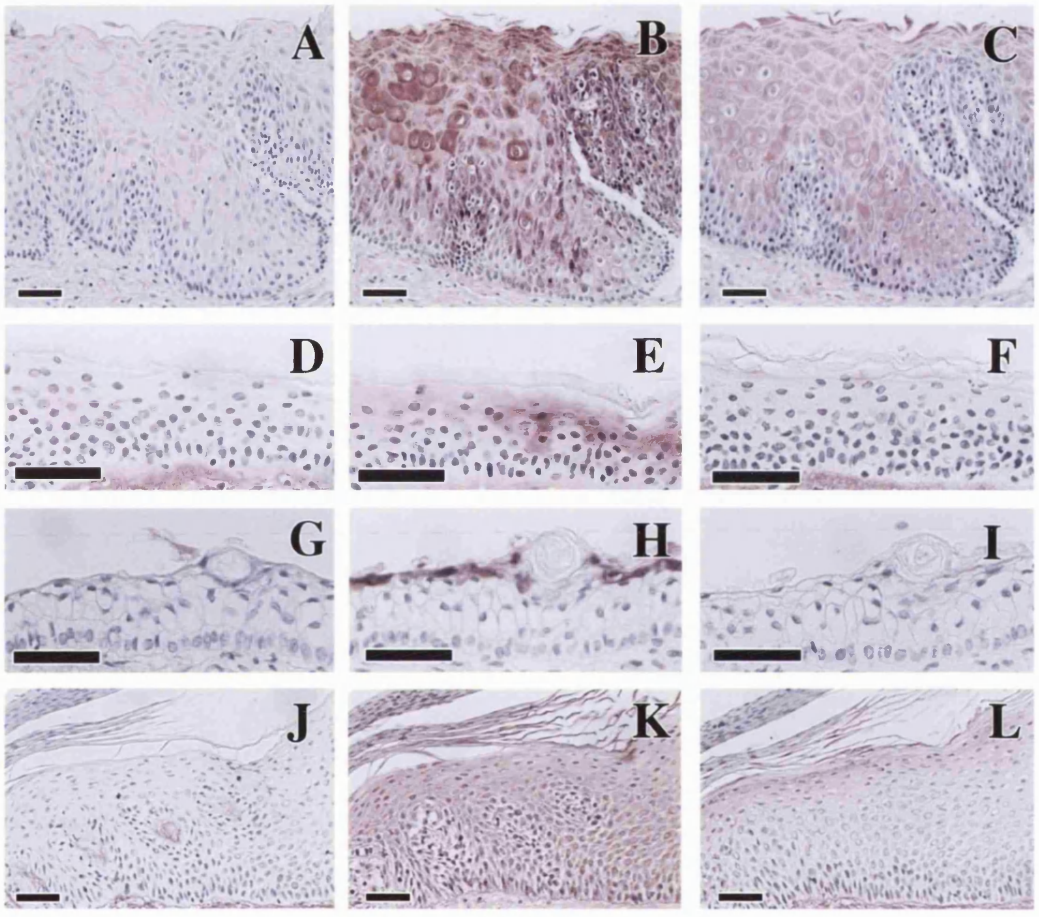

Figure 3.10: S100A12 Expression in Stratified Squamous Epithelia.
Immunohistochemistry of human tissues staining with the control sera (**A**, **D**, **G** and **J**), the MRP-14 antisera (**B**, **E**, **H** and **K**) and the S100A12 antisera (**C**, **F**, **I** and **L**) at 1 in 1,000. The tissues stained were oesophagus (**A-C**), skin (**D-F**), foetal scalp (**G-I**) and psoriatic skin (**J-L**). Scale bar: 50μm. This immunohistochemistry was performed by G. Elia (Histopathology Unit, ICRF).

Tissue	Expression of	
	S100A12	MRP-14
Lymph Node	− (+)[a]	− (+)[a]
Tonsil	−	+[b]
Thymus	−	−
Lung	−	−
Salivary Gland	−	−
Stomach	−	− (+)
Colon	−	− (+)[c]
Appendix	−	− (+)[c]
Kidney	−	− (+)
Foetal Trachea	−	− (+)

Table 3.1: S100A12 Expression in Other Tissues
A summary of the tissue distribution of S100A12 and MRP-14 as determined by immunohistochemistry performed with the relevant antisera at 1 in 1,000. − signifies no staining seen; − (+) signifies no general tissue staining, but occasional sporadic positive cells; and + signifies positive tissue staining observed. [a] Positive leukocytes largely restricted to the red pulp areas. [b] Capsular epithelium stained positive. [c] Positive cells mainly seen in lamina propria. This immunohistochemical study was performed by G. Elia (Histopathology Unit, ICRF).

3.2.f S100A12 is not Associated with the MRP Proteins

In human neutrophils MRP-8 and MRP-14 are noncovalently associated in a complex (Edgeworth et al., 1991; Teigelkamp et al., 1991). S100A12 consistently co-purifies with MRP-8 and MRP-14, using a protein purification protocol including Mono Q and Mono S chromatography ((Edgeworth et al., 1991) and data not shown). Together with the similar cell specific expression and subcellular localisation (Guignard et al., 1995; Vogl et al., 1999), it was considered that S100A12 might exist in complex with MRP8/14. To test whether S100A12 and MRP-14 could be co-immunoprecipitated from neutrophil lysate, immunoprecipitates with S100A12, MRP-14 and control antisera were analysed by Western blotting. This revealed that MRP-14 antisera precipitated both MRP-8 and -14, suggesting that under the lysis conditions the complex remained intact (Fig 3.11, Lane 3). However, no S100A12 co-precipitated with the MRP-14 antisera, and the S100A12 antisera did not co-precipitate MRP-8 or MRP-14 (Fig 3.11, Lane 3 and 2). Furthermore, activation of neutrophils by fMLP or ionomycin, which can induce subcellular translocation of both the MRP proteins (Lemarchand et al., 1992) and S100A12 (Guignard et al., 1995), did not cause S100A12 and MRP-14 to co-immunoprecipitate (Fig 3.11, Lanes 5, 6, 8 and 9). The immunoprecipitations were specific as the control antisera failed to precipitate any of the three proteins from resting and activated neutrophils (Fig 3.11, Lanes 1, 4 and 7). Therefore, under lysis conditions that maintain the MRP-8 and -14 interaction, S100A12 was found not to be complexed with the MRP proteins in either resting or activated neutrophils.

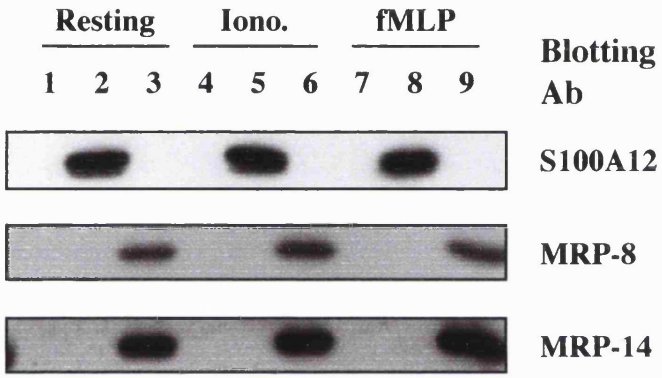

Figure 3.11: Failure to Co-Immunoprecipitate S100A12 and MRP-14
Immunoprecipitates of S100A12 antisera (Lane 2, 5 and 8), MRP-14 antisera (Lane 3, 6 and 9) and the control sera (Lane 1, 4 and 7) were made from the NP40 lysates of resting (Lanes 1-3), fMLP-activated (Lanes 4-6) and ionomycin-activated (Lanes 7-9) neutrophils. The immunoprecipitate from 25μg of total protein was loaded per lane. Shown is the Western blot analysis with the antisera against S100A12, MRP-8 and MRP-14 used at 1 in 10,000, 1 in 5,000 and 1 in 10,000, respectively.

3.2.g rS100A12 Does Not Induce or Inhibit Leukocytes Adhesion to Fibrinogen

Work from this laboratory has shown that rMRP-14 induces Mac-1-mediated adhesion of neutrophils to fibrinogen in a static adhesion assay (Newton and Hogg, 1998). As MRP-14 is the closest homologue to S100A12, whether rS100A12 stimulated neutrophil binding in similar fashion was investigated. Over a concentration range in which rMRP-14 is functional, rS100A12 failed to induce neutrophil adhesion to fibrinogen (Fig 3.12A). As murine MRP-8 is functional at much lower concentrations, rS100A12 was titrated down to 20pM, but still did not stimulate binding (Fig 3.12B).

Recombinant human MRP-8 (rMRP-8) specifically inhibits rMRP-14 induced adhesion of neutrophils, probably by heterodimer formation. As a control rMRP-8 did not effect fMLP-stimulated binding (Newton and Hogg, 1998). Consequently, rS100A12 inhibition of rMRP-14- and fMLP-stimulated adhesion of neutrophils to fibrinogen was evaluated. Over a concentration range in which rMRP-8 is functional, rS100A12 failed to inhibit the adhesion stimulated by either rMRP-14 or fMLP (Fig 3.13A and B).

rMRP-14 stimulation of neutrophil binding is inhibited by pertussis toxin, thus indicating that rMRP-14 induced binding is mediated by a G protein coupled receptor (Newton and Hogg, 1998). rMRP-14 also stimulates T lymphoblasts and the promonocytic cell line THP-1 to adhere to fibrinogen, because presumably these cells also possess the putative MRP-14 receptor. rS100A12 did not induce T lymphoblasts or THP-1 cell adhesion (Fig 3.14A and data not shown), suggesting these cells do not possess a functionally similar receptor for rS100A12. Additionally, rS100A12 did not inhibit the rMRP-14 stimulated adhesion of T lymphoblasts and THP-1 cells (Fig 3.14B and data not shown) in a similar fashion to rMRP-8 and (Newton, 1997). Therefore, rS100A12 does not have a proadhesive function similar to rMRP-14, and it does not regulate rMRP-14 like rMRP-8.

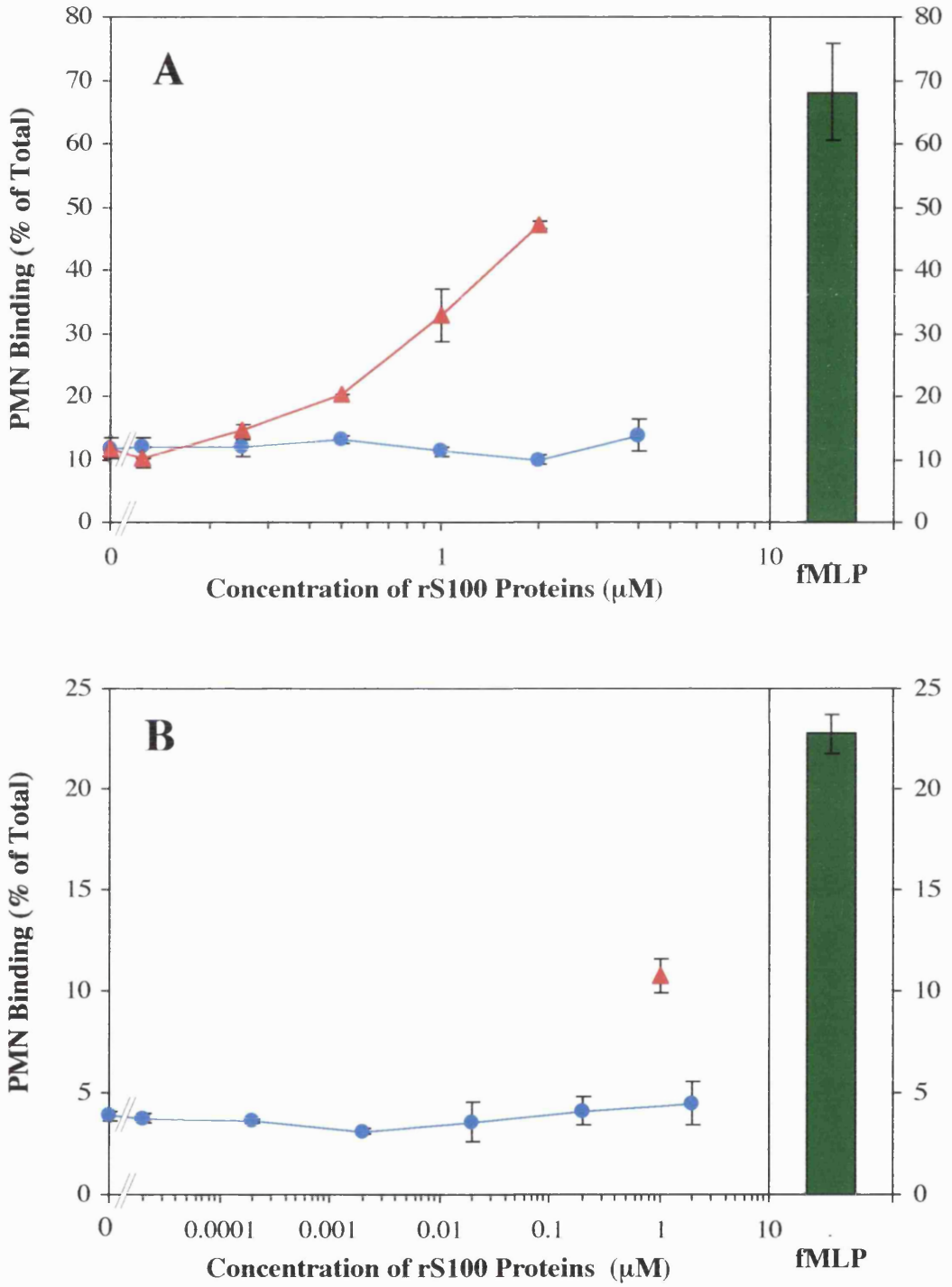

Figure 3.12: S100A12 Does Not Induce Neutrophil Binding to Fibrinogen
rS100A12 (●) as a stimulus in the neutrophil binding to fibrinogen static adhesion assay, as compared to rMRP-14 (▲). rS100A12 is titrated over a similar range to rMRP-14 (**A**) and over a more extensive range (**B**). 100nM fMLP (■) acted as a positive control in each experiment. Data are means of triplicates ± SD. Both **A** and **B** are representative experiments of four.

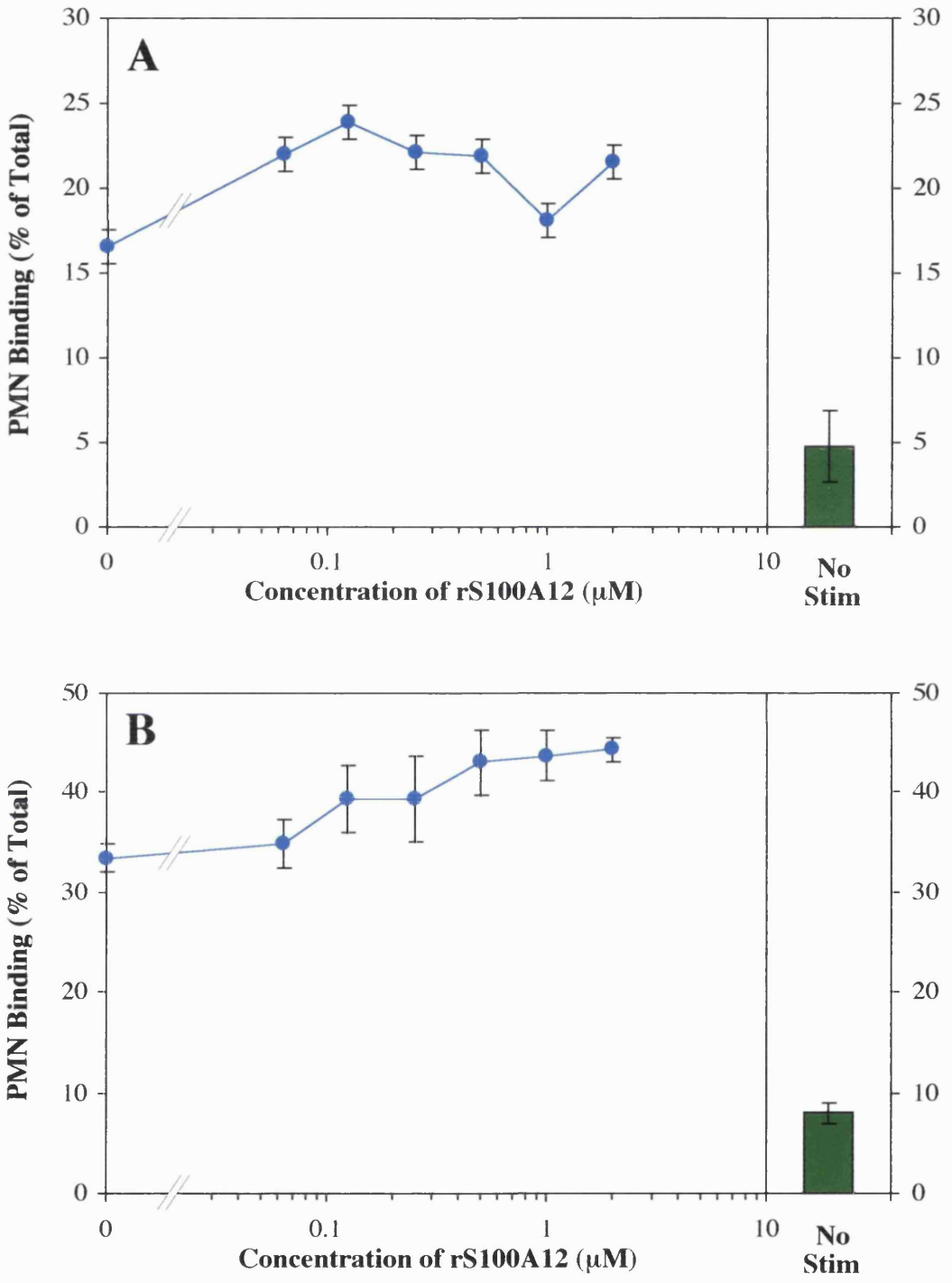

Figure 3.13: S100A12 Does Not Inhibit rMRP-14 or fMLP Stimulated Neutrophil Binding to Fibrinogen

The effect of S100A12 (●) on 1μM rMRP-14 (**A**) and 10nM fMLP (**B**) stimulated neutrophil adhesion to fibrinogen in the static adhesion assay. The no stimulation controls (no rMRP-14, fMLP or S100A12) are shown (■). Data are means of triplicates ± SD. Representative experiments of two for **A** and three for **B** are shown.

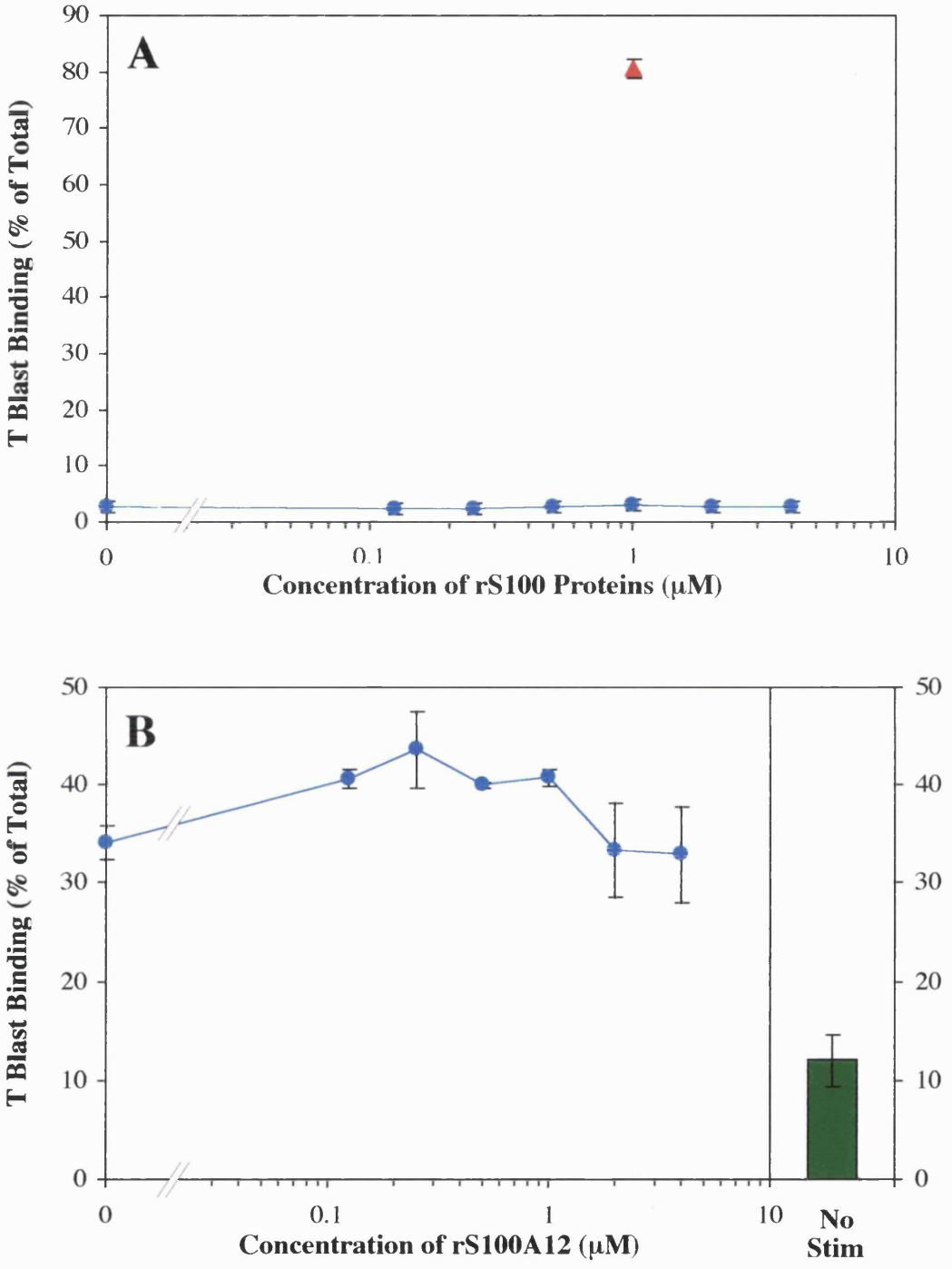

Figure 3.14: S100A12 Does Not Induce T Lymphoblast Binding to Fibrinogen or Inhibit rMRP-14 Stimulated Binding

A) rMRP-14 (▲) and rS100A12 (●) as stimuli in the T lymphoblast binding to fibrinogen static adhesion assay. **B**) The effect of rS100A12 (●) on 1μM rMRP-14 induced binding of T lymphoblasts to fibrinogen in the static adhesion assay. The binding in the absence of stimulus is shown (■). Data are means of triplicates ± SD. Representative experiments of four for **A** and two for **B** are shown.

3.2.h rS100A12 Does Not Induce Mac-1 Upregulation or L-Selectin Shedding by Neutrophils

rMRP-14 is an unusual activator of neutrophils, because, under all tested conditions, it does not stimulate degranulation, superoxide burst or shape change (Newton and Hogg, 1998). An increase in Mac-1 expression and the shedding of L-selectin are good indicators of general neutrophil activation. 1μM rS100A12, like rMRP-14, did not induce Mac-1 expression or L-selectin shedding (Fig 3.15). Although a general activator was not used as a positive control in the same assays, under the same assay conditions fMLP caused upregulation of Mac-1 and shedding of L-selectin (data not shown). Therefore, these cell surface indicators of neutrophils activation are not modulated by rS100A12, suggesting S100A12 does not activate neutrophils.

3.2.i rS100A12 in the Air Pouch, an In Vivo Model of Chemotaxis

Recombinant murine MRP-14 is not chemotactic for murine neutrophils in vitro, but induces the influx of millions of leukocytes, primarily neutrophils, into the mouse air pouch, an in vivo model of chemotaxis (May, R. et al, manuscript in preparation). This is mediated by induction of chemokines, including MIP-2 and KC, from an unknown source. In the air pouch model, rS100A12 did induce a statistically significant influx, as compared to the PBS injected control. However, this influx was very small, as compared with other stimuli such as recombinant murine MRP-14, TNFα and LPS (Fig 3.16 and data not shown). Additionally, the influx over a titration range did not form the bell-shaped curve observed with other chemoattractants.

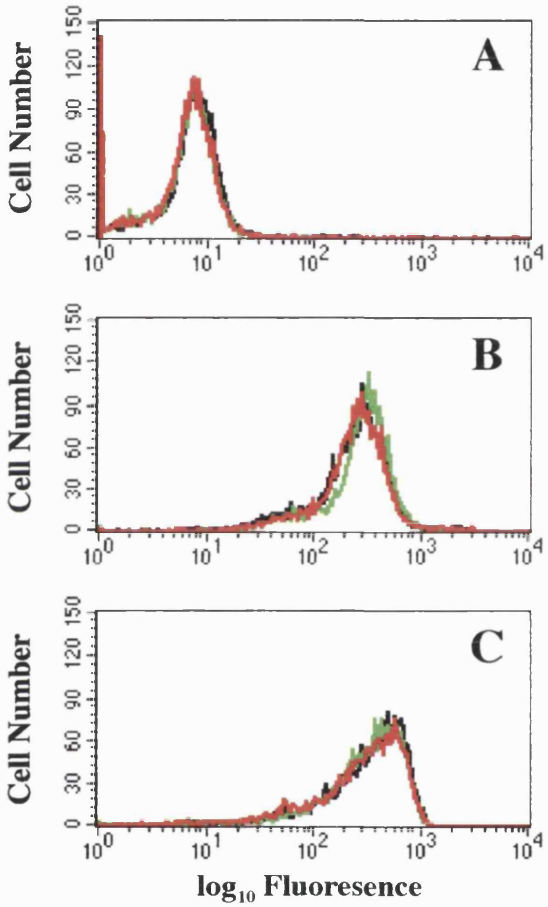

Figure 3.15: Effect of rS100A12 and rMRP-14 on Neutrophil Expression of Mac-1 and L-Selectin

The effect of no stimulus (—), 1μM rS100A12 (—) and 1μM rMRP-14 (—) on neutrophil expression of CD11b (**B**) and L-selectin (**C**) as compared to a control mAb (**A**) using mAbs: ICRF44, Lam 1.3 and 52U, respectively. The data is from 5,000 cells, and a representative experiments of three is shown.

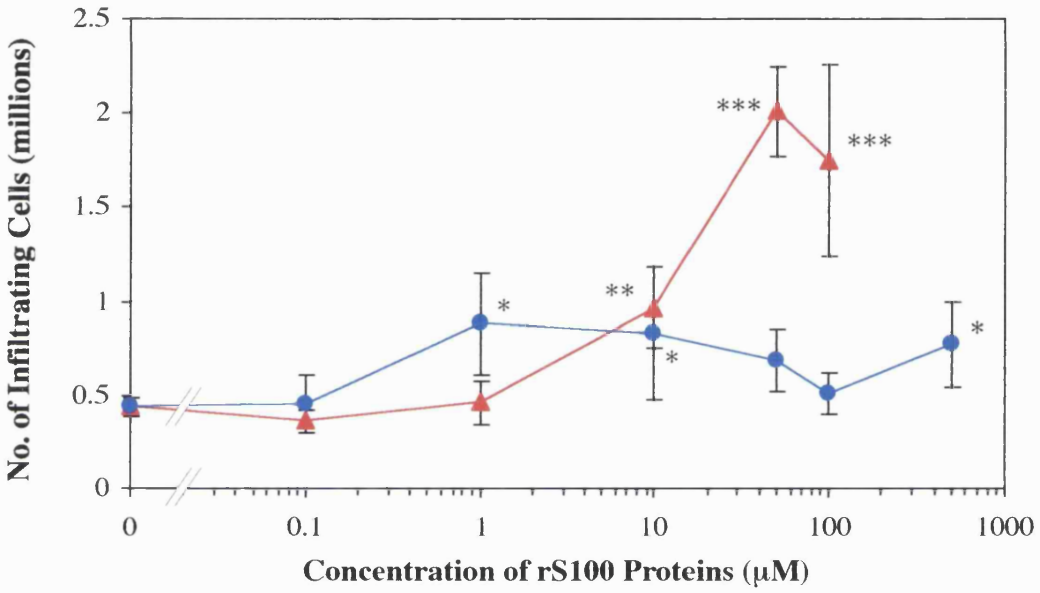

Fig 3.16: rS100A12 in the Air Pouch, an In Vivo Model of Chemotaxis
Total leukocytes migrating into the air pouch 6 hours following injection of recombinant murine MRP-14 (▲) and rS100A12 (●) into the air pouch. The data is the mean of 3-18 mice ± S.E.M. Significance by the T test is indicated by: * $P<0.05$ but >0.01; ** $P<0.01$; and *** $P<0.0001$.

3.3 Discussion

3.3.a Cloning S100A12 cDNA and Expression of rS100A12

As an initial approach to cloning the cDNA encoding S100A12, two primers were designed from the terminal amino acids sequences of the protein (Marti et al., 1996) using the most common codons. PCR with these primers successfully amplified the cDNA encoding S100A12 from bone marrow cDNA. The sequence of two clones agreed with the nucleotide sequence, which was published while this work was in progress (Wicki et al., 1996).

Tagging sequences are often added to recombinant proteins to aid purification. However, they are ideally cleaved by proteolysis for functional assays, which can cause complications and/or add contaminants. S100 proteins are relatively easy to purify, because they are small, have a very low pI, bind calcium and are soluble in saturated ammonium sulphate solution. Consequently, the cDNA encoding S100A12 was inserted into the pET3A vector. pET3A is a simple protein expression vector, which does not add any tagging sequences. rS100A12 was purified to homogeneity from the bacterial cytosol and stored, using a protocol developed from that of rMRP-14. As rMRP-14 is active, it was considered that by using the same purification and storage protocol the rS100A12 also should be functional.

3.3.b Expression of S100A12 by Leukocytes

Human neutrophils are known to express high levels of S100A12, constituting about 5% of the cytosolic protein. Preparations of PBMCs have also been shown to be positive (Dell'Angelica et al., 1994; Guignard et al., 1995; Vogl et al., 1999), but the expressing cell type has been controversial. The primary reason for this confusion has been the use of cell populations purified from whole blood, thus contaminating neutrophils could not be excluded as the source of S100A12. To

overcome this problem, analysis was performed at the single cell level, by cytospin staining, and it was proven that monocytes were clearly positive for S100A12. However, a recent report claims that monocytes analysed by cytospin staining and intracellular flow cytometric analysis were negative for S100A12 (Vogl et al., 1999). This conflicting result may have been due to the authors use of a less sensitive or low titre antisera, as the monocyte expression of S100A12 was relatively low.

T and B cell lines including Jurkat cells, erythroleukemia cell line K-562 and microvascular endothelial cell line HMEC-1, were all negative for S100A12 and the MRP proteins. The early monocytic cell line, THP-1, was weakly positive for MRP-8 and MRP-14, but negative for S100A12. The less mature myeloid cell lines, U-937 and HL-60, were negative for all three S100 proteins. Interestingly, HL60 differentiated to monocytes by 1α,25-dihydroxy-vitamin D_3 and to neutrophils by DMSO express MRP-14 and MRP-8 (Koike et al., 1992), but not S100A12 (Vogl et al., 1999). These results are consistent with MRP-8 and MRP-14 being expressed by monocytes and neutrophils, but only late in maturation at the metamyelocyte stage (Hessian et al., 1993). Because S100A12 is not expressed by THP-1 cells or differentiated HL-60 cells but is detected in fully mature circulating myeloid cells, it is possible that S100A12 is expressed at an even later stage of myeloid differentiation than the MRP proteins. However, a more detailed study of bone marrow and circulating myeloid cells would be required to evaluate this hypothesis.

The S100A12 antisera did not stain any non-lymphoid non-epithelial tissues, including liver, thymus and lung, which are highly populated by resident tissue macrophages. Therefore, this is strong evidence that, like the MRP proteins, resident tissue macrophages in non-inflammatory situations do not express S100A12. In two lymphoid tissues, the spleen and lymph node, neutrophil-like S100A12 positive cells were observed in the red pulp areas and in particular in the perifollicular zone in the spleen. Macrophages at chronic inflammatory sites, such as Crohn's disease, express the MRP proteins. A Crohn's disease biopsy contained S100A12 positive cells. However, the only positively identified cell type was the infiltrating neutrophil.

Therefore, these results do not fully elucidate the expression of S100A12 by tissue leukocytes. However, infiltrating neutrophils appear to be S100A12 positive, and resident tissue macrophages of normal tissue are probably negative. Double labelling with cell lineage markers is required to fully and conclusively determine the S100A12 expressing cell types.

3.3.c Expression of S100A12 in Epithelial Tissues

The expression of MRP-8 and -14 by some squamous epithelial tissues is strictly regulated in differentiation and by disease processes (see Section 1.3.c.ii). The supra-basal cells of oesophagus epithelium were S100A12 and MRP-14 positive. This implies that the expression of both proteins is switched on very early in the differentiation of oesophageal cells. The detection of S100A12 in oesophagus was subsequently reported by Hitomi et al. (Hitomi et al., 1998).

The MRP-14 positive non-mucosal epithelia analysed were negative for S100A12, except in the skin inflammatory condition psoriasis. In two psoriatic biopsies, MRP-14 was detected strongly and evenly in all layers including the basal layer, whereas S100A12 stained mainly the upper layers. This too was subsequently published (Mirmohammadsadegh et al., 2000). S100A12 was not detectable in any of the non-epithelial and non-lymphoid tissues stained.

Overall, the expression of S100A12 in epithelia was similar to, but more limited than the MRP proteins. Interestingly, as for leukocytes, S100A12 was not detected in cells that did not express the MRP protein. Currently, the function of the MRP proteins in epithelium is unknown, but they have been linked with the differentiation of hyperproliferating cells (see Section 1.3.c.ii). The S100A12 expression data presented here and the growth arrest induced by transfecting oesophageal carcinoma cell line with S100A12 (Hitomi et al., 1998) are consistent with a similar function for S100A12. Whether or not these S100 proteins contribute

to the pathology of dermatoses by inducing and/or aiding inflammation also is unknown.

3.3.d Potential Functions of S100A12

In this laboratory, it has been shown rMRP-14 stimulates the binding of neutrophils, T lymphoblasts and a promonocytic cell line (THP-1) to fibrinogen. S100A12 is most homologous to MRP-14, and thus was used in the above assays. rS100A12 did not stimulate adhesion of these leukocytes to fibrinogen, nor did the recombinant protein inhibit rMRP-14 induced binding, like rMRP-8. The functional assay for recombinant murine MRP-14, in the laboratory, is the induction of neutrophil influx in to the air pouch. rS100A12 induced a statistically significant influx of leukocytes, but the influx was very low and did not titrate, and consequently, this was not investigated further.

The assays described above were unable to elucidate any potential function for S100A12. This could be due to many reasons. Firstly, the recombinant form may not be functional. This is always a possibility with recombinant proteins as they may be misfolded. However, this was thought not to be the case for rS100A12, because it was purified and stored in a similar fashion to the active rMRP-14. Also the rS100A12 bound to the hydroxyapatite column, suggesting it is capable of binding calcium. Secondly, S100A12 may require posttranslational modification to be functional. Although, this is not the case for the MRP proteins, and such a modification of native S100A12 has not been reported. Thirdly, one of the many variables in the assays may not have been optimal for rS100A12 function. However, by using assays based on recombinant murine and human MRP-14 it was hoped to largely circumvent this problem. Finally, the function of S100A12 may not be linked to those of the MRP proteins that were assayed for. All four reasons are possible and complex to investigate, so it was decided that none of these routes would be investigated directly. Rather, the mechanism of action of rMRP-14 would be

investigated with the hope that any discovery would shed light on a potential function for S100A12. Thus, the investigations reported in the following chapters were based on rMRP-14, with rS100A12 being evaluated subsequently.

Since this investigation, rS100A12 was reported to be proinflammatory via an interaction with the receptor for advanced glycation end products (RAGE) (Hofmann et al., 1999). The neutrophil, T lymphoblast and THP-1 expression of RAGE is unknown, and thus the proadhesive effect of S100A12 on a cell known to express the putative receptor has not been knowingly evaluated. The chemotactic activity of rS100A12 in vivo, shown by Hoffman et al. (Hofmann et al., 1999), appears to conflict with the failure of rS100A12 to induce a sizeable influx of leukocytes in the air pouch model. However, there are considerable differences between the sub-cutaneous foot pad injection and the air pouch model, e.g. a 24 hour against a 6 hours time point. Initial investigations, performed in collaboration with A. McDowall and J. Hobbs (both of this laboratory), have failed to show rS100A12 to be chemotactic for peripheral blood monocytes and T lymphoblasts in vitro. Although preliminary, these results would also appear to contradict those of Hofmann et al (Hofmann et al., 1999).

Chapter 4

THE PROADHESIVE EFFECT OF rMRP-14

4.1 Introduction

The β_2 integrin Mac-1 (CD11b/CD18) is a promiscuous adhesion receptor predominantly expressed on neutrophils, monocytes and NK cells. Upon activation, Mac-1 is able to mediate adhesion to: several extracellular matrix proteins, such as fibronectin and laminin (Thompson and Matsushima, 1992); coagulation proteins, fibrinogen (Wright et al., 1988), kininogen (Sheng et al., 2000) and Factor X (Altieri and Edgington, 1988); and the endothelial proteins, ICAM-1 and –2 (Gahmberg, 1997b). Additionally, Mac-1 has been shown to mediate binding to several other proteins, including denatured BSA (Davis, 1992). The β_2 integrin is proposed to have a role in the adhesion, migration and invasion of myeloid and NK cells. Mac-1 can also act as a phagocytic receptor for iC3b opsonised bodies (Ross et al., 1985) and some bacterial glycoconjugates (reviewed by (Ehlers, 2000)).

Only a minor subset of T lymphocytes, approximately 5%, express the β_2 integrin Mac-1. This low level of expression is only increased by about twofold following phorbol ester stimulation (Muto et al., 1993). Thus T lymphocyte function is thought to be largely Mac-1 independent, and indeed T cell interactions with and transmigration through endothelium does not require Mac-1 (Andrew et al., 1998).

R. Newton, in this laboratory, demonstrated that rMRP-14 induced T lymphoblast adhesion to fibrinogen by a Mac-1 dependent mechanism. When the T lymphoblast expression of Mac-1 was investigated, only a minor population of the cells had detectable levels of cell surface Mac-1. However, upon rMRP-14 activation, but not phorbol ester stimulation, all the T lymphoblasts expressed Mac-1. The expression was induced in 30 minutes, and, therefore, was assumed to be independent of de novo protein synthesis. The activation of Mac-1 was similar to

that seen on neutrophils, as the 24 epitope was also upregulated (Newton, 1997). The 24 epitope is a reporter of high affinity β_2 integrins, and distinguishes these conformations from high avidity β_2 integrins that mediate binding by clustering (Stewart et al., 1996b). This was further supported by rMRP-14 induced binding of soluble fibrinogen (Newton, 1997), because high affinity, but not high avidity, β_2 integrins bind soluble ligands (Stewart et al., 1996b). It was therefore proposed that MRP-14 anchored on the endothelium proximal to inflammatory site would induce upregulation and activation of Mac-1 on T lymphocytes.

The aim of this project was to further characterise the rMRP-14 induced expression and activation of Mac-1.

4.2 Results

4.2.a T Lymphoblast Binding to Mac-1 Ligands

rMRP-14 induced T lymphoblast binding to the Mac-1 ligand, fibrinogen, was blocked by the ascitic fluid of the anti-CD11b monoclonal antibody, 2H3 (Newton, 1997). Because it was discovered rMRP-14 did not stimulate T lymphoblasts to adhere to fish skin gelatin (FSG), the adhesion assay was developed by blocking the fibrinogen-coated plates with FSG. It was hoped that the use of a blocking agent would simplify future investigations into adhesion to different ligands. Adding a FSG blocking step did not effect rMRP-14 stimulated binding to fibrinogen (Fig 4.1A), and the 2H3 ascitic fluid still was able to block the binding (Fig 4.1B).

Mac-1 is a very promiscuous receptor, so adhesion to other known ligands was determined. Because Mac-1 is known to ligate both denatured and native BSA (Davis, 1992), they were compared to fibrinogen and fish skin gelatin (FSG), as ligands in the T lymphoblast adhesion assay. rMRP-14 induced binding to urea denatured BSA was comparable to fibrinogen. Native BSA, as a ligand, supported

more binding than FSG, but required increased rMRP-14 concentrations to stimulate binding equivalent to denatured BSA or fibrinogen (Fig 4.2). Additionally, rMRP-14 also induced T lymphoblast binding to keyhole limpet haemocyanin (data not shown), another reported Mac-1 ligand (Shappell et al., 1990).

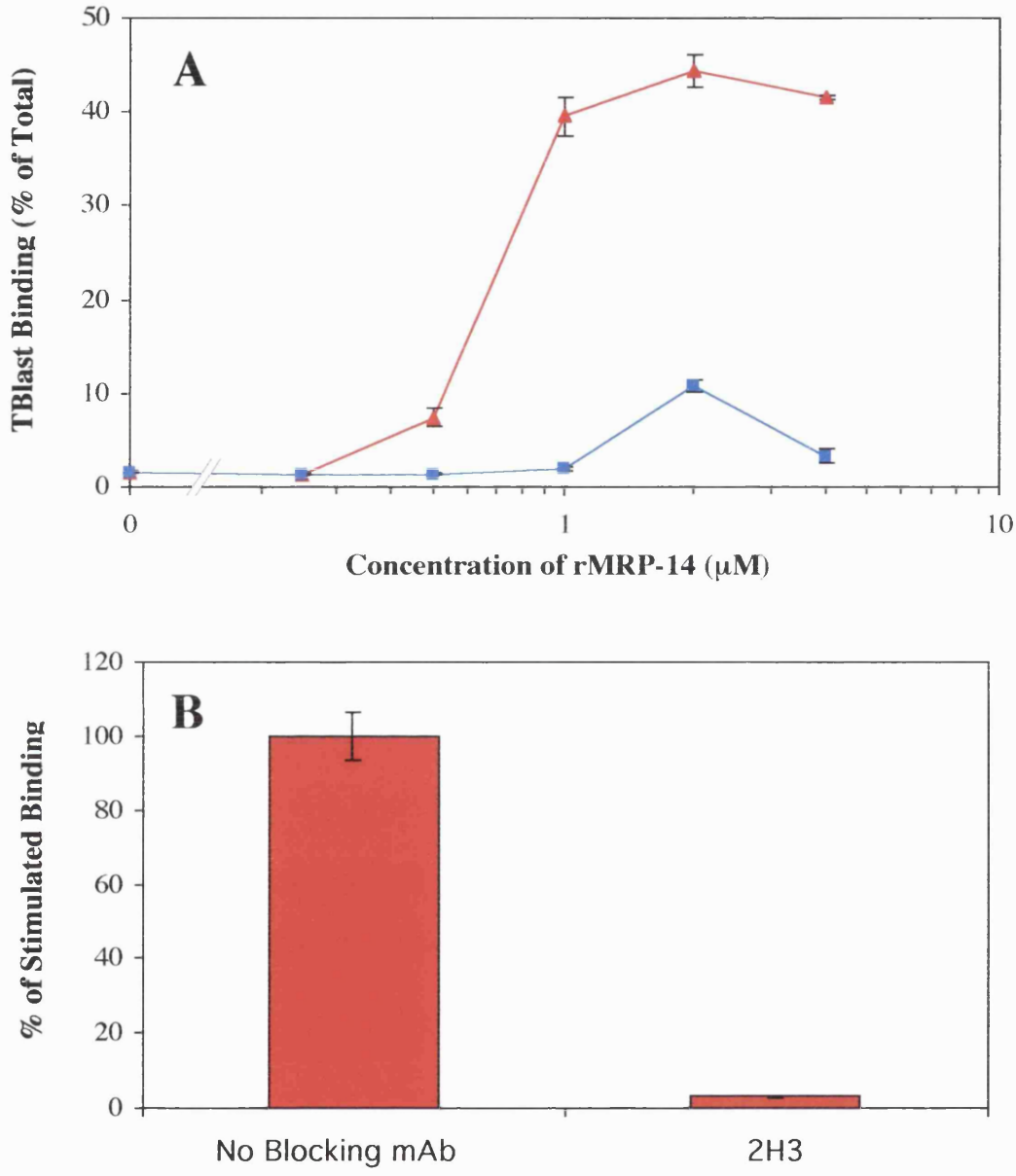

Figure 4.1: rMRP-14-Stimulated Binding of T lymphoblasts to FSG Blocked Fibrinogen and Blocking with 2H3

A) rMRP-14 stimulated binding of T lymphoblasts to fish skin gelatin (FSG; ■) and fibrinogen blocked with FSG (▲) in the static adhesion assay. **B**) The blocking of 1μM rMRP-14 stimulated binding of T lymphoblasts to fish skin gelatin blocked fibrinogen with the anti-Mac-1 ascites, 2H3, diluted at 1 in 100. Data are means of triplicates ± SD. Representative experiments of four (**A**) and two (**B**) are shown.

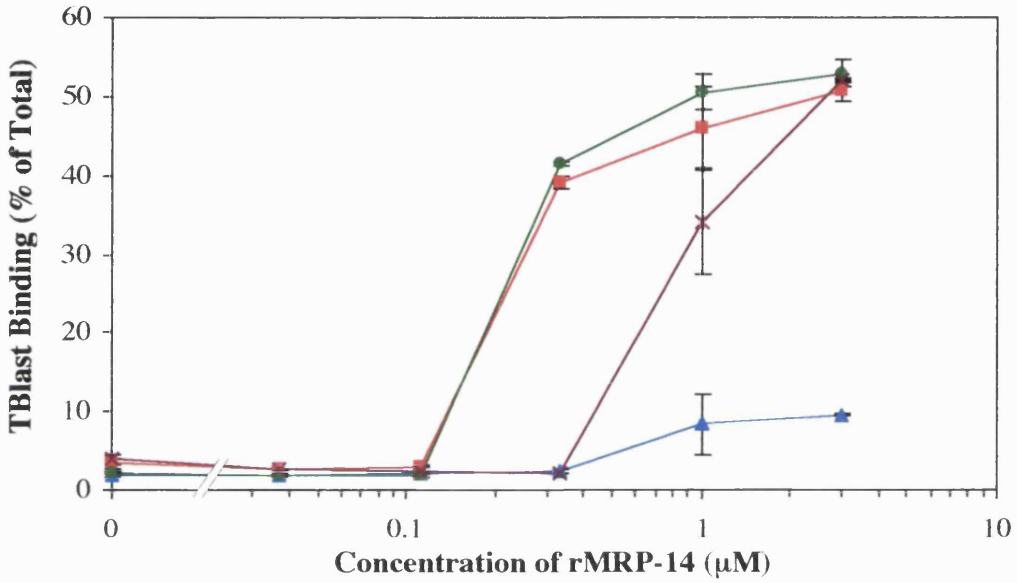

Figure 4-2: rMRP-14 Induces T Lymphoblast Binding to Various Mac-1 Ligands

rMRP-14 induces binding of T lymphoblasts to fish skin gelatin (▲), fibrinogen (■), native BSA (X) and denatured BSA (●) in the static adhesion assay. Data are means of triplicates ± SD. A representative experiment of three is shown.

4.2.b rMRP-14-Induced T Lymphoblast Adhesion to Fibrinogen is not Mediated by Mac-1

Ascitic fluids are crude peritoneal washes and contain protein components other than the monoclonal antibody. To determine if the 2H3 blocking of T lymphoblast binding to fibrinogen was mediated by the antibody, the null ascitic fluid, SP-2, was used as a control. SP-2 ascites is produced by the unfused myeloma cell line, and therefore does not contain monoclonal antibody. At the lower dilution of 1 in 400, 2H3 blocked 1μM rMRP-14-stimulated T lymphoblast binding to fibrinogen, but this blocking was reduced when diluted 1 in 800. The null ascites inhibited the rMRP-14-stimulated adhesion almost exactly as well as 2H3. This contrasted with binding stimulated by the phorbol ester, PdBu, which was blocked effectively by both dilutions of 2H3, but not SP-2 (Fig 4.3). These results infer that, 2H3 blocking of rMRP-14 induced binding of T lymphoblast to fibrinogen was non-specific. In addition, the rMRP-14 proadhesive effect may not be mediated by Mac-1, because at 1 in 800 the 2H3 ascites completely blocked PdBu but only partially blocked rMRP-14 stimulated binding. Alternatively, the PdBu-stimulated binding was lower than that induced by rMRP-14, and consequently may be weaker and more easily blocked.

To further evaluate the contribution of Mac-1 to rMRP-14-stimulated binding of T lymphoblast to fibrinogen, purified mAbs were used as blocking agents. Four mAbs, reported to block Mac-1-mediated adhesion, were selected. Namely, these were: the anti-CD11b antibody, 2LPM19c (Diamond et al., 1993); and the anti-CD18 antibodies, TS1/18 (Diamond et al., 1993), 6.5E (Au et al., 1994) and IB4 (Wright et al., 1983). The purified mAbs blocked PdBu-stimulated adhesion, but failed to block the rMRP-14-induced binding (Fig 4.4A). Preincubating the T lymphoblasts with IB4 prior to activation failed to enhance the blocking (Fig 4.4B), thereby eliminating a temporal difference in PdBu and rMRP-14 activation, as an explanation of the observed difference in blocking.

Integrin mediated adhesion is an active process, and therefore is optimal at 37°C and reversed at 4°C. Performing the static assay at 4°C and using chilled buffers was able to completely inhibit PbBu-activated binding, but did not effect rMRP-14-stimulated adhesion as compared to that achieved at 37°C (Fig 4.5). This further suggests that the observed adhesion is not integrin mediated, unless rMRP-14 binds directly to the integrin and induces a conformational change.

Like all integrins, cell surface expression of the α subunit of Mac-1 is dependent on the β subunit (Springer et al., 1984). $SK\beta_2.7$ is a T lymphoblast cell line that has been mutated to lack expression of CD18 (Weber et al., 1997), and thus does not express Mac-1 (also see Fig 4.11D). The parental cell line, SKW3, adhered to fibrinogen in a similar fashion to T lymphocytes. The $SK\beta_2.7$ cells failed to bind to fibrinogen when activated by PdBu, but bound when treated with rMRP-14 (Fig 4.6). This excludes the possibility that rMRP-14 stimulated binding is mediated by a β_2 integrin, such as Mac-1.

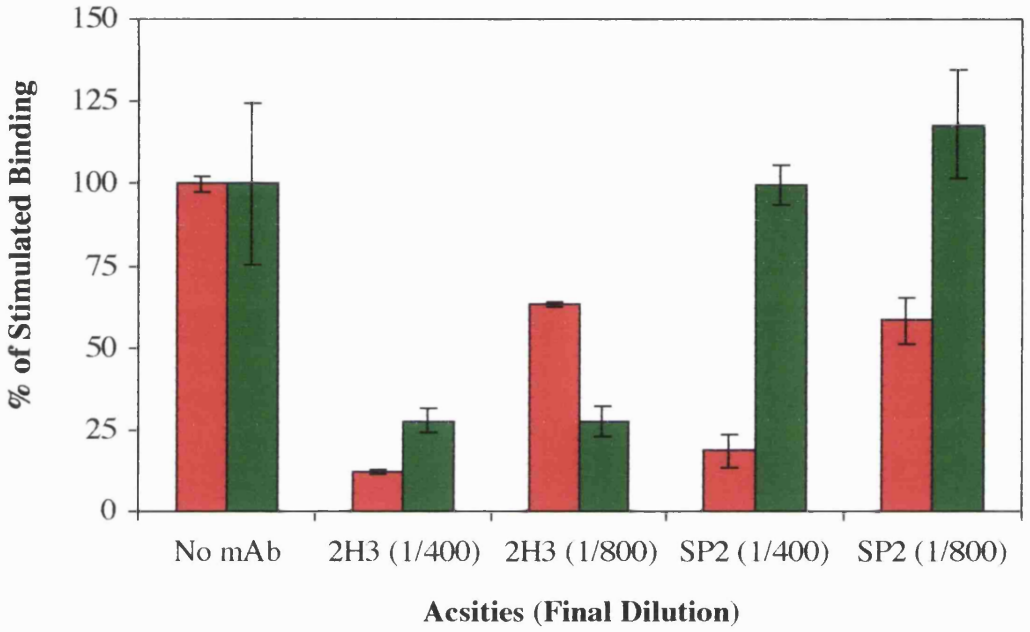

Figure 4-3: 2H3 and SP-2 Ascitic Fluid Blocking of Stimulated T Lymphoblast Binding to Fibrinogen

The effect of the anti-Mac-1 mAb, 2H3, and control ascites, SP-2, diluted 1 in 400 and 1 in 800 on 1μM rMRP-14 (■) and PdBu (■) stimulated binding of T lymphoblasts to fibrinogen in the static adhesion assay. Data are means of triplicates ± SD. Representative experiments of three for 1μM rMRP-14 and two for PdBu are shown.

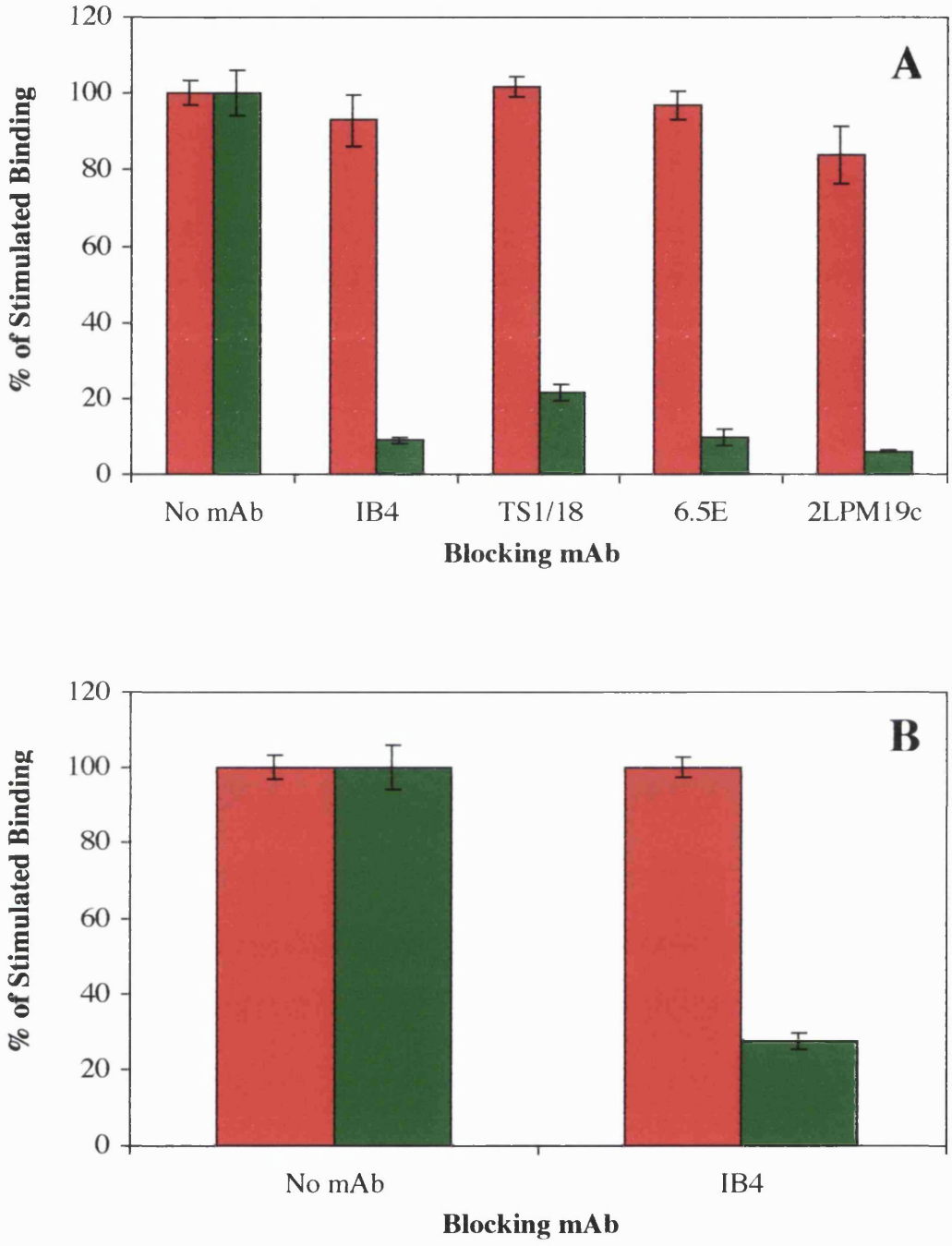

Figure 4.4: The Blocking of Stimulated T Lymphoblast Binding to Fibrinogen by Purified Anti-CD11b and -CD18 Antibodies

A) The effect of purified anti-CD18 blocking mAbs, IB4, TS1/18 and 6.5E, and the anti-Mac-1 blocking mAb, 2LPM19c on 1μM rMRP-14 (■) and PdBu (■) stimulated binding of T lymphoblasts to fibrinogen in the static adhesion assay. **B**) The effect of the anti-CD18 mAb IB4 on the same assay following preincubation with the cells. The anti-CD18 mAbs were used at 10 μg/ml and 2LPM19c at an optimal dilution. Data are means of triplicates ± SD. **A** is a representative experiment of three, where as **B** is a representative of two.

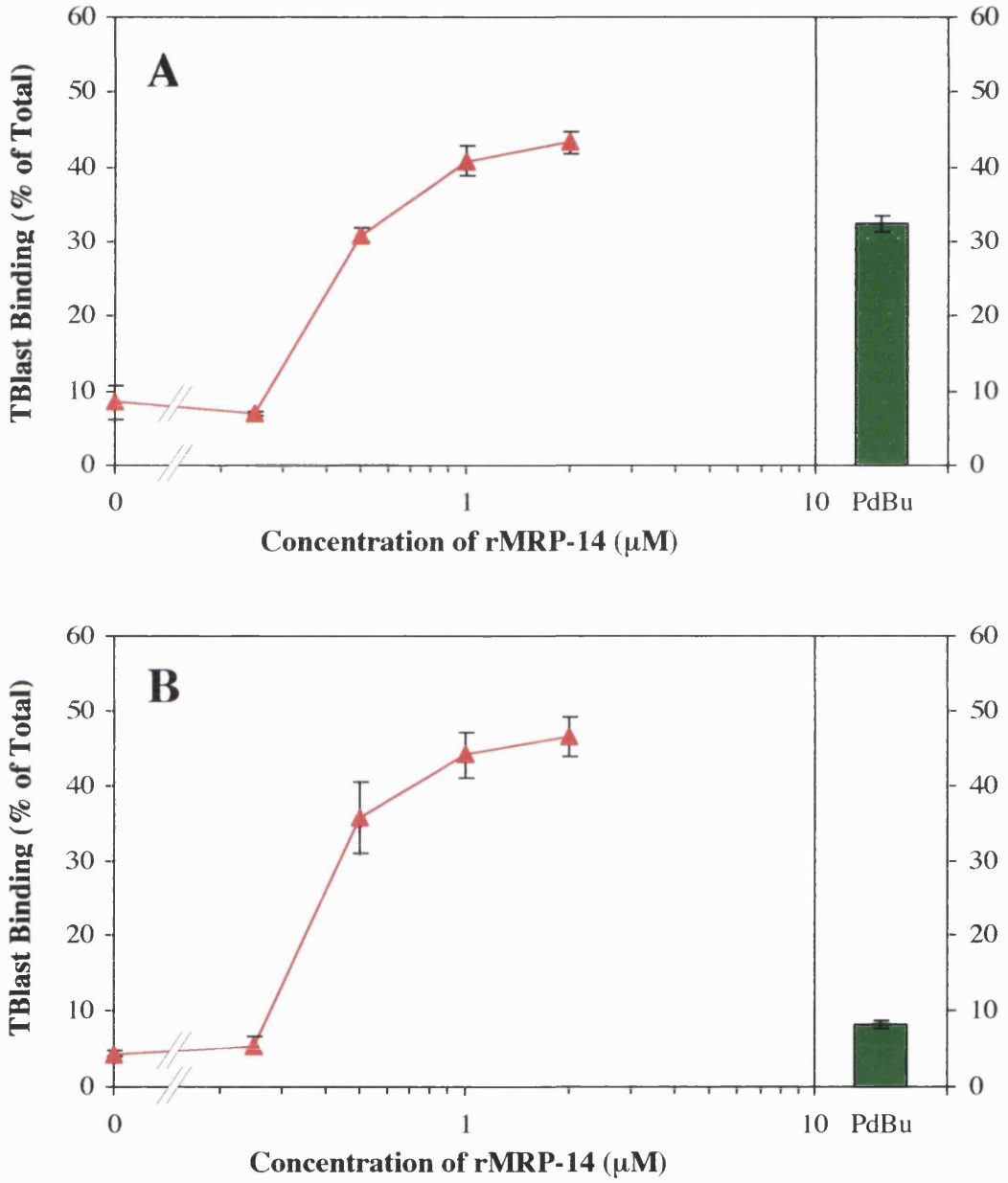

Figure 4.5: rMRP-14-Stimulated Binding of T lymphoblasts to Fibrinogen at 37°C and 4°C

rMRP-14 (▲) and 50nM PdBu (■) stimulated binding of T lymphoblasts to fibrinogen in the static adhesion assay at **A**) 37°C and **B**) 4°C. Data are means of triplicates ± SD. A representative experiment of two is shown.

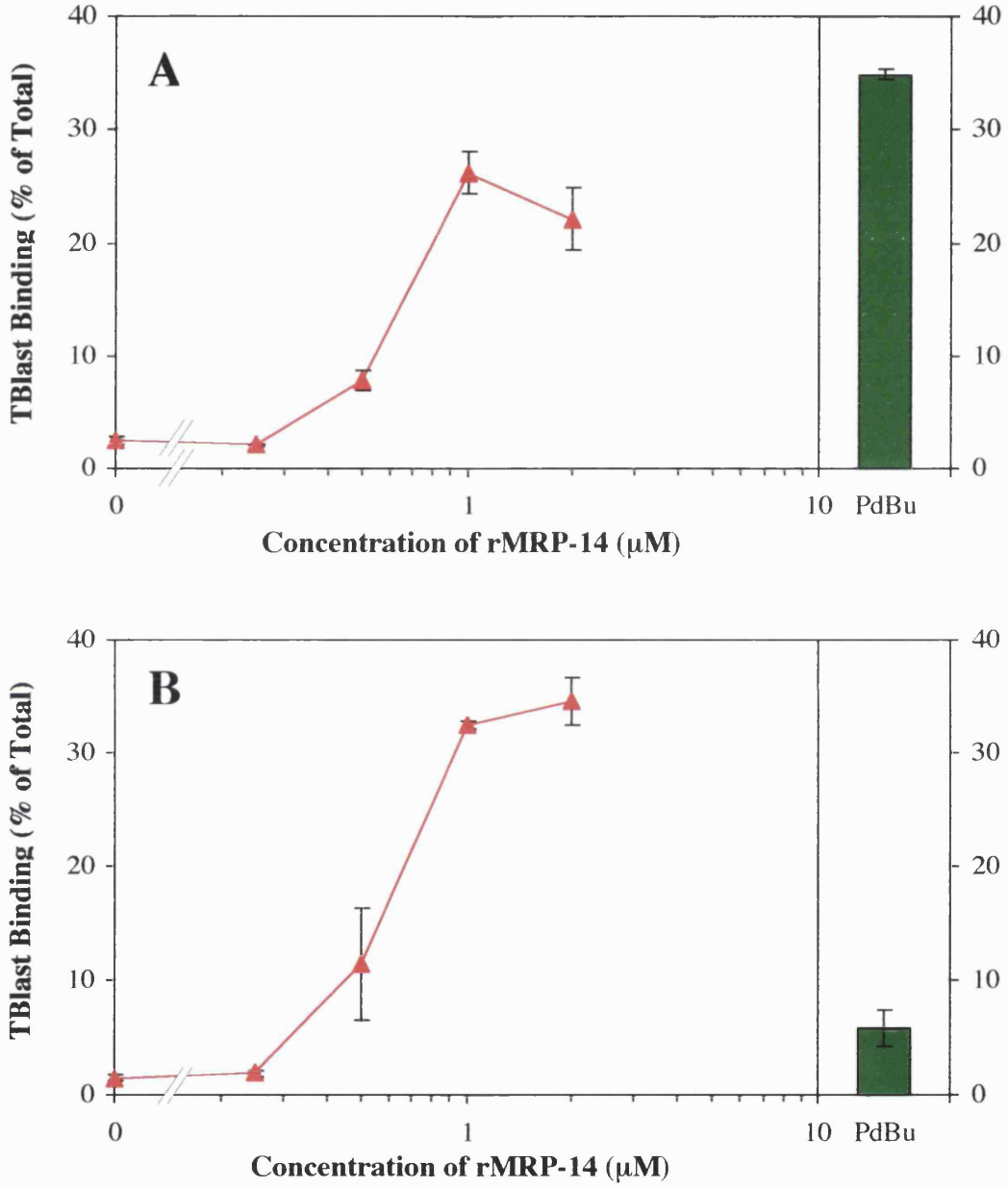

Figure 4.6: rMRP-14-Stimulated Binding of SKW3 and SKβ_2.7 Cells to Fibrinogen

rMRP-14 (▲) and 50nM PdBu (■) stimulated binding of **A**) SKW3 and **B**) SKβ_2.7 cells to fibrinogen in the static adhesion assay. Data are means of triplicates ± SD. A representative experiment of two is shown.

4.2.c rMRP-14-Stimulated Neutrophil Binding to Fibrinogen is not Mac-1 Mediated.

R. Newton reported that rMRP-14 stimulated adhesion of neutrophils to fibrinogen was blocked by 2LPM19c, and, therefore, was mediated by Mac-1 (Newton and Hogg, 1998). These blocking studies were conducted with both purified mAb and ascites, but in light of the above results these neutrophil experiments were re-investigated. The blocking of fMLP-stimulated neutrophil adhesion by purified anti-CD18 mAbs differed: TS1/18 only partially blocked, whereas IB4 and 6.5E almost completely inhibited the binding. The anti-CD11b mAb, 2LPM19c, was titrated to block optimally in the assay. This changed dramatically when rMRP-14 was used as a stimulus, as TS1/18 and 6.5E did not block the induced adhesion. IB4 reduced adhesion by about 30%, but this was not observed in two repeat experiments. 2LPM19c also failed to block the rMRP-14 stimulated binding (Fig 4.7). This result therefore contradicts the reported data.

In the fibrinogen adhesion assay, the binding to the blocking agent, FSG, was also determined as a control. Unstimulated neutrophils bound poorly to both FSG and fibrinogen. rMRP-14 stimulated binding to fibrinogen, but not FSG, as with T lymphoblasts. However, fMLP-activated neutrophils bound to FSG and fibrinogen to a similar level (Fig 4.8A and B). This binding to FSG was blocked with the anti-CD18 mAb, IB4 (Fig 4.8C). Thus FSG is probably a ligand for the promiscuous Mac-1, but rMRP-14 does not induce binding to this ligand. These results infer that not only is the rMRP-14 adhesion not dependent on Mac-1, but also that Mac-1 is not activated by rMRP-14.

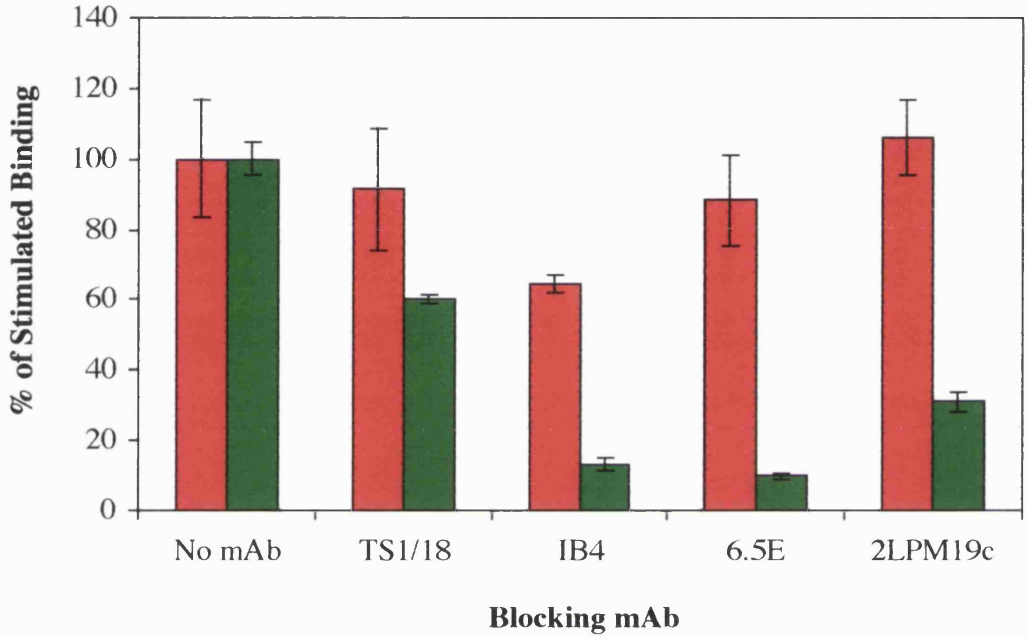

Figure 4.7: The Blocking of rMRP-14- and fMLP-Stimulated Neutrophil Binding to Fibrinogen by Purified Anti-CD11b and -CD18 mAbs

The effect of the anti-CD18 mAbs, TS1/18, IB4 and 6.5E at 10μg/ml and the anti-CD11b mAb, 2LPM19c at an optimal dilution, on 1μM rMRP-14 (■) and 100nM fMLP (■) stimulated binding of neutrophils to fibrinogen in the static adhesion assay. Data are means of triplicates ± SD. A representative experiment of three (or two for 6.5E and 2LPM19c) is shown.

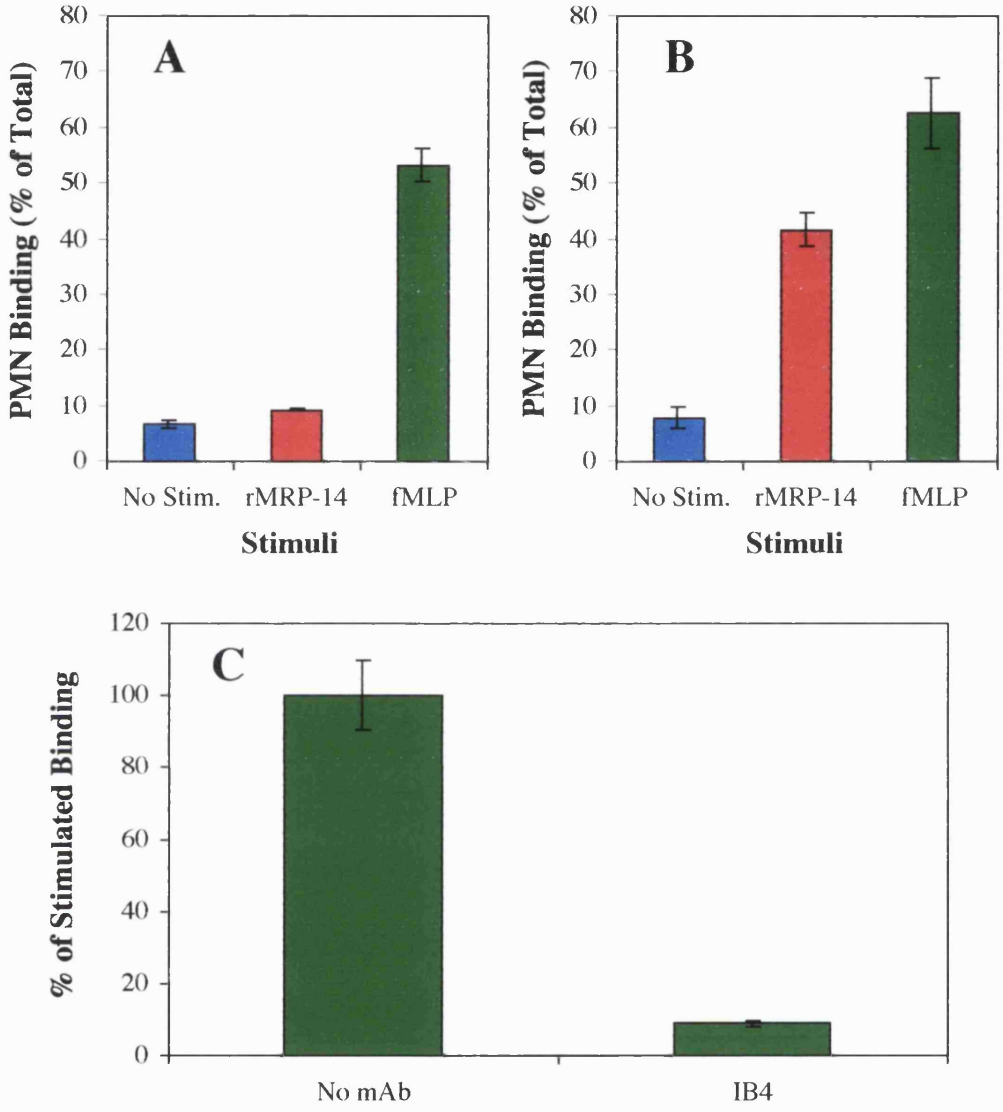

Figure 4.8: The rMRP-14- and fMLP-Stimulated Neutrophil Binding to FSG and Fibrinogen

A & B) Unstimulated (■), 1μM rMRP-14- (■) and 100nM fMLP-(■) stimulated binding of neutrophils to **A**) FSG and **B**) fibrinogen in the static adhesion assay. **C**) The effect of 10μg/ml IB4 on fMLP-stimulated binding to FSG. Data are means of triplicates ± SD. Representative experiments of three or two for **C** are shown.

4.2.d The Specificity of rMRP-14-Induced T Lymphoblast Expression of Cell Surface Molecules

R. Newton demonstrated that rMRP-14 upregulated the expression of Mac-1 and p150,95 on T lymphoblast (Newton, 1997). This could explain the high level of adhesion observed, as T lymphoblast normally express low levels of Mac-1. Further, rMRP-14 increased surface expression of the mAb 24 epitope (Newton, 1997), a reporter of high affinity β_2 integrin. However, as the rMRP-14-induced adhesion subsequently proved not to be Mac-1 mediated, this upregulation was reinvestigated. The mAbs 10.1 (CD16) and UCHM1 (CD14) were used as control IgG1 and IgG2a mAbs, respectively, and were not induced to bind to T lymphoblasts by rMRP-14 (Fig 4.9B and C). An increase in expression was seen with the anti-CD11b mAb, ICRF44; the anti-CD11c mAb, 3.9; and the high affinity β_2 integrin reporter, mAb 24 (Fig 4.9D, E and F). Thus suggesting rMRP-14 upregulated Mac-1, p150,95 and stimulated a high affinity β_2 integrin.

A more extended range of mAbs was analysed. rMRP-14 stimulation did not modulate the cell surface binding of mAbs specific for other adhesion receptors, namely: 38 (CD11a, LFA-1); P5D2 (CD29, β_1 integrin subunit); HP1/2 (CD49d, α_4 integrin subunit); Sam-1 (CD49e, α_5 integrin subunit); Lam 1.3 (CD62L, L-selectin) and 15.2 (CD54, ICAM-1) (data not shown). However, mAb E11 against CD35 (CR1) and the anti-CD32 (FcγRII) mAb FL18.26 showed a distinct increase in expression (Fig 4.9G and data not shown). Both CR1 and FcγRII are reported to be expressed by only a minor subset of T lymphocytes (Rodgaard et al., 1995; Sandilands et al., 1997). The greatest increase in mAb binding was seen with 4U (Fig 4.9H). T lymphoblasts do not express the 4U epitope (N. Hogg personal communication), so this latter upregulation was apparently epitope independent. When compared by SDS PAGE to the isotype control, UCHM1, 4U was heavily degraded (data not shown). This loss of integrity was due to the mAb being sensitive to an acidification step in the purification procedure (M. Stubbs, ICRF mAb Service,

personal communication). Because of the induced binding of E11, FL18.26 and 4U, the validity of the Mac-1, p150, 95 and 24 epitope upregulations was investigated further.

To evaluate whether the increased binding of antibodies was epitope dependent, three different CD11b specific mAbs were used in the induction of cell surface molecule expression assay. Although ICRF44 showed a significant rMRP-14 induced increase in cell surface binding, neither 2LPM19c nor MEM170 demonstrated a similar increase (Fig 4.10). Consequently, the rMRP-14 mediated increase in ICRF44 binding was probably also not epitope dependent.

The epitope dependency of rMRP-14-stimulated increase in binding of the β_2 integrin mAbs was further investigated with the SKβ_2.7 cells. Both the parental cells, SKW3, and the SKβ_2.7 cells did not show rMRP-14 induced binding of the IgG1 and IgG2a isotype controls (data not shown). However both cell lines showed increased binding of mAbs, ICRF44, 3.9 and 24 (Fig 4.11). The epitopes of these mAbs are dependent on the expression of CD18, and thus cannot be expressed by SKβ_2.7 cells. This and the results above inferred that the rMRP-14-mediated increased expression of Mac-1, p150,95 and the 24 epitopes was an artefact.

The most common epitope independent binding of antibodies is by Fc receptors. Additionally, FcγRII binds aggregated IgG molecules (Hulett and Hogarth, 1994), and, as such, may alone explain the apparent induction of other cell surface molecules. Fab' preparations of mAbs ICRF44 and 24 were analysed in the induction of cell surface molecule assay to eliminate Fc-mediated binding of the mAbs. The ICRF44 Fab' showed no significant increase in binding following rMRP-14 stimulation (Fig 4.12B), unlike the whole mAb (Fig 4.12A). Conversely, the 24 Fab' showed a higher expression than intact mAb 24 (Fig 4.12C and D), and consequently the increased binding of mAbs to the cell surface cannot be Fc-mediated.

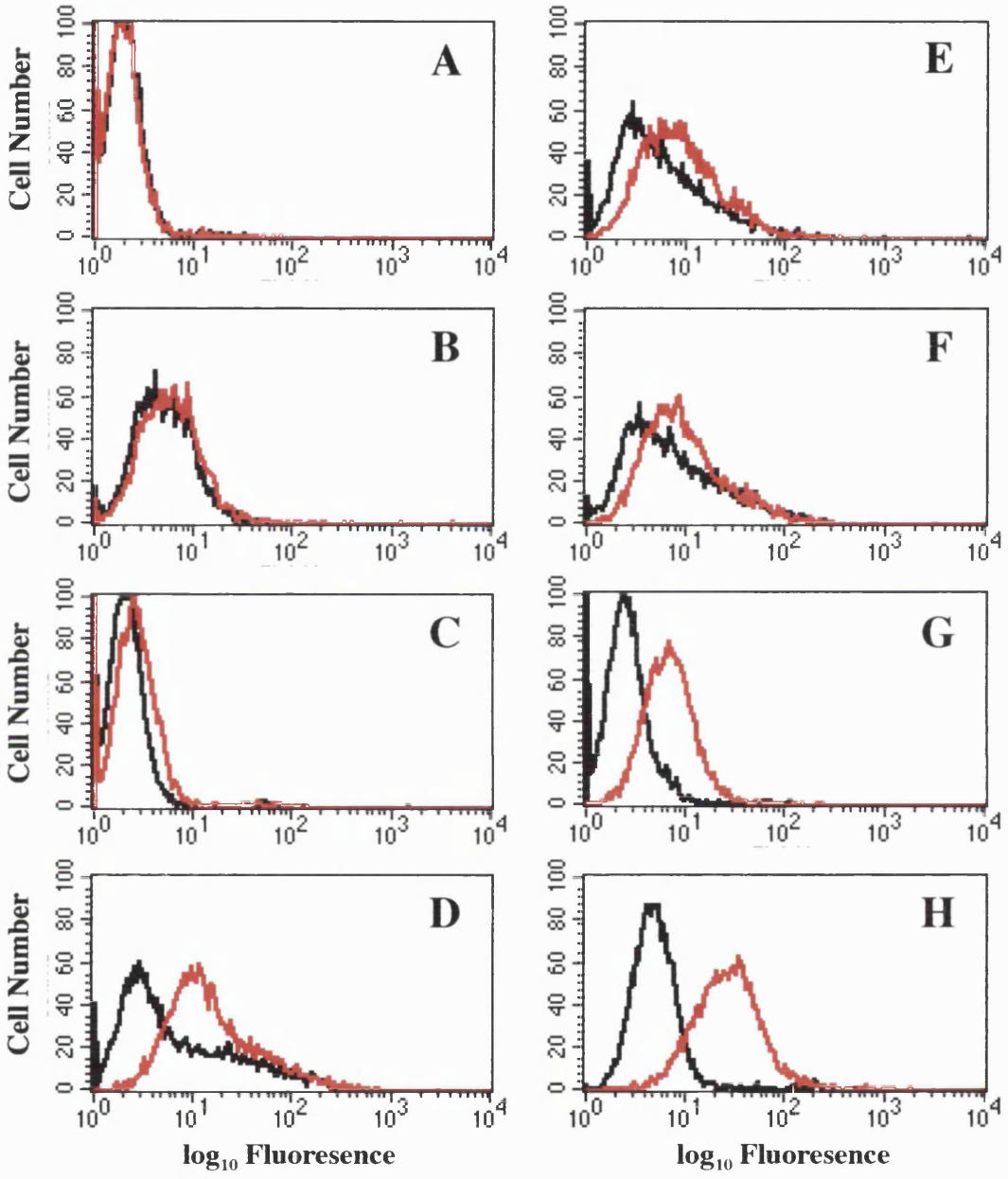

Figure 4.9: The Effect of rMRP-14 on the Expression of Cell Surface Molecules by T lymphoblasts as Detected by mAb Binding

The binding of various mAbs to unstimulated (—) and 1μM rMRP-14-stimulated (—) T lymphoblasts; **A**) No primary mAb, **B**) 10.1 (CD16), **C**) UCHM-1 (CD14), **D**) ICRF44 (CD11b), **E**) 3.9 (CD11c), **F**) 24, **G**) E11 (CD35) and **H**) 4U. All mAbs were used at 10μg/ml. The data are from 5,000 cells, and a representative experiment of three is shown.

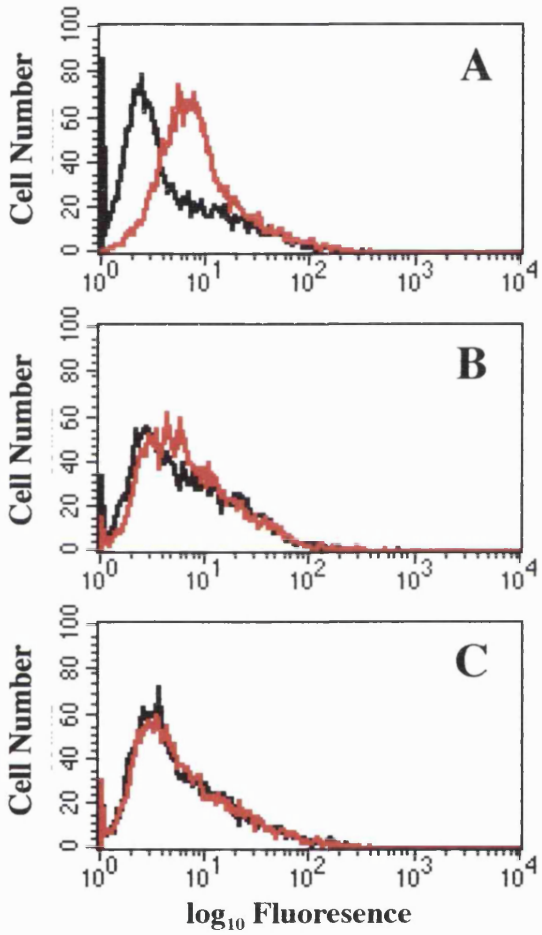

Figure 4.10: The Effect of rMRP-14 on the Expression of Mac-1 by T Lymphoblasts as Detected by Various Anti-Mac-1 mAbs

Flow cytometric analysis of the binding of various anti-CD11b mAbs to unstimulated (—) and 1μM rMRP-14-stimulated (—) T lymphoblasts; **A**) ICRF44, **B**) 2LPM19c and **C**) MEM170. ICRF44 was used at 10μg/ml, and 2LPM19c and MEM170 at an optimal dilution for FACS. A representative experiment of three is shown.

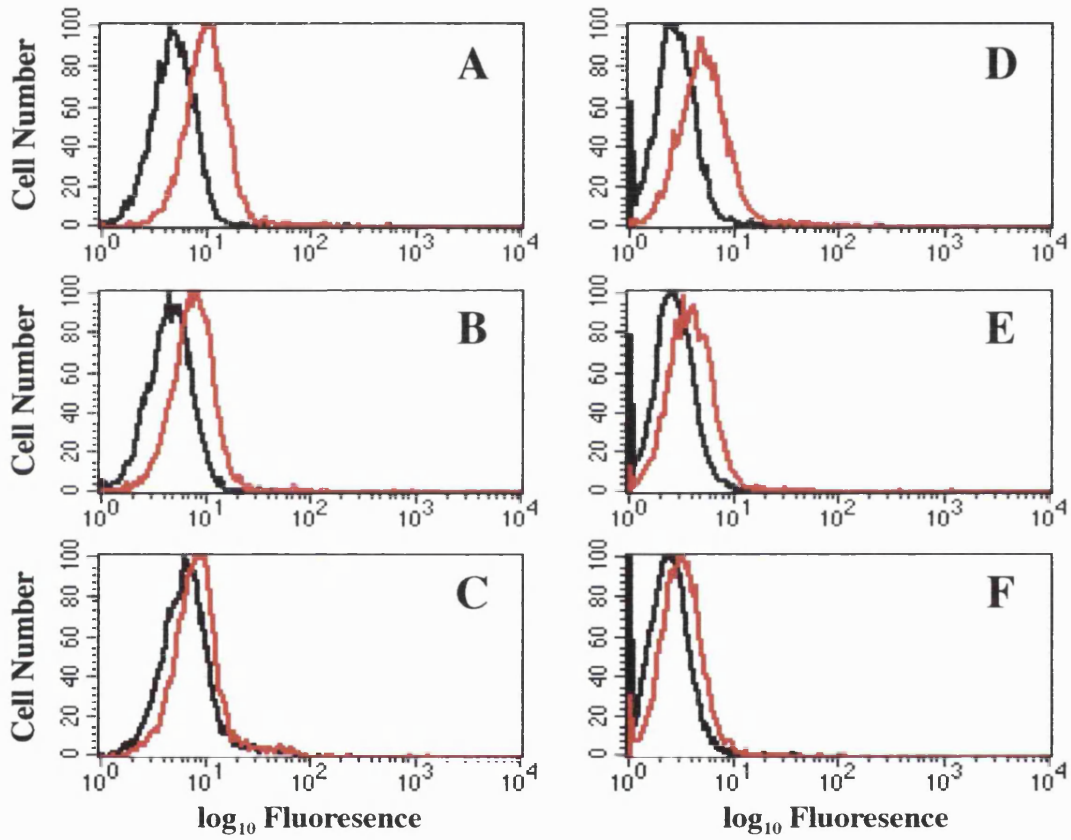

Figure 4.11: The Effect of rMRP-14 on the Binding of Various mAbs to SKW3 and SKβ_2.7 Cells
The binding of various mAbs to unstimulated (—) and 1μM rMRP-14-stimulated (—) **A-C**) SKW3 and **D-E**) SKβ_2.7 cells: **A & D**) ICRF44 (CD11b), **B & E**) 3.9 (CD11c), and **C & F**) 24. All mAbs were used at 10μg/ml. A representative experiment of two is shown.

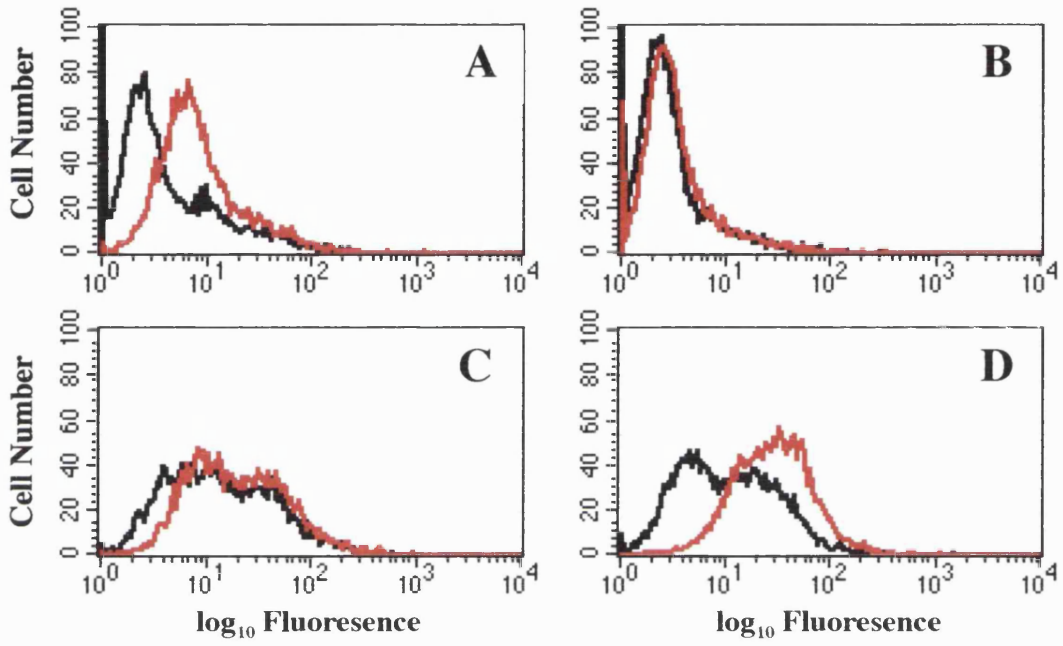

Figure 4.12: The Effect of rMRP-14 on the Binding of Whole mAbs and Fab's of ICRF44 and 24 to T Lymphoblasts

Flow cytometric analysis of the binding of whole mAbs and FAb' of ICRF44 and 24 to unstimulated (—) and 1μM rMRP-14-stimulated (—) T lymphoblasts: **A**) intact ICRF44, **B**) Fab' of ICRF44, **C**) intact 24 and **D**) Fab' of 24. All antibodies were used at 10μg/ml, except Fab' of 24 which was used at an optimal dilution. A representative experiment of three is shown.

4.3 Discussion

rMRP-14 induced T lymphoblasts to adhere to various Mac-1 ligands. Anti-CD11b and CD18 mAbs blocked similar binding stimulated by phorbol ester, but not the rMRP-14 induced adhesion. Further, the binding occurs at 4°C and consequently is unlikely to be mediated by another integrin. Integrin-mediated adhesion is usually further characterised by cation dependency, but this was not investigated for rMRP-14 because it is also a cation binding protein. However, the phorbol ester-stimulated adhesion to fibrinogen was low, and consequently could be more susceptible to blocking. To eliminate this possibility, the β_2 integrin lacking cell line SKβ_2.7 was used. rMRP-14 induced SKβ_2.7 cells to bind fibrinogen in a similar fashion to the parental cell line, thus excluding a Mac-1 mediated mechanism.

The rMRP-14 induced neutrophil adhesion was not investigated in as much detail as the T lymphoblast adhesion. mAb blocking data demonstrated the neutrophil adhesion is not dependent on Mac-1. However, it was reported that rMRP-14 induced binding of neutrophils to fibrinogen can be blocked by the anti-Mac-1 mAb 2LPM19c (Newton and Hogg, 1998). This may, in part, be due to the antibody being used as an ascitic fluid in some previous instances. Also, the purified 2LPM19c used in earlier studies was a different batch from that used here, and unfortunately a direct comparison of the different batches was not possible. The batch used in these studies blocked fMLP-activated neutrophil adhesion to fibrinogen, and thus was deemed functional. Previous batches may also have contained some denatured or degraded material, which could have blocked the binding non-specifically (see below). fMLP, but not rMRP-14, stimulated neutrophil adhesion to fish skin gelatin (FSG). This was blocked by an anti-CD18 mAb, and therefore is probably mediated by Mac-1, the most promiscuous β_2 integrin. This lack of induced neutrophil adhesion would suggest that rMRP-14 does not activate neutrophil Mac-1.

The MRP-14 induced binding of neutrophils and T lymphoblasts shared many characteristics: the adhesive ligand; the concentration of rMRP-14 that induces adhesion; and the blocking by ascitic fluid but not purified mAbs. Therefore it seems probable that the mechanism of induced adhesion is the same for both cell types.

The rMRP-14 induced upregulation of various cell surface molecules was also shown to be an artefact, as the increased binding of the detecting antibody was not epitope dependent. This binding was also not Fc mediated. Rather, it appeared to be specific for particular detecting mAbs with no obvious common characteristics, such as isotype. The mAb that had the highest induced binding, 4U, was heavily degraded. Because of this finding and also that denatured BSA was a good ligand for the rMRP-14 induced adhesion, 4U may have been acting like a soluble ligand for the proadhesive effect. Interestingly, 4U blocked the rMRP-14 induced adhesion to fibrinogen, further supporting the theory it could act as a soluble ligand (data not shown). The extension of this hypothesis is that the smaller increases seen with other mAbs may be due to contaminating degraded or denatured products, although no degradation could be detected by SDS PAGE (data not shown). This hypothesis may also explain the blocking of adhesion by ascitic fluids, because denatured and/or aggregated components could have inhibited binding by acting as a competing soluble ligand. Further, the blocking seen with previous batches of 2LPM19c may be due to denatured or degraded material in the preparations.

Therefore, rMRP-14, acting either directly or indirectly, caused neutrophil and T lymphoblast binding to ligands with characteristics that are superficially similar to those of the β_2 integrin Mac-1. However, the detailed analysis in this chapter demonstrated, for the first time, that the mechanism is independent of integrins. Most interestingly, the recognised features of the ligands appear to include characteristics revealed upon protein degradation and denaturation.

Chapter 5

rS100 Proteins Binding to Proteinaceous Ligands

5.1 Introduction

The proadhesive effect of rMRP-14 on neutrophils and T lymphoblasts is not mediated by Mac-1. Thus other possible mechanisms for the rMRP-14 induced binding, which are not dependent on Mac-1, were considered. One model would be that MRP-14 interacts with a specific receptor, which subsequently signals to an adhesive molecule. This mechanism is supported by rMRP-14 stimulated binding of neutrophils to fibrinogen being sensitive to pertussis toxin, an inhibitor of G protein signalling (Newton and Hogg, 1998). This is also consistent with S100A2 chemotaxis, which is also pertussis toxin sensitive (Komada et al., 1996). However, the toxin only blocked the rMRP-14 induced adhesion at a concentration higher than that required to inhibit fMLP stimulated binding (Newton, 1997). Thus it is possible the inhibition seen with pertussis toxin was non-specific, like the blocking by ascitic fluids and the mAb 4U. More crucially, T lymphoblast adhesion occurred at 4°C, which is inconsistent with G-protein signalling. Further any mechanism dependent on intracellular signalling conflicts with this data, as signalling is generally dependent on enzymes. Additionally, no obvious candidate adhesion receptor, that is promiscuous and expressed by neutrophils, THP-1 cells and T lymphoblast, has been described. Thus, it is not likely that this mechanism mediates the proadhesive effect.

An alternative putative mechanism is that rMRP-14 binds directly to an adhesive receptor or associated protein, and activates the receptor by inducing a conformational change. This would be more consistent with the data. However, again the putative adhesive receptor would also probably be a novel protein. A third hypothesis is that, rMRP-14 acts as a "molecular glue" by interacting with both the

cell surface and immobilised ligand. Again this would not conflict with the cell binding data, because, in such a model, the blocking agents could compete with either the cell or ligand binding of rMRP-14. Finally, rMRP-14 could transform the immobilised ligands into an adhesive state, which then binds the leukocytes.

The aim of this project is to investigate the proadhesive effect of rMRP-14. As it was assumed that rMRP-14 induced the binding of both T lymphoblasts and neutrophils by a similar process, the mechanism of T lymphoblast adhesion to the ligands was analysed first. T lymphoblasts were chosen because of the low Mac-1 levels, which simplified the assay and reduced background binding.

5.2 Results

5.2.a T Lymphocyte Binds to rMRP-14 Pre-treated Ligands

The latter two models of the proadhesive effect proposed above require rMRP-14 to bind to the immobilised ligand. As an initial test of these models, the ligands, fibrinogen, denatured BSA, native BSA and FSG, were pre-treated with rMRP-14, washed, and then the T lymphoblasts allowed to adhere. When directly compared to the standard adhesion assay, pre-incubating the rMRP-14 with ligands and washing did not alter binding characteristics of the assay (Fig 5.1A and B). This suggests that sufficient rMRP-14 is immobilised on the ligands in the static adhesion assay to mediate cell binding.

To initially characterise the binding of T lymphoblasts to rMRP-14 pre-treated fibrinogen and denatured BSA, the non-specific blocking agents, BSA and heparin were used. When added with the cells, both 100μg/ml heparin and 1% BSA were able to inhibit T lymphoblast binding to the rMRP-14 pre-treated ligands by 60-70% (Fig 5.1C). This implies the T lymphoblast adhesion was quite non-specific.

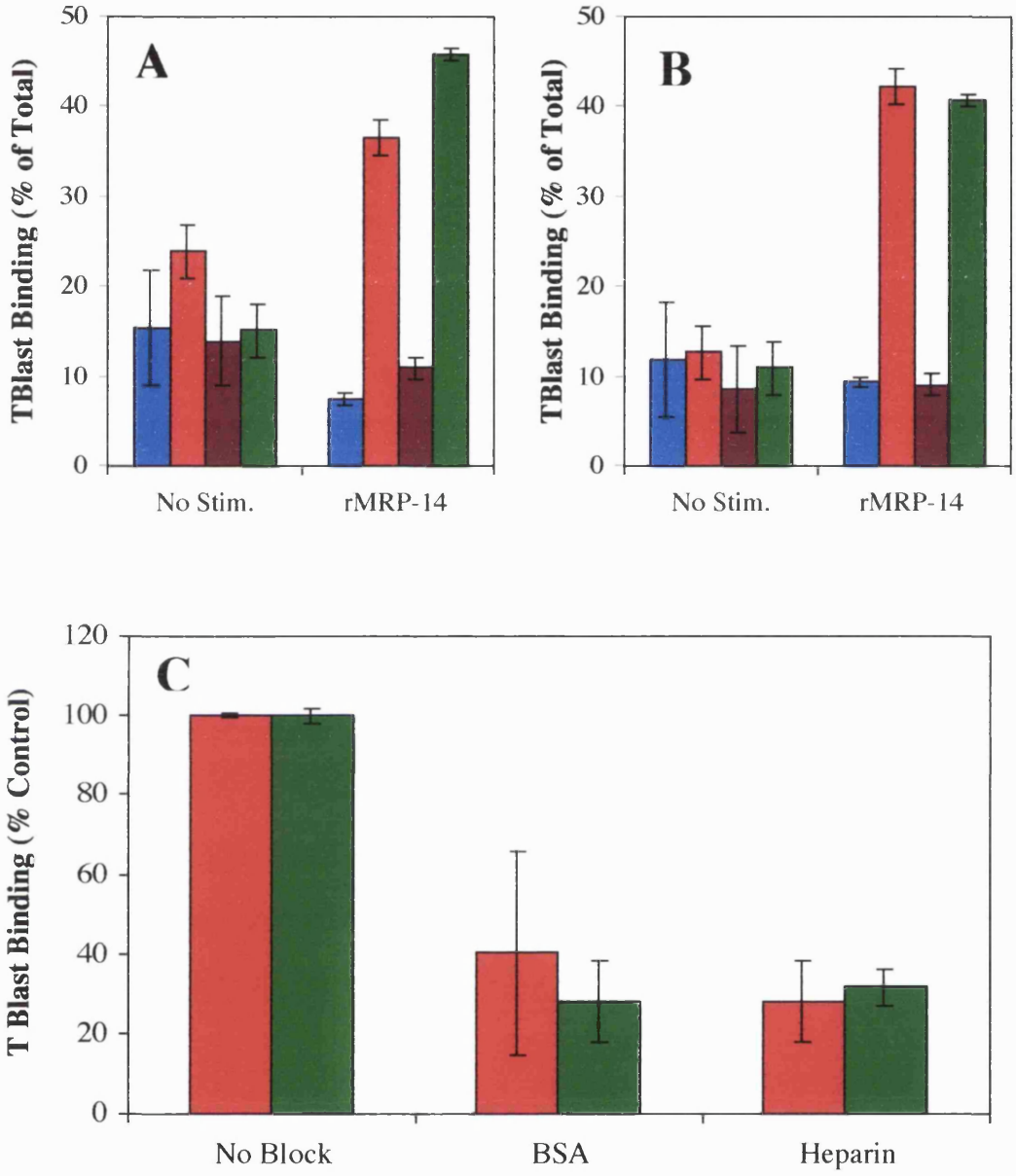

Figure 5.1: T Lymphoblasts Binding to rMRP-14-Pretreated Ligands With and Without Blocking by BSA and Heparin

1μM rMRP-14-induced binding of T lymphoblast to fish skin gelatin (■), fibrinogen (■), native BSA (■) and denatured BSA (■) in the static adhesion assay. **A**) rMRP-14 incubated with the cells as standard. **B**) rMRP-14 pretreated with the ligands, and the cells allowed to bind following washing. **C**) The effect of 1% BSA and 100μg/ml heparin on cells binding to rMRP-14-pretreated ligands. Data are means of triplicates ± SD. Representative experiments of four for **A** and **B**, and of two for **C** are shown.

5.2.b rMRP-14 Binding to Proteinaceous Ligands.

Because the binding of T lymphoblast to rMRP-14 pre-treated ligands appeared non-specific, the putative interaction between rMRP-14 and the ligands was investigated first. Initially the amount of rMRP-14 bound to the various ligands following pre-treatment was assayed. The bound recombinant protein was detected with a monospecific antisera (See Fig 3.6) in an enzyme linked immunosorbent assay (ELISA), based on an established MRP-14 ELISA (G. Ivanov, personal communication). rMRP-14 bound to all the ligands, but with different affinities. Denatured BSA was the most avid ligand with FSG being the worst ligand. Fibrinogen was similar to denatured BSA, and native BSA had an intermediate affinity (Fig 5.2). The ELISA based detection was specific for MRP-14, because replacing the anti-MRP-14 antisera with control sera or anti-S100A12 antisera gave no signal (data not shown). The binding directly mirrored the ligand specific binding seen in the static adhesion assay (see Fig 4.2), strongly implying rMRP-14 binding to the ligand is a significant step in the induced T lymphoblast adhesion.

The nature of the interactions of rMRP-14 with fibrinogen and denatured BSA was investigated. A protein-protein interaction can be characterised in many ways, but because one of the ligands was denatured, the contribution ionic and hydrophobic bonds to the interaction were of particular interest. Detergents characteristically disrupt hydrophobic bonds, so the effect of detergent on rMRP-14 binding was evaluated. Washing rMRP-14 that was bound to fibrinogen and denatured BSA with assay buffer containing 1% Tween-20, Triton X-100, NP-40 or Brij 96 did not disrupt the interaction. A wash containing 1% CHAPS, a zwitterionic detergent, slightly reduced the binding to denatured BSA, but this was insignificant ($P>0.2$) and did not repeat. Thus the interaction was not predominantly hydrophobic in nature. 0.1% and 1% SDS were able to completely disrupt the interaction with both fibrinogen and denatured BSA (Fig 5.3).

High salt concentrations disrupt ionic bonds, and so a salt wash is a common method used break protein-protein interactions mediated by these bonds. rMRP-14 binding to fibrinogen and denatured BSA was resistant to washing with assay buffer containing 1M NaCl (Fig 5.4). This is strong evidence the interaction is not solely dependent on ionic bonds, as this salt wash contains Hank's Balances Salt Solution as well as the 1M NaCl giving it a very high ionic potential.

Because MRP-14 has been shown to bind both calcium (Siegenthaler et al., 1997) and zinc (Raftery et al., 1996) ions, the divalent cation requirement of the rMRP-14 interaction with fibrinogen and denatured BSA was established. The binding of rMRP-14 to fibrinogen and denatured BSA was cation dependent. Specifically calcium and zinc, but not magnesium, were required for the interactions (Fig 5.5).

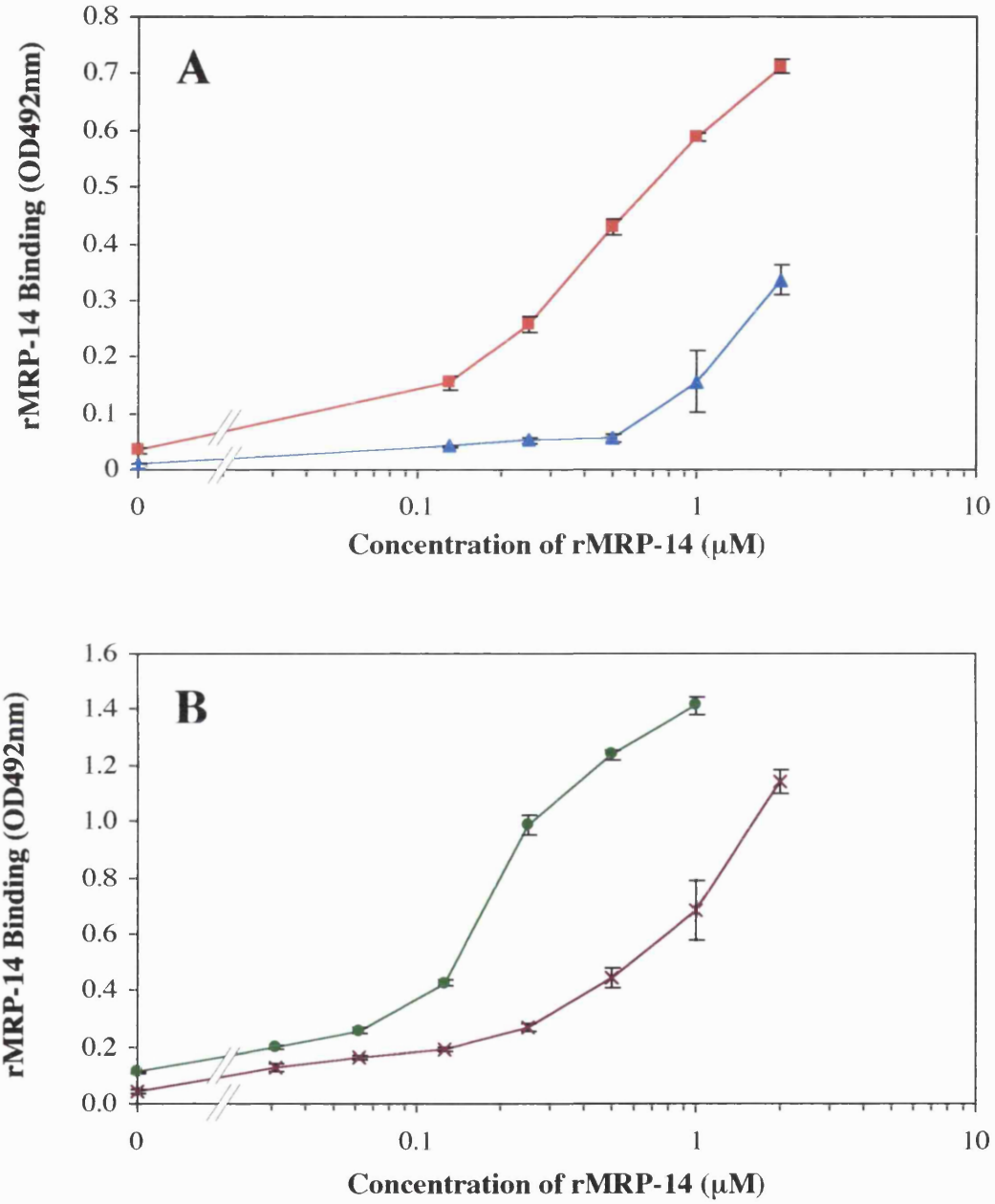

Figure 5-2: rMRP-14 Binding to Various Ligands
rMRP-14 binding directly to **A**) fish skin gelatin (▲) and fibrinogen (■) and **B**) native BSA (X) and denatured BSA (●). Data are means of triplicates ± SD. Representative experiments of four are shown.

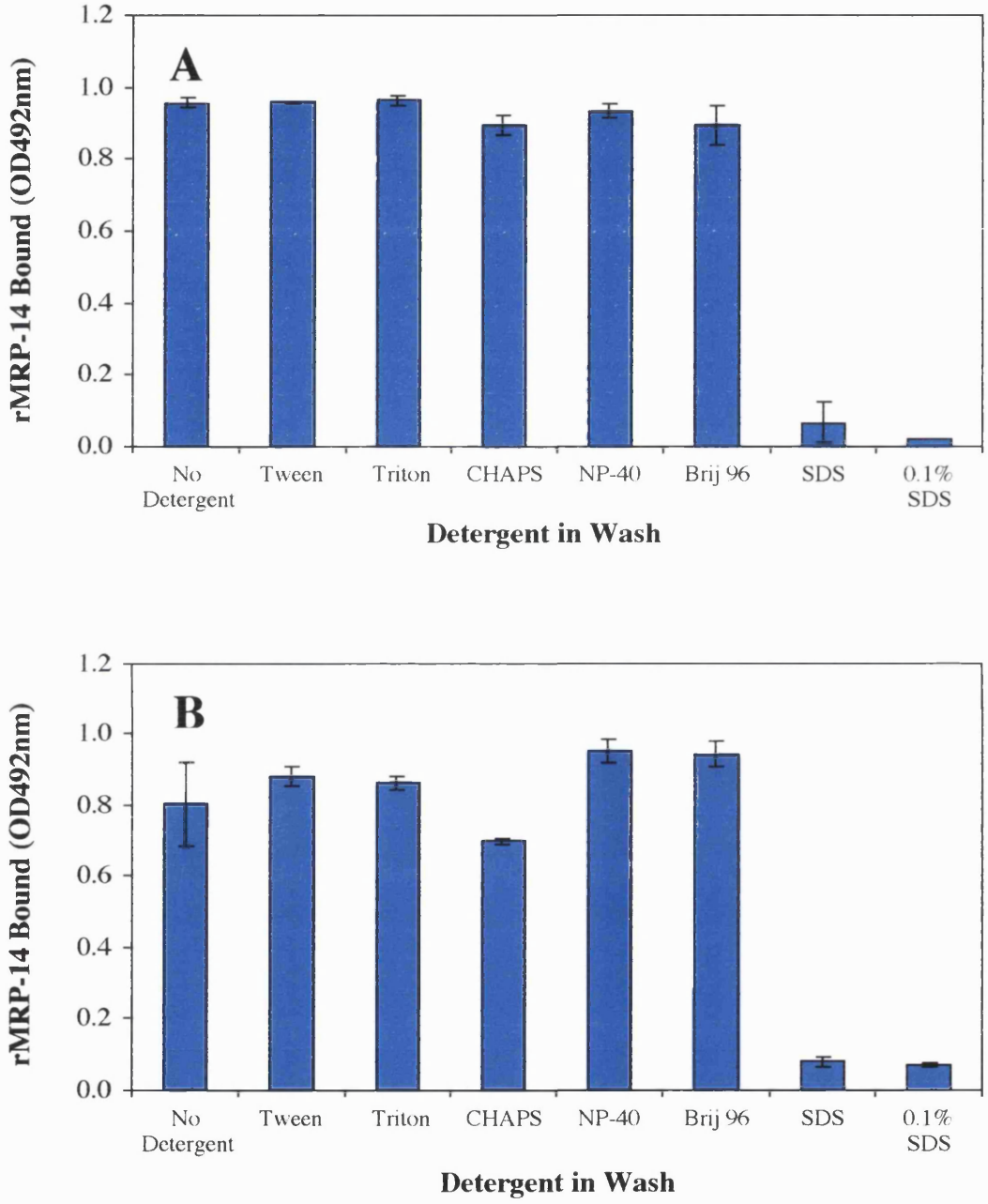

Figure 5.3: The Effect of Detergent Washes on rMRP-14 Bound to Various Ligands

The effect of a wash containing 1% Tween 20, Triton X-100, CHAPS, NP-40, Brij 96 or SDS or 0.1% SDS following 1μM rMRP-14 binding to **A**) fibrinogen and **B**) denatured BSA on the level of rMRP-14 bound. Data are means of triplicates ± SD. Representative experiments of **A**) three and **B**) two are shown.

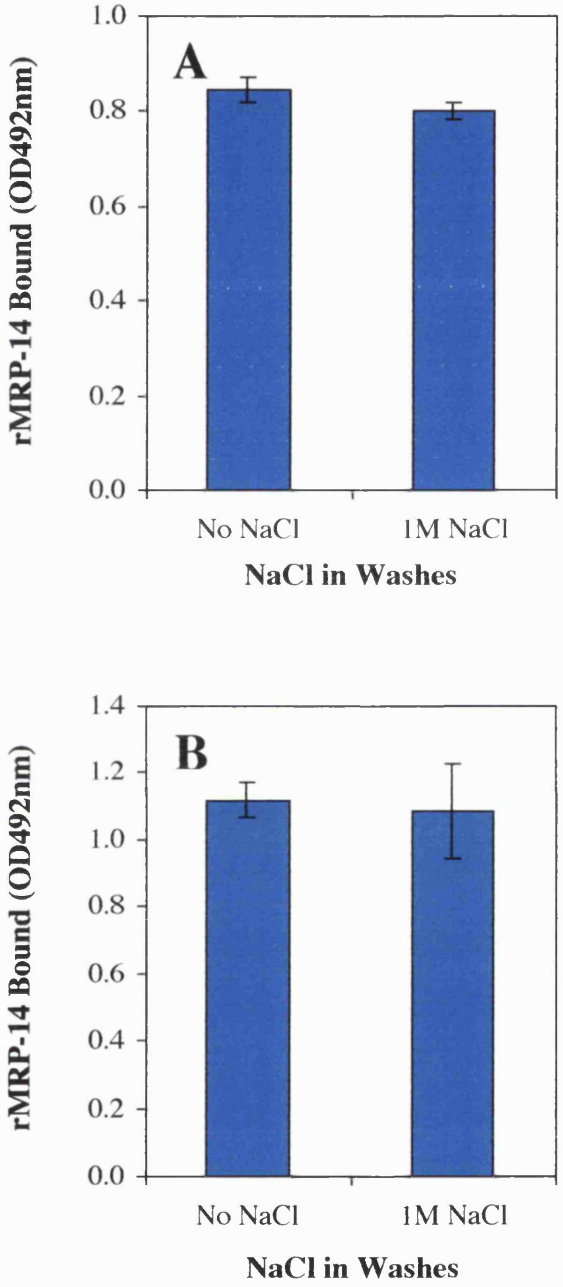

Figure 5.4: rMRP-14 Binding to Fibrinogen and Denatured BSA is Resistant to a 1M NaCl Wash

The effect of a 1M NaCl wash following 1μM rMRP-14 binding to **A**) fibrinogen and **B**) denatured BSA on the level of rMRP-14 bound. Data are means of triplicates ± SD. Representative experiments of three are shown.

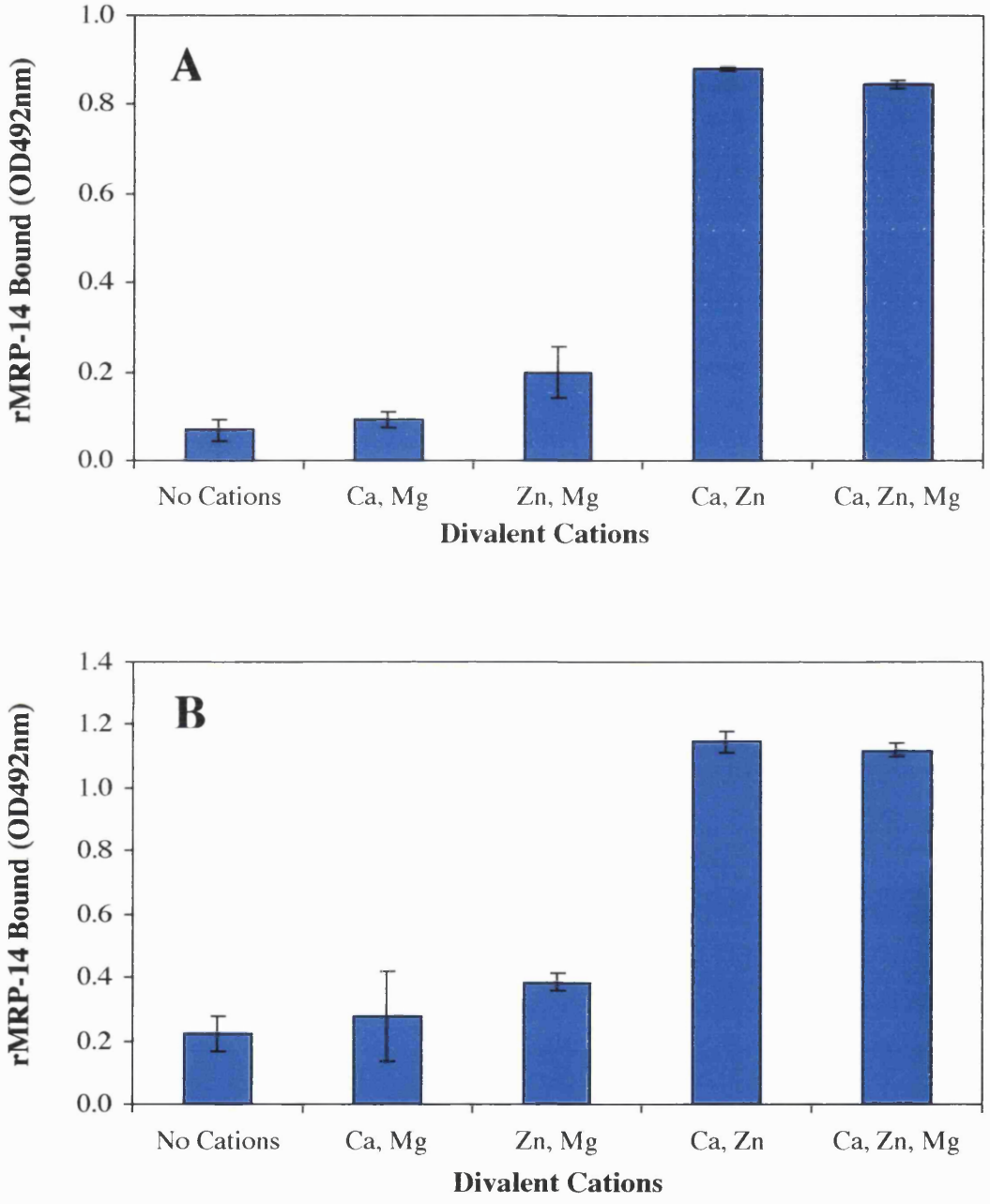

Figure 5.5: Divalent Cation Dependency of rMRP-14 Binding to Fibrinogen and Denatured BSA

The requirement of different divalent cations for 1μM rMRP-14 binding directly to **A**) fibrinogen and **B**) denatured BSA. Data are means of triplicates ± SD. Representative experiments of two are shown.

5.2.c Blocking of the Interaction of rMRP-14 with Fibrinogen and Denatured BSA.

1% BSA and 100μg/ml heparin non-specifically block adhesion of T lymphoblasts to rMRP-14 pre-treated fibrinogen and denatured BSA (see Fig 5.1C). Therefore, rMRP-14 binding to fibrinogen and denatured BSA in the presence of these blocking agents was assessed. 100μg/ml heparin did not affect the interaction between rMRP-14 and the ligands, but 1% BSA reduced binding by more than 80% (Fig 5.6A and B). Further 1% BSA was able to compete rMRP-14 from both ligands even following pre-treatment (data not shown). This strongly implies the native BSA site is the same site that interacts with the high affinity ligands.

Blocking monoclonal antibodies (mAbs) can often provide more information about the binding site of an interaction. Four previously uncharacterised anti-rMRP-14 mAbs were investigated in the binding assay. The mAbs were pre-incubated with rMRP-14 prior to adding to the denatured BSA for the standard ligand binding assay. Two mAbs, 1H9 and 1F5, did not block the interaction, but two, 6E1 and 6G4, blocked by 60% and 75%, respectively (Fig 5.6C). These mAbs were not degraded, as determined by SDS PAGE (data not shown). This implies a specific site on the surface of rMRP-14 molecule mediates the interaction with denatured BSA. Preliminary data suggests that another two anti-MRP-14 mAbs, 6F5 and 1A9, do not block the interaction, and also that 6E1 and 6G4, but not 1H9, block rMRP-14 binding to fibrinogen (data not shown). Therefore, the interaction of rMRP-14 with both these ligands appears to be mediated by the same distinct site.

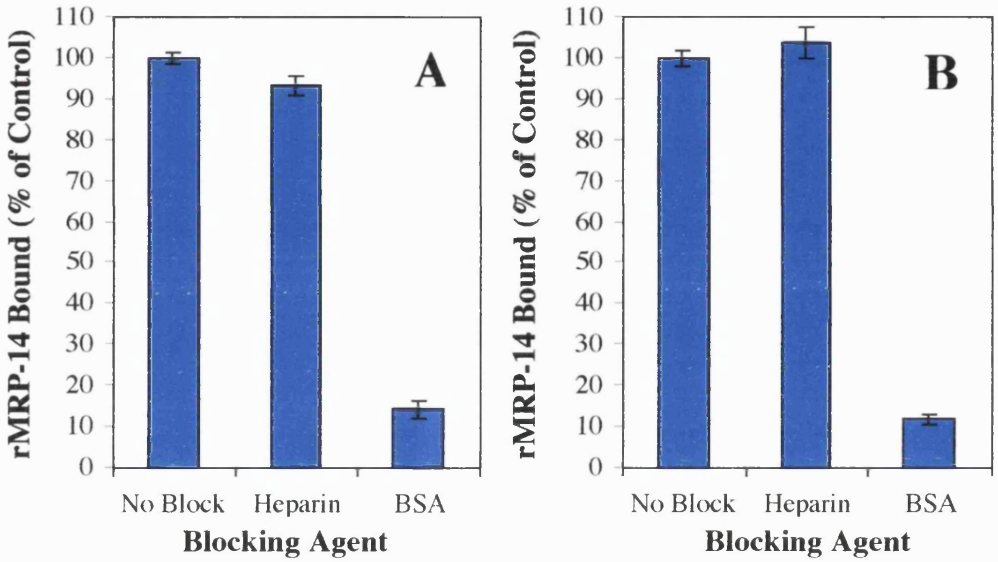

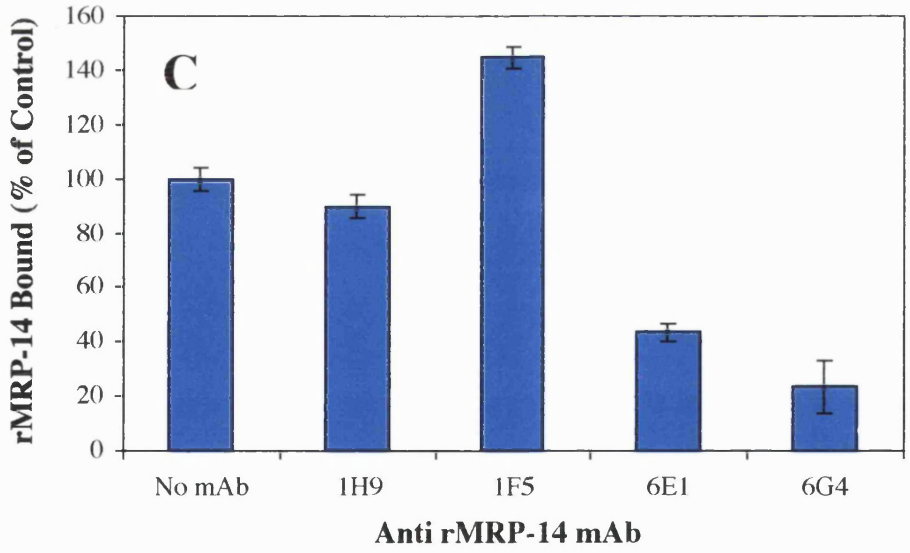

Figure 5.6: BSA, Heparin and Anti-MRP-14 mAbs as Blocking Agents in rMRP-14 Binding to Fibrinogen and Denatured BSA

A & **B**) Blocking agents in rMRP-14 binding to fibrinogen and denatured BSA. The effect of 1% BSA and 100μg/ml heparin on 1μM rMRP-14 binding to **A**) fibrinogen and **B**) denatured BSA. **C**) The effect of 20μg/ml anti-MRP-14 mAbs on 0.3μM rMRP-14 binding to denatured BSA. Data are the mean of triplicates (± SD). Representative experiments of three (for **A** & **C** except 1F5) and two (**B** & **C**-1F5) are shown.

5.2.d rMRP-8 Does Not Bind to the Proteinaceous Ligands.

rMRP-14-mediated T lymphoblast adhesion to fibrinogen and denatured BSA appears to be dependent on rMRP-14 binding to the ligands. rMRP-8 is not proadhesive, rather it inhibits rMRP-14 induced adhesion (Newton, 1997). MRP-8 is the closest homologue of MRP-14, and thus rMRP-8 binding to fibrinogen and denatured BSA was of interest. rMRP-8, up to 3μM, did not bind to FSG, fibrinogen, native BSA or denatured BSA, under the rMRP-14 binding assay conditions (Fig 5.7A). As a control in the same experiment, 1μM rMRP-14 showed good binding to fibrinogen and denatured BSA (Fig 5.7B). Unfortunately, as a ligand for MRP-8 was not found there was no positive control for rMRP-8 binding in the assay. However, the detecting antisera is functional, because, under the same conditions, it recognises rMRP-8 in a MRP-8 ELISA (G. Ivanov, unpublished data). This is interesting, as it implies that the rMRP-14 interaction with ligands, as described in this chapter, does not apply to at least one other S100 protein.

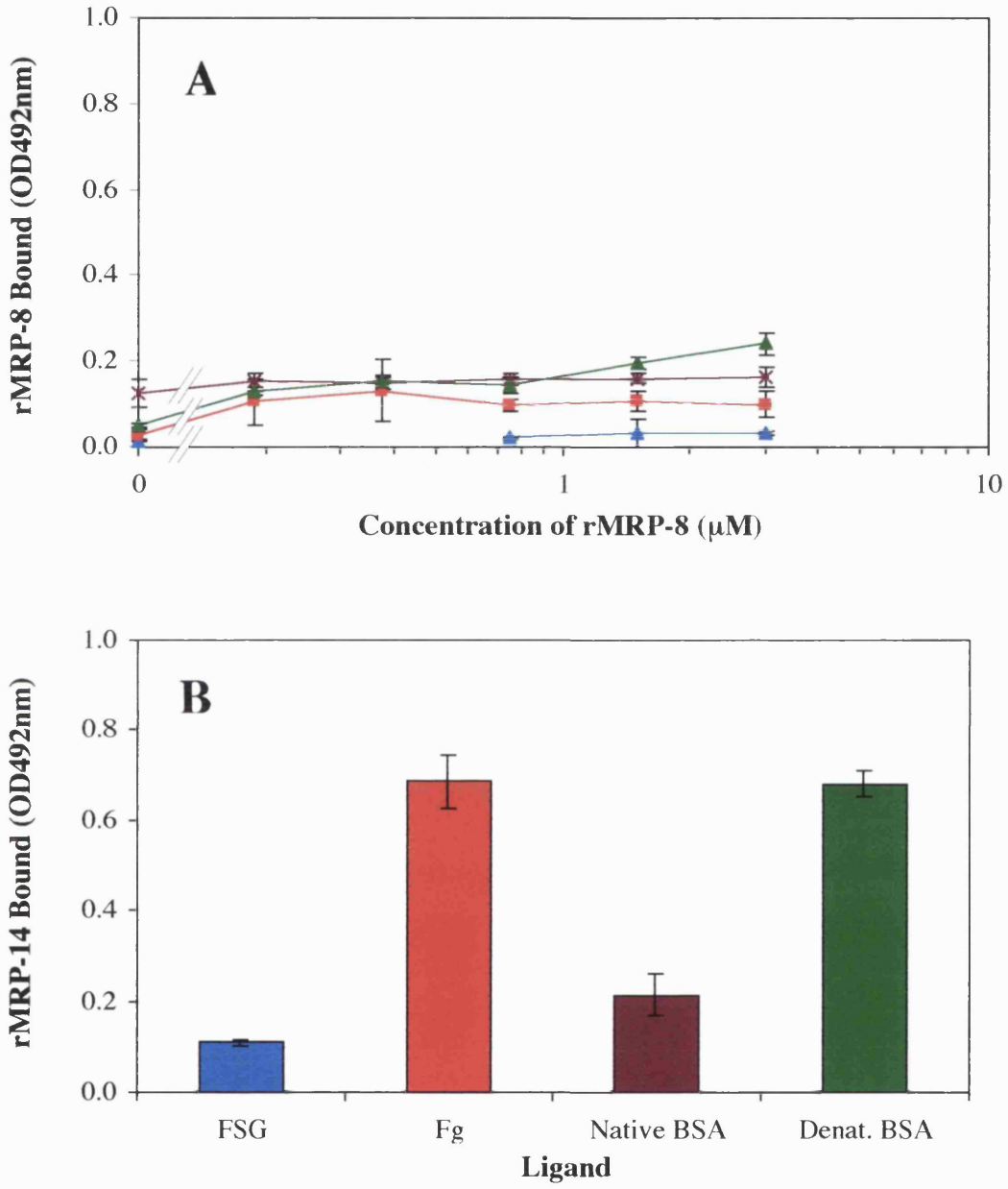

Figure 5.7: rMRP-8 Binding to Various Ligands

A) rMRP-8 and **B**) 1μM rMRP-14 binding directly to fish skin gelatin (▲), fibrinogen (■), native BSA (X) and denatured BSA (●). Data are means of triplicates ± SD. A representative experiment of two is shown.

5.2.e rS100A12 Binding to Proteinaceous Ligands

rS100A12 is unable to induce neutrophil and T lymphoblast adhesion to fibrinogen (see Fig 3.12 and 3.14), but is highly homologous to MRP-14. In the ligand binding assay, rS100A12 bound denatured BSA apparently with a higher affinity than rMRP-14. The interaction between S100A12 and fibrinogen was of slightly lower affinity, but still higher than that observed with rMRP-14. rS100A12, up to 2μM, did not bind to native BSA and FSG (Fig 5.8A). Interestingly, 2μM rMRP-14 consistently bound to native BSA and FSG (see Fig 5.2), and in the same experiment 1μM rMRP-14 bound to native BSA (Fig 5.8B). Therefore, rS100A12 bound to the good ligands (fibrinogen and denatured BSA) with a higher affinity than rMRP-14, but did not bind the poor ligands (native BSA and FSG).

The nature of the interactions of rS100A12 with fibrinogen and denatured BSA was compared to rMRP-14 binding. Washing rS100A12 bound to fibrinogen and denatured BSA with assay buffer containing 1% Tween-20, Triton X-100, NP-40 or Brij 96 did not disrupt the interaction, as with rMRP-14. Unlike rMRP-14, a 1% CHAPS wash variably reduced the binding to the ligands by up to 50%, but this was inconsistent. 0.1% and 1% SDS were able too completely disrupt the interaction with both fibrinogen and denatured BSA (Fig 5.9). rS100A12 binding to fibrinogen and denatured BSA was resistant to washing with assay buffer containing 1M NaCl (Fig 5.10). Therefore, like rMRP-14, the interaction of rS100A12 with ligands appears not to be predominantly mediated by hydrophobic or ionic bonds.

S100A12 binds calcium and zinc ions (Dell'Angelica et al., 1994), and thus the cation requirements of the rS100A12 interaction with fibrinogen and denatured BSA was established. Like the rMRP-14 interactions, the binding of rS100A12 to fibrinogen and denatured BSA was dependent on calcium. However, the interaction with ligand did not require zinc ions (Fig 5.11), unlike rMRP-14.

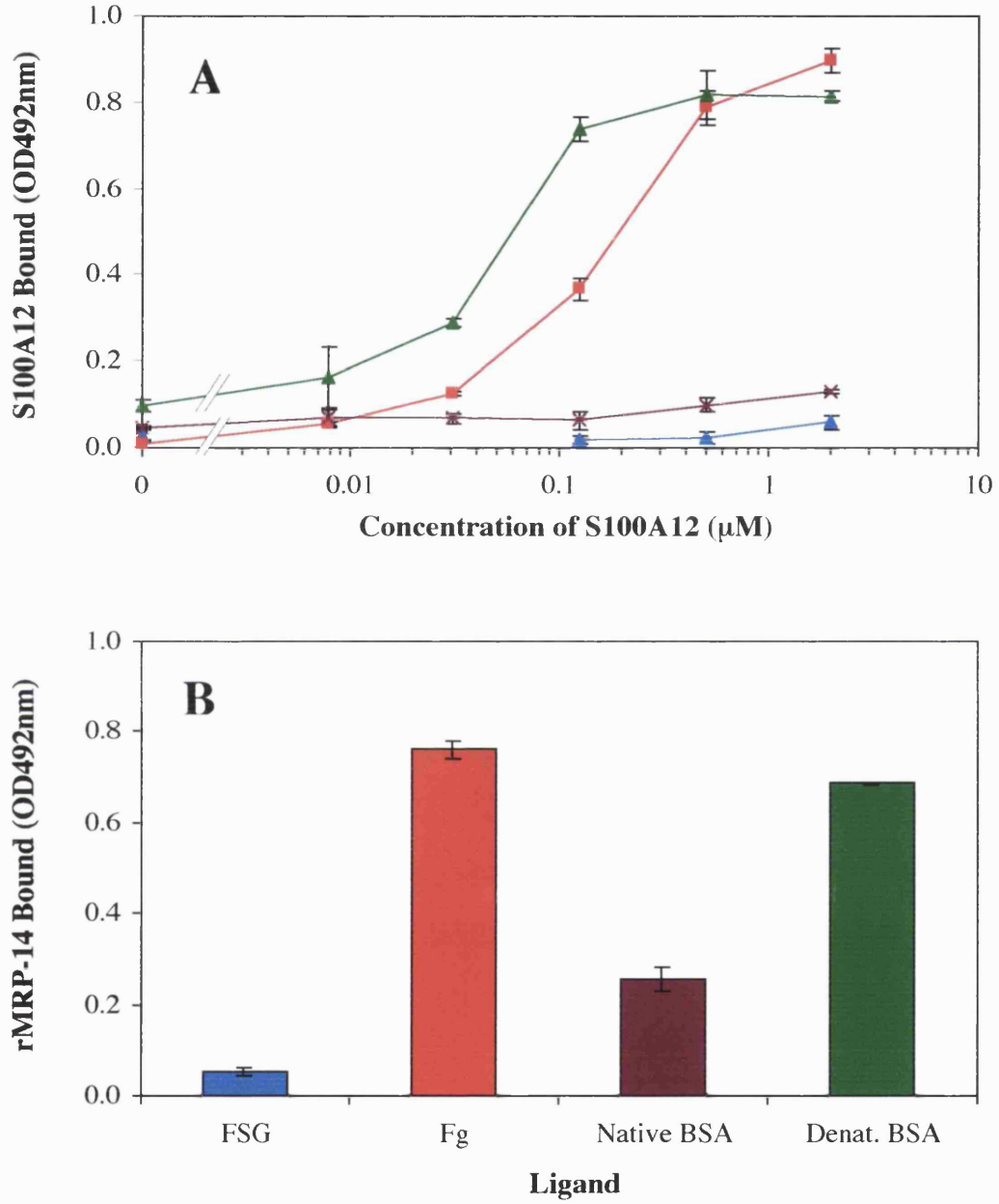

Figure 5.8: S100A12 Binding to Various Ligands

A) S100A12 and **B**) 1μM rMRP-14 binding directly to fish skin gelatin (▲), fibrinogen (■), native BSA (X) and denatured BSA (●). Data are means of triplicates ± SD. A representative experiment of three is shown.

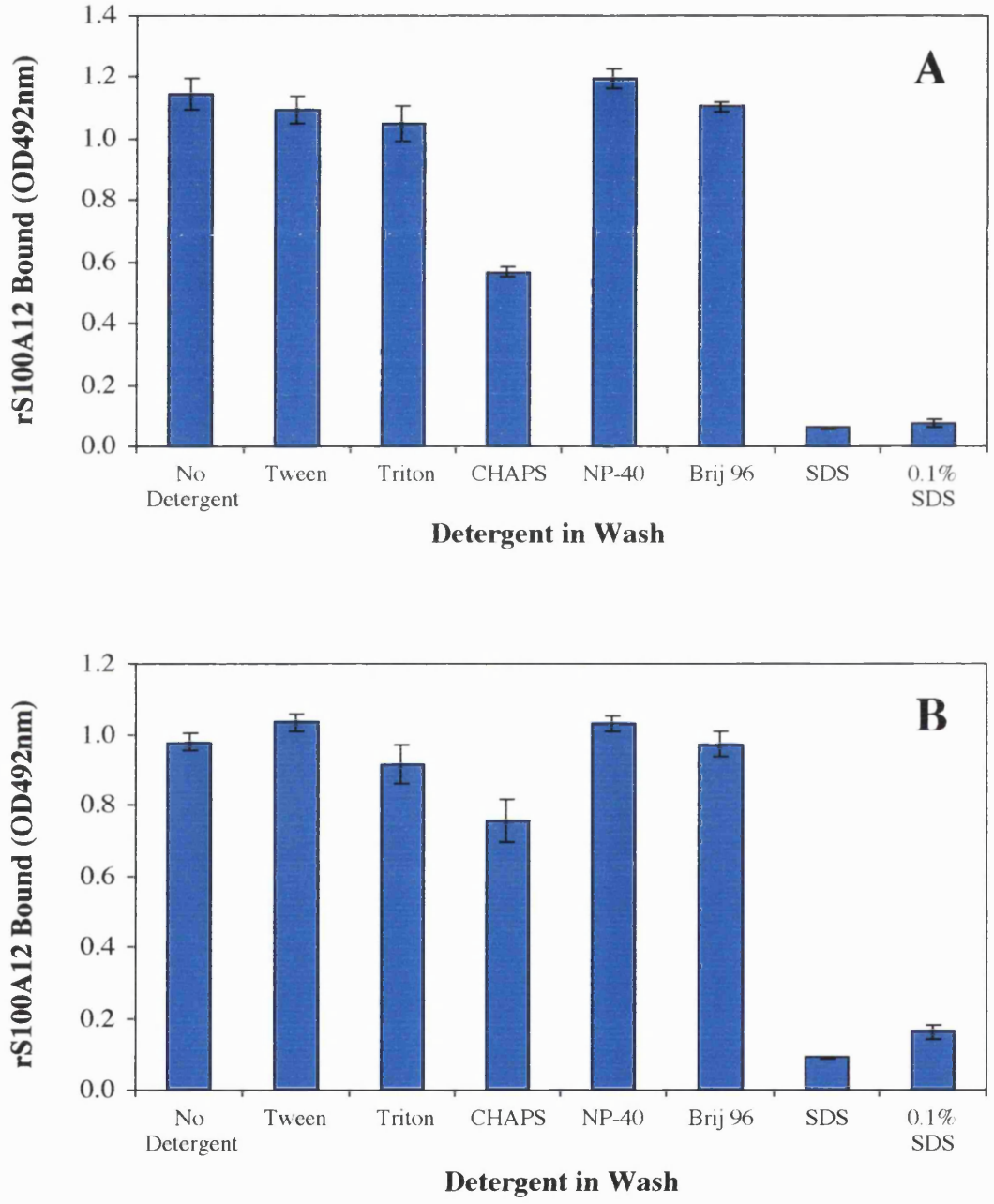

Figure 5.9: The Effect of Detergent Washes on rS100A12 Bound to Various Ligands

The effect of a wash containing 1% Tween 20, Triton X-100, CHAPS, NP-40, Brij 96 or SDS or 0.1% SDS following 1μM rS100A12 binding to **A**) fibrinogen and **B**) denatured BSA on the level of rS100A12 bound. Data are means of triplicates ± SD. Representative experiments of **A**) three and **B**) two are shown.

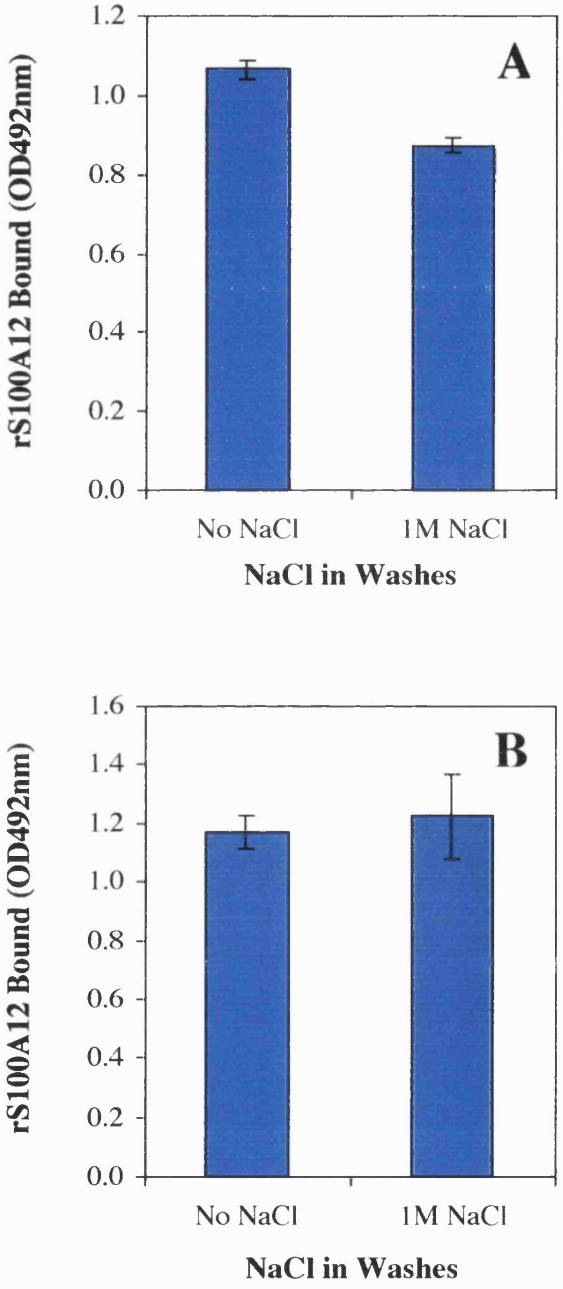

Figure 5.10: rS100A12 Binding to Fibrinogen and Denatured BSA is Resistant to a 1M NaCl Wash

The effect of a 1M NaCl wash following 1μM rS100A12 binding to **A**) fibrinogen and **B**) denatured BSA on the level of rS100A12 bound. Data are means of triplicates ± SD. Representative experiments of two are shown.

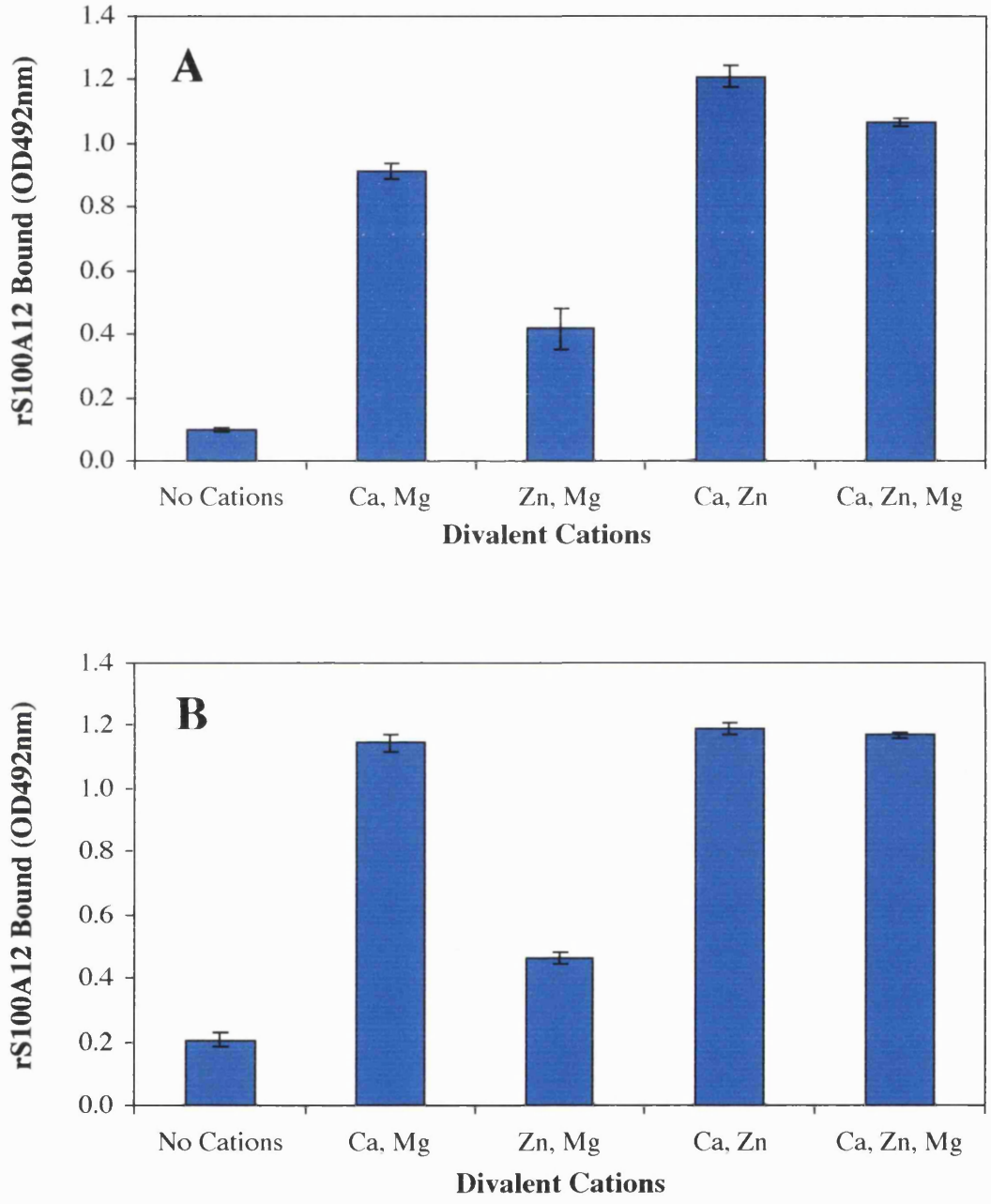

Figure 5.11: Divalent Cation Dependency of rS100A12 Binding to Fibrinogen and Denatured BSA

The requirement of different cations for 1μM rS100A12 binding directly to **A**) fibrinogen and **B**) denatured BSA. Data are means of triplicates ± SD. Representative experiments of two are shown.

5.3 Discussion

rMRP-14 stimulates the adhesion of T lymphoblasts and neutrophils to various ligands by an unknown mechanism. When the ligands were pre-treated with rMRP-14, washed and then T lymphoblasts allowed to adhere, the binding was equivalent to rMRP-14 being incubated with the cells. The relative affinity of rMRP-14 for the ligands directly paralleled that of T lymphoblast induced adhesion by the recombinant protein. Further, the induced cell binding occurred at a concentration of rMRP-14 roughly equal to those at which the protein bound maximally to the respective ligand. This data strongly implies the interaction of rMRP-14 with the ligand is required for the cell adhesion. Additionally, it may be inferred that rMRP-14 binding to the ligand was the limiting step. This is consistent with both the "molecular glue" and the rMRP-14-induced adhesive conformation of the immobilised ligand models of the proadhesive effect.

Denatured proteins can cause other proteins to unfold and aggregate. So, denatured BSA could potentially denature the recombinant protein, which would then non-specifically bind the ligand. However, this was thought unlikely because the immobilised rMRP-14 was detected by an antibody and a similar signal was obtained with a range of monoclonal antibodies (data not shown). Additionally, native BSA was able to compete the rMRP-14 from the denatured BSA, which is not consistent with this non-specific mechanism.

Amino acids of protein-protein interaction sites between two independent molecules generally reflect the nature of surface residues. As such, these interactions are usually mediated by electrostatic bonds between hydrophilic residues, with hydrophobic bonds contributing little (reviewed by (Sheinerman et al., 2000)). However, denaturation of proteins, such as BSA, will expose core residues, thus giving the protein surface a complex mix of hydrophobic and hydrophilic residues. Therefore, the nature of the interaction between rMRP-14 and the high affinity ligands was analysed. Four non-ionic detergents and the zwitterionic detergent,

CHAPS, did not disrupt the interaction with either ligand. Non-ionic detergents are considered non-denaturants, as they only disrupt the most hydrophobic protein-protein interactions. Zwitterionic detergents are more efficient at breaking protein-protein interactions, but CHAPS failed to significantly reduce the amount of rMRP-14 bound to either ligand. SDS, an anionic detergent, almost completely disrupted the interaction between rMRP-14 and the two high affinity ligands. However, unfortunately this reveals little about the nature of the bonds, as SDS disrupts virtually all protein-protein interactions and even denatures many proteins. The binding was also resistant to high salt, which disrupts ionic bonds. These results imply the binding is not solely dependent on ionic or hydrophobic interactions. Therefore, the interaction of rMRP-14 with fibrinogen and denatured BSA may be complex and maintained by both electrostatic and hydrophobic bonds. Certainly the nature of the interaction with both ligands appears to be similar. This may be due to fibrinogen being a large poorly soluble protein and thus may have surface features similar to those of denatured protein.

The interaction of rMRP-14 with the high affinity ligands required both calcium and zinc ions. Although fibrinogen can bind calcium (Marguerie et al., 1977), this was presumably due to the requirement of rMRP-14 for the divalent cations, as the same cations were required for binding to denatured BSA. Therefore, only the Ca^{2+}- and Zn^{2+}-bound conformation appears to bind to fibrinogen and denatured BSA. Calcium binding by some S100 proteins, such as S100B, causes a conformational change that leads to the creation of a hydrophobic and acidic crevice. This crevice has been shown to be the binding site of Ca^{2+}-dependent target proteins. Interestingly, Zn^{2+}-binding by S100A7 constricts this hydrophobic pocket (see Section 1.2.d). The Zn^{2+}-chelating residues of S100A7 are conserved in MRP-14. Fluorescence data with the MRP-8/-14 heterodimer shows that the binding of Ca^{2+} exposes some hydrophobic residues, and zinc ions restrict the solvent accessibility of these residues (Kerkhoff et al., 1999a). Together, this data indicates that, like S100A7, Zn^{2+}-binding to Ca^{2+}-bound MRP-14 may restrict an exposed hydrophobic

patch. The involvement of such a reduced hydrophobic patch in ligand binding may explain why the interaction appears to be mediated by both electrostatic and hydrophobic bonds.

Both BSA and heparin blocked T lymphoblast adhesion to rMRP-14 pre-treated fibrinogen and denatured BSA. 1% BSA blocked rMRP-14 binding to both ligands, and further it competed rMRP-14 from the ligands when pre-treated. This strongly implies that native BSA binds to the same site on rMRP-14 as the two higher affinity ligands. Also, native BSA probably blocks the cell adhesion by competing the rMRP-14 from the immobilised ligand. However, heparin did not block rMRP-14 binding to ligand, therefore heparin may interfere with the cell binding to rMRP-14-treated ligands.

Two anti-MRP-14 mAbs blocked rMRP-14 binding to denatured BSA, and also probably to fibrinogen. Four other anti-MRP-14 mAbs did not effect this interaction with denatured BSA. This would imply the same discrete site on rMRP-14 mediates the interaction with both ligands. Unfortunately, the binding site of the mAbs, and therefore also the high affinity ligands by association, could not be localised by peptide blocking (data not shown) or phage display analysis (J. Steel, ICRF Hybridoma Fusion Laboratory, personal communication). Interestingly, preliminary data from peptide blocking experiments demonstrated a peptide consisting of the C-terminal tail residues of MRP-14 (89-114) greatly reduced rMRP-14 binding to denatured BSA. Although five other peptides spanning the rest of the molecule did not block, the scrambled and reversed control peptides also blocked the interaction (data not shown). There appeared to be nothing unique about the three blocking peptides, apart from the composition, that would explain this inhibitory effect. Consequently, these initial experiments did not determine the discrete binding site for fibrinogen and denatured BSA, and, in fact, suggest that it is cryptic.

rMRP-14 binds to two very distinct ligands in a similar fashion, suggesting this interaction has limited specificity. In addition, the affinity of rMRP-14 for

native BSA and FSG was not greatly different, i.e. within an order of magnitude. Unfortunately, the standard specificity check for a protein-protein interaction, the binding in the presence of BSA, was not possible because BSA is a competing ligand. However, this limited specificity appears to conflict with the nature of the binding site on rMRP-14, which is discrete and conformation dependent. Therefore, I propose that a specific binding site on rMRP-14 binds to a feature that may be characteristic of many proteins. Further, the data above and in chapter 4 indicate that denaturation and/or degradation of a protein can reveal this rMRP-14 interacting feature.

rMRP-8 did not bind to the ligands in a similar fashion, which is further evidence that the rMRP-14 interaction is specific. This data also discounts rMRP-8 blocking the rMRP-14 binding sites of fibrinogen, as a possible mechanism of inhibition in the T lymphoblast adhesion assay.

rS100A12 bound both the high affinity ligands (fibrinogen and denatured BSA) better than rMRP-14, but did not bind the poor ligands (native BSA and FSG). The binding, like rMRP-14, was resistant to salt and non-ionic detergents, but the zwitterionic detergent, CHAPS, had a greater effect. Although significant, this gives little information about the nature of the interaction, as CHAPS will also disrupt some electrostatic bonds. Another parallel with rMRP-14 is that the interactions of rS100A12 required calcium, and thus were probably dependent on the conformation of the recombinant protein. Interestingly, despite having the same putative zinc binding site, the interaction of rS100A12 with the ligands was not zinc dependent. However, overall it would appear the characteristics of the interactions of these two S100 proteins are similar, and the affinities for the good ligands were not too different. Preliminary results suggest the binding of rS100A12 to denatured BSA and fibrinogen was not blocked by BSA, thus implying the interaction is more specific. This further supports the theory that, BSA only blocks the rMRP-14 because it is a weak ligand and not due to non-specificity.

The above study was based on the in vitro cell adhesion assay, and indicates that the binding of rMRP-14 to the immobilised ligands is a vital step in the proadhesive effect. Unfortunately, these assays reveal little about the physiological interactions of both MRP-14 and S100A12, and the features of the ligands that bind to the recombinant proteins. However, a continuation of the project, by investigating other ligands and further characterising the mAbs, could address these issues.

Chapter 6

rMRP-14 AND rS100A12 BINDING TO CELL SURFACES AND GLYCOSAMINOGLYCANS

6.1 Introduction

Glycosaminoglycans (GAGs) are linear co-polymers composed of alternating hexuronic acid and hexosamine units. The predominant mammalian GAGs are heparin, heparan sulphate, chondroitin sulphates, keratan sulphate and hyaluronan. GAGs exist either independently or linked to a core protein, known as a proteoglycan. Together these constitute a major proportion of extracellular matrices, and proteoglycans decorate the surface of most cells. The large size, complexity and variability of these structures has made them difficult to study, but recently the biochemistry of this field has advanced rapidly.

6.1.a Glycosaminoglycans Synthesis and Structure

Each GAG chain is synthesised by enzymatic addition of saccharide units and substitutions. Therefore, the structure is not as tightly regulated as for proteins or nucleic acids. Below is a brief summary of GAG structure and function as reviewed recently (Bernfield et al., 1999; Habuchi et al., 1998; Hardingham and Fosang, 1992; Kjellen and Lindahl, 1991; Lindahl et al., 1998; Rosenberg et al., 1997).

Heparin has been the most widely studied GAG, because of its therapeutic uses. Heparin is synthesised by mast cells and basophils as a proteoglycan of about $1x10^6$ Da. The co-polymers are initiated on tetrasaccharide linkers, which are in turn covalently attached to the core protein through O-glycosidic links. The alternating addition of N-Acetyl-D-glucosamine (GlcNAc) and glucuronic acid (GlcA) units then build up the GAG chains of heparin. Each polysaccharide chain may vary in length by up to an order of magnitude, but usually consists of 50-200 disaccharide

units. The co-polymers are sequentially modified by several enzymes, with the product of one enzyme being the substrate of the next. Initially, a N-deactetylase/N-sulphotransferase converts GlcNAc to N-Sulpho-D-glucosamine (GlcNSulpho). This allows a C5-epimerase to convert the adjoining GlcA residue to an iduronic acid (IdoA). The disaccharide unit is then susceptible to O-sulphation on the C-2 of IdoA, the C-6 of GlcNSulpho and the C-3 of the same residue. Because the enzymatic modifications do not always go to completion, the process can result in 24 different disaccharides. This introduces considerable structural heterogeneity even within a single chain. The GAG chains of heparin are generally very highly modified with typically only 10% of the GlcA units remaining unaltered. In fact, heparin is so heavily sulphated it is the most negatively charged polyelectrolyte found in mammalian tissues. On degranulation of mast cells and basophils, the heparin proteoglycan is proteolytically cleaved into glycoconjugates of about 13,000Da.

Heparan sulphate chains are synthesised by the same mechanism as heparin, but generally are modified to a much lesser extent than heparin. Unlike heparin, the N-deactetylase/N-sulphotransferase only modifies clusters of GlcNAc residues. Consequently, heparan sulphate typically has highly sulphated domains of 6-10 disaccharides units with intervening unmodified domains of 16-20 units.

Chondroitin sulphate GAG chains are co-polymers of D-galactosamine (GalNAc) and GlcA. The polysaccharides are synthesised in a similar fashion to heparin, and are attached to a core protein by the same tetrasaccharide linker. The chains can be divided in to three groups depending on subsequent modifications. Chondroitin-4-sulphate is largely sulphated on the C-4 of the GalNAc residues and the same residue is predominantly sulphated on C-6 in chondroitin-6-sulphate. Dermatan sulphate is similar to chondroitin-4-sulphate, but is more heavily sulphated and a significant portion of the GlcA residues are epimerised to IdoA.

Keratan sulphate is a co-polymer of galactose (Gal) and GlcNAc with both residues being O-sulphated primarily at the C-6 position. Again the chains are synthesised on a protein core, but the carbohydrate linker is different.

Hyaluronan differs greatly, as it is not synthesised on a core protein and is unmodified. Rather the chains are homogenous non-sulphated co-polymers of alternating GlcA and GlcNAc residues.

6.1.b Glycosaminoglycans Functions in Cell Adhesion

A function for GAGs has been implied in many processes, such as cell division, adhesion, spreading, migration, chemoattraction, axon guidance, matrix assembly, lipoprotein uptake, extracellular proteolysis, tumour invasion and microbial entry. However, the precise role of the GAGs is often unclear. Additionally, these structures have several mechanical functions, including exclusion of macromolecules, load distributions and tensile strengthening. Cell surface proteoglycans modulate cell adhesion by mediating cell to extracellular matrix binding and by interacting with soluble factors.

6.1.b.i Cell to Extracellular Matrix Binding

Many extracellular matrix proteins bind to GAGs. Several of these interactions occur within the matrices with constituent GAGs and/or proteoglycans, thereby giving increased mechanical strength (reviewed by (Iozzo, 1998)). GAG binding proteins of matrices also bind to proteoglycans of cell surfaces (reviewed by (Iozzo, 1998) and (Bernfield et al., 1999)), but these are often low affinity interactions. However, the proteoglycans are thought to function as co-receptors for integrins, the major class of extracellular matrix binding cellular receptors. Thus on integrin mediated cell binding to an extracellular matrix, the cell surface proteoglycans are brought into contact with GAG binding proteins. This allows the formation of several low affinity interactions .

Syndecans, a family of proteoglycans, have been identified as the primary co-receptors for extracellular matrices, and have recently been reviewed in (Woods and Couchman, 1998) and (Carey, 1997). Four syndecan core proteins, with low homology, have been identified. They are type I membrane proteins, and typically carry 3-5 heparan sulphate chains on the extracellular domain. The expression of each member is cell type restricted and developmentally regulated. Several studies indicate that the role of syndecans is not just as an adhesive receptor, because they have been shown to link the extracellular matrix with the cell cytoskeleton and to be required for focal contact assembly. However, the precise mechanism by which these proteoglycans act as activating receptors is yet to be fully elucidated.

6.1.b.ii Binding of Soluble Proteins

Several soluble proteins also interact with GAG chains. These proteins have a wide range of affinities, 10^{-5} to 10^{-9}M, and include enzymes, enzyme inhibitors, growth factors, growth factor binding proteins, morphogens and cytokines (reviewed by (Tanaka et al., 1998) and (Bernfield et al., 1999)). Most of these proteins were originally found to interact with heparin, but the restricted expression of heparin suggests heparan sulphate is probably the physiological ligand. This and other analysis indicate that the highly sulphated domains of heparan sulphate are the primary binding sites. Dermatan sulphate is the other major ligand identified.

Despite GAG chains often being thought as non-specific polyanions, proteins often bind to specific sequences (reviewed by (Gallagher, 1997) and (Lindahl et al., 1998)). The best known example is the heparin binding protein, anti-thrombin III, which binds a unique pentasaccharide structure with specific sulphate substitutions (Lindahl et al., 1984). These sequence specific protein binding sites typically comprise 5-15 saccharide units. The iduronic acid residues, found in heparin, heparan sulphate and dermatan sulphate, are a feature of many protein binding sequences. Iduronic acid has a flexible structure, and this is thought to be important

in these GAG-protein interactions (Casu et al., 1988). Other proteins show some selectivity in binding GAG chain microdomains that may not be as precise, for example the chemokines IL-8 and GROα, but not PF-4, preferentially bind the same sub-population of heparin molecules (Witt and Lander, 1994).

Analysis of small subsets of heparin binding proteins has given rise to different putative heparin binding motifs, such as xBBxBx, xBBBxxBx and TxxBxxTBxxxTBB (where x is any amino acid, B is a basic residue and T is a turn). However, these have not stood up to more expansive analysis. The three dimensional structures of heparin binding proteins appear to suggest that the sites are generally comprised of basic residues, but are often cryptic (reviewed by (Hileman et al., 1998) and (Spillmann and Lindahl, 1994)). Studies have indicated preferences amongst the basic amino acids, such that they can be ordered by contribution to heparin binding: Arg>Lys>Glu>His (see (Hileman et al., 1998)).

Several roles have been suggested for the binding of soluble proteins to GAG chains, and these can differ greatly between proteins (reviewed by (Nelson et al., 1995), (Tanaka et al., 1998) and (Bernfield et al., 1999)). A common function is to simply immobilise the soluble protein at the target site, thus effectively causing a localised increase in concentration. This is most evident with chemokines, which can be immobilised on the on the luminal face of endothelial cells by proteoglycans. This is especially vital in blood flow to prevent the chemokines from being washed away (also see (Tanaka et al., 1993)). In these cases the GAG chains often facilitate ligand-receptor engagement, but are not essential. In a growing number of cases the proteoglycan actually modulates the interaction of a soluble effector with the signalling receptor. The best studied examples are the fibroblast growth factors (FGFs), which require heparan sulphate or heparin to induce a signal via dimerisation of the high affinity receptors (FGFRs). Although the exact mechanism is not known, the polysaccharide can dimerise the FGFs, increase the affinity for the FGFRs and decrease the dissociation constant. The FGFRs also contain a heparin binding site that is contiguous with an equivalent site on FGF when complexed.

Therefore, it seems likely that the three molecules form a complex, and this is required for signalling (for details see (Schlessinger et al., 1995) and (Ornitz, 2000)). Proteoglycan binding of soluble proteins also has been shown to protect them from degradation especially by proteases (Webb et al., 1993). Cell surface GAG chains have also been implicated in the internalisation of soluble proteins, for example low density lipoproteins (Fuki et al., 1997).

6.1.c Aims

The aim of this project was to further characterise the rMRP-14 induced binding of T lymphoblasts to the proteinaceous ligands (see Fig 4.2). The results from chapter 5 demonstrate that rMRP-14 binds directly to the proteinaceous ligands and T lymphoblasts adhere to this complex (see Fig 5.1A and B). The data also demonstrate that heparin can block T lymphoblast binding to the complex (see Fig 5.1C). Specifically this project has attempted to address two questions. Firstly does rMRP-14 interact directly with T lymphoblasts? This was thought to be possible, because T lymphoblasts adhere poorly to the proteinaceous ligands but well to the complex. Secondly, what is the mechanism of heparin blocking of T lymphoblasts binding to the complex? This is of interest because heparin blocks the cell binding, but does not effect rMRP-14 binding to the proteinaceous ligands.

6.2 Results

6.2.a rMRP-14 Binds to the Cell Surface of T Lymphoblasts and HMEC-1

rMRP-14 bound to T lymphoblasts, as detected by the monospecific antisera, was saturable and titrated with half maximal binding being achieved between 1 and 3μM rMRP-14. Similar binding characteristics were observed with two anti-rMRP-14 mAbs (data not shown), and rMRP-14 directly labelled with FITC (R. Newton, unpublished data). This interaction with the T lymphoblast cell surface was inhibited by 100μg/ml heparin (Fig 6.1A).

rMRP-14 also bound to cells of the human microvascular endothelial cell line HMEC-1 in a similar fashion. The affinity of the interaction with HMEC-1 cells was higher than that observed with T lymphoblast, as half maximal binding was achieved between 0.1 and 0.3 μM rMRP-14. 100μg/ml heparin blocked the binding of low concentrations of rMRP-14, but higher concentrations of rMRP-14 overcame this inhibition. Interestingly, HMEC-1 cells removed from gelatin by trypsinisation showed little binding of rMRP-14, suggesting the rMRP-14 receptor is trypsin sensitive (Fig 6.1B).

The cell surface binding of rMRP-14 appears to be promiscuous, as preliminary data shows the recombinant protein bound to all the tested cell lines. Namely rMRP-14 can interact with: the myeloid cell lines, HL60 and THP-1; the fibroblast cell line, COS-1 cells (data not shown) and the bone marrow leukemic cell line, K-562 (Newton, 1997).

The blocking by heparin was further characterised by evaluating the effect of the other GAGs. Dermatan sulphate at 10μg/ml, but not 1μg/ml, blocked 9μM rMRP-14 binding to T lymphoblasts, which was as potent as heparin. Heparan sulphate, chondroitin-4-sulphate and chondroitin-6-sulphate also inhibited the interaction, but only at 100μg/ml. Hyaluronan and keratan sulphate did not effect the binding (Fig 6.2A). The situation changed when the GAGs were used to disrupt the

interaction between 0.3μM rMRP-14 and HMEC-1 cells surfaces. Heparin was more potent at blocking binding to HMEC-1 than to T lymphoblasts, as 1μg/ml of GAG inhibited the interaction. However, this increase in potency probably is due to the lower concentration of rMRP-14 used in the HMEC-1 binding assay. Dermatan sulphate was almost as effective as heparin. Heparan sulphate and chondroitin-4-sulphate both partially reduced the amount of rMRP-14 binding to the HMEC-1 at 100 μg/ml, whilst chondroitin-6-sulphate, hyaluronan and keratin sulphate had little or no effect on the interaction (Fig 6.2B). Therefore, the GAG blocking of rMRP-14 binding to the cell surface of T lymphoblasts and HMEC-1 appears to be similar with heparin and dermatan sulphate being potent inhibitors, whilst heparan sulphate and chondroitin-4-sulphate were poor blocking agents. Hyaluronan and keratan sulphate did not block. The most significant difference was that chondroitin-6-sulphate blocked rMRP-14 binding to T lymphoblasts but not to HMEC-1 cells.

The only known receptor for a S100 protein is the Receptor for Advanced Glycation End products (RAGE). S100A12 ligation of RAGE is blocked by glycated proteins (Hofmann et al., 1999), the first reported ligand for RAGE (Schmidt et al., 1994). As an attempt to discount rMRP-14 binding to RAGE on the cell surfaces, 1mg/ml glycated BSA was used as a blocking agent. The glycated BSA did not inhibit the interaction of rMRP-14 with either T lymphoblasts or HMEC-1 cells (Fig 6.3).

Both calcium and zinc were required for rMRP-14 to interact with fibrinogen and denatured BSA. The same two cations also were required for binding to the cell surface of T lymphoblasts and HMEC-1, with the removal of magnesium having little or no effect on the amount of the recombinant protein binding (Fig 6.4).

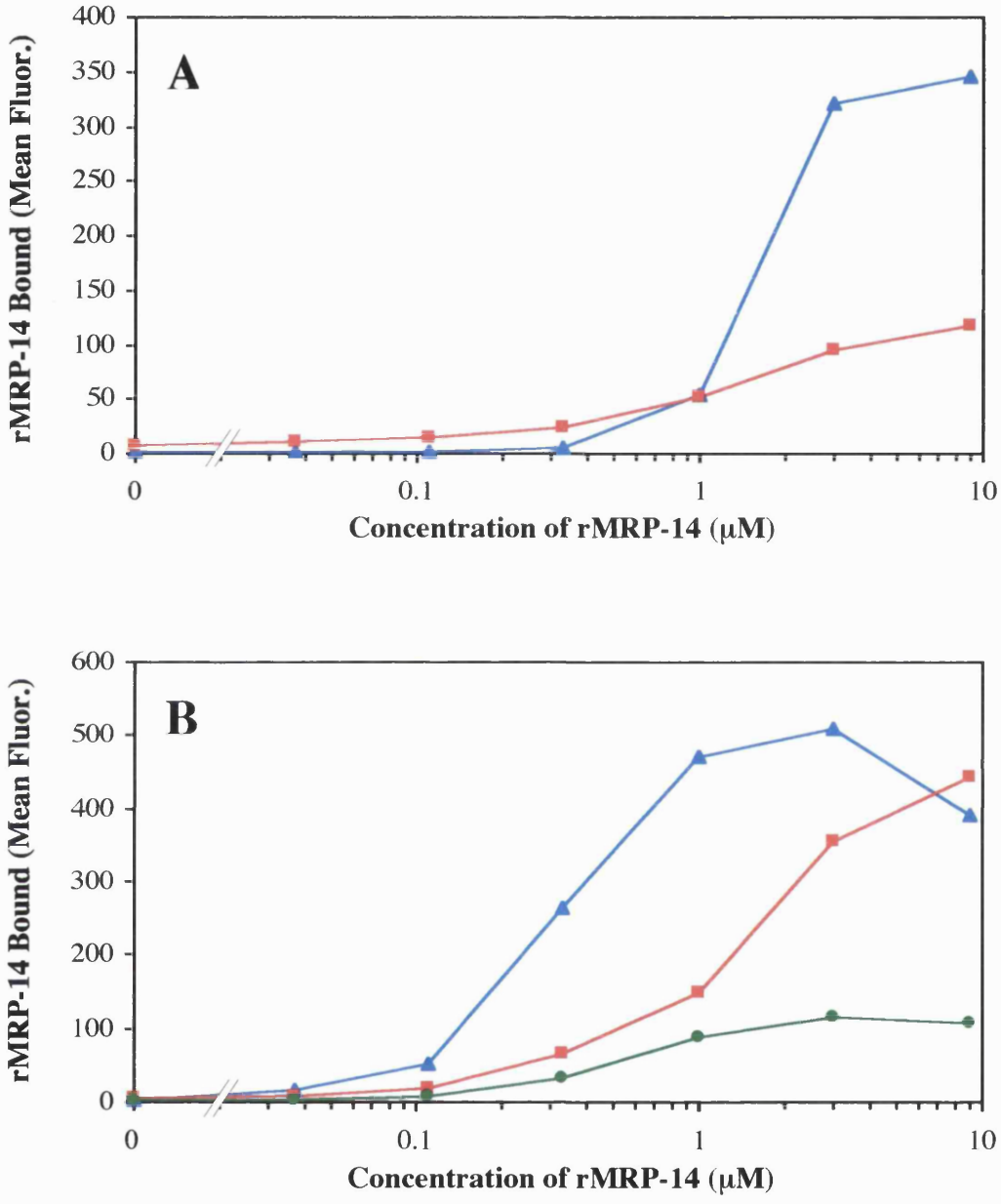

Figure 6.1: rMRP-14 Binding to the Cell Surface of T Lymphoblasts and HMEC-1 cells

rMRP-14 binding to the cell surface of **A**) T lymphoblasts and **B**) HMEC-1 cells in the absence of (▲) and presence of (■) 100μg/ml heparin. The effect of trypsin treatment of HMEC-1 is also shown (●). Data are geometric mean fluorescence of 5000 cells. Representative experiments of at least three are shown.

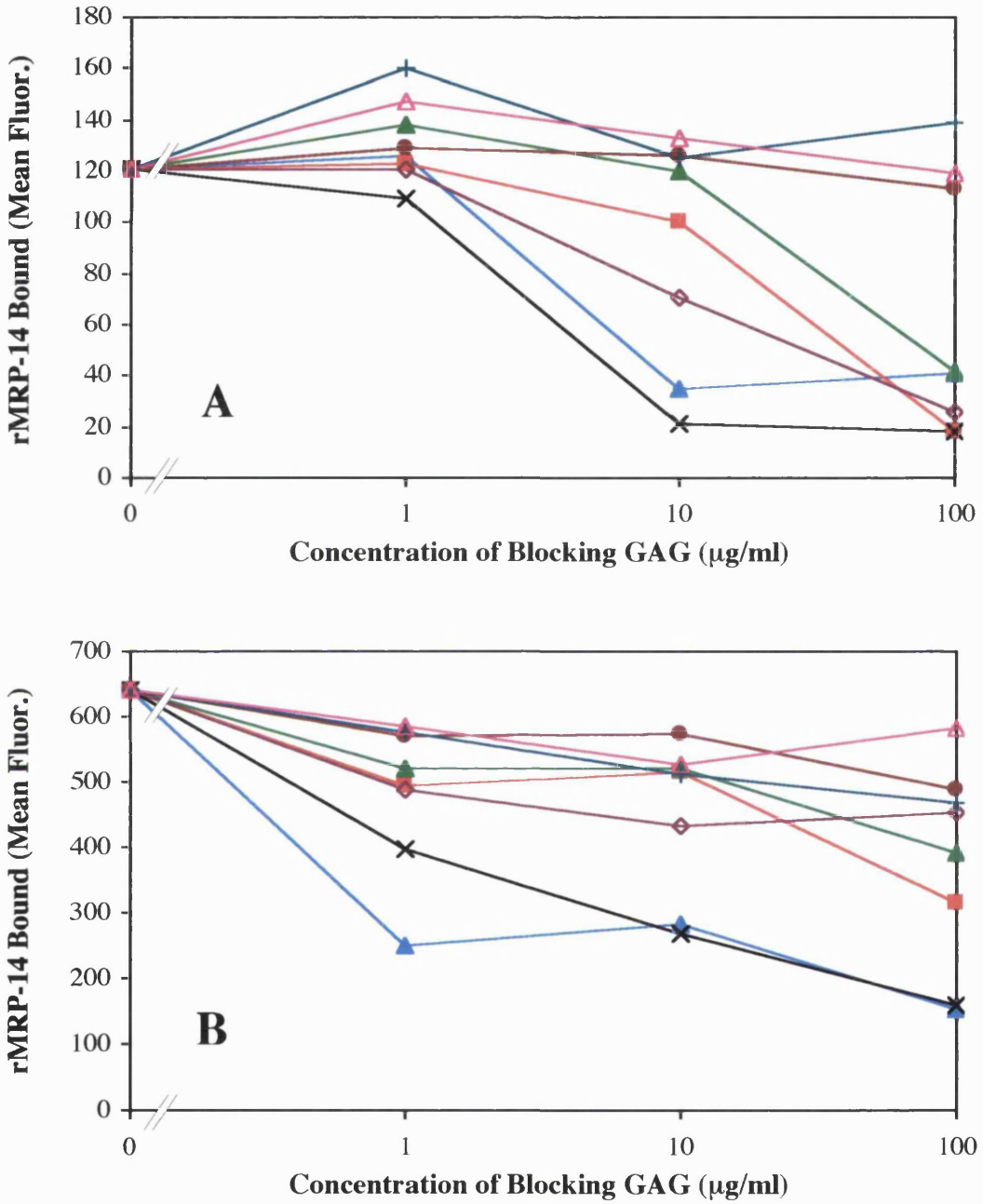

Figure 6.2: rMRP-14 Binding to T Lymphoblasts and HMEC-1: GAGs as Blocking Agents

The binding of **A)** 9µM rMRP-14 to T lymphoblasts and **B)** 0.33µM rMRP-14 to HMEC-1 in the presence of heparin (▲), heparan sulphate (■), dermatan sulphate (X), chondroitin-4-sulphate (▲), chondroitin-6-sulphate (◇), keratan sulphate (△), hyaluronan (●) or a buffer control for hyaluronan (+). Data are geometric mean fluorescence of 5,000 cells. Representative experiments of three are shown.

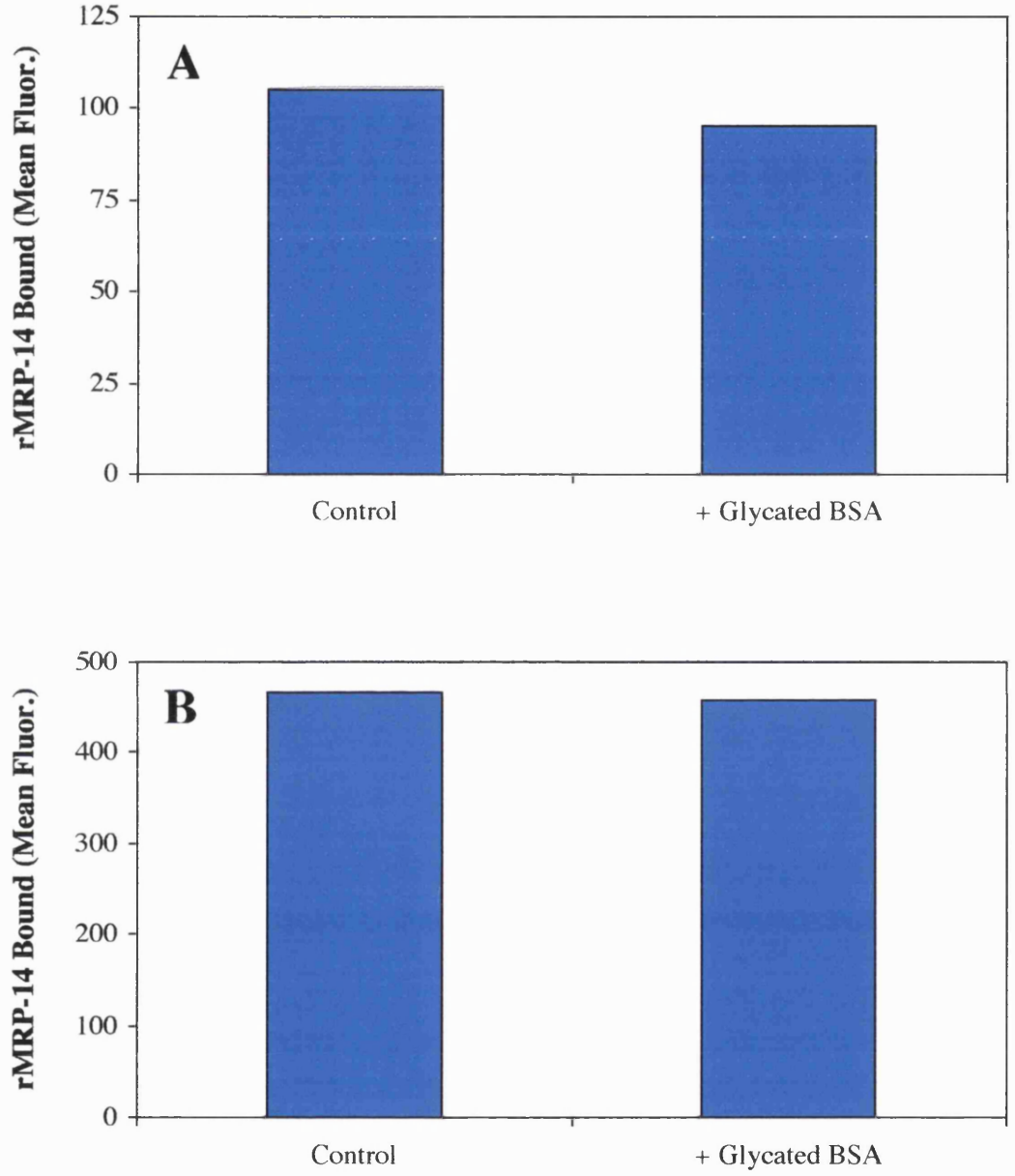

Figure 6.3: rMRP-14 Binding to T Lymphoblasts and HMEC-1: The Effect of Glycated BSA

The effect of 1mg/ml glycated BSA on **A**) 9μM rMRP-14 binding to T lymphoblasts and **B**) 0.33μM rMRP-14 binding to HMEC-1. Data are geometric mean fluorescence from 5,000 cells. Representative experiments of three for **A** and two for **B** are shown.

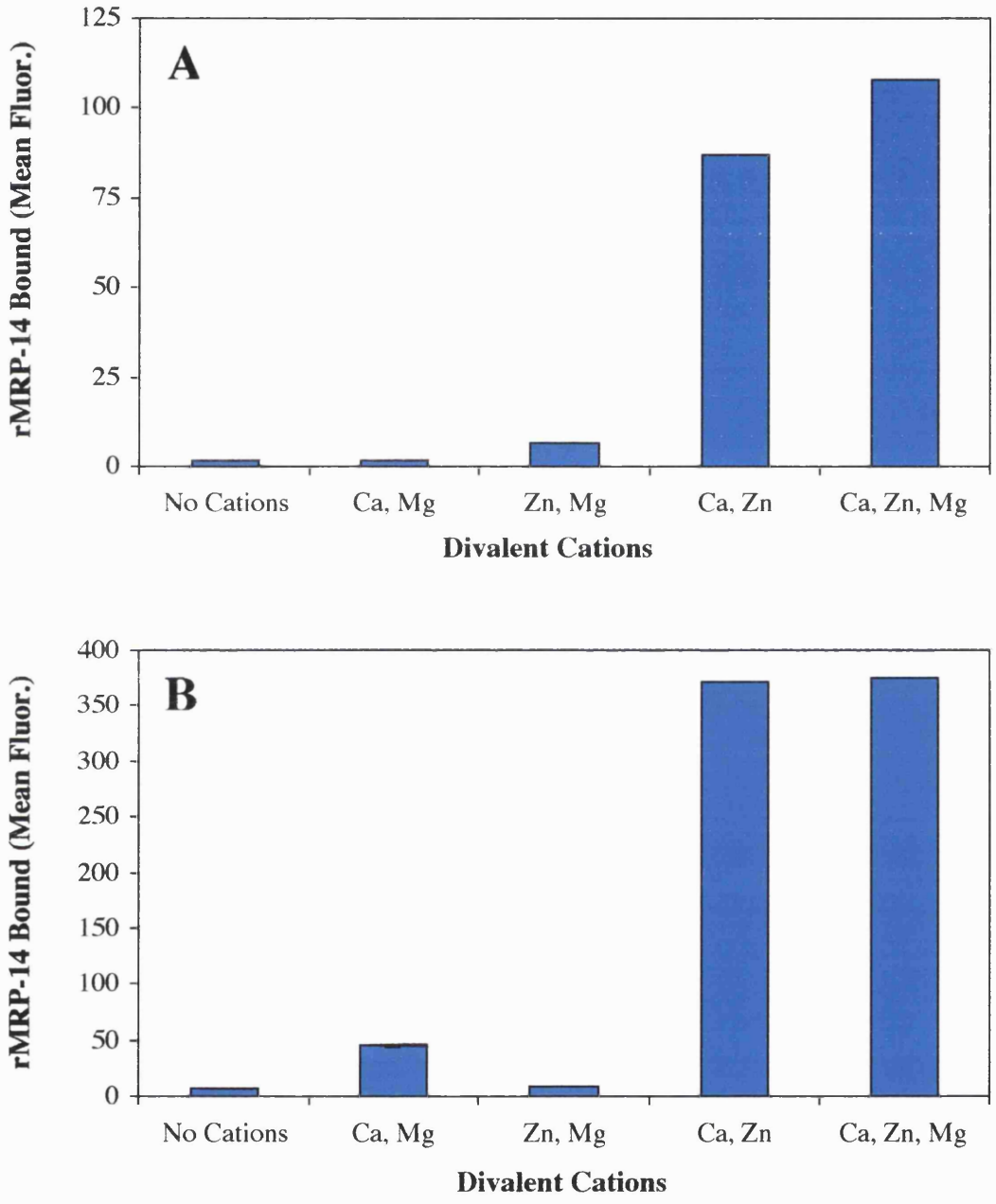

Figure 6.4: rMRP-14 Binding to T Lymphoblasts and HMEC-1: Divalent Cation Dependency

The requirement of different divalent cations for **A**) 9μM rMRP-14 binding to T lymphoblasts and **B**) 0.33μM rMRP-14 binding to HMEC-1. Data are geometric mean fluorescence from 5,000 cells. Representative experiments of three are shown.

6.2.b rMRP-14 Interaction with Heparin

In an assay that quantified the amount of [3H] heparin binding to rMRP-14 immobilised on mAb 1H9, heparin bound to rMRP-14 with high affinity and was saturable. The binding was specific, because it was almost completely inhibited with 100μg/ml cold heparin. In addition, 1H9 did not bind heparin in the absence of rMRP-14 (Fig 6.5A). Scatchard analysis of [3H] heparin binding after 1 hour determined the Kd to be 79±44 ng/ml (See Fig 6.5B, n=5). This did not significantly differ from the Kd determined after 30 minutes (97±77 ng/ml, n=3) and after 2 hours (92±26 ng/ml, n=3) of binding. Thus the 1 hour time point was chosen. Using the mid point value of the heparin molecular weight range (i.e. 13,000 Da) gave a Kd of 6.1±3.4 nM (as determined at 1 hour).

To investigate the specificity of the interaction between rMRP-14 and heparin, the effect of various GAGs on 100ng/ml [3H] heparin binding to rMRP-14 was assessed. Cold heparin blocked the interaction even at the lowest concentration, 10μg/ml. Both dermatan sulphate and chondroitin-4-sulphate partially inhibited the binding at 100μg/ml and reduced it completely at 500μg/ml. Heparan sulphate, chondroitin-6-sulphate and keratan sulphate did not effect the interaction at concentrations up to 500μg/ml. Hyaluronan slightly increased the amount of [3H] heparin binding, but the buffer control also had this effect (Fig 6.6A). Therefore, this improved binding is probably due to the reduced pH, which often increases the affinity of protein-GAG interactions. A parallel experiment demonstrated that the GAGs at 500μg/ml did not significantly reduce the amount of rMRP-14 anchored to the mAb, 1H9 (Fig 6.6B).

Modified preparations of heparin were also used to block 100ng/ml [3H] heparin binding to rMRP-14. Heparin blocked the interaction with an IC_{50} of 10-100ng/ml. This IC_{50} is lower than the concentration of [3H] heparin, which probably indicates the two preparations of heparin differed somewhat. Removal of the amino-linked sulphate groups of heparin (de-N-sulphated heparin) greatly reduced the

potency of heparin as a blocking agent by about three orders of magnitude. Acteylation of the amino groups following de-N-sulphation (N-acetyl heparin) did not greatly effect the blocking of the heparin-rMRP-14 interaction as compared to de-N-sulphated heparin. Removal of O-linked sulphate groups from this acetylated de-N-sulphated heparin (N-acetyl-de-O-sulphated heparin) completely removed the capacity of heparin to block the interaction (Fig 6.7A). A parallel experiment demonstrated that these preparations of modified heparin at 500μg/ml did not significantly reduce the amount of rMRP-14 anchored to mAb 1H9 (Fig 6.7B). This suggests the binding of rMRP-14 to heparin is dependent on the sulphate substitutions.

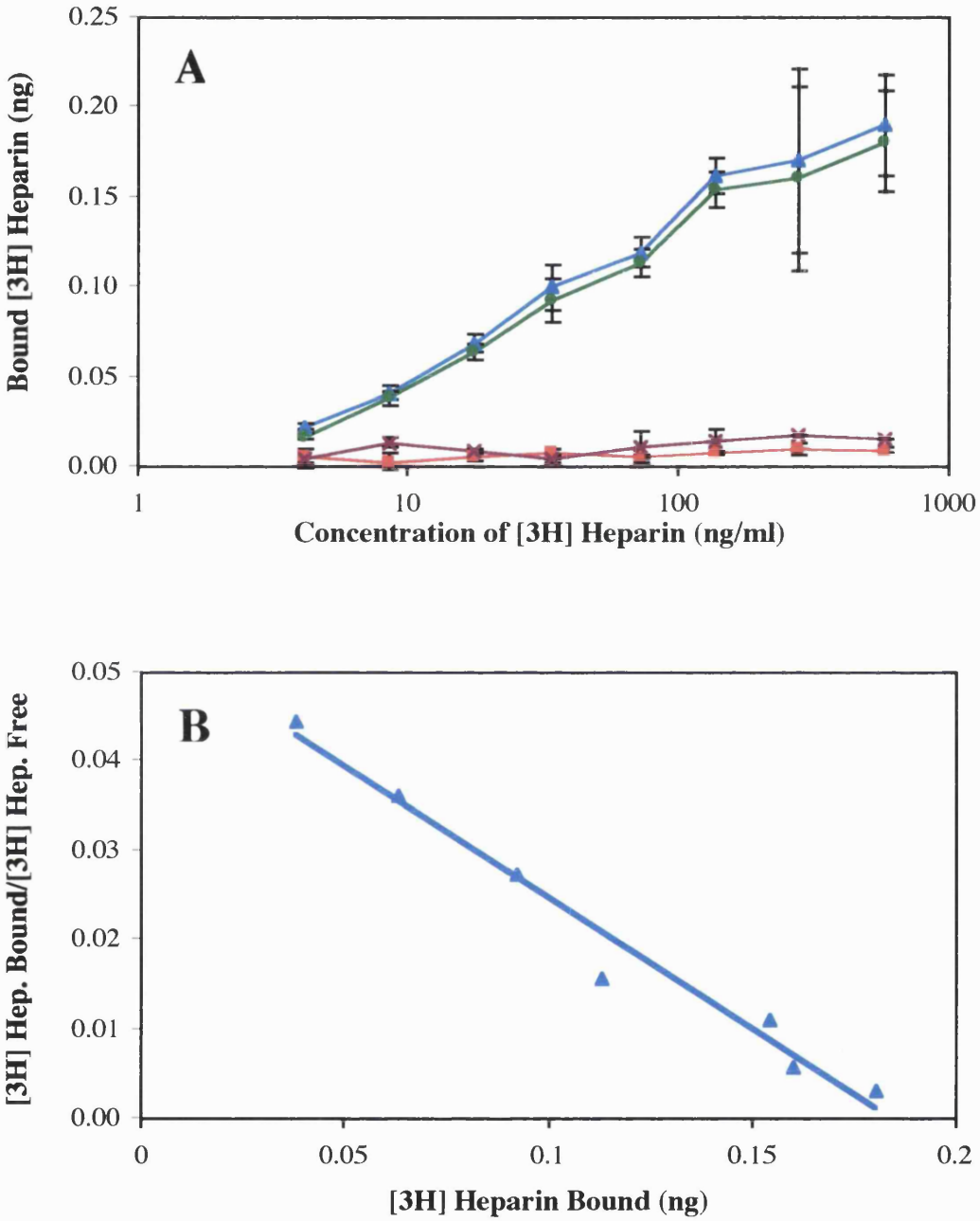

Figure 6.5: [3H] Heparin Binding to rMRP-14

A) [3H] Heparin binding to rMRP-14 after 1 hour (▲), binding in the presence of 100µg/ml cold heparin (■), binding in the absence of rMRP-14 (X) and specific binding to rMRP-14 (●). Data are means of triplicates ± SD. **B)** Scatchard analysis of [3H] Heparin binding to rMRP-14. A representative experiment of five is shown.

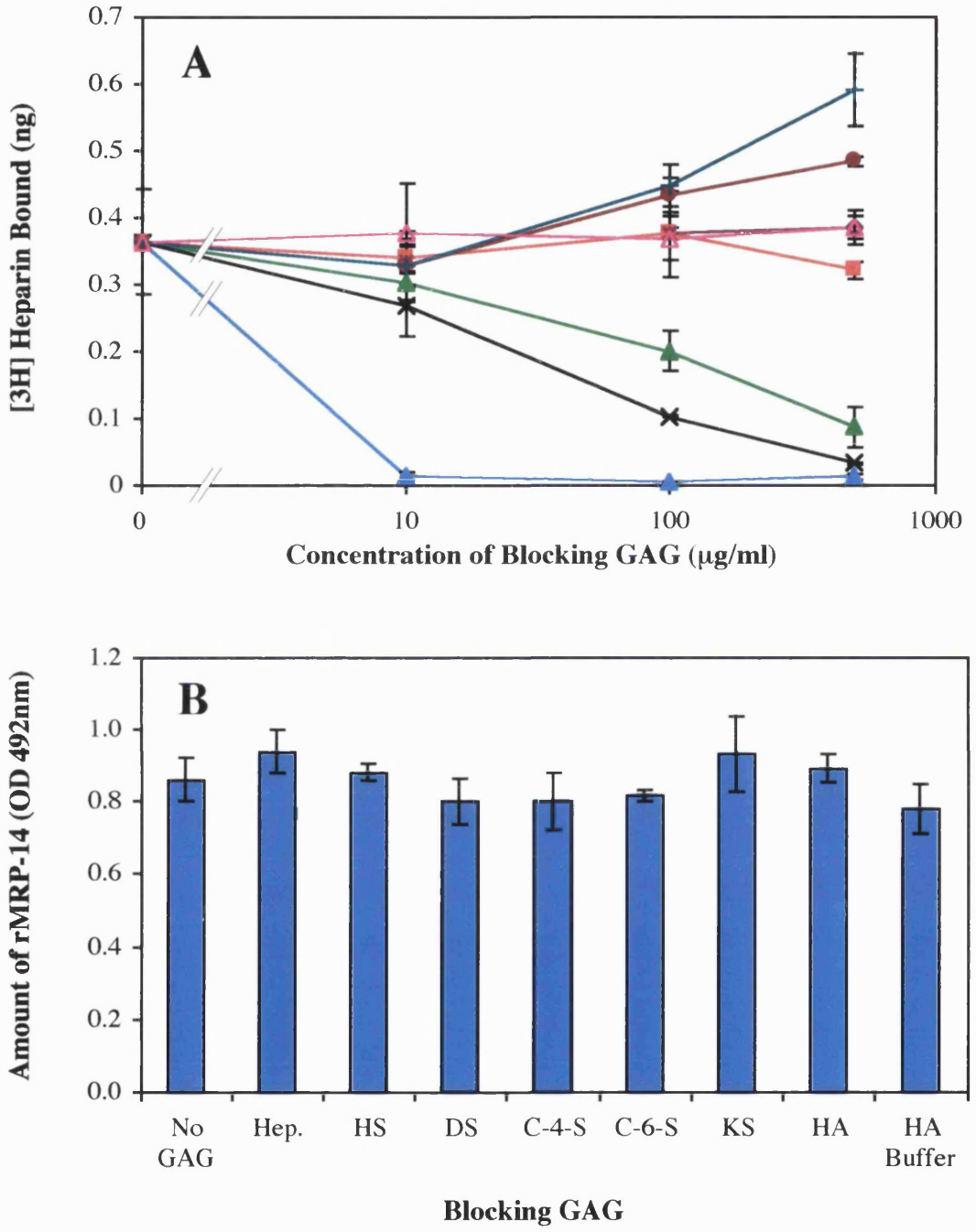

Figure 6.6: [3H] Heparin Binding to rMRP-14: GAGs as Blocking Agents
A) 100ng/ml [3H] Heparin binding to rMRP-14 immobilised on 1H9 in the presence of heparin (▲), heparan sulphate (■), dermatan sulphate (X), chondroitin-4-sulphate (▲), chondroitin-6-sulphate (◇), keratan sulphate (△), hyaluronan (●) or a buffer control for hyaluronan (+). **B)** The effect of the same GAGs at 500µg/ml on the amount of rMRP-14 immobilised on 1H9. Data are means of triplicates ± SD. A representative experiment of three is shown.

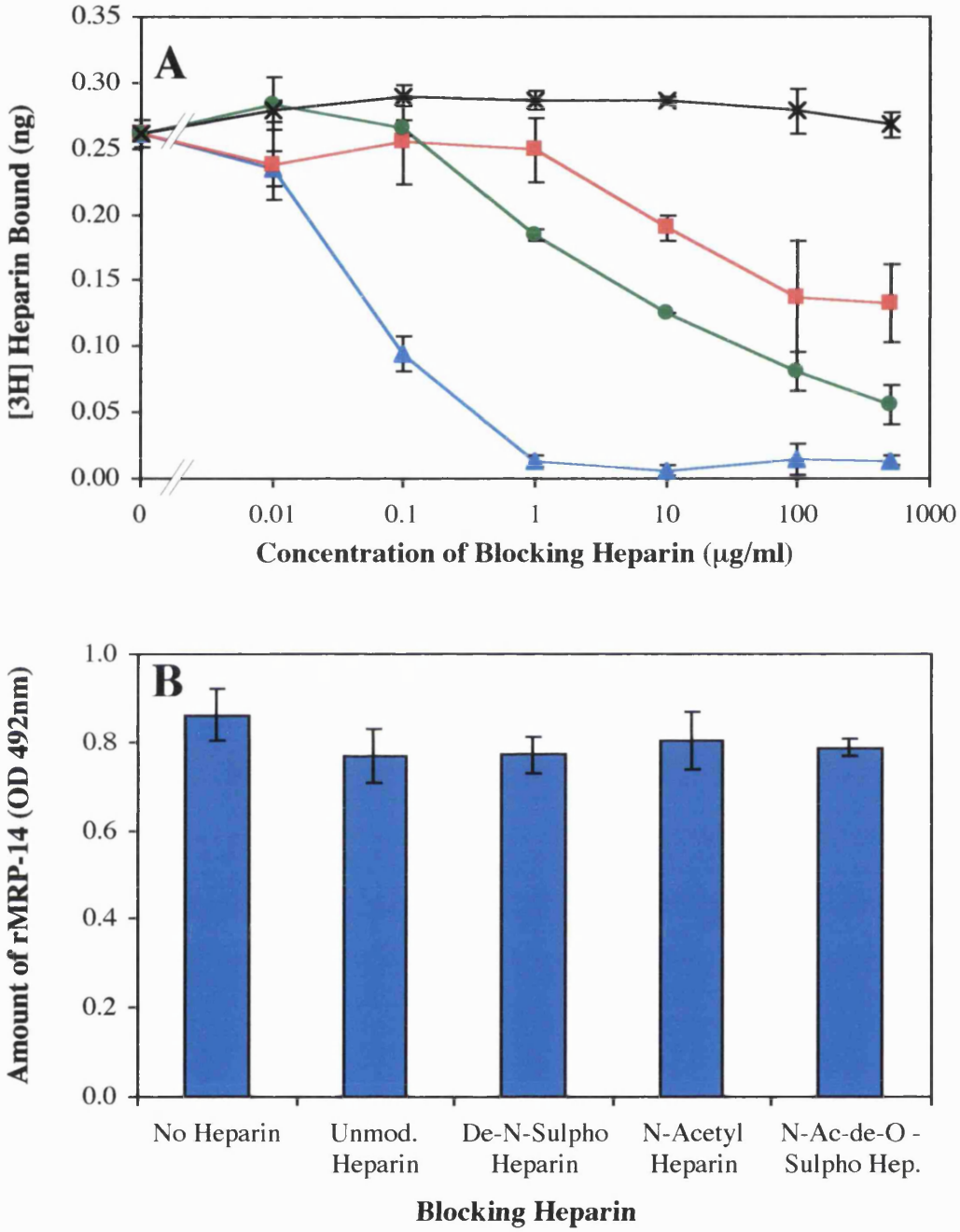

Figure 6.7: [3H] Heparin Binding to rMRP-14: Modified Heparin as Blocking Agents

A) 100ng/ml [3H] heparin binding to rMRP-14 immobilised on 1H9 in the presence of unmodified heparin (▲), de-N-sulphated heparin (■), N-acetyl heparin (●) or N-acetyl-de-O-sulphated heparin (X). **B**) The effect of the same GAGs at 500µg/ml on the amount of rMRP-14 immobilised on 1H9. Data are means of triplicates ± SD. A representative experiment of three is shown.

6.2.c Characterising the rMRP-14 Interaction with Heparin

The interaction of rMRP-14 with heparin differs greatly from that with proteinaceous ligands. The affinity of the binding to heparin is considerably higher. The binding was also unaffected by BSA, as the assay buffer contained 2% BSA and removing this did not significantly alter the binding characteristics (data not shown). In addition, the heparin bound to rMRP-14 was disrupted by washing with assay buffer containing 0.5M NaCl (Fig 6.8A). Again, a parallel experiment demonstrated the salt wash did not reduce the amount rMRP-14 anchored by mAb 1H9 (Fig 6.8B).

To further elucidate the differences between rMRP-14 binding to heparin and the proteinaceous ligands, the effect of anti-rMRP-14 mAbs on 100ng/ml [3H] heparin binding rMRP-14 was established. When rMRP-14 was anchored on 1H9, the same mAb at 20μg/ml partially reduced the amount of [3H] heparin binding. However, the 1H9 also reduced the amount of rMRP-14 immobilised. Although this was not significant, it suggests the inhibition was due to competing rMRP-14 from the anchoring mAb. 6E1 and 1F5 blocked the binding of [3H] heparin without reducing the amount of rMRP-14 anchored. Interestingly, 6G4 consistently increased the amount of [3H] heparin bound by approximately two fold (Fig 6.9). 6G4 does not directly ligate [3H] heparin (data not shown).

To evaluate the effect of 1H9 and to further investigate the mAb blocking, the effect of anti-rMRP-14 mAbs on 100ng/ml [3H] heparin binding rMRP-14 anchored on 6G4 was assessed. Preliminary data suggests [3H] heparin binds to rMRP-14 immobilised on 6G4 with the same affinity and a similar maximal binding, as rMRP-14 anchored to 1H9 (data not shown). 1H9 did not significantly effect the interactions, which is consistent with the reduction in binding seen previously being due to the competing of rMRP-14 from the anchoring mAb. Surprisingly, 6E1 also did not inhibit the binding of [3H] heparin. This differs from the previous results when 1H9 anchored the rMRP-14. Another difference is that 6G4 did not induce an increase in [3H] heparin binding. 1F5, again, completely inhibited the interaction of

[3H] heparin with rMRP-14. However, 1F5 was also able to partially reduce the amount of rMRP-14 anchored to 6G4, but the amount of rMRP-14 displaced is unlikely to be completely responsible for the level of blocking observed in the heparin binding assay (Fig 6.10). Therefore 1F5 appears to block the interaction between heparin and rMRP-14, and 6E1 also blocks but only when in combination with 1H9.

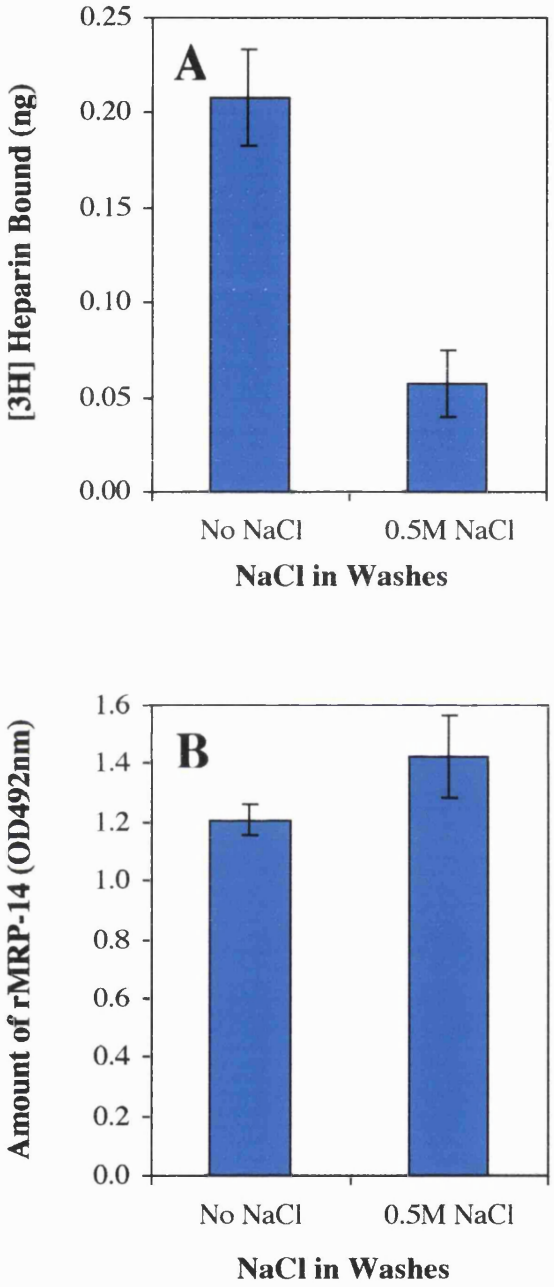

Figure 6-8: [3H] Heparin Binding to rMRP-14: The Effect of 0.5M NaCl
A) [3H] heparin at 100ng/ml was bound to rMRP-14 immobilised on 1H9 and washed three times with assay buffer with and without 0.5M NaCl. **B**) The effect of the 0.5M NaCl wash on the amount of rMRP-14 immobilised on 1H9. Data are means of triplicates ± SD. A representative experiments of two is shown.

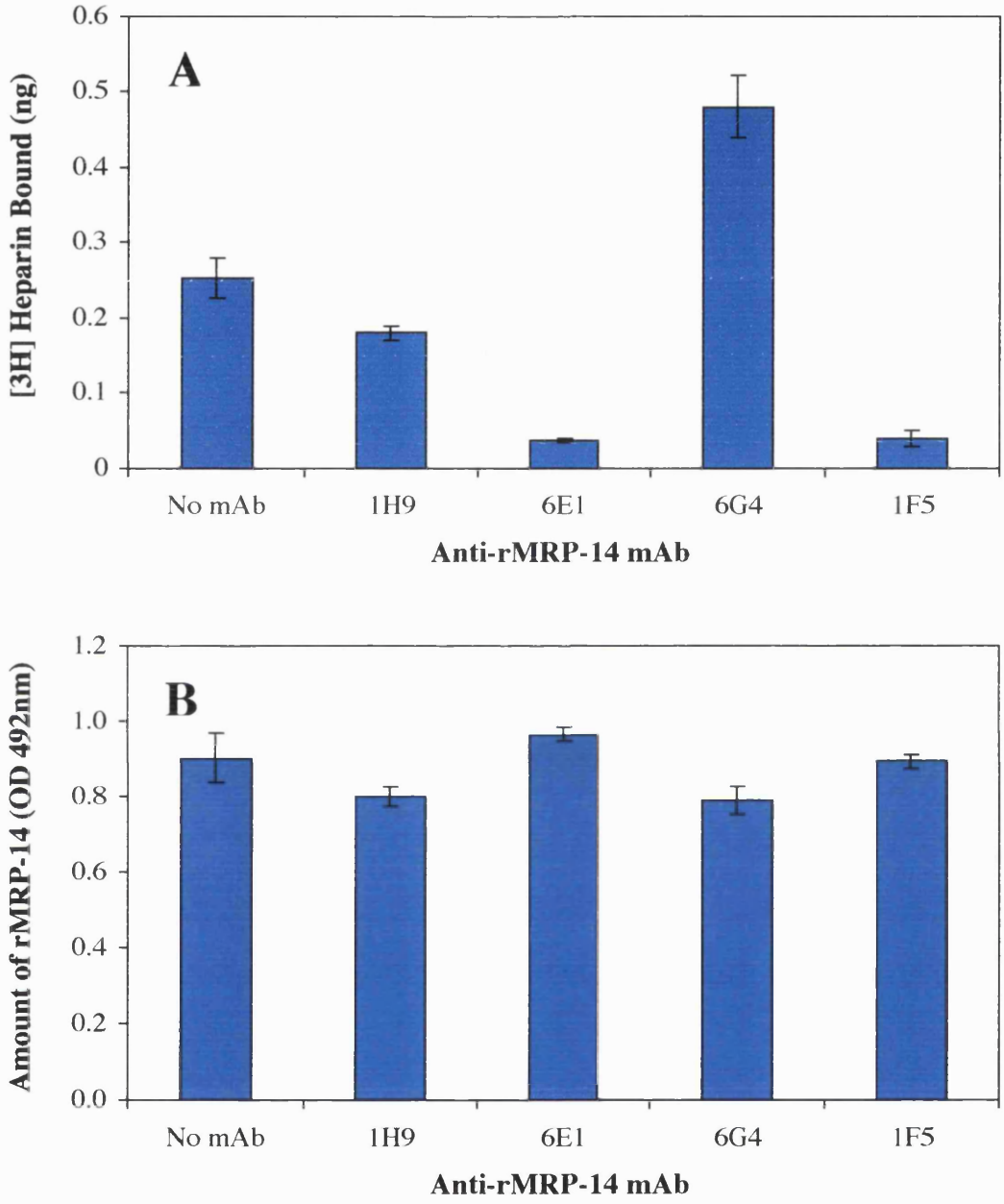

Figure 6.9: [3H] Heparin Binding to rMRP-14: Anti-rMRP-14 mAbs as Blocking Agents

A) The effect of anti-rMRP-14 mAbs at 20μg/ml on 100ng/ml [3H] heparin binding to rMRP-14 immobilised on 1H9. **B**) The effect of the same mAbs under identical conditions on the amount of rMRP-14 immobilised. Data are means of triplicates ± SD. A representative experiments of three is shown.

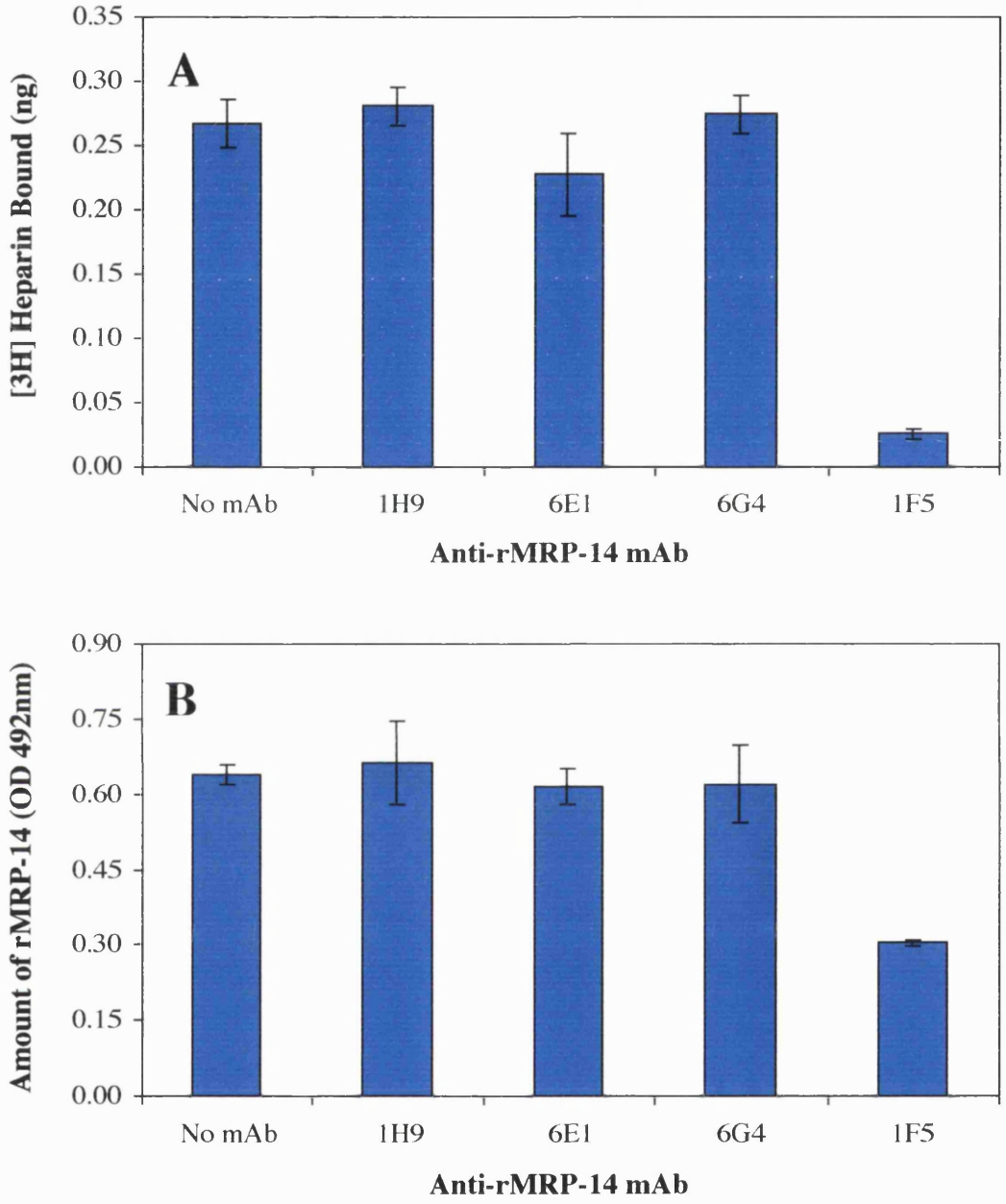

Figure 6.10: [3H] Heparin Binding to rMRP-14: Anti-rMRP-14 mAbs as Blocking Agents

A) The effect of anti-rMRP-14 mAbs at 20μg/ml on 100ng/ml [3H] heparin binding to rMRP-14 immobilised on 6G4. **B)** The effect of the same mAbs under identical conditions on the amount of rMRP-14 immobilised. Data are means of triplicates ± SD. A representative experiments of two is shown.

6.2.d rS100A12 Binding to Cell Surfaces

rS100A12 bound to fibrinogen in a similar fashion to rMRP-14, but did not induce T lymphoblast adhesion to the same ligand. Therefore, it was of interest to determine if rS100A12 bound to the cell surface of T lymphoblasts. rS100A12 bound to T lymphoblasts and this was saturable. Half maximal binding was achieved at approximately 0.3μM rS100A12, which implies the interaction was of higher affinity than that observed with rMRP-14. This binding was almost completely blocked with 100μg/ml heparin (Fig 6.11). Interestingly, rS100A12 binds to heparin columns (J. Edgeworth, personal communication). Preliminary data also shows rS100A12 binds [3H] heparin in a similar fashion to rMRP-14, but unfortunately this has not been fully characterised yet. However, an initial study indicates the interaction is sensitive to salt and that the preparations of modified heparin block in a similar fashion to rMRP-14.

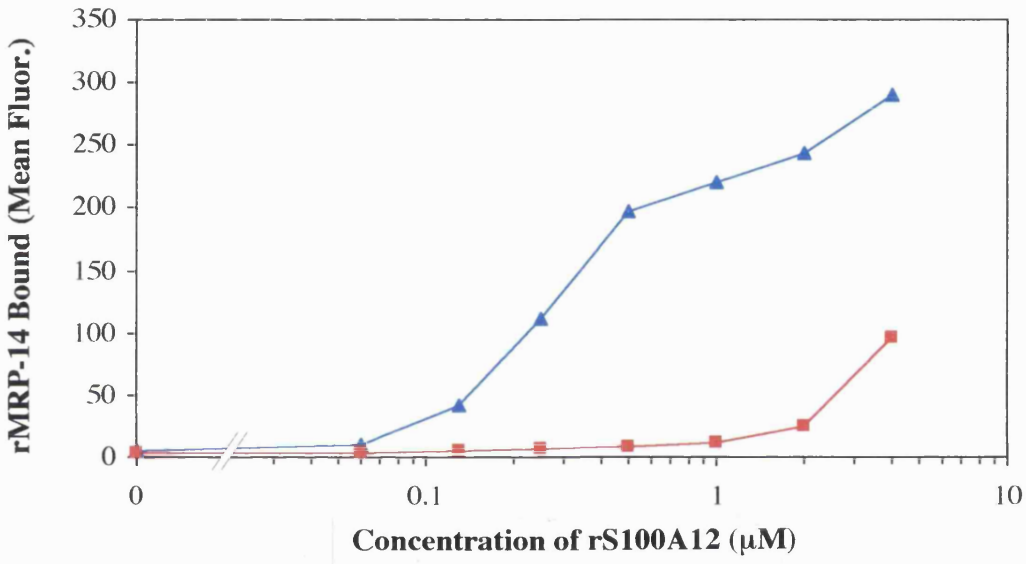

Figure 6.11: rS100A12 Binding to the Cell Surface of T Lymphoblasts
rS100A12 binding to the cell surface of T lymphoblasts in the absence of (▲) and presence of (■) 100μg/ml heparin. Data are geometric mean fluorescence of 5,000 cells. A representative experiment of three is shown.

6.3 Discussion

The proadhesive effect of rMRP-14 appears to be dependent on rMRP-14 directly ligating the immobilised proteinaceous ligand, and cells binding to this complex. Unstimulated T lymphoblasts bind very poorly to both fibrinogen and denatured BSA, thus the ability of rMRP-14 to directly ligate T lymphoblasts was investigated. rMRP-14 bound to T lymphoblasts in a saturable and monophasic fashion. The interaction with the T lymphoblast cell surface was blocked by heparin. This is interesting because heparin blocked T lymphoblast binding to rMRP-14 treated ligands, but did not effect the interaction of the recombinant protein with the immobilised ligand. This is strong evidence that, in the adhesion assay, T lymphoblasts adhere to rMRP-14 immobilised on the proteinaceous ligand, rather than to the proteinaceous ligand in an adhesive state.

rMRP-14 also bound to the human microvascular endothelial cell line HMEC-1 in a similar fashion as to T lymphocytes with heparin again blocking the interaction. This is reminiscent of many proinflammatory molecules, such as the chemokines, which bind to GAG structures on the endothelium (see (Tanaka et al., 1993)). The rMRP-14 receptor on HMEC-1 cells was trypsin sensitive, which demonstrates that the receptor is, at least in part, comprised of protein. The receptor for MRP-14 on T lymphoblasts and HMEC-1 cells did not appear identical, because the affinity of the S100 protein for HMEC-1 cells was higher than that for T lymphoblasts. Additionally, the heparin blocking of rMRP-14 binding to HMEC-1 could be overcome with high concentrations of rMRP-14, which could be consistent with the MRP-14 receptor on HMEC-1 being of higher affinity.

The expression of the putative MRP-14 receptor(s) appears to be widespread, because preliminary data shows the recombinant protein also binds to two myeloid cell lines, a fibroblast cell line and a bone marrow leukemic cell line.

Heparin is a highly charged polyelectrolyte and a multivalent ligand. Consequently heparin can non-specifically block the binding of low affinity ligands

to other higher affinity receptors. To investigate the specificity of the heparin blocking, other GAG preparations were used as blocking agents in rMRP-14 binding to T lymphoblasts and HMEC-1 cells. Dermatan sulphate, another highly sulphated GAG and frequent ligand for proteins, blocked the binding to both cell types with a similar potency to heparin. Heparan sulphate, chondroitin-6-sulphate and chondroitin-4-sulphate all blocked the binding to T lymphoblast at higher concentrations, but showed little or no inhibition of the interaction with HMEC-1 cells. Thus, these results again suggest that there may be some differences between the receptors on the two cells. Hyaluronan and keratan sulphate had no effect on rMRP-14 binding to either cell type. This indicates the GAG blocking has some structural specificity, because dermatan sulphate and keratan sulphate typically contain a similar number of sulphate substitutions (1-2 per disaccharide unit). Iduronic acid is most abundant in heparin and dermatan sulphate, and therefore may be structurally important. This is particularly of interest as iduronic acid is a frequent constituent of protein binding sites (see (Casu et al., 1988)).

The S100A12 receptor, RAGE, is expressed on endothelium, but there is no evidence of this molecule on lymphocytes. As an initial attempt to exclude this molecule as the rMRP-14 receptor, the S100A12 competing ligand glycated BSA (Hofmann et al., 1999) was used as a blocking agent. Glycated BSA did not greatly effect the binding of rMRP-14 to either cell type, which suggests RAGE is not the receptor. However, this is not conclusive as the appropriate control for the blocking by glycated BSA was not done. Quantifying the amount of RAGE expressed by the rMRP-14 binding cell lines is hoped to address this issue more conclusively. Interestingly, the binding required the presence of both zinc and calcium, suggesting that the binding to the cell surface receptor was conformation dependent, like the interaction with proteinaceous ligand.

In summary, the binding of rMRP-14 to both HMEC-1 cells and T lymphoblasts appears to be monophasic, saturable and blocked by some GAG preparations. Blocking by GAGs alone is not conclusive evidence for their

involvement in the ligand binding, as GAGs can sequester low affinity ligands from other high affinity receptors. Several features of the cell surface binding are more typical of a ligand for a proteoglycan rather than a proteinaceous receptor, such as: the specific blocking by different GAG preparations; the cell type promiscuous binding; and the cell type specific differences in the receptor. However, the data above is not conclusive evidence that rMRP-14 interacts with a cell surface proteoglycan, and further studies are required to elucidate the nature of the receptor. The only conclusive evidence is that the receptor is, at least in part, comprised of protein, as it is trypsin sensitive. This does not exclude a proteoglycan or other protein linked carbohydrate moiety from being the receptor.

To elucidate the mechanism of the heparin mediated blocking, rMRP-14 binding to heparin was investigated. rMRP-14 bound heparin in a monophasic and saturable fashion, which produced a straight line in the Scatchard plot. The Kd for the interaction was estimated to be 6.1±3.4 nM, which is very high affinity for a GAG binding protein (typically $1x10^{-9}$ to $1x10^{-5}$ M). Interestingly, the blocking of this interaction with other GAG preparations was similar, but distinct from the blocking of cell surface binding. Dermatan sulphate and chondroitin-4-sulphate were poor blocking agents, whereas heparan sulphate, chondroitin-6-sulphate, keratan sulphate and hyaluronan failed to block. However, this assay differed from the cell surface binding in many respects, such as the concentration of BSA and the temperature. Another significant difference was the amount of rMRP-14, and the fact it was immobilised on to the plate. Therefore, direct comparisons are hard to draw, but dermatan sulphate appears to consistently mimic the heparin blocking to some extent.

Chemically modified heparin preparations were used as blocking agents in the heparin to rMRP-14 binding assay, in order to determine the contribution of sulphate substitutions to the binding. Removal of the N-sulphations reduced the blocking potential of heparin, and cleaving off N- and O-linked sulphate substitutions knocked out blocking. Therefore, the sulphate substitutions of heparin

are absolutely required for heparin binding, with both N- and O-sulphations contributing. Interestingly, the interaction was also shown to be sensitive to salt washes. Thus it seems likely that rMRP-14 interacts with heparin via ionic bonds formed with the sulphate groups. This differs considerably from the salt insensitive interaction between rMRP-14 and the proteinaceous ligands.

To try and further define this heparin-binding site anti-MRP-14 mAbs were used as blocking agents. When rMRP-14 was immobilised on the plate by the mAb 1H9, the same mAb appeared to have slight blocking effect on the interaction. However, the data suggests that this may be due to rMRP-14 being competed from the anchoring mAb, and the same reduction in binding was not seen when rMRP-14 was tethered to another mAb, 6G4. 6G4, which greatly reduced the binding to proteinaceous ligands, increased the binding of heparin to rMRP-14. The explanation for the activity of this mAb awaits further investigation, but preliminary data suggest it is not due to an increase in affinity. Therefore, this mAb may stabilise the interaction by maintaining an altered rMRP-14 conformation. Intriguingly, another mAb that inhibited the interaction with proteinaceous ligands, 6E1, blocked heparin binding, but only when 1H9 anchored the rMRP-14. Therefore, this blocking is probably due to 6E1 and 1H9 blocking in combination. An alternative explanation is that 6E1 does not recognise, and, therefore, block an altered conformation induced by 6G4. Unfortunately, the mechanism has yet to be investigated. 1F5, an anti-rMRP-14 mAb that did not effect the binding to proteinaceous ligands, greatly reduced the binding of heparin to rMRP-14.

Together the mAb blocking data strongly indicates a specific site on rMRP-14 mediates the interaction with heparin, which is distinct from the proteinaceous ligand binding site. This is supported by the failure of BSA to block the interaction, and the ionic nature of the bonds formed. Additionally, rMRP-14 tethered on fibrinogen and denatured BSA also binds heparin (data not shown), suggesting the sites do not interfere with each other.

rS100A12 bound to T lymphoblasts in a very similar fashion to rMRP-14, but with a higher affinity. Unfortunately, this data is preliminary and thus the follow up studies are yet to be performed. However, early data suggests rS100A12 binds to heparin with a similar affinity to rMRP-14. Other initial results indicate that rS100A12 forms ionic interactions with the sulphate groups of heparin in a similar fashion to rMRP-14.

Chapter 7

DISCUSSION AND FUTURE DIRECTIONS

7.1 Discussion of Results

Recombinant human MRP-14 (rMRP-14) induced T lymphoblast and neutrophil adhesion to several proteinaceous ligands. The results presented in this thesis demonstrate that this was not due to a Mac-1 mediated mechanism, as has been reported previously (Newton and Hogg, 1998). Thus other mechanisms were considered. As rMRP-14 did not appear to cause cell activation and the binding occurred at 4°C, the mechanism was thought to be independent of intracellular signal transduction. Therefore, three putative mechanisms were proposed: rMRP-14 binds to a promiscuous adhesion receptor or associated molecule on the cell surface and directly activates the receptor; rMRP-14 induces the proteinaceous ligands to change into an adhesive state; or rMRP-14 binds to both the leukocytes and ligands, thereby acting as a "molecular glue".

The latter two mechanisms proposed above would require rMRP-14 to bind to the immobilised proteinaceous ligands that the cells adhere to. When investigated rMRP-14 interacted directly with the proteinaceous ligands under the same conditions as required for cell adhesion. The level of rMRP-14 bound to the good cell ligands (fibrinogen and denatured BSA) was sufficient to induce the adhesion of T lymphoblasts added subsequently. However, the level of rMRP-14 bound to the bad cell ligands (native BSA and FSG) was not sufficient to mediate cell adhesion. Interestingly, native BSA blocked both the binding of rMRP-14 to proteinaceous ligands and the T lymphoblast adhesion to rMRP-14 treated ligands. This data suggests that the interaction between rMRP-14 and the immobilised ligands was critical for cell adhesion. Further, the amount of rMRP-14 required to achieve a high level of binding to a specific ligand closely paralleled the amount of recombinant

protein necessary to induce leukocyte adhesion to the same ligand. This indicates that the interaction between rMRP-14 and the ligand was a limiting factor in cell adhesion. Thus, the mechanism of cell adhesion appears to be dependent on rMRP-14 binding to the immobilised proteinaceous ligand. This is consistent with either the rMRP-14 inducing the ligands to adopt an adhesive state or the "molecular glue" mechanism of cell binding.

The nature of the interaction between rMRP-14 and the proteinaceous ligands was briefly investigated. The data indicated that a discrete site on rMRP-14 mediated the binding to the ligands, which was only revealed in the Ca^{2+}- and Zn^{2+}-bound conformation of rMRP-14. The nature of the interaction was complex, and was not solely mediated by hydrophobic or ionic bonds. The feature of the diverse proteinaceous ligands that is recognised by the rMRP-14 remains to be investigated. However, the data presented in this thesis indicate that denaturation and/or degradation of a protein may reveal or enhance the rMRP-14 binding characteristics.

rMRP-14 also bound heparin. This interaction was of very high affinity (Kd $\approx$ 6 nM), and mediated by a discrete site on rMRP-14. The binding to heparin was dependent on both N- and O-linked sulphations, and was disrupted by some other glycosaminoglycans (GAGs) at higher concentrations. The nature of this interaction with heparin differed from that with proteinaceous ligands. The interaction with heparin appeared to be dependent on ionic bonds, as it was sensitive to salt. Additionally, the heparin and proteinaceous ligands bound to different sites on the rMRP-14, because native BSA did not disrupt the binding to heparin and the two interactions were blocked by different anti-MRP-14 mAbs. Therefore, rMRP-14 appears to have two distinct binding sites, one for proteinaceous ligands and one for GAGs.

rMRP-14 also interacts with cell surfaces, but due to time constraints the nature of this interaction was not fully investigated. Therefore, the contributions of the GAG- and/or the proteinaceous ligand-binding sites of rMRP-14 to this binding remain unclear. The affinity and divalent cation dependency of the interaction with

cell surfaces was reminiscent of the proteinaceous ligand-binding site. However, the blocking effect of GAGs was characteristic of the GAG-binding site. It is possible that this blocking was due to the multivalent GAGs sequestering the recombinant protein rather than directly competing for the cell surface-binding site, but this did not occur in the proteinaceous ligand-binding studies. Therefore, I propose these initial results indicate that the GAG-binding site on rMRP-14, at least in part, mediated the interaction with cell surfaces. Further studies using BSA and the MRP-14 mAbs as blocking agents will hopefully establish the significance of the two sites for the cell surface-binding of rMRP-14.

The nature of the rMRP-14 receptor on the cell surfaces is not elucidated in this study. Trypsinisation removed the receptor demonstrating it is either a protein or conjugated to a protein. Together with the GAG blocking data, this suggests that rMRP-14 binds to proteoglycans. The differences in affinity of rMRP-14 for different cell types suggests variability in the receptor structure, which is also more typical of a glycoconjugate than a protein. Thus, the results presented in this thesis indicate that the MRP-14 receptor may be a proteoglycan, but further work is required to determine this.

Heparin blocked both rMRP-14 binding to cell surfaces and cell adhesion to rMRP-14 pretreated proteinaceous ligands. This is strong evidence that the cells adhered to immobilised rMRP-14, rather than to the proteinaceous ligands in an induced adhesive state. Further, the heparin blocking of cell binding also indicates that rMRP-14 ligates the cells via the GAG-binding site in the cell adhesion assay as well as in solution. Therefore, the data presented in this thesis support the "molecular glue" mechanism of rMRP-14 induced cell adhesion, where rMRP-14 binds to the immobilised ligand via the proteinaceous ligand-binding site, and to the cell via the GAG-binding site. This model is depicted in Fig 7.1.

rS100A12, like rMRP-14, interacted with proteinaceous ligands, heparin and cell surfaces, but did not induce cell adhesion. However, the relative amount of

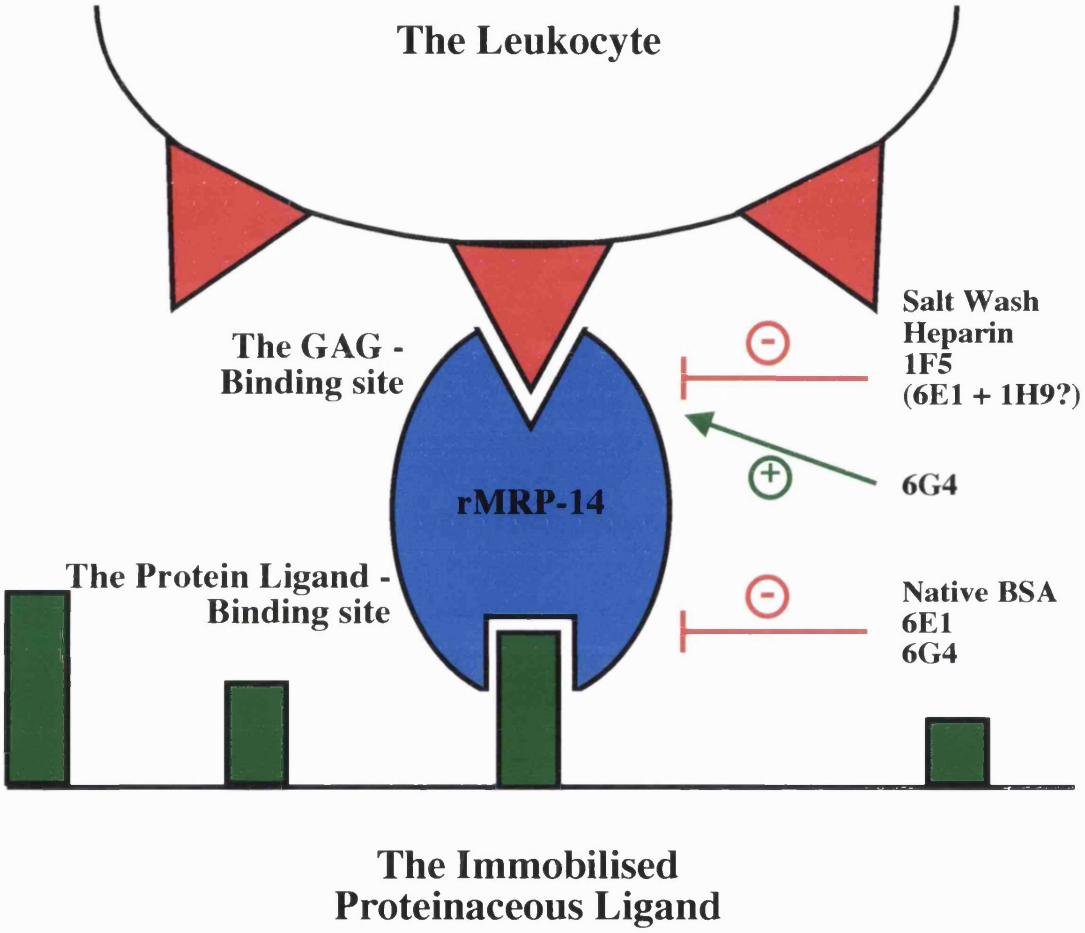

Figure 7.1: The "Molecular Glue" Model of Cell Adhesion
A diagrammatic representation of the "molecular glue" mechanism of rMRP-14 induced leukocyte adhesion to an immobilised proteinaceous ligand. rMRP-14 is proposed to bind to both the ligand and the cell surface, with the latter being mediated by the GAG-binding site on rMRP-14. The proteinaceous ligand-binding site is blocked by native BSA and mAbs 6E1 and 6G4. Whereas, the GAG-binding site is aided by mAb 6G4 and blocked by heparin, high salt concentrations, mAb 1F5 and possibly mAbs 6E1 and 1H9 in combination.

rS100A12 bound to cell surfaces and proteinaceous ligands was not been determined. Also the cross competition between the sites was not evaluated.

7.2 Putative Physiological Functions

Most of the work in this thesis is based on elucidating the mechanism of an in vitro assay. Therefore, it is important to consider the physiological relevance of the observations discussed above. In vivo, extracellular MRP-8 and –14 have frequently been observed on the endothelium of venules proximal to inflammatory sites (see Section 1.3.c.iv and Fig 1.5). The MRP proteins could potentially be immobilised by either the GAG- or proteinaceous ligand-binding site of MRP-14.

MRP-14 appears to bind proteoglycans on the surface of cultured endothelial cells, thus this could be the mechanism by which the MRPs are immobilised on the vessel wall. The possible functions of the immobilised MRPs are also not directly addressed in this thesis. The MRP-14 may act by increasing the adhesiveness of the endothelium for leukocytes, in a similar fashion to ligand immobilised rMRP-14. The location and tethering is reminiscent of the anchoring of chemokines and cytokines on the vascular wall during inflammation (Tanaka et al., 1993). The GAG chains on inflammatory venule endothelium also are proposed to be involved in the rolling of leukocytes, as a ligand for L-selectin. How MRP-14 may effect these functions is unknown, but would be interesting to investigate.

Another possibility is that the MRPs are immobilised by the proteinaceous ligand-binding site of MRP-14. Adherent activated leukocytes, and especially neutrophils, can cause vascular endothelial damage by releasing a variety of oxidants and proteinases (reviewed by (Lentsch and Ward, 2000)). This vascular damage could lead to exposure of the basement membrane and/or an increase in vascular permeability. Thus the MRPs may bind to the more accessible basement membrane or extracellular matrix. The proteinase degradation of both the basement membrane

and/or extracellular matrix could potentially cause these structures to become MRP-14 ligands.

One possible function of MRP-14 binding to exposed surfaces, such as the basement membrane, could be the inhibition of high molecular weight kininogen (HMWK) binding. HMWK binds to several surfaces, as part of a complex that initiates intrinsic coagulation, which results in fibrin deposition. This binding of HMWK is in part mediated by domain 5, which is homologous to the C-terminal extension of MRP-14. MRP-14, alone or complexed to MRP-8, was able to compete with HMWK binding to kaolin, and delay the resulting fibrin formation (Hessian et al., 1995). Therefore, MRP-14 may inhibit fibrin formation on venules at sites of chronic inflammation that could limit leukocyte emigration.

rMRP-8 inhibited rMRP-14 induced cell adhesion (Newton, 1997), but the mechanism of this blocking is unknown. rMRP-8 could have acted as a competitive inhibitor of the proteinaceous ligand-binding site or alternatively one of the binding sites on MRP-14 may not exist in the heterodimer. The understanding of this mechanism is crucial to interpreting the results in this thesis within a physiological context, as in vivo the MRPs exist largely as a heterodimer.

7.3 Future Directions

This project aimed to investigate the mechanism of rMRP-14 induced adhesion. The "molecular glue" hypothesis seems to largely explain this proadhesive effect of rMRP-14, but this project has given rise to several more questions. Some of these are briefly listed below, and may help to elucidate the physiological relevance of the above findings.

What is the nature of the cell surface receptor for rMRP-14? The use of BSA and MRP-14 mAbs as blocking agents, as well as a salt wash should finally determine whether the GAG- and/or proteinaceous ligand-binding sites of rMRP-14

participate in the cell binding. The nature of the receptor could also be investigated further by enzymatic degradation of cell surface molecules, e.g. with heparinases, and inhibition of protein conjugate synthesis. Further characterisation of blocking agents, such as GAG fragments, would also help define the receptor.

Whether the MRP proteins also interact with the reported S100A12 receptor, RAGE, or a homologue is also critical to understanding the physiological functions of the MRPs. The elucidation of this should be easier following the above studies, and when reliable RAGE reagents become available.

What is the feature recognised by the proteinaceous ligand-binding site? Expanding the range of proteins to which rMRP-14 binds, may allow the identification of a common characteristic. The enzymatic degradation and denaturation of good and bad ligands may also clarify the features that interact with rMRP-14 .

What is the structure of the rMRP-14 binding site in heparin? Using heparin based oligosaccharides as blocking agents has successfully defined the structural requirements of some GAG-binding proteins. Fractionation and subsequent analysis of rMRP-14 binding and non-binding heparin molecules may also help to define the rMRP-14 binding structure. In practice, these studies can involve complex biochemistry, and produce low yields.

Does native MRP-14 bind GAGs and proteinaceous ligands in a similar fashion to the recombinant protein? How does MRP-8 effect rMRP-14 binding to GAGs and proteinaceous ligands? The use of rMRP-8 and the native complex should answer these questions easily. It is also possible to purify native MRP-8 and -14 from the complex by reverse phase chromatography.

What is nature of the binding sites on S100A12? A comparison of the binding activities of rS100A12 and rMRP-14, together with cross-blocking studies should allow this question to be answered.

Is rMRP-14 bound to the endothelium proadhesive? This could easily be addressed in vitro by investigating whether rMRP-14 treatment of HMEC-1 cells induces leukocyte adhesion.

How does rMRP-14 affect fibrin formation? The reagents described in this thesis may help to further define the mechanism of rMRP-14 inhibition of high molecular weight kininogen triggered coagulation.

REFERENCES

Ades, E.W., F.J. Candal, R.A. Swerlick, V.G. George, S. Summers, D.C. Bosse, and T.J. Lawley. 1992.
HMEC-1: establishment of an immortalized human microvascular endothelial cell line.
J. Invest. Dermatol. **99**:683-690.

Aida, Y., and M.J. Pabst. 1990.
Removal of endotoxin from protein solutions by phase separation using Triton X-114.
J. Immunol. Methods **132**:191-195.

Altieri, D.C., and T.S. Edgington. 1988.
The saturable high affinity association of factor X to ADP-stimulated monocytes defines a novel function of the Mac-1 receptor.
J. Biol. Chem. **263**:7007-7015.

Andrew, D.P., J.P. Spellberg, H. Takimoto, R. Schmits, T.W. Mak, and M.M. Zukowski. 1998.
Transendothelial migration and trafficking of leukocytes in LFA-1-deficient mice.
Eur. J. Immunol. **28**:1959-1969.

Au, B.T., T.J. Williams, and P.D. Collins. 1994.
Zymosan-induced IL-8 release from human neutrophils involves activation via the CD11b/CD18 receptor and endogenous platelet-activating factor as an autocrine modulator.
J. Immunol. **152**:5411-5419.

Baggiolini, M., B. Dewald, and B. Moser. 1994.
Interleukin-8 and related chemotactic cytokines-CXC and CC chemokines.
Adv. Immunol. **55**:97-179.

Baggiolini, M., B. Dewald, and B. Moser. 1997.
Human chemokines: an update.
Annu. Rev. Immunol. **15**:675-705.

Barger, S.W., S.R. Wolchok, and L.J. Van Eldik. 1992.
Disulfide-linked S100 β dimers and signal transduction.
Biochim Biophys Acta **1160**:105-112.

Barraclough, R. 1998.
Calcium-binding protein S100A4 in health and disease.
Biochim. Biophys. Acta **1448**:190-199.

Barritt, G.J. 1999.
Receptor-activated Ca^{2+} inflow in animal cells: a variety of pathways tailored to meet different intracellular Ca^{2+} signalling requirements.
Biochem. J. **337**:153-169.

Baudier, J., N. Glasser, and D. Gerard. 1986.
Ions binding to S100 proteins. I. Calcium- and zinc-binding properties of bovine brain S100 αα, S100a (αβ), and S100b (ββ) protein: Zn^{2+} regulates Ca^{2+} binding on S100b protein.
J. Biol. Chem. **261**:8192-8203.

Baudier, J., and R.D. Cole. 1989.
The Ca^{2+}-binding sequence in bovine brain S100b protein β-subunit. A spectroscopic study.
Biochem. J. **264**:79-85.

Baudier, J., C. Delphin, D. Grunwald, S. Khochbin, and J.J. Lawrence. 1992.
Characterization of the tumor suppressor protein p53 as a protein kinase C substrate and a S100b-binding protein.
Proc. Natl. Acad. Sci. U S A **89**:11627-11631.

Baudier, J., E. Bergeret, N. Bertacchi, H. Weintraub, J. Gagnon, and J. Garin. 1995.
Interactions of myogenic bHLH transcription factors with calcium-binding calmodulin and S100a (αα) proteins.
Biochemistry **34**:7834-7846.

Bernfield, M., M. Gotte, P.W. Park, O. Reizes, M.L. Fitzgerald, J. Lincecum, and M. Zako. 1999.
Functions of cell surface heparan sulfate proteoglycans.
Annu. Rev. Biochem. **68**:729-777.

Bhardwaj, R.S., C. Zotz, G. Zwadlo-Klarwasser, J. Roth, M. Goebeler, K. Mahnke, M. Falk, G. Meinardus-Hager, and C. Sorg. 1992.
The calcium-binding proteins MRP8 and MRP14 form a membrane-associated heterodimer in a subset of monocytes/macrophages present in acute but absent in chronic inflammatory lesions.
Eur. J. Immunol. **22**:1891-1897.

Bianchi, R., M. Garbuglia, M. Verzini, I. Giambanco, A. Spreca, and R. Donato. 1995.
S-100 protein and annexin II_2-$p11_2$ (calpactin I) act in concert to regulate the state of assembly of GFAP intermediate filaments.
Biochem. Biophys. Res. Commun. **208**:910-918.

Bianchi, E., J.R. Bender, F. Blasi, and R. Pardi. 1997.
Through and beyond the wall: late steps in leukocyte transendothelial migration.
Immunol. Today **18**:586-591.

Brandtzaeg, P., I. Dale, and M.K. Fagerhol. 1987.
Distribution of a formalin-resistant myelomonocytic antigen (L1) in human tissues. II. Normal and aberrant occurrence in various epithelia.
Am. J. Clin. Pathol. **87**:700-707.

Brodersen, D.E., J. Nyborg, and M. Kjeldgaard. 1999.
Zinc-binding site of an S100 protein revealed. Two crystal structures of Ca^{2+}-bound human psoriasin (S100A7) in the Zn^{2+}-loaded and Zn^{2+}-free states.
Biochemistry **38**:1695-1704.

Bruggen, J., L. Tarcsay, N. Cerletti, K. Odink, M. Rutishauser, G. Hollander, and C. Sorg. 1988.
The molecular nature of the cystic fibrosis antigen.
Nature **331**:570.

Brun, J.G., G. Haland, H.J. Haga, M.K. Fagerhol, and R. Jonsson. 1995.
Effects of calprotectin in avridine-induced arthritis.
APMIS **103**:233-240.

Burgoyne, R.D., S.E. Handel, A. Morgan, M.E. Rennison, M.D. Turner, and C.J. Wilde. 1991.
Calcium, the cytoskeleton and calpactin (annexin II) in exocytotic secretion from adrenal chromaffin and mammary epithelial cells.
Biochem. Soc. Trans. **19**:1085-1090.

Burwinkel, F., J. Roth, M. Goebeler, U. Bitter, V. Wrocklage, E. Vollmer, A. Roessner, C. Sorg, and W. Bocker. 1994.
Ultrastructural localization of the S-100-like proteins MRP8 and MRP14 in monocytes is calcium-dependent.
Histochemistry **101**:113-120.

Calabretta, B., R. Battini, L. Kaczmarek, J.K. de Riel, and R. Baserga. 1986.
Molecular cloning of the cDNA for a growth factor-inducible gene with strong homology to S-100, a calcium-binding protein.
J. Biol. Chem. **261**:12628-12632.

Carey, D.J. 1997.
Syndecans: multifunctional cell-surface co-receptors.
Biochem. J. **327**:1-16.

Carlos, T.M., and J.M. Harlan. 1994.
Leukocyte-endothelial adhesion molecules.
Blood **84**:2068-2101.

Casu, B., M. Petitou, M. Provasoli, and P. Sinay. 1988.
Conformational flexibility: a new concept for explaining binding and biological properties of iduronic acid-containing glycosaminoglycans.
Trends Biochem. Sci. **13**:221-225.

Chin, D., and A.R. Means. 2000.
Calmodulin: a prototypical calcium sensor.
Trends Cell Biol. **10**:322-328.

Clapham, D.E. 1995.
Calcium signaling.
Cell **80**:259-268.

Cornish, C.J., J.M. Devery, P. Poronnik, M. Lackmann, D.I. Cook, and C.L. Geczy. 1996.
S100 protein CP-10 stimulates myeloid cell chemotaxis without activation.
J. Cell. Physiol. **166**:427-437.

Davies, B.R., M.P. Davies, F.E. Gibbs, R. Barraclough, and P.S. Rudland. 1993.
Induction of the metastatic phenotype by transfection of a benign rat mammary epithelial cell line with the gene for p9Ka, a rat calcium-binding protein, but not with the oncogene EJ-ras-1.
Oncogene **8**:999-1008.

Davis, G.E. 1992.
The Mac-1 and p150,95 β_2 integrins bind denatured proteins to mediate leukocyte cell-substrate adhesion.
Exp. Cell Res. **200**:242-252.

Davies, M.P., P.S. Rudland, L. Robertson, E.W. Parry, P. Jolicoeur, and R. Barraclough. 1996.
Expression of the calcium-binding protein S100A4 (p9Ka) in MMTV-neu transgenic mice induces metastasis of mammary tumours.
Oncogene **13**:1631-1637.

Delabie, J., C. de Wolf-Peeters, J.J. van den Oord, and V.J. Desmet. 1990.
Differential expression of the calcium-binding proteins MRP8 and MRP14 in granulomatous conditions: an immunohistochemical study.
Clin. Exp. Immunol. **81**:123-126.

Dell'Angelica, E.C., C.H. Schleicher, and J.A. Santome. 1994.
Primary structure and binding properties of calgranulin C, a novel S100-like calcium-binding protein from pig granulocytes.
J. Biol. Chem. **269**:28929-28936.

Devery, J.M., N.J. King, and C.L. Geczy. 1994.
Acute inflammatory activity of the S100 protein CP-10. Activation of neutrophils in vivo and in vitro.
J. Immunol. **152**:1888-1897.

Diamond, M.S., J. Garcia-Aguilar, J.K. Bickford, A.L. Corbi, and T.A. Springer. 1993.
The I domain is a major recognition site on the leukocyte integrin Mac-1 (CD11b/CD18) for four distinct adhesion ligands.
J. Cell Biol. **120**:1031-1043.

Donato, R. 1999.
Functional roles of S100 proteins, calcium-binding proteins of the EF-hand type.
Biochim. Biophys. Acta **1450**:191-231.

Dooley, D.C., J.F. Simpson, and H.T. Meryman. 1982.
Isolation of large numbers of fully viable human neutrophils: a preparative technique using percoll density gradient centrifugation.
Exp. Hematol. **10**:591-599.

Drohat, A.C., J.C. Amburgey, F. Abildgaard, M.R. Starich, D. Baldisseri, and D.J. Weber. 1996.
Solution structure of rat apo-S100B(ββ) as determined by NMR spectroscopy.
Biochemistry **35**:11577-11588.

Drohat, A.C., D.M. Baldisseri, R.R. Rustandi, and D.J. Weber. 1998.
Solution structure of calcium-bound rat S100B(ββ) as determined by nuclear magnetic resonance spectroscopy.
Biochemistry **37**:2729-2740.

Duncan, A.M., J. Higgins, R.J. Dunn, R. Allore, and A. Marks. 1989.
Refined sublocalization of the human gene encoding the β subunit of the S100 protein (S100B) and confirmation of a subtle t(9;21) translocation using in situ hybridization.
Cytogenet. Cell Genet. **50**:234-235.

Edgeworth, J., P. Freemont, and N. Hogg. 1989.
Ionomycin-regulated phosphorylation of the myeloid calcium-binding protein p14.
Nature **342**:189-192.

Edgeworth, J., M. Gorman, R. Bennett, P. Freemont, and N. Hogg. 1991.
Identification of p8,14 as a highly abundant heterodimeric calcium binding protein complex of myeloid cells.
J. Biol. Chem. **266**:7706-7713.

Ehlers, M.R. 2000.
CR3: a general purpose adhesion-recognition receptor essential for innate immunity.
Microbes Infect. **2**:289-294.

Engelkamp, D., B.W. Schafer, M.G. Mattei, P. Erne, and C.W. Heizmann. 1993.
Six S100 genes are clustered on human chromosome 1q21: identification of two genes coding for the two previously unreported calcium-binding proteins S100D and S100E.
Proc. Natl. Acad. Sci. U S A **90**:6547-6551.

Filipek, A., C.W. Heizmann, and J. Kuznicki. 1990.
Calcyclin is a calcium and zinc binding protein.
FEBS Lett. **264**:263-266.

Foxman, E.F., E.J. Kunkel, and E.C. Butcher. 1999.
Integrating conflicting chemotactic signals. The role of memory in leukocyte navigation.
J. Cell Biol. **147**:577-588.

Franz, C., I. Durussel, J.A. Cox, B.W. Schafer, and C.W. Heizmann. 1998.
Binding of Ca^{2+} and Zn^{2+} to human nuclear S100A2 and mutant proteins.
J. Biol. Chem. **273**:18826-18834.

Freemont, P., N. Hogg, and J. Edgeworth. 1989.
Sequence identity.
Nature **339**:516.

Fritz, G., C.W. Heizmann, and P.M. Kroneck. 1998.
Probing the structure of the human Ca^{2+}- and Zn^{2+}-binding protein S100A3: spectroscopic investigations of its transition metal ion complexes, and three-dimensional structural model.
Biochim. Biophys. Acta **1448**:264-276.

Fuki, I.V., K.M. Kuhn, I.R. Lomazov, V.L. Rothman, G.P. Tuszynski, R.V. Iozzo, T.L. Swenson, E.A. Fisher, and K.J. Williams. 1997.
The syndecan family of proteoglycans. Novel receptors mediating internalization of atherogenic lipoproteins in vitro.
J. Clin. Invest. **100**:1611-1622.

Fulle, S., M.A. Mariggio, S. Belia, I. Nicoletti, and G. Fano. 1997.
Nerve growth factor inhibits apoptosis induced by S-100 binding in neuronal PC12 cells.
Neuroscience **76**:159-166.

Gabrielsen, T.O., I. Dale, P. Brandtzaeg, P.S. Hoel, M.K. Fagerhol, T.E. Larsen, and P.O. Thune. 1986.
Epidermal and dermal distribution of a myelomonocytic antigen (L1) shared by epithelial cells in various inflammatory skin diseases.
J. Am. Acad. Dermatol. **15**:173-179.

Gahmberg, C.G., M. Tolvanen, and P. Kotovuori. 1997a.
Leukocyte adhesion-structure and function of human leukocyte β_2-integrins and their cellular ligands.
Eur. J. Biochem. **245**:215-232.

Gahmberg, C.G. 1997b.
Leukocyte adhesion: CD11/CD18 integrins and intercellular adhesion molecules.
Curr. Opin. Cell Biol. **9**:643-650.

Gallagher, J.T. 1997.
Structure-activity relationship of heparan sulphate.
Biochem. Soc. Trans. **25**:1206-1209.

Garbuglia, M., R. Bianchi, M. Verzini, I. Giambanco, and R. Donato. 1995.
Annexin II2-p11(2) (calpactin I) stimulates the assembly of GFAP in a calcium- and pH-dependent manner.
Biochem. Biophys. Res. Commun. **208**:901-909.

Garbuglia, M., M. Verzini, G. Sorci, R. Bianchi, I. Giambanco, A.L. Agneletti, and R. Donato. 1999.
The calcium-modulated proteins, S100A1 and S100B, as potential regulators of the dynamics of type III intermediate filaments.
Braz. J. Med. Biol. Res. **32**:1177-1185.

Gerke, V., and S.E. Moss. 1997.
Annexins and membrane dynamics.
Biochim. Biophys. Acta **1357**:129-154.

Goebeler, M., J. Roth, C. van den Bos, G. Ader, and C. Sorg. 1995.
Increase of calcium levels in epithelial cells induces translocation of calcium-binding proteins migration inhibitory factor-related protein 8 (MRP8) and MRP14 to keratin intermediate filaments.
Biochem. J. **309**:419-424.

Golitsina, N.L., J. Kordowska, C.L. Wang, and S.S. Lehrer. 1996.
Ca^{2+}-dependent binding of calcyclin to muscle tropomyosin.
Biochem. Biophys. Res. Commun. **220**:360-365.

Gottsch, J.D., and S.H. Liu. 1997.
Cloning and expression of bovine corneal antigen cDNA.
Curr. Eye Res. **16**:1239-1244.

Gottsch, J.D., and S.H. Liu. 1998.
Cloning and expression of human corneal calgranulin C (CO-Ag).
Curr. Eye Res. **17**:870-874.

Gottsch, J.D., S.W. Eisinger, S.H. Liu, and A.L. Scott. 1999.
Calgranulin C has filariacidal and filariastatic activity.
Infect. Immun. **67**:6631-6636.

Griffin, W.S., L.C. Stanley, C. Ling, L. White, V. MacLeod, L.J. Perrot, C.L. White, and C. Araoz. 1989.
Brain interleukin 1 and S-100 immunoreactivity are elevated in Down syndrome and Alzheimer disease.
Proc. Natl. Acad. Sci. U S A **86**:7611-7615.

Guignard, F., J. Mauel, and M. Markert. 1995.
Identification and characterization of a novel human neutrophil protein related to the S100 family.
Biochem. J. **309**:395-401.

Guignard, F., J. Mauel, and M. Markert. 1996.
Phosphorylation of myeloid-related proteins MRP-14 and MRP-8 during human neutrophil activation.
Eur. J. Biochem. **241**:265-271.

Habuchi, H., O. Habuchi, and K. Kimata. 1998.
Biosynthesis of Heparan Sulfate and Heparin How are the Multifunctional Glycosaminoglycans built up?
Trends Glycosci. Glycotechol. **10**:65-80.

Haines, K.A., S.L. Kolasinski, B.N. Cronstein, J. Reibman, L.I. Gold, and G. Weissmann. 1993.
Chemoattraction of neutrophils by substance P and transforming growth factor-β1 is inadequately explained by current models of lipid remodeling.
J. Immunol. **151**:1491-1499.

Hardingham, T.E., and A.J. Fosang. 1992.
Proteoglycans: many forms and many functions.
FASEB J. **6**:861-870.

Harris, E.S., T.M. McIntyre, S.M. Prescott, and G.A. Zimmerman. 2000.
The leukocyte integrins.
J. Biol. Chem. **275**:23409-23412.

Hasan, A.A.K., T. Zisman, and A.H. Schmaier. 1998.
Identification of cytokeratin 1 as a binding protein and presentation receptor for kininogens on endothelial cells.
Proc. Natl. Acad. Sci. U S A **95**:3615-3620.

Heizmann, C.W., and W. Hunziker. 1991.
Intracellular calcium-binding proteins: more sites than insights.
Trends Biochem. Sci. **16**:98-103.

Heizmann, C.W., and J.A. Cox. 1998.
New perspectives on S100 proteins: a multi-functional Ca^{2+}-, Zn^{2+}- and Cu^{2+}-binding protein family.
Biometals **11**:383-397.

Henderson, B., and M. Wilson. 1996.
Cytokine induction by bacteria: beyond lipopolysaccharide.
Cytokine **8**:269-282.

Hersh, D., J. Weiss, and A. Zychlinsky. 1998.
How bacteria initiate inflammation: aspects of the emerging story.
Curr. Opin. Microbiol. **1**:43-48.

Hessian, P.A., J. Edgeworth, and N. Hogg. 1993.
MRP-8 and MRP-14, two abundant Ca^{2+}-binding proteins of neutrophils and monocytes.
J. Leukoc. Biol. **53**:197-204.

Hessian, P.A., L. Wilkinson, and N. Hogg. 1995.
The S100 family protein MRP-14 (S100A9) has homology with the contact domain of high molecular weight kininogen.
FEBS Lett. **371**:271-275.

Hileman, R.E., J.R. Fromm, J.M. Weiler, and R.J. Linhardt. 1998.
Glycosaminoglycan-protein interactions: definition of consensus sites in glycosaminoglycan binding proteins.
Bioessays **20**:156-167.

Hitomi, J., K. Yamaguchi, Y. Kikuchi, T. Kimura, K. Maruyama, and K. Nagasaki. 1996.
A novel calcium-binding protein in amniotic fluid, CAAF1: its molecular cloning and tissue distribution.
J. Cell Sci. **109**:805-815.

Hitomi, J., T. Kimura, E. Kusumi, S. Nakagawa, S. Kuwabara, K. Hatakeyama, and K. Yamaguchi. 1998.
Novel S100 proteins in human esophageal epithelial cells: CAAF1 expression is associated with cell growth arrest.
Arch. Histol. Cytol. **61**:163-178.

Hofmann, M.A., S. Drury, C. Fu, W. Qu, A. Taguchi, Y. Lu, C. Avila, N. Kambham, A. Bierhaus, P. Nawroth, M.F. Neurath, T. Slattery, D. Beach, J. McClary, M. Nagashima, J. Morser, D. Stern, and A.M. Schmidt. 1999.
RAGE mediates a novel proinflammatory axis: a central cell surface receptor for S100/calgranulin polypeptides.
Cell **97**:889-901.

Hogg, N., D.G. Palmer, and P.A. Revell. 1985.
Mononuclear phagocytes of normal and rheumatoid synovial membrane identified by monoclonal antibodies.
Immunology **56**:673-681.

Hogg, N., C. Allen, and J. Edgeworth. 1989.
Monoclonal antibody 5.5 reacts with p8,14, a myeloid molecule associated with some vascular endothelium.
Eur. J. Immunol. **19**:1053-1061.

Hosfield, C.M., J.S. Elce, P.L. Davies, and Z. Jia. 1999.
Crystal structure of calpain reveals the structural basis for Ca^{2+}-dependent protease activity and a novel mode of enzyme activation.
EMBO J. **18**:6880-6889.

Hulett, M.D., and P.M. Hogarth. 1994.
Molecular basis of Fc receptor function.
Adv. Immunol. **57**:1-127.

Hunter, M.J., and W.J. Chazin. 1998.
High level expression and dimer characterization of the S100 EF-hand proteins, migration inhibitory factor-related proteins 8 and 14.
J. Biol. Chem. **273**:12427-12435.

Ikebuchi, N.W., and D.M. Waisman. 1990.
Calcium-dependent regulation of actin filament bundling by lipocortin-85.
J. Biol. Chem. **265**:3392-3400.

Ikura, M. 1996.
Calcium binding and conformational response in EF-hand proteins.
Trends Biochem. Sci. **21**:14-17.

Ilg, E.C., B.W. Schafer, and C.W. Heizmann. 1996a.
Expression pattern of S100 calcium-binding proteins in human tumors.
Int. J. Cancer **68**:325-332.

Ilg, E.C., H. Troxler, D.M. Burgisser, T. Kuster, M. Markert, F. Guignard, P. Hunziker, N. Birchler, and C.W. Heizmann. 1996b.
Amino acid sequence determination of human S100A12 (P6, calgranulin C, CGRP, CAAF1) by tandem mass spectrometry.
Biochem. Biophys. Res. Commun. **225**:146-150.

Iozzo, R.V. 1998.
Matrix proteoglycans: from molecular design to cellular function.
Annu. Rev. Biochem. **67**:609-652.

Ishikawa, K., A. Nakagawa, I. Tanaka, M. Suzuki, and J. Nishihira. 2000.
The structure of human MRP8, a member of the S100 calcium-binding protein family, by MAD phasing at 1.9 A resolution.
Acta Crystallogr. D Biol. Crystallogr. **56**:559-566.

Isobe, T., N. Ishioka, and T. Okuyama. 1981.
Structural relation of two S-100 proteins in bovine brain; subunit composition of S-100a protein.
Eur. J. Biochem. **115**:469-474.

Janeway, C.A., P. Travers, M. Walport, and J.D. Capra. 1999.
Immunobiology. 4th Edition.
Elsevier Science Ltd, London.

Jinquan, T., H. Vorum, C.G. Larsen, P. Madsen, H.H. Rasmussen, B. Gesser, M. Etzerodt, B. Honore, J.E. Celis, and K. Thestrup-Pedersen. 1996.
Psoriasin: a novel chemotactic protein.
J. Invest. Dermatol. **107**:5-10.

Johne, B., M.K. Fagerhol, T. Lyberg, H. Prydz, P. Brandtzaeg, C.F. Naess-Andresen, and I. Dale. 1997.
Functional and clinical aspects of the myelomonocyte protein calprotectin.
Mol. Pathol. **50**:113-123.

Johnson-Leger, C., M. Aurrand-Lions, and B.A. Imhof. 2000.
The parting of the endothelium: miracle, or simply a junctional affair?
J. Cell Sci. **113**:921-933.

Joseph, K., B. Ghebrehiwet, E.I. Peerschke, K.B. Reid, and A.P. Kaplan. 1996.
Identification of the zinc-dependent endothelial cell binding protein for high molecular weight kininogen and factor XII: identity with the receptor that binds to the globular "heads" of C1q (gC1q-R).
Proc. Natl. Acad. Sci. U S A **93**:8552-8557.

Kaplan, A.P., K. Joseph, Y. Shibayama, S. Reddigari, B. Ghebrehiwet, and M. Silverberg. 1997.
The intrinsic coagulation/kinin-forming cascade: assembly in plasma and cell surfaces in inflammation.
Adv. Immunol. **66**:225-272.

Kerkhoff, C., M. Klempt, and C. Sorg. 1998.
Novel insights into structure and function of MRP8 (S100A8) and MRP14 (S100A9).
Biochim. Biophys. Acta **1448**:200-211.

Kerkhoff, C., T. Vogl, W. Nacken, C. Sopalla, and C. Sorg. 1999a.
Zinc binding reverses the calcium-induced arachidonic acid-binding capacity of the S100A8/A9 protein complex.
FEBS Lett. **460**:134-138.

Kerkhoff, C., M. Klempt, V. Kaever, and C. Sorg. 1999b.
The two calcium-binding proteins, S100A8 and S100A9, are involved in the metabolism of arachidonic acid in human neutrophils.
J. Biol. Chem. **274**:32672-32679.

Kerkhoff, C., I. Eue, and C. Sorg. 1999c.
The regulatory role of MRP8 (S100A8) and MRP14 (S100A9) in the transendothelial migration of human leukocytes.
Pathobiology **67**:230-232.

Kilby, P.M., L.J. Van Eldik, and G.C. Roberts. 1996.
The solution structure of the bovine S100B protein dimer in the calcium-free state.
Structure **4**:1041-1052.

Kitayama, J., M.W. Carr, S.J. Roth, J. Buccola, and T.A. Springer. 1997.
Contrasting responses to multiple chemotactic stimuli in transendothelial migration: heterologous desensitization in neutrophils and augmentation of migration in eosinophils.
J. Immunol. **158**:2340-2349.

Kjellen, L., and U. Lindahl. 1991.
Proteoglycans: structures and interactions.
Annu. Rev. Biochem. **60**:443-475.

Klempt, M., H. Melkonyan, W. Nacken, D. Wiesmann, U. Holtkemper, and C. Sorg. 1997.
The heterodimer of the Ca^{2+}-binding proteins MRP8 and MRP14 binds to arachidonic acid.
FEBS Lett. **408**:81-84.

Kligman, D., and D.C. Hilt. 1988.
The S100 protein family.
Trends Biochem. Sci. **13**:437-443.

Koike, T., N. Harada, T. Yoshida, and M. Morikawa. 1992.
Regulation of myeloid-specific calcium binding protein synthesis by cytosolic protein kinase C.
J. Biochem. (Tokyo) **112**:624-630.

Komada, T., R. Araki, K. Nakatani, I. Yada, M. Naka, and T. Tanaka. 1996.
Novel specific chemtactic receptor for S100L protein on guinea pig eosinophils.
Biochem. Biophys. Res. Commun. **220**:871-874.

Kunz, M., J. Roth, C. Sorg, and G. Kolde. 1992.
Epidermal expression of the calcium binding surface antigen 27E10 in inflammatory skin diseases.
Arch. Dermatol. Res. **284**:386-390.

Kuznicki, J., J. Kordowska, M. Puzianowska, and B.M. Wozniewicz. 1992.
Calcyclin as a marker of human epithelial cells and fibroblasts.
Exp. Cell. Res. **200**:425-430.

Lackmann, M., P. Rajasekariah, S.E. Iismaa, G. Jones, C.J. Cornish, S. Hu, R.J. Simpson, R.L. Moritz, and C.L. Geczy. 1993.
Identification of a chemotactic domain of the pro-inflammatory S100 protein CP-10.
J. Immunol. **150**:2981-2991.

Laemmli, U.K. 1970.
Cleavage of structural proteins during the assembly of the head of bacteriophage T4.
Nature **227**:680-685.

Lagasse, E., and R.G. Clerc. 1988.
Cloning and expression of two human genes encoding calcium-binding proteins that are regulated during myeloid differentiation.
Mol. Cell. Biol. **8**:2402-2410.

Lagasse, E., and I.L. Weissman. 1992.
Mouse MRP8 and MRP14, two intracellular calcium-binding proteins associated with the development of the myeloid lineage.
Blood **79**:1907-1915.

Lemarchand, P., M. Vaglio, J. Mauel, and M. Markert. 1992.
Translocation of a small cytosolic calcium-binding protein (MRP-8) to plasma membrane correlates with human neutrophil activation.
J. Biol. Chem. **267**:19379-19382.

Lentsch, A.B., and P.A. Ward. 2000.
Regulation of inflammatory vascular damage.
J. Pathol. **190**:343-348.

Li, Y., J. Wang, J.G. Sheng, L. Liu, S.W. Barger, R.A. Jones, L.J. Van Eldik, R.E. Mrak, and W.S. Griffin. 1998.
S100 β increases levels of beta-amyloid precursor protein and its encoding mRNA in rat neuronal cultures.
J. Neurochem. **71**:1421-1428.

Lindahl, U., L. Thunberg, G. Backstrom, J. Riesenfeld, K. Nordling, and I. Bjork. 1984.
Extension and structural variability of the antithrombin-binding sequence in heparin.
J. Biol. Chem. **259**:12368-12376.

Lindahl, U., M. Kusche-Gullberg, and L. Kjellen. 1998.
Regulated diversity of heparan sulfate.
J. Biol. Chem. **273**:24979-24982.

Longbottom, D., J.M. Sallenave, and V. van Heyningen. 1992.
Subunit structure of calgranulins A and B obtained from sputum, plasma, granulocytes and cultured epithelial cells.
Biochim. Biophys. Acta **1120**:215-222.

Loomans, H.J., B.L. Hahn, Q.Q. Li, S.H. Phadnis, and P.G. Sohnle. 1998.
Histidine-based zinc-binding sequences and the antimicrobial activity of calprotectin.
J. Infect. Dis. **177**:812-814.

Lugering, N., T. Kucharzik, A. Lugering, G. Winde, C. Sorg, W. Domschke, and R. Stoll. 1997.
Importance of combined treatment with IL-10 and IL-4, but not IL-13, for inhibition of monocyte release of the Ca^{2+}-binding protein MRP8/14.
Immunology **91**:130-134.

Madsen, P., H.H. Rasmussen, H. Leffers, B. Honore, K. Dejgaard, E. Olsen, J. Kiil, E. Walbum, A.H. Andersen, B. Basse et al. 1991.
Molecular cloning, occurrence, and expression of a novel partially secreted protein "psoriasin" that is highly up-regulated in psoriatic skin.
J. Invest. Dermatol. **97**:701-712.

Mailliard, W.S., H.T. Haigler, and D.D. Schlaepfer. 1996.
Calcium-dependent binding of S100C to the N-terminal domain of annexin I.
J. Biol. Chem. **271**:719-725.

Mani, R.S., W.D. McCubbin, and C.M. Kay. 1992.
Calcium-dependent regulation of caldesmon by an 11-kDa smooth muscle calcium-binding protein, caltropin.
Biochemistry **31**:11896-11901.

Mani, R.S., and C.M. Kay. 1995.
Effect of caltropin on caldesmon-actin interaction.
J. Biol. Chem. **270**:6658-6663.

Mantovani, A., F. Bussolino, and E. Dejana. 1992.
Cytokine regulation of endothelial cell function.
FASEB J. **6**:2591-2599.

Mantovani, A., F. Colotta, S. Sozzani, P. Allavena, and E. Dejana. 1994.
Vasodilation in multistep paradigm of leucocyte extravasation.
Lancet **343**:1499-1500.

Marguerie, G., G. Chagniel, and M. Suscillon. 1977.
The binding of calcium to bovine fibrinogen.
Biochim. Biophys. Acta **490**:94-103.

Marti, T., K.D. Erttmann, and M.Y. Gallin. 1996.
Host-parasite interaction in human onchocerciasis: identification and sequence analysis of a novel human calgranulin.
Biochem. Biophys. Res. Commun. **221**:454-458.

Matsumura, H., T. Shiba, T. Inoue, S. Harada, and Y. Kai. 1998.
A novel mode of target recognition suggested by the 2.0 A structure of holo S100B from bovine brain.
Structure **6**:233-241.

McNutt, N.S. 1998.
The S100 family of multipurpose calcium-binding proteins.
J. Cutan. Pathol. **25**:521-529.

Millward, T.A., C.W. Heizmann, B.W. Schafer, and B.A. Hemmings. 1998.
Calcium regulation of Ndr protein kinase mediated by S100 calcium-binding proteins.
EMBO J. **17**:5913-5922.

Mirmohammadsadegh, A., E. Tschakarjan, A. Ljoljiic, K. Bohner, G. Michel, T. Ruzicka, M. Goos, and U.R. Hengge. 2000.
Calgranulin C is overexpressed in lesional psoriasis.
J. Invest. Dermatol. **114**:1207-1208.

Moll, T., E. Dejana, and D. Vestweber. 1998.
In vitro degradation of endothelial catenins by a neutrophil protease.
J. Cell Biol. **140**:403-407.

Murao, S., F.R. Collart, and E. Huberman. 1989.
A protein containing the cystic fibrosis antigen is an inhibitor of protein kinases.
J. Biol. Chem. **264**:8356-8360.

Muto, S., V. Vetvicka, and G.D. Ross. 1993.
CR3 (CD11b/CD18) expressed by cytotoxic T cells and natural killer cells is upregulated in a manner similar to neutrophil CR3 following stimulation with various activating agents.
J. Clin. Immunol. **13**:175-184.

Nagasawa, K., and Y. Inoue. 1980.
De-N-sulphation.
Methods Carbohydr. Chem. **8**.

Nelson, R.M., A. Venot, M.P. Bevilacqua, R.J. Linhardt, and I. Stamenkovic. 1995.
Carbohydrate-protein interactions in vascular biology.
Annu. Rev. Cell Dev. Biol. **11**:601-631.

Newton, R.A. 1997.
A role for S100 proteins,MRP-8 and MRP-14 in leukocyte adhesion.
University College London, PhD Thesis.

Newton, R.A., and N. Hogg. 1998.
The human S100 protein MRP-14 is a novel activator of the β_2 integrin Mac-1 on neutrophils.
J. Immunol. **160**:1427-1435.

Norgard-Sumnicht, K.E., N.M. Varki and A.Varki. 1993.
Calcium-dependent heparin-like ligands for L-selectin in nonlymphoid endothelial cells.
Science **261**:480-483.

Odink, K., N. Cerletti, J. Bruggen, R.G. Clerc, L. Tarcsay, G. Zwadlo, G. Gerhards, R. Schlegel, and C. Sorg. 1987.
Two calcium-binding proteins in infiltrate macrophages of rheumatoid arthritis.
Nature **330**:80-82.

Onions, J., S. Hermann, and T. Grundstrom. 1997.
Basic helix-loop-helix protein sequences determining differential inhibition by calmodulin and S-100 proteins.
J. Biol. Chem. **272**:23930-23937.

Ornitz, D.M. 2000.
FGFs, heparan sulfate and FGFRs: complex interactions essential for development.
Bioessays **22**:108-112.

Passey, R.J., E. Williams, A.M. Lichanska, C. Wells, S. Hu, C.L. Geczy, M.H. Little, and D.A. Hume. 1999.
A null mutation in the inflammation-associated S100 protein S100A8 causes early resorption of the mouse embryo.
J. Immunol. **163**:2209-2216.

Potts, B.C., J. Smith, M. Akke, T.J. Macke, K. Okazaki, H. Hidaka, D.A. Case, and W.J. Chazin. 1995.
The structure of calcyclin reveals a novel homodimeric fold for S100 Ca^{2+}-binding proteins.
Nat. Struct. Biol. **2**:790-796.

Raftery, M.J., C.A. Harrison, P. Alewood, A. Jones, and C.L. Geczy. 1996.
Isolation of the murine S100 protein MRP14 (14 kDa migration-inhibitory-factor-related protein) from activated spleen cells: characterization of post-translational modifications and zinc binding.
Biochem. J. **316**:285-293.

Raftery, M.J., L. Collinson, and C.L. Geczy. 1999.
Overexpression, oxidative refolding, and zinc binding of recombinant forms of the murine S100 protein MRP14 (S100A9).
Protein Expr. Purif. **15**:228-235.

Rammes, A., J. Roth, M. Goebeler, M. Klempt, M. Hartmann, and C. Sorg. 1997.
Myeloid-related protein (MRP) 8 and MRP14, calcium-binding proteins of the S100 family, are secreted by activated monocytes via a novel, tubulin-dependent pathway.
J. Biol. Chem. **272**:9496-9502.

Renne, T., J. Dedio, G. David, and W. Muller-Esterl. 2000.
H-kininogen utilizes heparan sulfate proteoglycans for accumulation on Endothelial cells.
J. Biol. Chem. (in press).

Rety, S., J. Sopkova, M. Renouard, D. Osterloh, V. Gerke, S. Tabaries, F. Russo-Marie, and A. Lewit-Bentley. 1999.
The crystal structure of a complex of p11 with the annexin II N-terminal peptide.
Nat. Struct. Biol. **6**:89-95.

Rety, S., D. Osterloh, J.P. Arie, S. Tabaries, J. Seeman, F. Russo-Marie, V. Gerke, and A. Lewit-Bentley. 2000.
Structural basis of the Ca^{2+}-dependent association between S100C (S100A11) and its target, the N-terminal part of annexin I.
Structure **8**:175-184.

Ridinger, K., E.C. Ilg, F.K. Niggli, C.W. Heizmann, and B.W. Schafer. 1998.
Clustered organization of S100 genes in human and mouse.
Biochim. Biophys. Acta **1448**:254-263.

Rodgaard, A., B.S. Thomsen, G. Bendixen, and K. Bendtzen. 1995.
Increased expression of complement receptor type 1 (CR1, CD35) on human peripheral blood T lymphocytes after polyclonal activation in vitro.
Immunol. Res. **14**:69-76.

Rosen, S.D., and C.R. Bertozzi. 1996.
Two selectins converge on sulphate. Leukocyte adhesion.
Curr. Biol. **6**:261-264.

Rosen, S.D. 1999.
Endothelial ligands for L-selectin: from lymphocyte recirculation to allograft rejection.
Am. J. Pathol. **155**:1013-1020.

Rosenberg, R.D., N.W. Shworak, J. Liu, J.J. Schwartz, and L. Zhang. 1997.
Heparan sulfate proteoglycans of the cardiovascular system. Specific structures emerge but how is synthesis regulated?
J. Clin. Invest. **100**:S67-75.

Ross, G.D., J.A. Cain, and P.J. Lachmann. 1985.
Membrane complement receptor type three (CR3) has lectin-like properties analogous to bovine conglutinin as functions as a receptor for zymosan and rabbit erythrocytes as well as a receptor for iC3b.
J. Immunol. **134**:3307-3315.

Roth, J., F. Burwinkel, C. van den Bos, M. Goebeler, E. Vollmer, and C. Sorg. 1993.
MRP8 and MRP14, S-100-like proteins associated with myeloid differentiation, are translocated to plasma membrane and intermediate filaments in a calcium-dependent manner.
Blood **82**:1875-1883.

Roulin, K., G. Hagens, R. Hotz, J.H. Saurat, J.H. Veerkamp, and G. Siegenthaler. 1999.
The fatty acid-binding heterocomplex FA-p34 formed by S100A8 and S100A9 is the major fatty acid carrier in neutrophils and translocates from the cytosol to the membrane upon stimulation.
Exp. Cell Res. **247**:410-421.

Rustandi, R.R., D.M. Baldisseri, and D.J. Weber. 2000.
Structure of the negative regulatory domain of p53 bound to S100B(ββ).
Nat. Struct. Biol. 7:570-574.

Saintigny, G., R. Schmidt, B. Shroot, L. Juhlin, U. Reichert, and S. Michel. 1992.
Differential expression of calgranulin A and B in various epithelial cell lines and reconstructed epidermis.
J. Invest. Dermatol. **99**:639-644.

Sakaguchi, M., M. Miyazaki, Y. Inoue, T. Tsuji, H. Kouchi, T. Tanaka, H. Yamada, and M. Namba. 2000.
Relationship between contact inhibition and intranuclear S100C of normal human fibroblasts.
J. Cell Biol. **149**:1193-1206.

Sandilands, G.P., S.A. MacPherson, E.R. Burnett, A.J. Russell, R.I. Downie, and R.N. MacSween. 1997.
Differential expression of CD32 isoforms following alloactivation of human T cells.
Immunology **91**:204-211.

Santhanagopalan, V., B.L. Hahn, and P.G. Sohnle. 1995.
Resistance of zinc-supplemented Candida albicans cells to the growth inhibitory effect of calprotectin.
J. Infect. Dis. **171**:1289-1294.

Sastry, M., R.R. Ketchem, O. Crescenzi, C. Weber, M.J. Lubienski, H. Hidaka, and W.J. Chazin. 1998.
The three-dimensional structure of Ca^{2+}-bound calcyclin: implications for Ca^{2+}-signal transduction by S100 proteins.
Structure **6**:223-231.

Sato, N., K. Isono, I. Ishiwata, M. Nakai, and K. Kami. 1999.
Tissue expression of the S100 protein family-related MRP8 gene in human chorionic villi by in situ hybridization techniques.
Okajimas Folia Anat. Jpn. **76**:123-129.

Schafer, B.W., R. Wicki, D. Engelkamp, M.G. Mattei, and C.W. Heizmann. 1995.
Isolation of a YAC clone covering a cluster of nine S100 genes on human chromosome 1q21: rationale for a new nomenclature of the S100 calcium-binding protein family.
Genomics **25**:638-643.

Schafer, B.W., and C.W. Heizmann. 1996.
The S100 family of EF-hand calcium-binding proteins: functions and pathology.
Trends Biochem. Sci. **21**:134-140.

Schafer, B.W., J. Fritschy, P. Murmann, H. Troxler, I. Durussel, C.W. Heizmann, and J.A. Cox. 2000.
S100A5 is a novel calcium-, zinc-, and copper ion-binding protein of the EF-hand superfamily.
J. Biol. Chem. **275**:30623-30630.

Schlessinger, J., I. Lax, and M. Lemmon. 1995.
Regulation of growth factor activation by proteoglycans: what is the role of the low affinity receptors?
Cell **83**:357-360.

Schluger, N.W., and W.N. Rom. 1997.
Early responses to infection: chemokines as mediators of inflammation.
Curr. Opin. Immunol. **9**:504-508.

Schmid, K.W., N. Lugering, R. Stoll, P. Brinkbaumer, G. Winde, W. Domschke, W. Bocker, and C. Sorg. 1995.
Immunohistochemical demonstration of the calcium-binding proteins MRP8 and MRP14 and their heterodimer (27E10 antigen) in Crohn's disease.
Hum. Pathol. **26**:334-337.

Schmidt, A.M., R. Mora, R. Cao, S.D. Yan, J. Brett, R. Ramakrishnan, T.C. Tsang, M. Simionescu, and D. Stern. 1994.
The endothelial cell binding site for advanced glycation end products consists of a complex: an integral membrane protein and a lactoferrin-like polypeptide.
J. Biol. Chem. **269**:9882-9888.

Shappell, S.B., C. Toman, D.C. Anderson, A.A. Taylor, M.L. Entman, and C.W. Smith. 1990.
Mac-1 (CD11b/CD18) mediates adherence-dependent hydrogen peroxide production by human and canine neutrophils.
J. Immunol. **144**:2702-2711.

Sheinerman, F.B., R. Norel, and B. Honig. 2000.
Electrostatic aspects of protein-protein interactions.
Curr. Opin. Struct. Biol. **10**:153-159.

Sheng, N., M.B. Fairbanks, R.L. Heinrikson, G. Canziani, I.M. Chaiken, D.M. Mosser, H. Zhang, and R.W. Colman. 2000.
Cleaved high molecular weight kininogen binds directly to the integrin CD11b/CD18 (Mac-1) and blocks adhesion to fibrinogen and ICAM-1.
Blood **95**:3788-3795.

Siegenthaler, G., K. Roulin, D. Chatellard-Gruaz, R. Hotz, J.H. Saurat, U. Hellman, and G. Hagens. 1997.
A heterocomplex formed by the calcium-binding proteins MRP8 (S100A8) and MRP14 (S100A9) binds unsaturated fatty acids with high affinity.
J. Biol. Chem. **272**:9371-9377.

Skelton, N.J., J. Kordel, M. Akke, S. Forsen, and W.J. Chazin. 1994.
Signal transduction versus buffering activity in Ca^{2+}-binding proteins.
Nat. Struct. Biol. **1**:239-245.

Smith, S.P., and G.S. Shaw. 1998a.
A novel calcium-sensitive switch revealed by the structure of human S100B in the calcium-bound form.
Structure **6**:211-222.

Smith, S.P., and G.S. Shaw. 1998b.
A change-in-hand mechanism for S100 signalling.
Biochem. Cell Biol. **76**:324-333.

Sohnle, P.G., C. Collins-Lech, and J.H. Wiessner. 1991.
The zinc-reversible antimicrobial activity of neutrophil lysates and abscess fluid supernatants.
J. Infect. Dis. **164**:137-142.

Spillmann, D., and U. Lindahl. 1994.
Glycoaminoglycan-protein interactions: a question of specificity.
Curr. Opin. Struct. Biol. **4**:677-682.

Springer, T.A., W.S. Thompson, L.J. Miller, F.C. Schmalstieg, and D.C. Anderson. 1984.
Inherited deficiency of the Mac-1, LFA-1, p150,95 glycoprotein family and its molecular basis.
J. Exp. Med. **160**:1901-1918.

Springer, T.A. 1994.
Traffic signals for lymphocyte recirculation and leukocyte emigration: the multistep paradigm.
Cell **76**:301-314.

Steinbakk, M., C.F. Naess-Andresen, E. Lingaas, I. Dale, P. Brandtzaeg, and M.K. Fagerhol. 1990.
Antimicrobial actions of calcium binding leucocyte L1 protein, calprotectin.
Lancet **336**:763-765.

Stewart, M.P., and N. Hogg. 1996a.
Regulation of leukocyte integrin function: affinity vs. avidity.
J. Cell. Biochem. **61**:554-561.

Stewart, M.P., C. Cabanas, and N. Hogg. 1996b.
T cell adhesion to intercellular adhesion molecule-1 (ICAM-1) is controlled by cell spreading and the activation of integrin LFA-1.
J. Immunol. **156**:1810-1817.

Stradal, T.B., and M. Gimona. 1999.
Ca^{2+}-dependent association of S100A6 (Calcyclin) with the plasma membrane and the nuclear envelope.
J. Biol. Chem. **274**:31593-31596.

Stradal, T.B., H. Troxler, C.W. Heizmann, and M. Gimona. 2000.
Mapping the zinc ligands of S100A2 by site-directed mutagenesis.
J. Biol. Chem. **275**:13219-13227.

Sudo, T., and H. Hidaka. 1999.
Characterization of the calcyclin (S100A6) binding site of annexin XI-A by site-directed mutagenesis.
FEBS Lett. **444**:11-14.

Tanaka, Y., D.H. Adams, and S. Shaw. 1993.
Regulation of leukocyte recruitment by proadhesive cytokines immobilized on endothelial proteoglycan.
Curr. Top. Microbiol. Immunol. **184**:99-106.

Tanaka, Y., K. Kimata, D.H. Adams, and S. Eto. 1998.
Modulation of cytokine function by heparan sulfate proteoglycans: sophisticated models for the regulation of cellular responses to cytokines.
Proc. Assoc. Am. Physicians **110**:118-125.

Teigelkamp, S., R.S. Bhardwaj, J. Roth, G. Meinardus-Hager, M. Karas, and C. Sorg. 1991.
Calcium-dependent complex assembly of the myeloic differentiation proteins MRP-8 and MRP-14.
J. Biol. Chem. **266**:13462-13467.

Tessier, P.A., P.H. Naccache, I. Clark-Lewis, R.P. Gladue, K.S. Neote, and S.R. McColl. 1997.
Chemokine networks in vivo: involvement of C-X-C and C-C chemokines in neutrophil extravasation in vivo in response to TNF-α.
J. Immunol. **159**:3595-3602.

Thompson, H.L., and K. Matsushima. 1992.
Human polymorphonuclear leucocytes stimulated by tumour necrosis factor-α show increased adherence to extracellular matrix proteins which is mediated via the CD11b/18 complex.
Clin. Exp. Immunol. **90**:280-285.

Treves, S., E. Scutari, M. Robert, S. Groh, M. Ottolia, G. Prestipino, M. Ronjat, and F. Zorzato. 1997.
Interaction of S100A1 with the Ca^{2+} release channel (ryanodine receptor) of skeletal muscle.
Biochemistry **36**:11496-11503.

van den Bos, C., J. Roth, H.G. Koch, M. Hartmann, and C. Sorg. 1996.
Phosphorylation of MRP14, an S100 protein expressed during monocytic differentiation, modulates Ca^{2+}-dependent translocation from cytoplasm to membranes and cytoskeleton.
J. Immunol. **156**:1247-1254.

Varki, A. 1994.
Selectin ligands.
Proc. Natl. Acad. Sci. U S A **91**:7390-7397.

Varki, A. 1997.
Selectin ligands: will the real ones please stand up?
J. Clin. Invest. **99**:158-162.

Vogl, T., C. Propper, M. Hartmann, A. Strey, K. Strupat, C. van den Bos, C. Sorg, and J. Roth. 1999.
S100A12 is expressed exclusively by granulocytes and acts independently from MRP8 and MRP14.
J. Biol. Chem. **274**:25291-25296.

Watt, K.W., I.L. Brightman, and E.J. Goetzl. 1983.
Isolation of two polypeptides comprising the neutrophil-immobilizing factor of human leucocytes.
Immunology **48**:79-86.

Webb, L.M., M.U. Ehrengruber, I. Clark-Lewis, M. Baggiolini, and A. Rot. 1993.
Binding to heparan sulfate or heparin enhances neutrophil responses to interleukin 8.
Proc. Natl. Acad. Sci. U S A **90**:7158-7162.

Weber, K.S., M.R. York, T.A. Springer, and L.B. Klickstein. 1997.
Characterization of lymphocyte function-associated antigen 1 (LFA-1)-deficient T cell lines: the α_L and β_2 subunits are interdependent for cell surface expression.
J. Immunol. **158**:273-279.

Wicki, R., I. Marenholz, D. Mischke, B.W. Schafer, and C.W. Heizmann. 1996.
Characterization of the human S100A12 (calgranulin C, p6, CAAF1, CGRP) gene, a new member of the S100 gene cluster on chromosome 1q21.
Cell Calcium **20**:459-464.

Wilkinson, M.M., A. Busuttil, C. Hayward, D.J. Brock, J.R. Dorin, and V. Van Heyningen. 1988.
Expression pattern of two related cystic fibrosis-associated calcium-binding proteins in normal and abnormal tissues.
J. Cell. Sci. **91**:221-230.

Witt, D.P., and A.D. Lander. 1994.
Differential binding of chemokines to glycosaminoglycan subpopulations.
Curr. Biol. **4**:394-400.

Woods, A., and J.R. Couchman. 1998.
Syndecans: synergistic activators of cell adhesion.
Trends Cell Biol. **8**:189-192.

Wright, S.D., P.E. Rao, W.C. Van Voorhis, L.S. Craigmyle, K. Iida, M.A. Talle, E.F. Westberg, G. Goldstein, and S.C. Silverstein. 1983.
Identification of the C3bi receptor of human monocytes and macrophages by using monoclonal antibodies.
Proc. Natl. Acad. Sci. U S A **80**:5699-5703.

Wright, S.D., J.I. Weitz, A.J. Huang, S.M. Levin, S.C. Silverstein, and J.D. Loike. 1988.
Complement receptor type three (CD11b/CD18) of human polymorphonuclear leukocytes recognizes fibrinogen.
Proc. Natl. Acad. Sci. U S A **85**:7734-7738.

Wu, T., C.W. Angus, X.L. Yao, C. Logun, and J.H. Shelhamer. 1997.
P11, a unique member of the S100 family of calcium-binding proteins, interacts with and inhibits the activity of the 85-kDa cytosolic phospholipase A2.
J. Biol. Chem. **272**:17145-17153.

Yamamura, T., J. Hitomi, K. Nagasaki, M. Suzuki, E. Takahashi, S. Saito, T. Tsukada, and K. Yamaguchi. 1996.
Human CAAF1 gene-molecular cloning, gene structure, and chromosome mapping.
Biochem. Biophys. Res. Commun. **221**:356-360.

Yang, Q., D. O'Hanlon, C.W. Heizmann, and A. Marks. 1999.
Demonstration of heterodimer formation between S100B and S100A6 in the yeast two-hybrid system and human melanoma.
Exp. Cell Res. **246**:501-509.

Yang, Z., M.J. deVeer, E.E. Gardiner, R.J. Devenish, C.J. Handley, J.R. Underwood, and H.C. Robinson. 1996.
Rabbit polymorphonuclear neutrophils form 35S-labeled S-sulfo-calgranulin C when incubated with inorganic [35S]sulfate.
J. Biol. Chem. **271**:19802-19809.

Yen, T., C.A. Harrison, J.M. Devery, S. Leong, S.E. Iismaa, T. Yoshimura, and C.L. Geczy. 1997.
Induction of the S100 chemotactic protein, CP-10, in murine microvascular endothelial cells by proinflammatory stimuli.
Blood **90**:4812-4821.

Yui, S., D. Yang, M. Mikami, and M. Yamazaki. 1993.
Characterization of cell growth-inhibitory factor in inflammatory peritoneal exudate cells of rats.
Microbiol. Immunol. **37**:961-969.

Yui, S., M. Mikami, and M. Yamazaki. 1995a.
Purification and characterization of the cytotoxic factor in rat peritoneal exudate cells: its identification as the calcium binding protein complex, calprotectin.
J. Leukoc. Biol. **58**:307-316.

Yui, S., M. Mikami, and M. Yamazaki. 1995b.
Induction of apoptotic cell death in mouse lymphoma and human leukemia cell lines by a calcium-binding protein complex, calprotectin, derived from inflammatory peritoneal exudate cells.
J. Leukoc. Biol. **58**:650-658.

Yui, S., M. Mikami, K. Tsurumaki, and M. Yamazaki. 1997.
Growth-inhibitory and apoptosis-inducing activities of calprotectin derived from inflammatory exudate cells on normal fibroblasts: regulation by metal ions.
J. Leukoc. Biol. **61**:50-57.

Zeng, F.Y., V. Gerke, and H.J. Gabius. 1993.
Identification of annexin II, annexin VI and glyceraldehyde-3-phosphate dehydrogenase as calcyclin-binding proteins in bovine heart.
Int. J. Biochem. **25**:1019-1027.

Zhao, X.Q., M. Naka, M. Muneyuki, and T. Tanaka. 2000.
Ca^{2+}-dependent inhibition of actin-activated myosin ATPase activity by S100C (S100A11), a novel member of the S100 protein family.
Biochem. Biophys. Res. Commun. **267**:77-79.

Zimmer, D.B., E.H. Cornwall, A. Landar, and W. Song. 1995.
The S100 protein family: history, function, and expression.
Brain Res. Bull. **37**:417-429.

Zimmer, D.B., J. Chessher, and W. Song. 1996.
Nucleotide homologies in genes encoding members of the S100 protein family.
Biochim. Biophys. Acta **1313**:229-238.

Zlotnik, A., and O. Yoshie. 2000.
Chemokines: a new classification system and their role in immunity.
Immunity **12**:121-127.

Zwadlo, G., R. Schlegel, and C. Sorg. 1986.
A monoclonal antibody to a subset of human monocytes found only in the peripheral blood and inflammatory tissues.
J. Immunol. **137**:512-518.

Zwadlo, G., J. Bruggen, G. Gerhards, R. Schlegel, and C. Sorg. 1988.
Two calcium-binding proteins associated with specific stages of myeloid cell differentiation are expressed by subsets of macrophages in inflammatory tissues.
Clin. Exp. Immunol. **72**:510-515.

PUBLICATIONS ARISING FROM THIS WORK

Robinson, M.J., and N. Hogg

A comparison of human S100A12 with MRP-14.

Biochem. Biophys. Res. Commun. **275**:865-870.